جامعة سيدي محمد بن عبد الله بفاس
UNIVERSITÉ SIDI MOHAMED BEN ABDELLAH DE FES

كلية العلوم والتقنيات فاس
FACULTÉ DES SCIENCES ET TECHNIQUES DE FÈS

Centre d'Etudes Doctorales : Sciences et Techniques de l'Ingénieur

N° d'ordre 45 /2020

THESE DE DOCTORAT

Présentée par

M^lle^: Manal EL RHAZI

Spécialité : Informatique

Sujet de la thèse :

3D facial aesthetic quality: Analysis and enhancement system

Thèse présentée et soutenue le Mardi 13 Octobre 2020 devant le jury composé de :

Nom Prénom	Titre	Etablissement	
Pr. KHARROUBI Jamal	PES	Faculté des Sciences et Techniques de Fès	Président
Pr. EL HASSOUNI Mohammed	PES	Faculté des Lettres et des Sciences Humaines Rabat	Rapporteur
Pr. AKSASSE Brahim	PES	Faculté des Sciences et Techniques d'Errachidia	Rapporteur
Pr. TALIBI ALAOUI Mohammed	PH	Faculté des Sciences et Techniques de Fès	Rapporteur
Pr. OUFKIR Ayat Allah	PES	Faculté de Médecine et de Pharmacie d'OUJDA	Examinatrice
Pr. ABBAD Khalid	PH	Faculté des Sciences et Techniques de Fès	Examinateur
Pr. ZARGHILI Arsalane Pr. MAJDA Aicha	PES PES	Faculté des Sciences et Techniques de Fès	Directeurs de thèse

Laboratoire d'accueil : Systèmes Intelligents et Applications.

Etablissement : Faculté des Sciences et Techniques de Fès

Acknowledgments

I would like to acknowledge the help and support of many people, without whom, my Ph.D. thesis would not have been possible and accomplished.

First of all, I would like to address my acknowledgements to the directors of my thesis Pr. ZARGHILI Arsalane and Pr. MAJDA Aicha for the endless encouragements, guidance, and useful advices during my PhD thesis. I am really grateful for their kindness and valuable remarks and it was a pleasure to be directed by them- thank you very much!

I am thankful to my dear friends KHADIJA and FATIMA ZAHRA for their help, advices and support in some hard times.

I would also thank all my colleagues at the Intelligent Systems and Application Laboratory (LSIA) for their help and support.

I am very grateful to my beloved family specially my parents ATMANE and FATIMA the source of my pride, for their encouragements and massive emotional support. Thank you dear father for the opportunities you have created for me to achieve my goals, for you love and support. Thank you lovely mother for your kindness, prayers, endless support and love. A warm gratitude goes to my sister SAMIA and brother YAHYA for their encouragements and for always being there, making the journey of my Ph.D. thesis amusing even if it was from a distance.

EL RHAZI Manal

Abstract

In the last few years, beauty industries have expanded quickly. Therefore, the analysis and assessment of facial attractiveness has attracted the interest of scientists, doctors and artists for its numerous applications in the entertainment industry, virtual media, plastic surgery and cosmetics. Facial aesthetic quality is one of the most important social characteristics of the individual's face, and many studies have demonstrated that the facial attractiveness is perceived as a key to both social and intellectual skills.

Through centuries, the common idea about the attractiveness was that beauty is "In the eye of the beholder", and that the attraction of a face is impossible to predict beyond our knowledge of the person's culture, historical era or even personal history. However, recent work suggests that the constituents of beauty are neither arbitrary nor culturally related, but that there is cross-cultural agreement on the face attractiveness of different ethnicities. These constituents are known by the canons of beauty and are essentially based on the face geometry: symmetry, golden ratio, neoclassical proportions, and angular profile.

Recently, various techniques of machine learning have been developed to analyze the attractiveness of the face by evaluating the characteristics of a given face. Nevertheless, these proposed techniques have not tested and combined the beauty canons in an overall system. Moreover, few of them have enhanced automatically the aesthetic quality of an analyzed face by applying the beauty canons to improve the appeal of faces.

Given the importance of facial attractiveness in our social life in addition to the increased demand of cosmetic and aesthetic surgeries, a need for an automatic system to analyze, assess and improve the attractiveness of a face is of a good deal.

Therefore, the aim of our project is to develop an automatic system to analyze the aesthetic quality of 3D faces, and then suggest the necessary modification to apply in order to enhance its attractiveness. This work as well aims to allow the plastic surgeon to apply the modifications to a virtual face before the surgery.

The step of localizing the facial landmarks is considered as a key step for any further analysis, thus the first contribution of this work is related to the esthetic quality analysis of 2D faces, and especially to 2D facial landmarks detection. Indeed, we developed a new approach by combining a method based skin color and facial geometric model characteristics with the Active Contour Detector "Snake". The second contribution consists of classifying the existing geometric information based methods to localize the 3D facial landmarks into four categories based on a mapping study. The third contribution is a new method to detect the 3D craniofacial landmarks on 3D face meshes. This method is based on the geometric information provided by the 3D mesh, and the last contribution is a Free Form deformation technique based on the Bézier function to edit the 3D faces in order to enhance their aesthetic quality.

Keywords: 3D faces; facial attractiveness; aesthetic quality analysis; attractiveness enhancement.

Résumé

Au cours des dernières années, les industries de la beauté ont connu une expansion rapide. Par conséquent, l'analyse et l'évaluation de l'attractivité faciale a suscité l'intérêt des scientifiques, des médecins et des artistes pour ses nombreuses applications dans l'industrie du divertissement, les médias virtuels, la chirurgie plastique et les cosmétiques. La qualité esthétique du visage est l'une des caractéristiques sociales les plus importantes du visage d'un individu, et de nombreuses études ont démontré que l'attractivité du visage est perçu comme un élément clé des compétences sociales et intellectuelles.

À travers des siècles, la notion commune dans la recherche sur l'attractivité d'un visage a été que la beauté est « dans l'œil du l'observateur », et que l'attraction d'un visage est impossible à prévoir au-delà de notre connaissance de la culture de la personne, son époque historique ou même son histoire personnelle. Cependant, des travaux récents suggèrent que les constituants de la beauté sont ni arbitraires ni liés à la culture, mais qu'il existe un accord interculturelles sur l'attractivité des visages de différentes ethnies. Ces constituants sont connus par les canons de beauté et se basent essentiellement sur la géométrie du visage, et sont : La symétrie, le nombre d'or, les proportions néoclassiques, et les angles de profil de visage.

Récemment, diverses techniques d'apprentissage automatique ont été développées pour analyser l'attractivité du visage en évaluant ses caractéristiques. Néanmoins, ces techniques proposées n'ont pas permis de tester et de combiner les canons de la beauté dans un système global. De plus, peu d'entre elles ont amélioré automatiquement la qualité esthétique d'un visage analysé en appliquant ses canons. Étant donné l'importance de l'attractivité du visage dans notre vie sociale, en plus de la demande accrue de chirurgies esthétiques et cosmétiques, il est nécessaire de disposer d'un système automatique pour analyser, évaluer et améliorer la qualité esthétique d'un visage. Par conséquent, le but de notre sujet est de développer un système automatique pour l'évaluation de la beauté d'un visage 3D, puis de proposer les modifications nécessaires pour améliorer son attractivité. Tout cela en permettant au chirurgien plasticien d'appliquer les modifications sur un visage virtuel avant l'intervention chirurgicale.

En effet, l'étape de la localisation des points caractéristiques est considéré une étape clé pour garantir des meilleur résultats d'analyse et d'amélioration de l'attractivité des visage, du coup, la première contribution de notre travail est au niveau d'analyse de la qualité esthétique des visages 2D, précisément la détection des points caractéristique du visage, en utilisant une combinaison d'une méthode basée sur la couleur de la peau et les caractéristiques du modèle géométrique du visage d'une part et le détecteur active contour « Snake » d'une autre part.

La deuxième contribution consiste à classer les méthodes géométriques existantes pour localiser les points caractéristiques des visages 3D en quatre catégories en se basant sur le mapping study.

La troisième contribution consiste en une nouvelle méthode de détection des points caractéristique sur un modèle de visage 3D, cette méthode se base essentiellement sur les propriétés géométriques des mailles 3D. La dernière contribution est au niveau de l'amélioration de la qualité esthétique des visages 3D ; Free Form Deformation technique basée sur la fonction de Bézier est utilisée pour modifier les visages 3D.

Mots-clés : visages 3D ; attractivité des visages 2D/3D ; analyse de la qualité esthétique ; amélioration de la qualité esthétique des visages.

ملخص

في السنوات القليلة الماضية ، توسعت صناعات التجميل بسرعة. لذلك ، اجتذب تحليل وتقييم جاذبية الوجه اهتمام العلماء والأطباء والفنانين لتطبيقاته العديدة في الوسائط الافتراضية والجراحة التجميلية. تعد الجودة الجمالية للوجه واحدة من أهم الخصائص الاجتماعية لوجه الفرد، وقد أثبتت العديد من الدراسات أن جاذبية الوجه تعتبر مفتاحًا لكل من المهارات الاجتماعية والفكرية.

عبر القرون، كانت الفكرة الشائعة عن الجاذبية هي أن الجمال "في عين الناظر"، وأن جاذبية الوجه من المستحيل التنبؤ بها بما يتجاوز معرفتنا بثقافة الشخص أو العصر التاريخي أو حتى التاريخ الشخصي. ومع ذلك ، تشير الأعمال الحديثة إلى أن مكونات الجمال ليست تعسفية ولا مرتبطة ثقافيًا ، ولكن هناك اتفاق عبر الثقافات على جاذبية الوجه للأعراق المختلفة. تُعرف هذه المكونات بشرائع الجمال وتستند أساسًا إلى هندسة الوجه: التناظر والنسبة الذهبية والنسب الكلاسيكية الجديدة و الجانب الزاوي.

في الآونة الأخيرة ، تم تطوير تقنيات مختلفة للتعلم الآلي لتحليل جاذبية الوجه من خلال تقييم خصائص وجه معين. ومع ذلك ، فإن هذه التقنيات المقترحة لم تختبر دمج شرائع الجمال في نظام شامل. علاوة على ذلك ، عزز عدد قليل منهم تلقائيًا الجودة الجمالية للوجه الذي تم تحليله من خلال تطبيق قوانين التجميل لتحسين جاذبية الوجوه.

نظرًا لأهمية جاذبية الوجه في حياتنا الاجتماعية بالإضافة إلى زيادة الطلب على العمليات التجميلية والتجميلية ، فإن الحاجة إلى نظام آلي لتحليل وتقييم وتحسين جاذبية الوجه أمر جيد. لذلك ، فإن الهدف من مشروعنا هو تطوير نظام آلي لتحليل الجودة الجمالية للوجوه ثلاثية الأبعاد ، ومن ثم اقتراح التعديل اللازم لتطبيقه من أجل تعزيز جاذبيته. يهدف هذا العمل أيضًا إلى السماح لجراح التجميل بتطبيق التعديلات على الوجه الافتراضي قبل الجراحة.

تعتبر خطوة تحديد معالم الوجه خطوة أساسية لأي تحليل إضافي ، وبالتالي فإن المساهمة الأولى لهذا العمل تتعلق بتحليل الجودة الجمالية للوجوه ثنائية الأبعاد ، وخاصةً الكشف عن معالم الوجه ثنائية الأبعاد. في الواقع ، لقد طورنا نهجًا جديدًا من خلال الجمع بين لون البشرة المستند إلى الأسلوب وخصائص النموذج الهندسي للوجه مع .Active Contour Detector تتكون المساهمة الثانية من تصنيف الأساليب القائمة على المعلومات الهندسية الحالية لتوطين معالم الوجه ثلاثية الأبعاد إلى أربع فئات بناءً على دراسة الخرائط. المساهمة الثالثة هي طريقة جديدة لاكتشاف المعالم ثلاثية الأبعاد على شبكات الوجه ثلاثية الأبعاد. تعتمد هذه الطريقة على المعلومات الهندسية التي توفرها الشبكة ثلاثية الأبعاد ، والمساهمة الأخيرة هي تقنية تشوه لتعديل الوجوه ثلاثية الأبعاد من أجل تحسين جودتها الجمالية.

الكلمات المفتاحية: وجوه ثلاثية الأبعاد ؛ جاذبية الوجوه ثنائية الأبعاد / ثلاثية الأبعاد ؛ تحليل الجودة الجمالية تحسين الجودة الجمالية للوجه.

Liste of publications

Journal papers:

- Manal El Rhazi, Arsalane Zarghili, Aicha Majda, Ayat Allah Oufkir, Anissa Bouzalmat **" Facial beauty analysis by age and gender."** Int. J. Intelligent Systems Technologies and Applications, Vol. 18, Nos. 1/2, 2019.

- Manal El Rhazi, Arsalane Zarghili, Aicha Majda **"Survey on the approaches based geometric information for 3D face landmarks detection."** IET Image Processing, Vol13, Issue8, 2019.

- Manal El Rhazi, Arsalane Zarghili, Aicha Majda **"Comparative Study of Harris and Active Contour Using Viola-Jones Algorithm for Facial Landmarks Detection."** Transactions on Machine Learning and Artificial Intelligence Vol5, No4, 2017.

- Manal El Rhazi, Arsalane Zarghili, Aicha Majda, Ayat Allah Oufkir **"3D Facial attractiveness enhancement using Free Form Deformation."** Journal of King Saud University - Computer and Information Sciences, Accepted for minor revision.

Conference papers:

- Manal EL Rhazi, Arsalane Zarghili, Aicha Majda **"Automated detection of craniofacial landmarks on a 3D facial mesh."** 11th edition of the International Conference on Integrated Design and Production CPI, Fez 2019.

- Manal EL Rhazi, Arsalane Zarghili, Aicha Majda **"Comparative Study of Harris and Active Contour Using Viola-Jones Algorithm for Facial Landmarks Detection."** ACMLIS'17 International Conference, Tétouan 19 Mai 2017.

Table of figures

Table of tables

Glossary

R.O-	Research Objectives
2D-	2 Dimension
3D-	3 Dimension
B.C-	Before Christ
NFr-	NasoFrontal angle
NFa-	NasoFacial angle
NM-	NasoMental
MeC-	MentoCervical
Na-	Nasal angle
Mx-	Maxillary angle
Mn-	Mandibular angle
MF-	MaxilloFacial angle
F-	Facial angle
NM-	Nasal Maxillary angle
H-	Holdaway's angle
CV-	Curriculum vitae
LFW-	Labeled Faces in the Wild
FDDB-	Face Detection Data Set and Benchmark
SIFT-	Scale Invariant Feature Transform
HoGs-	Histograms of oriented Gradients
LBPs-	Local Binary Patterns
CNNs-	Convolutional Neural Networks
DCNNs-	Deep Convolutional Neural Networks
DPM-	Deformable Parts based Model
LBP-	Local Binary Patterns
KL boosting-	Kullback-Leibler Boosting
YIQ-	Y In-phase Quadrature
HSV-	Hue, Saturation, Value
CARTs-	Classification and Regress Tree
R-CNNs-	Region based Convolutional neural networks
AlexNet-	Alex Networks
GoogLeNet-	Google Networks
GPUs-	Graphics Processing Unit
ReLU-	Rectified Linear Unit
DDFD-	Deep Dense Face Detector
SVM-	Support Vector Machine
AAM-	Active Appearance Model
CLM-	Constrained Local Model
AOM-	Active Orientation Model
PCA-	Principal Component Analysis

PDM-	Point Distribution Model
CLNF-	Constrained Local Neural Field
DRMF-	Discriminative Response Map Fitting
ICA-	Independent Component Analysis
TCDCN-	Tasks-Constrained Deep Convolutional Network
RNN-	Recurrent Neural Network
KNN-	k Nearest Neighbors
RANSAC-	RANdom Sample Consensus
3DMM-	3 Dimensional Morphable Models
VAAM-	View based Active Appearance Model
FLM-	Facial Landmarks Model
LDA-	Latent Dirichlet Allocation
HONV-	Histogram of Oriented Normal Vectors
SIFT-	Scale Invariant Feature Transform
APSC-	Asymmetry Patterns Shape Contexts
FRGC-	Face Recognition Grand Challenge
BU-3DFE-	Binghamton University 3D Facial Expression
SI-	Shape Index
SS-	Spin Image
K-	Gaussian Curvature
H-	Mean Curvature
k1,k2-	Principal Curvatures
EGBM-	Elastic Graph Bunch Matching
HONV-	Histogram of Oriented Normal Vectors
LNBP-	Local Normal Binary Patterns
FRGCv2-	Face Recognition Grand Challenge version2
LCC-	Local Coordinates Coding
SI-SSM-	Shape index based statistical shape model
SFAM-	Statistical Facial feAture Model
FFD-	Free Form Deformation
CMYK-	Cyan- Magenta- Yellow- Black
RGB-	Red- Green-Blue
CIE-	International Commission on Illumination
FEI-	Fundação Educacional Inaciana (Faculty of Industrial Engineering)
ECVP-	European Conference on Visual Perception in Utrecht
BFM-	Basel Face Model
PC-	Personal Computer
RAM-	Random Access Memory
ROI-	Regions of interest
NURBS-	Non-Uniform Rational Bézier Spline
CPU-	Central Processing Unit

Table of content

Introduction

1 Motivation

Facial attractiveness plays an important role in human life and always been one of the most debated subjects in many fields because of the different perceptions of attractiveness by individuals.

In the literature, many studies have defined what makes a face attractive, thus unifying the attractiveness criterions and making it universal and not related to the historical era or ethnicity of a person, which means that people all over the world have the same criterions on judging facial attractiveness.

Physical attractiveness has an important and great influence in human social life as been demonstrated in several researches during the last decades [1][2]. It was also widely linked to the possession of a variety of positive qualities that makes an individual better than the others as summarized in the statement of Dion, Berscheid, and Walster's in 1972 [3], who claimed that " what is beautiful is good". Indeed, physical attractiveness offers many advantages to individual life especially in a society obsessed with beauty and attractiveness. These advantages are proved by daily experiences such as in the intersexual selection [4], as attractive people have more chance to find their mate easily. Physical attractiveness can also affect individual self-esteem and cause psychological disorders [5][1]. In general, attractive people are better treated comparing with less attractive ones and are likely to be better which let them enjoy many advantages like to be hired for jobs more than equally qualified but less attractive people[6][7], having more friends and getting higher incomes [8].

As consequences to the attractiveness influence, people tend to look more and more attractive using makeup or in most of time plastic surgeries. By asking the surgeons about the reasons that make people asking for a plastic surgery, they mentioned that there exist different types of demanding; for example, a type who is just looking for perfection in their body even that they don't look strange or ugly or have any abnormalities, another type of people want to look younger. In addition, there is a type who is trying to look like others like TV stars, as the media shows their beauty as the perfect one and therefore dictates what an attractive face for example should look like. On the other hand, there is a type who wants to be liked, be accepted by others and wishing to develop self-esteem, which is the most largely used reason to have plastic surgery. Therefore, since 2000, overall plastic surgeries have risen considerably due to the continued growth of surgeries demanding as well as the money spent for that purpose.

In parallel to the increased need to plastic surgeries, the need to simplify and show how the face will look like after the surgery is recommended, to plan the procedures, verify the satisfaction of the patient, and reduce the risks during the surgery as well.

These days, in the industry field, working with 3D models of facial procedures is an essential tool to plan the surgical procedures and evaluate the postsurgical results. Indeed, there exist two ways for 3D face modelling of plastic surgery; 3D face printing and 3D face model software. Each way of those is manipulated by the surgeon and the patient, manually, before the final

results. Therefore, an automatic tool for facial attractiveness analysis based on the beauty canons defined in the literature is needed, which is considered a great challenge for researchers.

2 Research objectives

The main relevant findings on enhancing facial attractiveness mainly deals with 2D face images. Authors in [9] developed a program to apply face makeup to a face image using the example of another image's appearance. This technique affects the colour and skin properties of a face whose shape remains unchanged, so it is similar to physical make-up. Nevertheless, these procedures are used to alter the initial image in such a way that the contour and geometry of the facial traits are not altered.

Nowadays, 3D visualization has been widely used in medical area; still few systems are dedicated for the plastic surgeries fields because of the high price of materials. The existing software to plan 3D facial procedures and evaluate the post surgery are manipulated based on the patient and what he want to look like as a results, with usually no respect to the real attractive face and the criterions that must be respected to achieve it.
The existing systems for visualizing 3D face (VECTRA 3D [10], MIRRORME 3D [11], CRISALIX [12]) do not suggest any standards of 3D facial attractiveness which makes the development of such a tool a necessary task to facilitate the work of the surgeons and patient at the same time, thereafter to address the lack of 3D systems to analyze the 3D facial attractiveness, to suggest the necessary modification to enhance its attractiveness based on the criterions defined by the researchers in that field, and finally to evaluate the results of the post-surgery on the 3D virtual model of the face.
In our thesis, we aim to address the following research objectives:

- **Research Objective One:** To analyze the 2D facial aesthetic quality and thereafter suggest the necessary modifications in order to improve its attractiveness.

- **Research Objective Two:** To assess the aesthetic quality of 3D faces and as the first research object, recommend the required modifications to enhance its attractiveness.

- **Research Objective Three:** To predict how the face will look like after applying the required modification, thus the post-surgery results.

- **Research Objective Four:** To assess the resulting face after the surgery by asking a domain expert in plastic surgery and conducting a survey.

3 Research methodology

To fulfill the research objectives cited previously, the figure 1 presents a summary of the methodology followed in our thesis.
The project has been divided into four stages; each one is related to the following stage, we started by a global literature review to localize our work and to establish the existing needs. Then as the first try, we analyzed the aesthetic quality of 2D face using a new method to detect the 2D

facial landmarks and then we suggested the necessary modifications to enhance its attractiveness. The second stage is to start working deeply into our project of the analysis of 3D facial attractiveness, after a systematic literature review and a mapping review, we selected the appropriate method to detect the 3D facial landmarks to be able to analyze the attractiveness of the 3D face and finally to predict how this face can look more attractive.
The third stage is the visualization of the 3D face after the applied modifications to verify the satisfaction of both the patient and the surgeon. Finally, the last stage is the evaluation of the obtained results, by asking a domain expert in plastic surgery to assess the obtained results and conducting a survey by asking the participants to vote for the most attractive face within two versions.

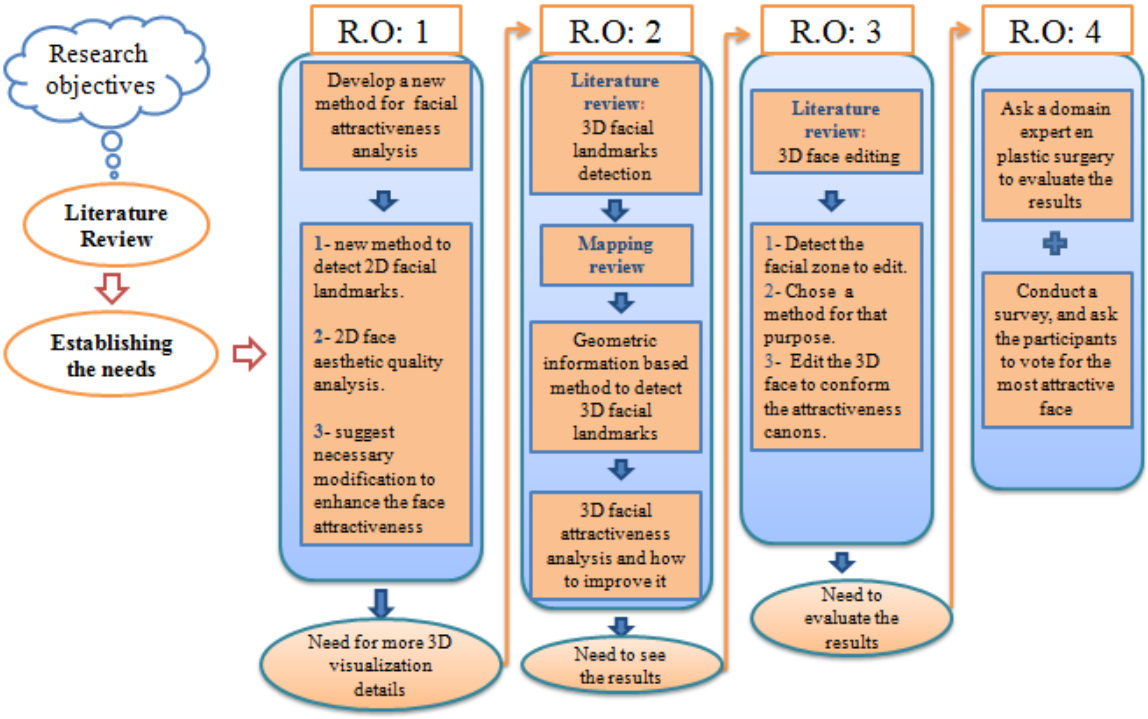

Figure 1: Overview of the research methodology

4 Summary of contributions

The contributions of this thesis are as follows:

1. **A new method to detect facial landmarks on a 2D image** [13]**.** This method is a combination of two approaches: the active contour (snake) and the approach based on the detection of the 2D face axes that go through some facial feature: the eyes, the nose, the mouth and the median axis. Once we get the facial axes that go along the facial features, we apply the active contour (snake) to the edge of the face and then to each facial feature to get the contour of each of them. Finally, we find the intersection of the axes and the points given by the active contour, these intersections must be localized in the skin zone of the face. The resulted intersection points are the final landmarks. This new method proves to be more efficient in detecting a large number of landmarks comparing with the other most used approaches in the literature like Haar wavelet [14].

2. The second contribution is a **comparative study of Harris and Active Contour using Viola-Jones algorithm for facial landmarks detection** [15]. Based on the first contribution, we have conducted a comparative study of the well know operator Harris and the Active Contour (Snake) using the Viola-Jones algorithm for 2D facial landmarks localization. In this study, we have localized the common landmarks that can be detected by both the competing methods which are: the eyes corners, the nose corners, and the mouth corners. The comparison is based essentially on comparing the success rate of detection of the landmarks using two different face databases. Experimental results have shown that both the Harris and the Active Contour using the Viola-Jones algorithm can localize the facial landmarks with good rates, still the Active Contour + Viola-Jones has shown an interesting localization results compared to the Harris+ Viola-Jones algorithm.
3. The third contribution is **a classification of the geometric information methods to localize the 3D facial landmarks into four categories** [16]**.** A mapping study is performed to characterize the existing geometric information based methods to localize the 3D facial landmarks and to classify them into categories. Actually a searching for the articles based geometric information techniques to detect the 3D facial landmarks is conducted in the period of 2010-2018, consequently, 30 papers were found after excluding paper that are not in the field. Thus, the geometric information based methods to localize the 3D facial landmarks can be classified into four categories; the first category is: methods based curvature analysis, the second category is: methods based on combining 2D texture with 3D shape information, the third category is: methods based on matching the 3D query face with a manually labeled one, and the fourth category is methods based on generic image descriptors.
4. The fourth contribution is **a new approach to detect 30 3D facial landmarks** [17], this approaches is based on the geometric information of the 3D face. For a given 3D face model, a preprocessing of this face is mandatory to normalize its orientation and angles to be ready for the localization of the 3D landmarks. Once the face is normalized, the 3D face landmarks are detected using the geometric information of the 3D face: the first landmark to detect is the nose tip, as it is the most identified point on the face by having the maximum Z value, then for the rest of the 29 landmarks, the detection is based on the first result obtained for the nose tip and other 3D facial characteristics. This method is able to localize 30 landmarks on a 3D face with a minimum error and standard deviation compared with the other studies in the literature.
5. The fifth contribution is a new method to **edit the 3D face model** in order to apply the necessary modification to enhance its attractiveness. This method is based on the use of a Free Form Deformation technique using the Bezier interpolation function. Indeed, for each zone of the face that need to be edited, the Free Form technique is used to apply the required modifications -obtained from the step of the aesthetic quality analysis- to improve its appeal in term of the beauty canons.

5 Thesis structure

The rest of this thesis is organized as follows:

- **Chapter one: State of the art on facial aesthetic quality analysis**

This chapter presents the state of the art of facial attractiveness studies and the methods used to analyze it. It gives the history of facial attractiveness and discusses the canons used to analyze the facial beauty such as the symmetry, the golden ratio, the face averageness, the neoclassical proportions, and the angular profile. This chapter also presents the steps used to analyze the aesthetic quality of 2D face; these steps include the localization of the face on a 2D image, and then the detection of the 2D facial landmarks, finally the analysis of the facial attractiveness using the canons discussed previously. The chapter discusses also the analysis of 3D facial aesthetic quality, firstly by detecting the 3D facial landmarks on 3D face, and then studying its attractiveness using the same beauty canons, but also adding those related to the profile side of the 3D face. Finally, this chapter is concluded by the 3D facial attractiveness enhancement and the different existing ways to achieve that purpose.

- **Chapter two: 2D facial aesthetic quality analysis methodology**

In this chapter, the details on how to analyze the aesthetic quality of 2D face and consequently to achieve the first research objective are presented. First, it gives an overview of the existing method to detect the facial zone on a 2D image and the selected approach in this thesis and then the different steps used to detect the 2D facial axes and landmarks, finally, it describes the approach used to analyze the aesthetic quality of a 2D face and how can the face look more attractive using the beauty canons defined by the literature studies.

- **Chapter three: 3D facial aesthetic quality analysis methodology**

This chapter presents the followed steps to analyze the aesthetic quality of a 3D face: first the pose and orientation of the 3D face must be normalized to be able to detect its landmarks on the both frontal and profile sides using the geometric information based method selected for that purpose. After the detection of the 3D landmarks, the followed steps is the analysis of the aesthetic quality of the 3D face, by first verifying if the 3D face satisfies the beauty canons or not, and then suggest the necessary modifications to improve its attractiveness.

- **Chapter four: 3D face attractiveness enhancement**

In this chapter, we describe how to enhance the aesthetic quality of the given 3D face by applying the different modifications required from the previous chapter (Chapter 3). Our tool for improving the attractiveness of faces for 3D faces is built on the concepts of neoclassical canons, symmetry, golden number and the definition of facial attractiveness standards in cosmetology. Our method is based on a parameterized free form deformation technique based on the Bezier interpolation function to correct and edit the geometry of a 3D face model in order to preserve its geometric details. As a result, we obtain a more attractive 3D face model while maintaining the main characteristics of the original face.

- **Chapter five: Evaluating of the 3D modified face**

  This chapter provides the evaluation of the modified 3D face after editing the face and applying the beauty canons. Firstly, a set of research questions is presented as a part of the work evaluation, followed by the finding of our thesis as the answers and the prototypes proposed as a solutions for each research question. Finally, this chapter is concluded by the verification of the proposed evaluation steps.

In brief, this general introduction presents a summary of the discussed research objectives in our thesis, the followed methodology to achieve our goals, in addition to the main contributions of this research.

Chapter 1: State of the art on facial aesthetic quality analysis

1 Introduction

This chapter presents the state of the art review of the existing researches in the literature to analyze the aesthetic quality of 2D and 3D faces and the different methods used to edit the 3D face in order to enhance its attractiveness. Indeed, this chapter is organized as follows: Section 2 discusses the history of facial beauty during the last decencies. Section 3 describes the different beauty canons existing in the literature research studies used to analyze the facial aesthetic quality; these canons include the facial symmetry, the golden ratio, the averageness, the neoclassical proportions, and the angular profile. Section 4 introduces the processes of the analysis of 2D facial aesthetic quality, this section is divided as well into several subsections, presenting the different approaches used to localize the face in a 2D image, the existing methods in the literature to detect 2D facial landmarks and finally, the existing methods to analyze the attractiveness of the 2D face are discussed. Section 5 presents the process of the analysis of 3D facial aesthetic quality; this section starts with the 3D face normalization step, which is of great importance. Then, it presents a literature review on the existing methods used to localize the 3D landmarks, and finally shows how the attractiveness of a 3D face can be analyzed by adding the profile side of the face. Section 6 describes the 3D facial attractiveness enhancement by editing the 3D facial shape. Finally, section 7 concludes this chapter.

2 The history of attractiveness

Attractiveness has always been a long debated topic by different disciplines such as human sciences, computer vision and medical area. Attractiveness is as well a source of issues related to people's discrimination based on their physical state.

Since the ancient Egyptian civilization, facial beauty has been idealized in art, and it was directly related to the facial proportions that must be respected in order to consider a face attractive. However, the study of beauty as a formal discipline started with the Greek civilization guided by artists and philosophers, having insisted that beauty means the harmony of proportions of the body or the face. The Renaissance artists afterward discussed the beauty and the proportions and defined therefore the ideal human form, which is well known by drawings of Leonardo da Vinci and the Vitruvian man.

Decades ago, the importance of attractiveness started serendipitously during researches done by Hatfield and colleagues in 1966 [18] that aim to paired randomly men and women for blind dates. In these researches participants were asked after the first date to fill in a questionnaire about the most interesting things about their random partners concerning their personality, historical background and if they are interested in another date with the same partner in order to have a survey at the end about the common points of interest in a population towards a partner. The results were not as expected by the researches, as there was a new criterion added by the participants to make their choice which is the physical attractiveness of the partner. This criterion proved to be a sign of a good health and having advantageous biological characteristics as mate [19]. The good health can be explained by having a good immune defense that can help the mate to be less susceptible to parasites.

Consequently, several studies have been conducted in many disciplines to analyze and demonstrate the attractiveness and its different sides in relation with the human life. These studies were formulated at the level of socio-psychological study and most of the research addressed three basic research questions: (1) Are attractive people perceived in any way different from unattractive people? (2) Are attractive people are treated unequally compared to unattractive people? (3) Do attractive people have different characteristics than unattractive people concerning their personality traits, skills and behavioural tendencies? [20]. The proposed research questions aims to discuss in the first place the how can attractiveness influence the social life of individuals under the stereotypes imposed from the perception of attractive individuals. The second research area discusses how these stereotypes can divide and discriminate peoples depending on their appearance, and finally, the last axis of research aims to describe the different characteristic of both attractive and unattractive people concerning their personality traits and behaviour.

Physical attractiveness has an important and great influence in human social life as been demonstrated in several researches during the last decades [1][2], it was also widely linked to the possession of a range of positive qualities that makes an individual better than the others as summarized in the statement of Dion, Berscheid, and Walster's in 1972 [3], who claimed that " what is beautiful is good", based on a classical experience using facial photographs of different individuals that were judged into three categories; low, medium, or high in physical attractiveness by the researches. The purpose of the study was to assign to each photograph various personality traits as well as life outcomes such as marital happiness and career success, as a result, the individuals that were assigned with more valuable traits are those judged physically attractive. This stereotype led to many researches [21][22][23][24] on attractiveness to examine its generality and how far its strength can influence.

As a conclusion to the study cited previously and to the statement, physical attractiveness offers many advantages to the individual life especially in a society obsessed with attractiveness and beauty. These advantages are proved by daily experiences such as in the intersexual selection [4], as attractive people have more chance to find their mate easily. Physical attractiveness can also affect individual self-esteem and cause psychological disorders [5][1]. In general, attractive people are more well treated comparing with less attractive ones and are likely to be better which let them enjoy many advantages like to be hired for jobs more than equally qualified but less attractive people[6][7], having more friends and getting higher incomes [8]. Due to the social consequences of the physical attractiveness, several researches guided by philosophers, artistes and scientists were established to define what beauty is and what turns a face into an attractive one.

Through centuries, the common idea in research on the face attractiveness was that beauty is 'in the eye of the beholder', which means that people vary in what they perceive to be attractive, and what is attractive now could, in a different time or place, be considered unattractive, furthermore, the attraction is impossible to predict beyond our knowledge of the culture of the person, his historical era or even his personal history [25]. This testament was also supported by [26] who claims in his research that attractiveness differs depending on the population and cross-culture,

such there is many individuals preferences that could not be the same for others from another population and culture, this preferences can be presented for example in the body weight, face shape, skin colour and even teeth filing.

However, recent works suggest that the components of facial beauty are not arbitrary or related to culture, but there is a cross-cultural agreement on the face attractiveness of diverse ethnic groups [27][28], also that the preferences of beauty may be biological and an innate part of the constitution of human nature rather than his culture and history [29][8][27][30][31]. These studies proved the infants with few months aged from 2 to 3 months and from 6 to 8 months old preferences during experience that aims to show them photographs of both male and female that have been already judged attractive and non attractive by a group of ratters. The obtained results show that the infants look at the photographs rated attractive for long time comparing with photographs judged unattractive regardless the age, gender and the race [32].

Accordingly, that suggests that people all around the world use similar criterions in their judgements on facial beauty. These criterions are related to some features and facial traits that determinate the attraction of the body and the face as well; hence we say that an individual is attractive if his facial features follow some rules that will be indicated later.

These traits are known as the beauty canons for both the body and its part, and they are defined by the advocates of the cross-cultural agreement of attractiveness since ancient times. The word canon was first defined by the Greek sculptor Polycleitus (circa 450 to 420 BC) trying to define the aesthetics in mathematical terms. He claims in his famous statue of Doryphorous that the height of the face is one-tenth the length of the whole body, the head one-eighth the length of the whole body, and the head and neck one-sixth the length of the whole body. Afterwards, during the renaissance times, new criterions called the classical and the neoclassical canons have been used [33][34][35] and still considered a reference by plastic surgeons nowadays to evaluate the aesthetic quality of a face.

3 Facial beauty canons

The ancient Egyptians (c 1350 BC) have created a harmonious status and painters for their kings and queens with ideal facial proportions and symmetry which explain how they immortalized the beauty that time. This mathematical treatise has been developed by the Greek mathematician Pythagoras (6th century BC) who has confirmed that beauty could be explained using mathematical and proportions laws. To describe beauty, Pythagoras used the term ‘cosmos’ that explain that the beauty was part of the mathematical order of the universe, hence the origin of the word ‘cosmetic’.

According to universal nature of the facial attractiveness [8], various hypotheses have been put forward to describe the common preferences for facial beauty hence answer the question; What makes a face attractive?. These hypotheses came with the idea that a face must respect some criterions which are known by beauty canons to be judged attractive. In our thesis we focused on three canons which are most used and have been widely discussed in many research studies that proved these canons importance in assessing facial beauty.

Trying to measure the facial attractiveness quantitatively was first suggested by psychologists and artists then investigated in computer science field and more recently by orthodontists and maxillofacial surgeons who have reported the increase demand of orthodontic treatments for aesthetic reasons from 25% in 1980 to over 75% in last two years [29][36][37][38][39][27]. Indeed, some facial characteristics have proven that the attractiveness of a face is determined by the symmetry, the closeness to averageness, the golden ratio and the physical characteristics of facial features and proportions which are known by the neoclassical proportions. Several studies have claimed that these characteristics are based on women's preferences, although most of them are also relevant for men. In the following subsections, a detailed explanation of each canon is given.

3.1 Symmetry

A common characteristic of faces judged beautiful is that their harmony came from balance [40], the symmetry refers to the ability that a face can be divided into two equal halves. Evolutionary psychology has focused on the perception of facial symmetry and reported that it is a factor of attractiveness, and many studies prove that the symmetry reflects the psychological state [41] and genetic conditions, as the bilateral symmetry of facial features is a sign of genetic heterozygosity and it also reflect the ability to resist parasites and different disturbances [19][42], thus can be considered as a sign of good health. In other hand, the face asymmetry may be related to a genetic abnormality that occurs with individuals who have been exposed to environmental disturbances, or diseases [42]. Men with lower fluctuant asymmetry have the chance to meet their mates as they are the choice of women and may have more offspring and fewer diseases [43]. And for women, a lower fluctuant asymmetry can reflect a good fertility and phenotypic quality [44].

A large number of studies have addressed the link between the symmetry and the attractiveness and moreover with the physical conditions of an individual such as growth rate, fertility and survival capacity [45]. This link can be considered as a pressure that the symmetry create when it comes to choose the mate for example, an individual always choose the mate that will provide him a healthy offspring [46], thus symmetry is often seen better than asymmetry. Preference over symmetry has been advocated in a number of research studies in which authors have claimed that the power of symmetry is not only affective for humans but also for animals such as macaque monkeys. In a study about the effect of facial symmetry, macaque monkeys were found to look longer at symmetrical manipulate faces than at asymmetrical images [47].

To study the effect of symmetry, early research studies have created symmetric faces by reflecting one side of the face around the vertical midline axis in order to get two symmetric parts [48][49], the obtained faces were judged non attractive because of the displayed abnormalities on the two facial sides; one side will show a narrow abnormality and the other side a wide one. These abnormalities can be seen at the eyes region and space between them, the nose and the ears shape and the mouth size. This type of facial symmetry has no preferences because of the different abnormalities that can be caused [50]. Authors in [51] [52][53] created symmetric faces by blending normal and reversed-mirror images, the resulted faces were claimed

to be more attractive than the original images, and better than the results obtained by chimeras in the earliest studies noted above.

However, despite the correlation between attractiveness and symmetry, it still not the primary way to judge the facial beauty [54][55], as others think that symmetry has a little impact on facial attractiveness [38] or no influence at all and only the highly asymmetrical faces are unattractive [54].

3.2 Golden proportions

The golden ratio is a famous mathematical proportion, which is applied in painting, sculpture, architecture, and also observed in nature [56]. It has nearly became a synonym for a beautiful and balanced form. The golden ratio Φ is derived from the name of the Greek sculptor Phidias and is an irrational number with the order of 1.618033988. It is obtained when a segment a + b can be divided into two sections such as a + b/a = a/b [56][57].

The golden ratio has been considered as a sign of beauty and pleasing to the eye as described by the mathematician Euclid (c. 325−265 BC) who first cited this notion in his treatise "the Elements". The mathematician Leonardo of Pisa known by Leonardo Fibonacci (1170−1240) has added some confidence to the golden proportions by creating the well-known concept of the Fibonacci sequence [58]. The Fibonacci sequence consists of Fibonacci numbers that are following integer sequence such that each number after the first two is the sum of the previous two, i.e. 1, 1, 2, 3, 5, 8,13, 21, 34, 55 etc. It was discovered that this sequence is actually connected to the golden ratio because two consecutive Fibonacci numbers have a ratio very similar to the Golden Ratio which is 1.618034. Scientists have discovered that the Fibonacci numbers appears in nature such in sunflowers, hurricanes and galaxies.

Through centuries starting from the ancient Greek era till our present days, the golden ratio has been in correlation with aesthetic and beauty, and mathematicians, scientists, architects, artists, and cosmetic surgeons have advocate the effect of its key role in perceiving attractiveness especially in the human face [58][59].

Recently, some studies [60] have shown that the proportions in a face generally perceived as being beautiful are intimately related to the golden ratio, so they conclude from an experience conducted at the University of California, San Diego and the University of Toronto that there exists a correlation between the golden ratio and beauty score given by human raters; most of the faces judged beautiful are those corresponding to the golden ratio.

Stephan Marquardt [39] used the golden proportion to create a mask to analyze and assess the facial attractiveness, by determining if the face is close or far from the ideal golden proportions. If the facial features shape doesn't fit the mask specified regions for these features, then the corresponding facial zone needs to be modified.

Although all the good attention that have been devoted to the golden proportions and their association with the attractiveness, authors in [61] have claimed that the golden proportions has no correlation with the facial attractiveness as Marquardt has indicated and that the phi-mask

doesn't really represent the female face as it has a prominent and strong supraorbital ridges, high cheekbones, low eyebrows, and a square jaw which are related to male facial characteristics. These observations comes with the conclusion that the golden proportions are a good criteria to judge attractiveness but still not sufficient to analyze and measure the facial attractiveness.

3.3 Averageness

Average face defines how a face looks like the other faces of a population [46]. It is considered more attractive because it represents an alignment of different facial characteristics which makes it one of the good biologically based preference [19]. An average face is closer to our mental prototype of a face which is easier to process by the brain [62], as people can build prototypes of distinct categories of characteristics and stimuli that aid the brain to detect new instances in the usual category. Hence each stimuli that match the prototype is preferred and easily processed by the brain which explain the preference for averageness.

Biologists confirm that the average face denotes developmental stability and genetic heterozygosity that may provide mate genetic diversity in defense against parasites unlike people with non-average face who are less resistant because of their homozygosity for alleles coding for proteins that the parasites are adapted for [19][63][42] which may provide genetic mutation, chromosomal abnormality, non-genetic congenital deformation and diseases. Therefore, this explains the association between the averageness and the health state of individuals.

Indeed, recent studies have supported the existence of a link between the averageness and the facial attractiveness, as the genetic heterozygosity is positively related to facial attractiveness [63]. Furthermore, Average faces are generally more symmetric and as it is already explained; symmetry is a separate factor in facial attractiveness. It has also been claimed that by combining a large number of facial images to get an average face, the resulted facial skin texture become smoother, and the imperfections such as blemishes or lines are averaged [64]. Those indices (the skin appearance and texture) are a major effect on judging facial attractiveness. An experience on the attractiveness of the average face was conducted in [54] and [65], where authors created a composite face using a set of photographs belonging to men and women and they claims that the resulted face is more closer to the average if the number of the composite photographs for both men and women rose, also by increasing that number, the attractiveness rating of the average face increases.

The close to averageness hypothesis was also supported by the caricature studies, indeed authors in [66] used caricature which are known by their exaggerated facial features, original faces and averaged faces, and they concluded that as the averageness increased, distinctiveness decreased and attractiveness increased. On the other hand, these experiments were conducted on different ethnic groups such as in North America, Britain, Australia, Japan [69] and in African hunter–gatherers who showed their preference for average faces [67].

Even if the composite face is claimed to be attractive, some research studies proved that the most attractive face is not necessarily close to the average [68][27], which means that the closeness to average is not sufficient and not even necessary for the attractiveness of a face.

3.4 Neoclassical proportions

Moreover, despite a perfectly proportioned face, there are endless variations of color and shape of every facial feature (eyebrows, eyes, nose, lips, etc.) which leads to the distinctive aspect of each race and allow infinite variations of beauty. The facial proportions or the neoclassical canons were formulated since the renaissance times by some artists like Durer and da Vinci [69], and they still very famous and largely used in the field of plastic surgeries, art and sculpture. The popular neoclassical canons are as follow:

On the frontal side of the face, the 'ideal' face may be divided into five equal vertical segments with each 5th is equal to the width of an eye [70][71].
Horizontally, between the hair line and the chin, the face may be divided into equal thirds, the upper third extends from the hairline to the glabella, the middle third from the glabella to the subnasale, and the lower third from the subnasale to the chin tip [70][71]. These thirds are not perfectly equals in all regions, for example East Asian people tend to have the middle third equals to the lower third and larger than the upper third, in the other hand the upper third is often smaller than the lower third.

Moreover, the lower third may be subdivided also into equal thirds that determine the upper lip, the lower lip and the chin zone. The first third extends from the subnasale to the horizontal line between the upper lip and the lower lip, the second third extends from the line between the upper lip and the lower lip to the sublabial and the last third extends from the sublabial to the chin tip. Furthermore, the width to the height of the head is typically 3:4. [70][71].

The corners of the mouth should be projected in the vertical descending from the pupil when the look is neutral and forward. Finally, the height of the chin should represent 1/9 of the height of the face (1/3 lower third). Figure 1.1 shows these proportions on an example frontal face.

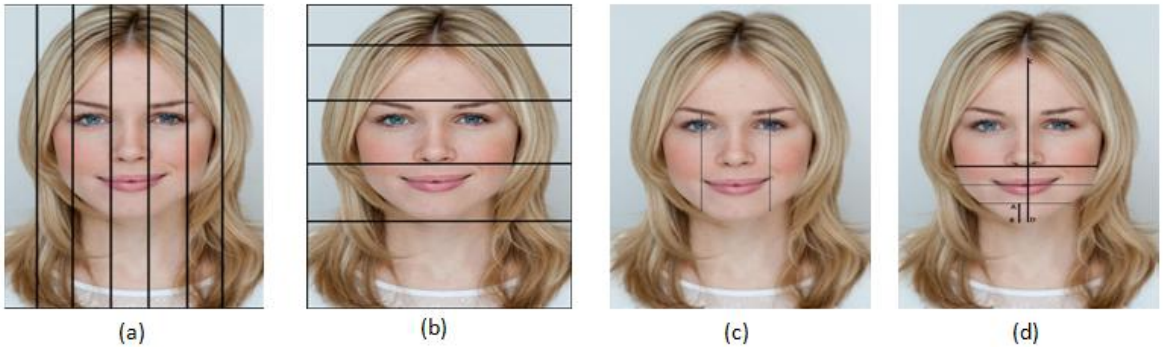

Figure 1.1: Frontal face proportions

On the profile side, a number of angles have to be verified in order to reflect the face profile proportions. In [72], author have defined four angles on the profile side of the face and they have described them as the " aesthetic triangle". It consists of first defining the vertical facial plan that extends from the glabella to the pogonion, and then the first angle is created by drawing a line from the nose tip to the nasion and from the nasion to the glabella, this angle is named the NasoFrontal angle. The second angle is created using the anterior facial plan and the line tangent to the dorsum of the nose, and this angle is named the NasoFacial angle. The third angle is created by drawing the line tangent to the dorsum of the nose and the line that connects the nose tip and the pogonion, this angle is called the NasoMental angle. The fourth angel is created using the intersection of the anterior facial plan and the line traced from the cervical point to the menton, this angle is called MentoCervical angle. These angles are explained in figure 1.2.

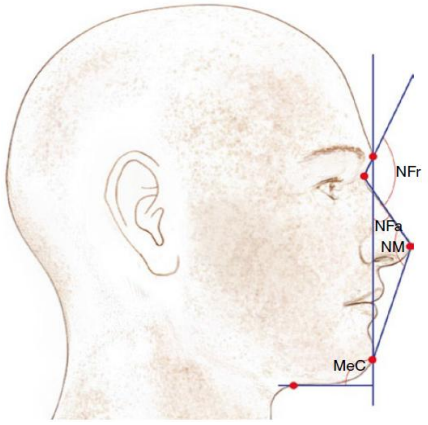

Figure 1.2: The aesthetic triangle

In the ideal female and male faces, these angles have to be within ranges as shown in table 1.1.

The angles	Mean values of the angles
NasoFrontal angle (NFr)	115° - 130°
NasoFacial angle (NFa)	30° - 40°
NasoMental angle (NM)	120° - 130°
MentoCervical angle(MeC)	80° - 95°

Table 1.1: Aesthetic triangle measurements

Authors in [73], have defined additional six angles to describe the vertical proportion of the profile side of the face. The first angle is created by the intersection of the drawn line from the nasion to the tragion and the line from the tragion to the nose tip, this angle measures the height of the nasal thus it is called the Nasal angle. The second angle is created by the intersection of the line from the nose tip to the tragion and the line from the tragion to the labiale superius, this angle measures the height of the maxillary and it is called the Maxillary angle. The third angle is formed by the intersection of the line that joining the labiale superius and the tragion, and the line from the tragion to the pogonion, this angle measures the height of the mandibular thus it is called the Mandibular angle. These three angles are presented in figure 1.3.

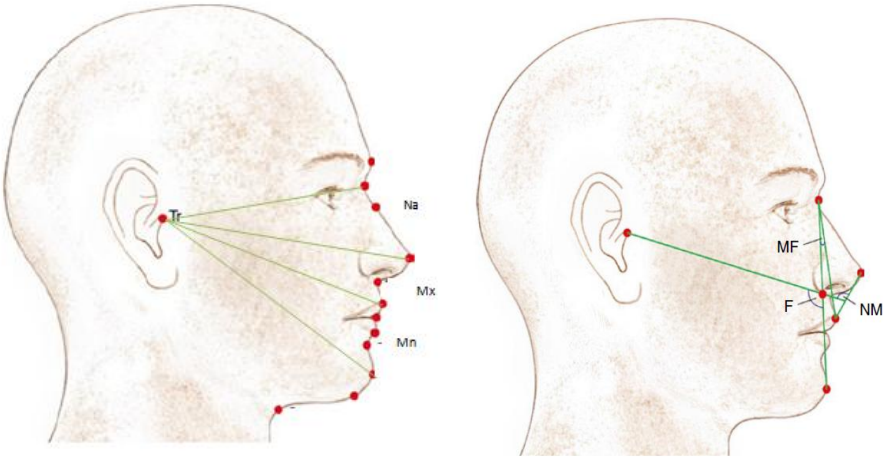

Figure 1.3: Peck and Peck angles

The fourth angle is defined by the intersection of the line from the nasion to the pogonion and the line from the nasion to the labial superius, this angle is called the maxilloFacial angle. The fifth angle is created by drawing the line that connects the nasion to the pogonion and the line that cross the tragion to form the oriental plan, this angle is called the Facial angle. The last angle is created by drawing the intersection of the line joining the labiale superius to the nose tip and the oriental plan, this angle is called the Nasal Maxillary angle. The authors have defined in their studies the mean value for each angle for Caucasians as presented in table 1.2.

The angles	Mean values of the angles
Nasal angle (Na)	23.3°
Maxillary angle (Mx)	14.1°
Mandibular angle (Mn)	17.1°
MaxilloFacial angle (MF)	5.9°
Facial angle (F)	102.5°
Nasal Maxillary angle (NM)	106.1°

Table 1.2: Peck and Peck angles

Holdaway in [74] has defined the H angle which is created by the line extended from the nasion to the pogonion and the line that connects the pogonion to the labial superius. The H angle describes the measurement of the maxillary- mandibular relationships [75], and its value is 10 degrees. This angle can be manipulated by orthodontists or chin's surgeries. Figure 1.4 presents the Holdaway's "H" angle.

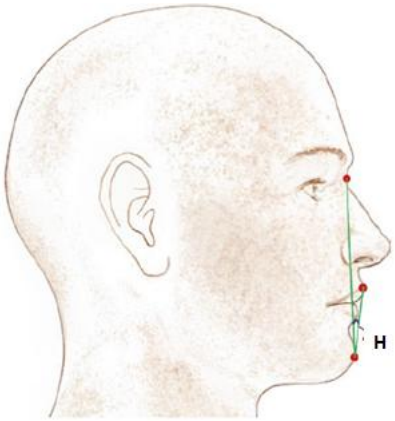

Figure 1.4: Holdaway's H angle

4 Facial aesthetic quality analysis on 2D images

The analysis of facial aesthetic quality has been an attractive area of research since ancient times by multidisciplinary fields. A number of artists, painters and scientists have proposed some canons to evaluate the attractiveness of a face, these canons are believed to be universal and people with different ethnicity, gender, and historical era have the same criterions to judge facial attractiveness. The defined beauty canons discussed in this part of our thesis are the symmetry, the golden ratio, the averageness and the facial proportions or neoclassical canons.

The analysis of facial attractiveness and then suggesting the necessary modification to improve its attractiveness can be applied for different purposes based on the area of application. For example, the study of facial attractiveness can be used for photo retouching for CVs and applying for jobs that require the face to be attractive. Furthermore, the analysis of facial attractiveness can be used as a beauty-ranking program and so many applications in diversity of fields.

In computer science society, the automatic analysis of facial beauty has first been done using 2D images of the face in order to develop and modeling real life application systems, as the use of 3D scans was too expensive because of the lack of 3D scanners and 3D models providers. A typical facial attractiveness analysis system is composed of some specific steps; the first step is to detect the face area in a 2D image in order to specify the work zone; the result is always the skin zone of the face. The second step is to localize the facial features on the detected skin zone, and the last step before the analysis is to localize the facial landmarks, this step is the most important in the process of the facial attractiveness analysis as the analysis results depend on the efficiency of the localization task.

The next steps after the detection of the 2D facial landmarks is to analyze the face attractiveness by verifying wither the face respects the beauty canons or not.

4.1 2D face detection methods in an image

2D face detection in an image consists on determining first of all if the face exists on the analyzed image and then detecting its position and extracting it from the background. This task

has attracted the attention of many researchers for decades who have claimed that the step of face detection in an image is very important and a key step for further image analysis.
There exists different constraints which may influence the result of the face detection; these constraints can be kind of some accessories such as the glasses, the beard and the mustache for male, the pose of the face in the image, some backgrounds, illumination conditions, orientation and camera distance.
Since 2001, and after the huge contribution of Viola and Jones algorithm, a significant progress has been made in face detection area to improve the results of the detection and to be able to localize faces "in the wild". Furthermore, recent face detection algorithms have made use of the other new factors such as the availability of databases and benchmarks for face and objects detection; LFW and FDDB. Moreover, the development of repositories of publicly available code such as the OpenCV series of releases [76] in addition to the recent huge efforts to make a repository of Convolutional Neural Network architectures [77] with a high quality. Finally the large availability of features extraction methods such as the Histograms of oriented Gradients (HoGs), Scale Invariant Feature Transform (SIFT) features, and Local Binary Patterns (LBPs) and their variations have made the 2D face detection easier than before.
To detect the face in an image, a large number of studies has been conducted trying to overcome the different problems that can occur during that process, these studies proposed many approaches; authors in [78] surveyed this topic and suggest that these approaches can be classified into two types; features based approaches and image based approaches. Each type can be divided as well into three approaches or models for more specification of the process used to detect the face. The first type of approaches (Features based approaches) is divided into: low level analysis, feature analysis and active shape models, while the second type (Image based approaches) is divided into: linear subspace models, neural networks and statistical approaches. Another survey was conducted by authors in [79], in this report authors have grouped the existing methods for extracting a face from a 2D image into four categories; feature invariant approaches, knowledge-based methods, appearance-based methods, and template matching methods. More recently a survey has been presented in [80] in which authors have claimed that the seminal work by Viola and Jones has made face detection practically achievable task in the real world and helped to make a significant progress in that field, furthermore, authors proposed to categorize the methods used to detect the 2D face into two main families of algorithms; the first family of algorithms is based on rigid-templates and includes mainly:

– Variations of boosting: Viola–Jones face detection algorithm and its variations.
– Algorithms based on Convolutional Neural Networks (CNNs) and Deep CNNs (DCNNs).

The second family of algorithms learns and applies a Deformable Parts based Model (DPM) to model a potential deformation between facial parts.

4.1.1 Face detection algorithms based rigid templates

This first family of algorithm includes two main axes of research; the first one is based on learning rigid templates using boosted cascades of classifiers and the second one is based on Deep Convolutional Neural networks.

a. Algorithms based variations of boosting

About the methods based learning rigid templates and more specifically based variations of boosting; the Viola Jones algorithm has shown to be the most effective detector on frontal images of faces, in addition, it can cope with 45° face rotation both around the vertical and horizontal axis. The three key concepts that allow it to work in real time are the integral image, AdaBoost and the cascade structure.

The Integral Image is an algorithm for cost-effective generation of the sum of pixel intensities in a defined rectangle in a given image. It is used to make the computation of Haar-like features fast. The popular boosting technique AdaBoost algorithm is used for construction of strong classifiers as linear combination of weak classifiers and then the Cascade of AdaBoost works as a classification model by which they discarded the background from an image, Finally, the Viola and Jones is a powerful method to avoid the detection of regions which does not contain the object of interest.

Using Viola Jones algorithm, Face detection is achieved by bounding the area of interest using a rectangle based on Haar-like features and cascade of classifiers learnt to detect a face zone on an image.

The figure 1.5 below presents the rectangles using in the detection by the extended Haar-like features:

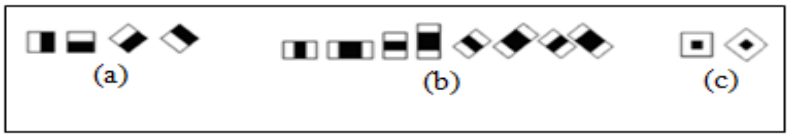

Figure 1.5: Extended Haar-like features: (a) edge features, (b) line features, (c) center surround features

These features are used to calculate the difference between the sum of the white pixels areas and the sum of the black pixels areas.

$$d = \sum (white\text{-}pixels) - \sum (black\text{-}pixels) \qquad (1)$$

To outline the face zone, a window of initial size of 24×24 (increased iteratively) scans the input image in every direction to locate the face zone. This operation generates many features, which make the use of integral image required for the speed of detection. Then, a cascade of adaboost-based classifiers is used to classify the face or non-face area according to the value of its descriptor obtained from the training using images of face and non-face.

A cascade classifier consists of several simple classifiers which are applied one after the other on a region of interest in an image, while Boosting means to combine the results obtained by several "weak" classifiers to build one more efficient.

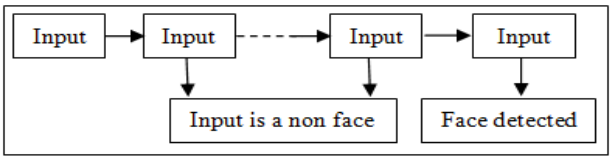

Figure 1.6: The cascade classifier

The integral image at the pixel (x,y) of an input image is calculated by summing the pixels above and left of the current pixel (x,y):

$$ii(x,y) = \sum_{x' \le x,\ y' \le y} (x', y') \qquad (2)$$

After this step, the algorithm of face detection returns the face region localized (Figure 1.7), which will be considered as inputs of the algorithm of facial features detection.

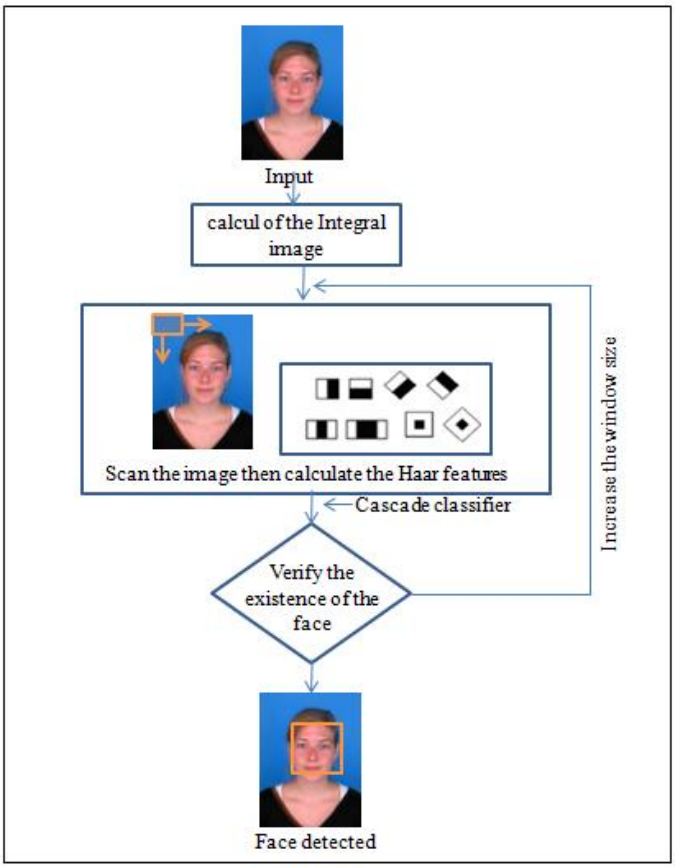

Figure 1.7: Example of face detection process from [15]

To improve the performance and the accuracy of the face detection, a large number of features in addition to Haar-like feature were proposed. These features include: Pixel-based features which includes Pixel pairs and Control point set, Binarized features that includes Modified census transform, LBP features and Locally assembled binary feature, Generic linear features including Anisotropic Gaussian filters, LNMF and Generic linear features with KL boosting RNDA, Statistics-based features which include Edge orientation histograms, Spectral histogram, Spatial histogram (LBP-based), HoG and LBP, Region covariance and SURF , Composite features and Shape features that includes LGB, BHOG, Integral Channel Features on HoG and LUV (Headhunter), HSV, HoG, LUV, RGB, Grayscale, Boundary/contour fragments, Gradient Magnitude, Edgelet and Shapelet.

In the work presented by Viola and Jones, AdaBoost was the boosting learning algorithm used, to improve the performance of the detection; following works have proposed other boosting algorithms such as the FloatBoost, GentleBoost and the RealBoost that were claimed to surpass the AdaBoost algorithm concerning the weak classifiers learning challenge.

The RealBoost is actually the new version of the Viola Jones algorithm in which the authors tried to outperform the oldest version by using real-valued week classifiers into the AdaBoost. RealBoost algorithm computes real-valued weak classifiers given real numbered feature values and then generates a linear combination of these weak classifiers that minimizes the training error. It is also known to consider the confidence of a weak classifier in a particular decision given a particular response.

The Floatboost algorithm aims to deal with the monotonicity of the AdaBoost learning following the floating search into the AdaBoost which not only attempts to add more features during the training but backtrack the existing features in order to remove those that can drops the performance of the detection. Authors claimed that the FloatBoost algorithm is a strong classifier that can use a fewer week classifiers to get the same results obtained using the AdaBoost.

The GentleBoost algorithm is a modified version of the RealBoost; it is used to select a set of features to get a given detection and error rate. In general, authors claimed that it is better to use it in combination with the Classification and Regress Tree (CARTs) week classifiers to enhance the detection results. GentleBoost algorithm can enhance the performance of the classifier and reduce computation by 10 to 50 times compared to Real AdaBoost.

b. Algorithms based on Convolution Neural Networks and Deep CNNs

During the past decade, improvements have been applied to the Viola Jones algorithm for face detection in order to enhance the accuracy of the detection and to reduce the error that can be occurred during the process as well. These improvements have been applied to the cascades boosted framework by using more efficient features which can reject false detections quickly during early stages in the process of the detection.

Deep learning Neural Networks have shown to be a good method to detect faces in the literature even before the introduction of the Viola Jones algorithm. In fact, deep learning aims to simulate the organization of the human brain's nerve and the structure of its work. One of the most popular methods of deep learning is the Convolutional Neural Network (CNN) [81] composed of two basic layers called Convolutional layers (C layers) and subsampling layers (S layers) respectively (figure 1.8). CNN has gained a great attention in the past years and has shown a good performance in face detection in uncontrolled environments as described in numerous papers presented in the recent past years; in [82] authors have concluded that the CNN can automatically get the feature extractors from the training examples, without making any assumptions about the features or the face to extract. Other work [83] has proposed a new structure of the CNN which is a jointly trained cascaded CNNs that combines the performances and the speed of the CNN on one hand and the efficiency of the proposed back propagation algorithm on the other hand, in order to obtain better face detection results.

Region based Convolutional neural networks (R-CNNs)[84] is considered to be one of the CNNs based methods for objects detection which aims to produce an independent region proposals, then for each region the CNN features have to be extracted in order to be able to classify the category of the given proposal. Furthermore, Convolutional neural networks based method, AlexNet and GoogLeNet have shown improved images classification results comparing to other competing work in the literature thus they have been deployed in commercial applications.

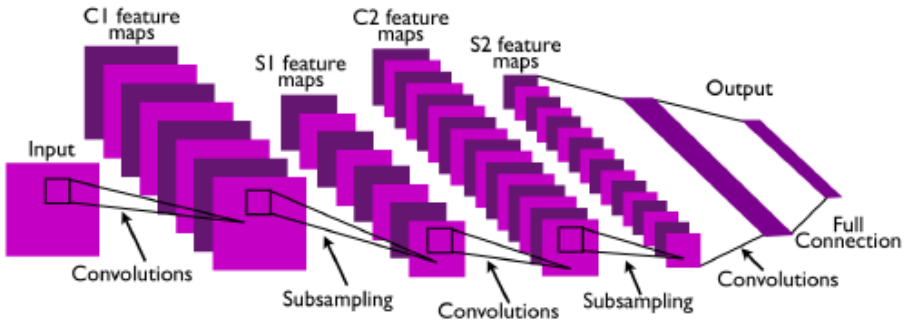

Figure 1.8: Example of Convolutional neural networks architecture with two feature stages from [85]

More recently, the Deep Convolutional Neural Network (DCNN) was considered a breakthrough of CNN as it has achieved outstanding performance. Therefore , DCNN has dominated the majority of the computer vision tasks such as face recognition [86], image classification and detection [87][84]. Unlike the previous neural networks so called traditional networks, the DCNN can use a large number of Convolution or fully connected layers that were before impossible to train using a shallow network. The progress of the performance in object classification and detection can be explained by: (a) the availability of large databases and a labeled data such as ImageNet [88], (b) the evolution of the GPUs which allow fast parallel computation, and (c) using new tricks and regularization techniques to prevent overfitting [80].

About the techniques used by the DCNN, ReLU and dropout [87] were used to train a multi-task DCNN for multiview face detection, and authors in [89] have claimed that a significant improvement has been achieved in face detection using the publicly available FDDB data set [90]. In another work [91], authors have proposed a new method to localize faces with different orientation on an image based on a deep learning approach called deep dense face detector (DDFD), the proposed method requires minimal complexity and is dependant of the recent deep learning common modules. In addition, DDFD is based sliding window approach and which showed to be more accurate comparing to the region based Convolutional neural network (R-CNN) for face detection.

4.1.2 Deformable parts-model for face detection

Face detection using deformable parts model (DPM) [92] structure has been used in a large number of research papers during the last years and has shown state of the art face detection results. This structure consists of representing the face as a set of parts where each part captures specific local proprieties on the face, and these parts are connected using spring-like connections that have to be trained during the deformable configuration.

DPM typically operate with the histogram of orientation gradients feature maps (HOG). In fact, they are actually considered to be an update for the pictorial structure models with new image features and more developed machine learning algorithms in order to achieve more accurate face detection results. In general, for a given image, in order to detect faces- if they exist- , DPM aims to first find the necessary parts on the face , and then the connections between them using the SVM algorithm in most of time.

To simplify the DPM model, actually it can be represented by a graph G (ν, ε), where ν (ν_1, ν_2 … ν_n) represents the vertices corresponding to the parts of the face while ε represents the edges that connect these vertices if only there is a connection between two parts of the face. Figure1.9 represents an example of the facial parts represented by the areas that englobe the facial landmarks. The parts as well as their connections can be learned automatically during training processes where each parts localization can be transformed to a new one by a linear transformation such as the SVM.

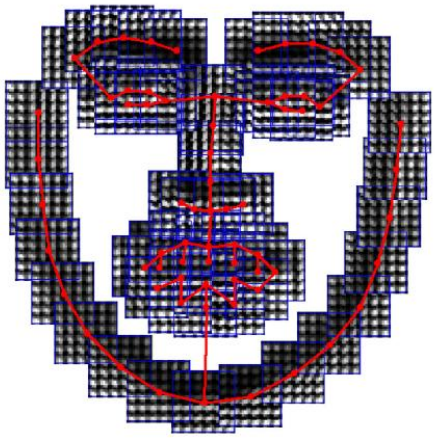

Figure 1.9: Example of structural models from [80]

To localize the face in an image using the DPM, the famous approach of sliding window is used to brows the given image and determines whether the window corresponds to a face or not. This process is achieved by finding a configuration with high matching score of the structural model on all the possible configuration of the sliding window.

Face detection based DPM structure using the HOG decreases when using faces with different illumination conditions and poses due to the features used in that process. To remedy these limitations, authors in [93] have replaced the standard image features used in DPM based HOG with a learned feature extractor (by a CNN), the final model is called DeepPyramid DPMs which shows a significant performances compared to the DPMs based histograms of oriented gradients features as well as the R-CNN. Another drawback of the DPMs structure is the high computational complexity and to solve that issue, efforts have been devoted in a number of papers to accelerate the DPM by using a Fourier Transform such as in [94], building cascade classifiers from the DPM [95] and using a Branch-and-Bound framework and a boosting classifiers [96].

4.2 2D facial landmarks detection

The detection of 2D facial features is an important initial step in various facial image interpretation works related to computer vision application, such as: face identification, facial expression recognition, facial features tracking, facial beauty analysis…. Moreover, in addition to facial features localization, the detection of facial landmarks is considered the key step for more analysis accuracy.

Facial landmarks detection has been a challenging task during the past decades; hence it has received a great attention and so many approaches have been proposed in the literature to localize the facial landmarks precisely. The existing methods can be divided into four types; the first type is the active appearance models based methods [97]; these methods use a combined statistical model of shape and texture in order to localize the facial landmarks. AAM were largely used in literature and they have shown an important detection results. The second type is the constrained local model based methods, this second type is known to be similar to the active appearance models (AAM), but with some strong properties regarding the presence of occlusions, facial expressions...even though, there is still some weakness and issues on these methods that prevent them from reaching the state of the art performances on some face datasets. The third and last type is the regression based methods which consist generally to predict the facial landmarks from the facial appearance using in the most of time a cascade regression approach.

In the following subsections, we present the aforementioned methods to localize the landmarks on 2D faces; the first subsection (1.4.2.1) presents the active appearance models based methods (AAM) for facial landmarks detection. The second subsection (1.4.2.2) describes the constrained local model based methods (CLM) for facial landmarks and the last subsection (1.4.2.3) presents the regression-based methods for facial landmarks localization.

4.2.1 Active Appearance Models based methods

The active appearance models (AAM) [97] is a generic face alignment approach and a joint statistical model of shape and appearance (figure 1.10), they are very famous and largely used for images segmentation and landmarks localization especially in the medical field where the shape information is required for various application [98].

AAM consists of modeling how instances of both shape and appearance of a well-determined object class – such as faces- are generated; furthermore, AAM can model the global appearance of the object using typically the PCA to both shape and texture. In general, AAM is an iterative fitting process to images aiming to update the model's parameters at each iteration by minimizing the error function between the model instance and the given image.

Figure 1.10: AAM: first row: learned shape variations using AAM model. Second row: learned appearance variations using AAM from [97]

In order to localize cephalometric landmarks automatically on the face, authors in [99] used the AAM method combined with mathematical morphology. To train the model, authors used 96 image manually labeled and after the test using images of clinical cases they achieved good

detection results with an average precision of 2.48 mm. Despite the good results, the average accuracy still high. This may be due to the images quality. In similar work [100], Authors proposed to use the AAM to localize the facial landmarks on cephalograms. The AAM was first built and trained using training set of 131 facial landmarks manually annotated and then the statistical model was generated using the PCA algorithm. For a given cephalogram, an initial template of the AAM is used over the image then the process of minimizing the cost function between the given image and the appearance model is applied.
The obtained results showed successful cephalometric landmarks detection, yet some wrong detection that are due to extreme shape variation.

Despite the accuracy and the performances of the AAM, the fitting process stills a difficult problem especially when working with unseen variations of illumination and expressions of images and this is due to the appearance model limitations. However, authors in [101] have proposed to pursue the AAM approach and to develop it to be able to overcome the mentioned limitations. For that purpose, they suggest the new active orientation model (AOM) that combines the power of the statistically robust appearance model and the principal components of images gradient orientations. The proposed AOM uses the same motion model and shape used in the AAMs but with a different appearance model and robust cost function to fit that model. Experiment results show that the AOM outperforms the AAM and some other state of the art methods for facial landmarks detection.

4.2.2 Constrained Local Model based methods

Constrained Local Models (CLM) [102] (figure 1.11) is a developed version of the AAM approach aiming to model a set of local feature templates instead of modeling the whole face as well as to avoid the previous limitations of the AAM. CLM is composed of three main parts; the first part is the point distribution model (PDM) which models the facial landmarks localization using a specific parameters. The second part is the patch experts that model the appearance of each local patch around the facial landmarks and the final part is the used fitting approach to estimates the best parameters of the model.
Generally, CLM consists of finding the best parameters for a face model in order to match the appearance of a given image. The CLM has some strong proprieties comparing to the AAM, for example, unlike the AAM, the CLM is generative to unseen faces variations. Additionally, the model can detect the facial landmarks in presence of illumination variations and occlusions.

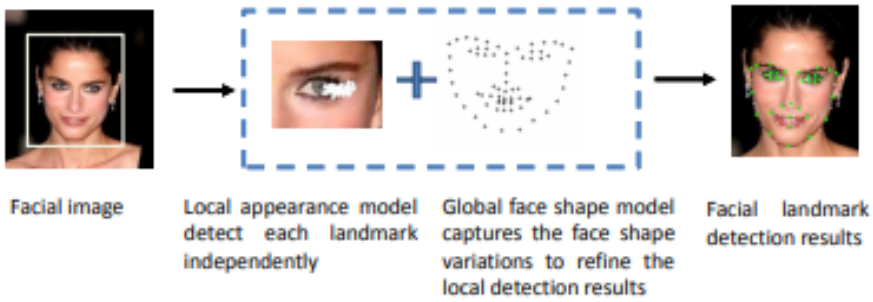

Figure 1.11: Constrained Local Model

CLM methods still suffer from some weakness especially when the detection is in complex scenes. For this reason various extensions of CLM have been proposed recently in the literature to overcome these problems; in [103] authors proposed a new extension of the CLM which is the constrained local neural field (CLNF) for facial landmarks detection. The proposed method has shown significant performances of detection comparing to the state of the art methods at that time. CLNF has introduced two novel techniques; a LNF patch expert and a Non-uniform Regularized Landmark Mean-Shift optimization technique that takes into account the reliabilities of each used patch expert. Another variant of the CLM is presented in [104] where the authors introduced a Discriminative Response Map Fitting (DRMF) method for facial landmarks localization. This approach uses well developed methodologies to compute the local response maps and then concluding the landmark locations. The DRMF for the CLM method shows an efficient detection results comparing to the state of the art methods at that time. In [105] authors present an automatic framework for Down syndrome detection and other genetic syndromes associated with facial dysmorphosis. The introduced technique is based on locating the anatomical facial landmarks using a hierarchical constrained local model based on independent component analysis (ICA) which shows to a powerful approach to create a statistical shape model. The obtained results of landmarks detection show that the HCLM based ICA outperform the traditional CLM and proved to be more accurate. Other extensions of the CLM were described in [106][107].

4.2.3 Regression based methods

Regression based methods for facial landmarks detection learn the mapping and predict the landmarks directly from the face image appearance. In general, the regression based methods can be used in three different way; direct regression methods, cascade regression methods and deep learning based regression methods.

The direct regression methods are characterized by the fact that they don't require any initial guess about the positions of the facial landmarks, thus they only learn the mapping directly from the appearance to the facial landmarks. Several works have been proposed in the literature to localize the facial landmarks using direct regression methods; in [108] authors presented a conditional regression forests method for facial features detection and landmarks positions estimation. The proposed method consists of modeling the facial landmarks conditional to the head position and the results have shown a significant performances using in the wild datasets. In [109], a Tasks-Constrained Deep Convolutional Network (TCDCN) is introduced to localize the facial landmarks accurately, as well as a set of multiple related tasks such as the head pose, the facial expressions and the appearance attributes using a deep learning approach similar to the CNN. Obtained results proved that the proposed method is robust to face occlusions and expressions comparing to the competing methods.

The cascaded regression methods (Figure 1.12) require having an initial estimation of the facial landmarks locations, then during the training process; these locations are updates iteratively using a regression functions learnt before in order to fit the given face. Several works have introduced the cascaded regression methods using different regression functions to localize the facial landmarks such as in [110] where authors have introduced two new components which are the locality principal and the local binary features. The proposed method aims to learn a set of

discriminating local binary properties for each facial landmark separately using the regression forests and then the local binary features obtained from all the landmarks are used to learn jointly the mapping model from the appearance to the global output. Other variations of cascaded regression methods is presented in [111][112][113].

Figure 1.12: Cascaded regression method from [114]**.**

Despite the significant performances of the cascaded regression based methods for facial landmarks localization compared to the direct regression methods, there still some problems concerning the initialization step of the landmarks locations.

As mentioned in the previous section, the deep learning based methods is the tendency in the computer vision problems as they have shown a significant performance in several tasks. To localize the facial landmarks, the deep learning based methods were used and they can be classified as a regression based methods. Nowadays, the CNN has become the leader models for facial landmarks localization, and a large number of papers have proved the outstanding detection results comparing to other proposed methods in the literature. In [109] and [115], authors used the CNN combined with a multi-task learning to localize the facial landmarks as well as a set of associated features. In [116], a new direction using a deeper model is introduced by extending the multi-task learning approach to predict jointly associated task such as age, gender, head pose…etc. Other improved cascaded based CNN methods have been suggested the deep auto-encoder model [117] and the deep Convolutional Recurrent Neural Network (RNN) [118].

4.3 2D facial aesthetic quality analysis

The obsession with beauty has always been a world wild and cross cultural phenomenon. Furthermore, facial attractiveness analysis has been discussed in a large number of research studies from various disciplines such as facial cosmetic, plastic, and reconstructive surgery, social, developmental, cognitive, and evolutionary psychology for many decades. In some studies about the assessment of facial attractiveness, some authors tend to use a group of human raters in order to vote for the face that looks more attractive for them based on the candidate face appearance, and then to estimate the different facial traits that affect the attractiveness; age, gender, smile… [119]. In [51] authors have used a group of human raters to assess the attractiveness of a face based on its symmetry, actually an original face, authors created left and right symmetric faces and then ask the raters to vote for the more attractive face. A similar work has been proposed by [65], and has proved by rating that the face symmetry and averageness have a positive influence on the facial attractiveness. In [120] 42 female volunteers have been asked to rate the attractiveness of male faces, showing that the results of the male attractiveness

depend on the hormonal state of the raters. In another paper [25], authors have investigated a machine learning techniques (K-NN, SVM and linear regression) to train a facial attractiveness predictor based on a set of face images and their average human ratings. The obtained results from the predictor showed a correlation with the human ratings. Similar work has been presented in [121][122][50][123][51][124].

As we can conclude from the huge amount of these works, they basically measure the correlations among the ratings given to the faces by human raters, or analyze the covariations of the face attractiveness with some facial traits like symmetry, averageness and some secondary sexual traits. These works however have some limitations that decrease the efficiency of the attractiveness analysis; these limitations include the use of a manual landmarking of faces and the human ratings of beauty which severely affects the results of the analysis.

To analyze the aesthetic quality of a face computationally, a large number of research studies have investigated some computer techniques as well as machine learning techniques. For this end, the localization of the cephalometric soft tissue landmarks is considered a critical and a key step, and as long as the landmarks detection is relevant, the results of the attractiveness analysis will be so. After the localization of the facial landmarks, the analysis of facial attractiveness can processed by verifying- for each given face- wether the canons of beauty are respected. Not all of the introduced works in the literature to analyze the aesthetic quality of the face used all the aforementioned beauty canons at the same time (symmetry, golden ration, neoclassical proportions…), for example in [125] a facial attractiveness has been analyzed using a regression analysis to perform a set of beauty canons: the neoclassic canons, the symmetry and the golden ratio. 29 facial landmarks have been detected and then authors have proceeded to analyze the role of each of the beauty canons in facial attractiveness. The obtained results were thereafter compared to a ground truth which is a group of human raters, and have concluded that the beauty canons have a significant impact on the beauty scores. In [126], after the localization of a set of facial landmarks, authors introduced an automated system capable of reproducing the average human judgments on facial attractiveness, results show that the scores respect the facial proportions. Another typical example is the Marquardt beauty analysis (http://www. beautyanalysis.com), which consists of a face mask for facial attractiveness. This mask is constructed based on the golden ratio and the facial beauty score is then defined by the matching degree between the given face and the mask.

5 3D Facial aesthetic quality analysis

The human face is an area of active research in numerous domains such as: virtual reality, computer vision, forensics, anthropology, psychology, medical genetics, etc... As the face is a great source of information and it also contains many zones each has its own geometry, the first step of the face studies is the detection of the facial landmarks, as it is the key step for any further analysis. Over the past decade, the human face has been investigated and analyzed using only the 2D image of a face- as explained in the previous chapter,- because the adoption of alternative representations such as 3D models was quite expensive given the limited availability of 3D scans that provide 3D face models. The results obtained using 2D face images were very satisfied but limited by the variations of the illumination and the pose. Lately, due to the growing

availability of 3D scans, getting a wide number of 3D face models has become an uncomplicated task in a short time, which helps to overcome the 2D images limitations.

5.1 3D face normalization

The 3D facial mesh pose and orientation normalization is an important step in 3D images processing, this step consists on recovering the canonical view of 3D faces under arbitrary conditions of pose and orientation. Essentially, it is crucial to improve the performances of the results of the post normalization processing steps such as 3D face recognition, 3D facial landmarks detection, 3D facial expressions detection...etc.

The 3D facial normalization process has to keep the 3D original face proprieties, and must be automatic and database independent. This is a challenge to many suggested method in literatures that aims to preprocess and normalize the faces before any further analysis, as the pose and the orientation of face can drop the performance of the analysis.

Many research studies have performed the 3D face normalization, for example in [127] authors did the facial pose normalization using their novel method which is matching meshSIFT features between the faces that need to be face pose normalized, this method is based on the SIFT algorithm for 3D face features detection. To eliminate some pose normalization error which can be due to false matches, a RANdom Sample Consensus (RANSAC) algorithm [128] is performed in order to get the rigid transformation matrix. To validate the results of the pose normalization, the available 3D landmarks in the Bosphorus database are used after the pose normalization of the face meshes. Authors calculate the distances between the same landmarks for all the faces, and the pose normalization is considered correct if the mean distance is less than 20mm.

In another work [129], authors have proposed a new method to align the pose of 3D faces. To do so, the symmetry between the left and the right sides of the face is used to align the yaw and the roll angles by determining the most central position of the face. The pitch angle was aligned by minimizing the difference between the chin height and the height of the forehead (equation 3). If the face is not symmetric, the 3D face can be aligned by finding the angular rotations of yaw and roll that minimize the difference between the left and the right side of the face.

$$Diff = \sum_{y=0}^{height} \sum_{x=0}^{width/2} \left| Image_{x,y} - Image_{width-x-1,y} \right| \quad (3)$$

In [130] authors have presented a new method for face pose and expression normalization using a 3D morphable model in order to preserve the face identity information. This method aims to estimate the depth information of the 3D mesh as well as its background and then a 3D transformation can be applied to normalize the pose and the face expressions. The depth information is estimated as shown in figure 1.13.

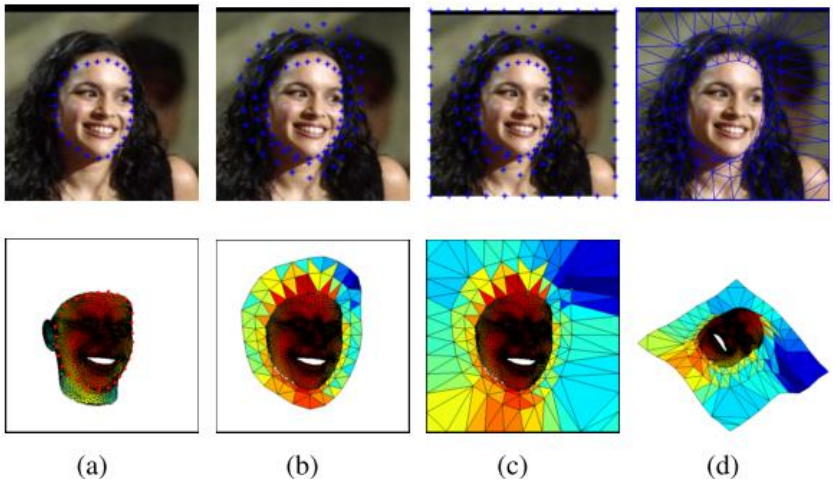

Figure 1.13: 2D and 3D view of 3D-meshing. (a) The boundary anchors. (b) The surrounding anchors. (c) The background anchors. (d) Triangulation and better view of depth information. From [130]

The depth of anchors is estimated from three groups, one is the boundary anchors which are located on the face contour and adjusted by landmark marching the second group is the surrounding anchors which enclose a larger region containing head back, ear and neck. The last group is the background anchors located on the image boundary.

After the detection of the anchors, the Delaunay algorithm is applied to triangulate anchors to get the 3D meshed face. The pose normalization can then be performed using the inverse rotation matrix R^{-1} as shown in Equation 4:

$$S_{img\_rn} = R^{-1} S_{img} \qquad (4)$$

Where S_{img} is the meshed face object containing 3D face model and anchors. R is the estimated rotation matrix in 3DMM fitting and S_{imgrn} is the rigidly normalized mesh, see Figure 1.14. After this step, filling and adjust the artifacts caused by the pose and expression normalization is required.

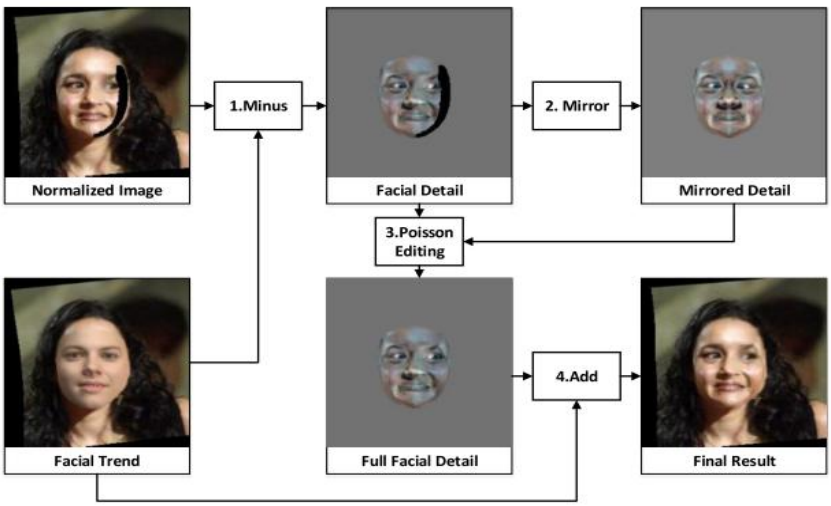

Figure 1.14: adjusting and filling the result of the 3D meshing and normalization from [130]

Authors in [131] presented a novel method for 3D face detection and pose normalization. After the detection of the face and estimating its pose and orientation, the authors performed a rasterization of the 3D mesh that aims to convert the 3D surface to a pixel representation thus synthesis a frontal view of the face. This is done using a hardware based OpenGL rasterization. Figure 1.15 shows the frontal mesh rasterization.

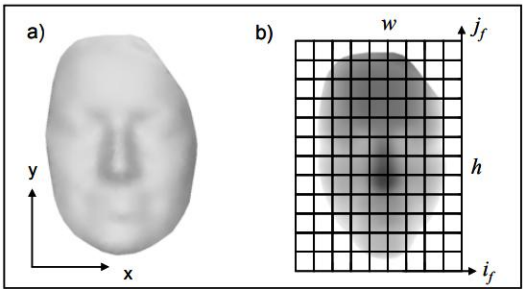

Figure 1.15: frontal mesh rasterization. A) 3D mesh model, b) Depth raster matrix. From [131]

The normalized face is then based on the depth raster matrix and they both have the same size. Figure 1.16 shows an example of the 3D mesh normalization.

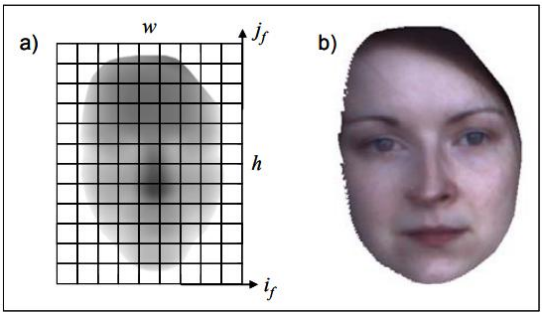

Figure 1.16: mesh normalization. A) Frontal depth raster, b) Corresponding normalized face. From [131]

In another work [132], in order to perform a 3D face recognition, authors have proceed by first detecting 3D face zone, crop it and denoising it, then they have corrected the face pose using the Hotelling transform [132]. This algorithm has proved to be facial expression invariant as well as hair tolerant. Figure 1.17 presents some of the obtained results of the pose correction.

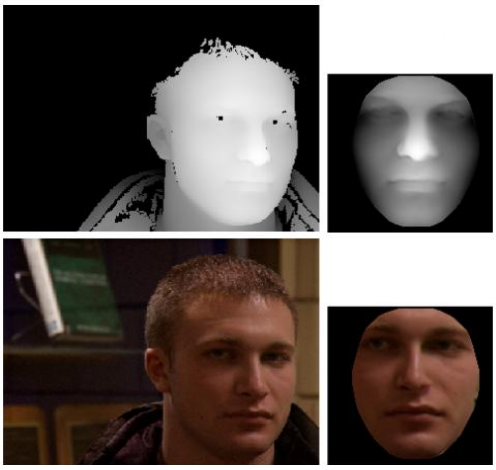

Figure 1.17: 3D face and its corresponding 2D image before and after the pose normalization. From [132]

In [133], authors present a new method for face normalization using the advantages of both 2D and 3D methods for face normalization. Indeed this approach is based on using the projected 3D landmarks to 2D image forming a dense grid. This grid is then used to establish a dense correspondence of faces across pose. Next, authors have estimated the transformation of the local patches around each landmark across pose using homography based on landmarks in the patch. With the estimated transformation, the non-linear texture warping across pose is corrected.

The last work we cite here is [134], in their paper authors presented a novel method to improve the accuracy of the face recognition system in the presence of variations in facial pose. This method is performed via 3D pose normalization.
To achieve the face normalization, the proposed method is based on automatically fitting the 3D face model to a 2D representation using the pose estimation based on the SVR and the VAAM (View based active appearance model) fitting. Finally, the image is projected back to the 3D face model to create a textured 3D face model. The methodology followed is shown in figure 1.18.

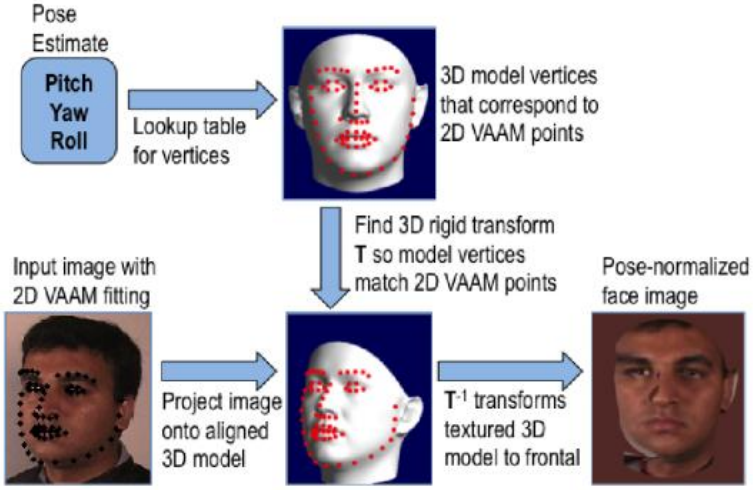

Figure 1.18: The followed methodology for facial pose normalization. From [134]

5.2 Literature review on 3D facial landmarks detection methods

3D face landmarks detection is an important step for 3D face analysis, that can be used for various objective such as the maxillofacial field, plastic, corrective surgery, and aesthetic area[135], which is considered as one of the largest applications where automatic landmarking is used, to avoid the significant amount of the manual detection of landmark process, as well as the errors committed in the landmarking labor.

To localize the 3D facial landmarks, various methodologies have been developed in the literature and a notable progress has been made in the recent decades. Early works have generally focused generally on simple 3D faces with neutral and frontal or near frontal position, whereas more advanced ones have addressed the detection of the 3D facial landmarks for various face positions and expressions. In [136][137] authors have used two methods' fusion scheme to localize the 3D facial landmarks. A different approach was presented in [138], where the nose tip and corners, and the eyes inners corners were localized using the x and the y-axes projections of the

curvature images. In [139] seven 3D facial landmarks have been localized by using Gabor wavelets to recover the faces curvature used afterwards in a coarse detection. In [140][141] authors have calculated 3D geometric information of the given face, thereafter, filtered out and labeled by matching them with the facial landmarks model (FLM), generated during the training part. In brief, a great number of approaches were proposed in the literature to automatically detect the 3D facial landmarks, yet testing these approaches has not been performed on large benchmarks of 3D face datasets [142] and most of them still encounter some problems related to the face pose and expressions variations as well [143][144]. A recent work [145] has demonstrated the strength of using the geometry characteristics information of the 3D face to localize a set of 8 facial landmarks. More lately, the Deep learning techniques have become more popular and have dominated the major part of the computer vision applications including 3D facial landmarking. In fact, in the majority of papers, this approach is often based on the projection the 3D face in 2D intensity images to localize the landmarks using the Convolutional Neural Networks (CNN) and then mapping back the obtained results into the 3D form [146]. In [147], authors applied the CNN directly on a 3D morphable model with pose variation omitting the step of 2D landmarks detection.
In the literature, the proposed methods for detecting the 3D facial landmarks can be classified into two main categories [140]: methods based trained statistical feature models, and methods based geometric information, and these two categories can either be used to detect the 3D facial landmarks on a neutral frontal faces or on 3D faces with pose and expression variations

Methods base trained statistical feature models aim at using a trained model that learns both the variations between landmarks locations and the local variations of geometry and texture surrounding each landmark. Thereafter, to localize the 3D facial landmarks on an input 3D face, the trained model is then used to determine the transformation to be performed between the landmarks on the template model and the input 3D face. In [148] authors used a detector formed by genetic to detect certain facial feature corners over a range images, in another work [149] a point distribution model is employed to localize 3D face landmarks, and further other examples in [150][151][152]. The geometric information based methods for 3D face landmarks detection have attracted a considerable attention as indicated by many research studies, which will be explained in the reminder of this section.

Despite the high number of articles suggesting approaches to detect 3D face landmarks, there is a lack of literature surveys that provide a synthesis of the existing methods used to localize 3D facial landmarks, and clearly explain each work's limitations and strengths. Therefore, the following subsection (5.2.1) provides a detailed review of recent literature studies (2010- 2018) associated to 3D facial landmarks detection methods based on the geometric information, as well as the performances of each study, and the second subsection (5.2.2) describes the recent suggested works (2010-2018) to localize the 3D facial landmarks using methods based on trained statistical feature models.

5.2.1 Approaches based geometric information

The growing accessibility to 3D scans, digitizing, and modeling tools led to more widespread the use of 3D face models. Over the past eight years (2010-2018), a great range of publications have highlighted the application of geometric information based methods to localize the 3D facial landmarks. Of these papers, authors have suggested approaches that may only be successful with 3D neutral and frontal or near frontal faces and others have introduced sophisticated approaches that can address different face pose and expression variations. The reviewed approaches for the last eight years are presented in the following subsections.

a. 3D facial landmarks detection for neutral and frontal or near frontal faces

Over the past eight years, various methods have been proposed to localize the 3D facial landmarks using with only faces with neutral expression and frontal or near frontal pose.

Gupta et al. in [153], introduced a novel method to automatically detect 10 anthropometric facial landmarks associated to the discriminatory anthropometric features. The published method operates with neutral and frontal 3D faces. To localize the nose tip, right and left alares, authors adopted a variety of shape descriptors; mean surface curvature, Gaussian surface curvature [154], and two principal curvatures. Subsequently, to localize the left nasion, mouth corners inner, and outer eyes corners, a 2D+3D elastic bunch graph matching is applied. This method has been only evaluated using the Texas 3D Face Recognition database where it demonstrated the ability to localize a large number of 3D landmarks accurately, but needs further improvement in order to localize these landmarks on faces with more extreme facial expressions, larger pose variations, and more extreme occlusions compared to those presented in the employed dataset.

Liang et al. in [135], reported a new approach to detect 20 landmarks on 3D face mesh, by initially applying a geometric technique on the 3D mesh to localize 17 facial landmarks, afterwards, a deformable transformation is employed between target and destination meshes to define a set of 20 established landmarks. The suggested approach detects a good number of 3D facial landmarks with accuracy using the introduced dataset that contains 3D neutral faces with no occlusions and expression variations. Figure 1.19 shows the deformable registration process.

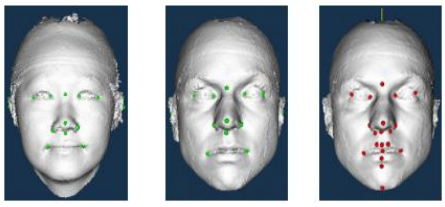

(a) *(b)* *(c)*

Figure 1.19: Process of the deformable registration: (a) and (b) are the target and the destination meshes with initial landmarks, (c) shows the destination with transferred landmarks, from [135]**.**

Perakis et al. in [155], have investigated a fusion method for 2D/3D landmarks detection using the spin images [156] and the shape index [157] to employ the 3D geometric information provided by the 3D scan, and Harris edge and corners detector [158] to use the 2D local appearance descriptors for the 2D intensity-based data. See equations (5) and (6).

$$\text{Shape Index}(P) = \frac{1}{2} - \frac{1}{\pi}\tan^{-1}\frac{K_{max}(P) + K_{min}(P)}{K_{max}(P) - K_{min}(P)} \qquad (5)$$

k_{max} and k_{min} are the principal curvatures values.

$$\text{Edge Response}(P) = \left(\frac{\partial I}{\partial x}\right)^2(P) + \left(\frac{\partial I}{\partial y}\right)^2(P) \qquad (6)$$

While I is the intensity image.

This method has been experimented on a great number of 3D faces to assess its effectiveness, and as described in the paper, the results have reached high accuracy compared to other methods. This approach may also be extended to work with 3D faces with various expression and illumination conditions as well.

Creusot et al. in [159], have suggested a trained off-line LDA classifier system to manually localize 14 3D landmarks identified on a training dataset. To do so, authors have computed a set of shape descriptors for every point on the training set faces and then assigned a descriptor value to each landmark. The proposed approach to detect the 3D landmarks is not solely geometric information based; the authors have used it in the initial steps to train the classifier which makes it robust and accurate. This method can also handle some facial expression variations but still weak regards pose variation and occlusions of the face.

Guo et al. in [160], introduced a new method to localize 17 3D facial landmarks automatically using the PCA feature recognition that follows 3D to 2D data transformation. Firstly, using a sphere fitting approach, the nose tip is localized, and then to detect additional 6 landmarks, the 3D data and texture were converted into 2D data to be able to use the Principal Component Analysis. Finally to localize 10 other points, texture constraints and geometric properties were used. The proposed method works showed a good detection results compared to early works in the literature; moreover, it has proven that it works well on 3D faces from different ethnicities which show the robustness of the approach.

Cheng et al. in [161], used a 3D Constrained Local Model framework to localize 3D facial landmarks. This framework is based on the use of different geometric features such as: Local Normal Binary Patterns (LNBP) [162], and Histogram of Oriented Normal Vectors (HONV) [163] which are known for their effective response map based 3D Point Distribution Model. Authors also argued that merging the intensity data and the 3D features enhance the detection performance. The presented method was evaluated on one 3D face dataset consisting of near frontal and neutral faces; hence some refinements are required to enhance the performances while using other developed 3D face databases.

Galvanek et al. in [164], proposed a novel algorithm to detect 14 landmarks automatically using the symmetric profile extraction and the surface curvature analysis. In this paper, authors have provided an effective method for visualizing the results, by first combining surface curvature analysis (minimal and maximal principal curvature) for each face feature, and then applying the symmetric profile extraction to localize the points on the profile side of the face based on peaks and valleys of the curve as demonstrated in Figure 1.20. The proposed approach allows the detection of a high number of 3D landmarks on neutral and frontal 3D faces yet with a high error rate; moreover, this approach is sensitive in the presence of certain facial accessories and beard for men.

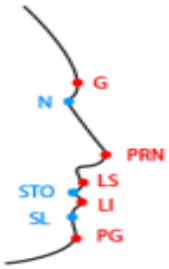

Figure 1.20: Landmarks detection on symmetry profile (red: local maxima, blue: local minima), from [164]**.**

Marcolin et al. in [165] employed 105 new geometric descriptors in order to localize 6 3D facial landmarks, the aim was achieved by deriving and composing some primitive descriptors such as Gaussian, mean and principal curvatures, shape index, curvedness, as well as the coefficients of the fundamental forms. The authors also proposed to apply some basic functions such as cosine, sine, and logarithm to employed descriptors. The new resulted descriptors have proven that they have numerous benefits over other well known descriptors such as: Gabor jets, LBP, and SIFT. The proposed method was experimented on neutral and frontal 3D faces acquired by a laser scanner, and not on some well established datasets to assess the strength of the introduced approach.

b. 3D facial landmarks detection for faces with expression and pose variations

Various advanced methods have been suggested in the literature to overcome the limitations of the first kind methods that work with only frontal or near frontal pose and neutral expression while detecting the 3D facial landmarks.

Mehryar et al. in [166], have detected 4 3D facial landmarks by initially identifying the peaks and valleys on the 3D surface based on the Mean curvatures and the Gaussian, afterwards, grouping the points that are closely clustered as the candidate landmarks and eliminating the others. At last, to get the resulted four points, a geometric model is used to impose some angles and distances constraints the candidate landmarks. The suggested method works very well on the used 3D face dataset as the success rate can achieve 98%; still there is a need to use it for other datasets that contains 3D faces with different poses and expressions as well as enhance the algorithm to be able to detect a larger number of landmarks. See Figure 1.21.

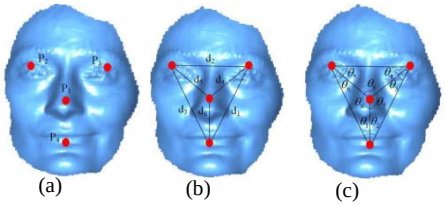

Figure 1.21: Geometric model constraints and landmark labeling: (a) detected landmarks, (b) relative distance constraints and (c) relative angle constraints. From [166]**.**

Creusot et al. in [167], presented a proof of concept for a face labeling method that can overcome the problem of localizing 14 facial landmarks under large pose variation and in the presence of occlusion. For a set of points containing manually placed landmarks as input data, the proposed

method aims to extract the landmarks within this set. For that purpose, authors suggested to calculate for each landmark a set of geometric descriptors that will help to create a generic graph model for the matching stage Figure 1.22. Then, the matching then is done by calculating for each point the matching score between an attribute value in the query graph and an attribute distribution in the model graph. The presented method can localize an important number of landmarks with high accuracy for the majority of the points, but likely to be decreased using other 3D face datasets. Thus, an improvement of the method is needed especially to detect the outer corner of the eyes and chin.

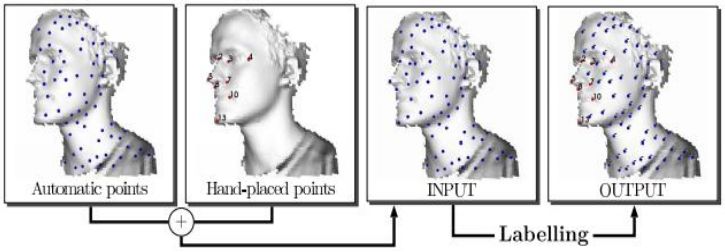

Figure 1.22: 3D facial landmarks labeling process. From [167]

Segundo et al. in [168], presented a method to detect 5 landmarks on 3D faces using the resulted combined relief curves [169] from the depth data and the obtained image of the surface curvature analysis [170]. To detect the eyes corners and the nose tip, authors have estimated the Gaussian and the mean curvatures for each region in the face and then classify the results into pits and peaks. In order to get more accurate results, authors computed the x and y projections of the depth information relief, and for the nose corners, they were found as the maximum variations in the obtained horizontal profile curve. This method was tested on two 3D face databases with different facial expressions and it has shown to be efficient (accuracy up to 99%). Despite the lower number of the detected landmarks, this method is a good benefit to face detection and recognition.

Berretti et al. in [171], detected 9 facial landmarks by localizing the nose tip and the two alare points in the first place using the curvature analysis (Gaussian surface curvature and the mean surface curvature) then the remaining points were detected using a solution based on the Scale Invariant Feature Transform (SIFT) [172] detector that was applied to local search windows around each feature. The landmarks are identified as the points with the largest scale. The suggested method was tested only on one dataset and it showed to have significant detection errors, which can be due to some facial accessories or large expression variations.
Vezzetti et al. in [173] and [174], proposed new approach based Differential Geometry to extract 9 3D facial landmarks. In their work a set of new and old geometric descriptors are presented in order to create a new structured methodology for facial landmarks formalization and automatic identification. These descriptors include: the first, the second and the mixed derivatives, the coefficients of the Fundamental Forms, the curvature, the shape and the curvedness Indexes and the Tangent Map. The detection errors reported in this work as well as the absence of some landmarks were claimed to be caused by the acquisition position of the 3D faces. For this reason, we believe that using some of the existing 3D face dataset is required to evaluate the performance and the accuracy of the proposed methods.

In another work [175], the authors developed an extension of the previous papers to detect new additional 8 landmarks based on the results already obtained. Firstly, the new search regions were localized then authors suggested to minimize the coefficient of the second fundamental form along a specific direction for the eyebrows landmarks and maximizing the curvedness index and the shape index for the cheilion landmarks. The new extension work can localize a larger number of landmarks with fewer errors and this is due to separating the working zones depending on the facial expressions. Furthermore, this work has been tested on an additional 3D face database.

Sangineto et al. in [176], proposed a method to detect 17 facial landmarks based on the SURF-like descriptor. The obtained results by this descriptor are used to establish a comparison of the 2D local landmarks classification using the Haar wavelets with the projected 3D shape vectors. Besides some wrong detection cases, the proposed algorithm localizes a large number of landmarks using 3D faces with pose and expression variations from the used dataset. Still as the majority of the presented papers, this work needs to be tested on different 3D databases to evaluate its performance.

Moos et al. in [177], proposed a new method to localize 13 landmarks on a 3D foetal face model in order to diagnose the prenatal cleft lip using various combinations of shape descriptors such as: the first, the second and the mixed derivatives, the coefficients of the fundamental forms E, F, G, e, f and g, the curvatures K, H, k1 and k2, and shape and curvedness indexes S and C as descriptors with the appropriate constraints and thresholds. This is the first automatic landmarking algorithm for this purpose, and it has shown to be depending on the quality of the echography. In good conditions, this method performs accurately due to the use of a variety of shape descriptors.

Gilani et al. in [178], in order to detect 18 3D face landmarks, they established a dense correspondence of 3D faces by minimizing the bending energy between landmarks of given faces and those of a reference face. The points of the reference face were extracted using adaptive level set curves with adaptive geometric speed functions. Then to identify the 3D landmarks on an unseen query face, a morphable model based on the dense corresponding points is performed for the correspondences transfer. The proposed method is considered one of the methods that can localize a large number of 3D landmarks accurately from two famous datasets; this number can be extended arbitrarily due to the use of the dense correspondence of 3D faces. See Figure 1.23.

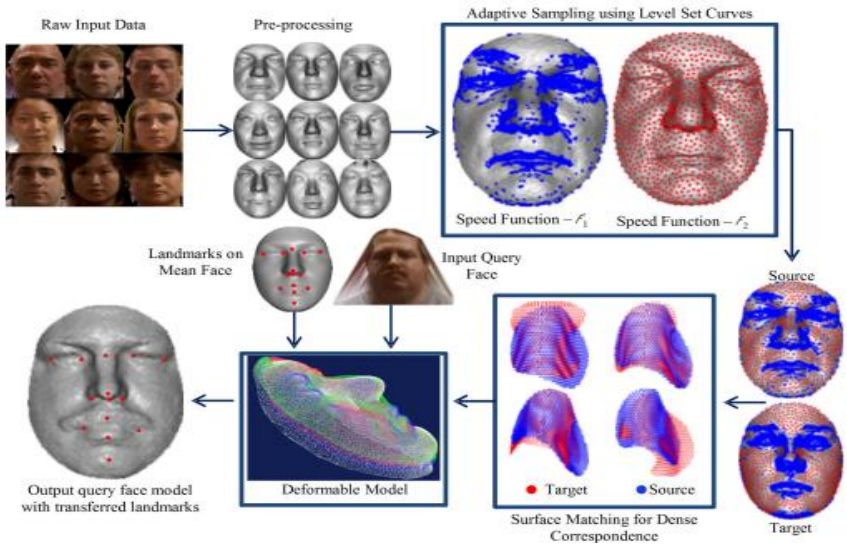

Figure 1.23: Diagram of the 3D facial landmarks detection using level set curves and the dense correspondence, from [178]**.**

Sukno et al. in [179], presented a shape regression with incomplete local features to detect 14 3D facial landmarks. By selecting the candidates points through local feature detection using the geometric descriptor APSC [180], authors then calculated the distance to each manually localized landmark on a set of 3D faces, finally, a partial set matching is used to conclude missing landmarks by regression. This method can handle missing data and occlusions due to the use of APSC descriptors, which showed its efficiency. Still the accuracy needs to be improved as the detection errors are a bit high compared to the recent methods.

Fan et al. in [181], detected 7 3D face landmarks by mapping the 3D facial models to 2D geometry image using a conformal mapping, then four 2D landmark detection methodologies are used in order to conclude the best one. Finally, the obtained landmarks from the 2D geometry images are mapped back to the 3D models, using point-to-point mapping. The proposed approach showed to be robust as it uses one of the best 2D landmarks detectors, in addition to the use of the conformal mapping, yet still weak in the case of missing data.
Li et al. in [182], have detected 25 landmarks on 3D facial scans by first calculating the mean curvature at every point on the mesh surface, then using a threshold to select the strong minimum and maximum in order to detect the landmarks regions and register the meshes to an adjusted position and orientation. Afterwards a training set is manually landmarked and used to create a mean face template, which is used to determine values for curvature thresholds, and to identify 17 control points. Finally, for a query facial mesh, the identified control points are used to register the template atlas to each mesh and subsequent transformation of the landmarks from the template to the mesh. The suggested method can localize a large number of 3D landmarks using essentially a set of shape descriptors and a face template, which makes it robust and accurate using the proposed set of 3D scans. Still this method needs to be tested on other 3D datasets to evaluate its performance.
Table 3 and Table 4 present a summary of the surveyed methods; it shows the details about authors, date of publication, the databases used in the experiments, the pose and expression of each set of the used database, and the number of the detected 3D landmarks. As can be noticed, some works used a known face databases like Bosphorus, Texas, FRGC, BU-3DFE…, and

others used cameras systems and scanners to capture the 3D model of the face, also the number of the detected landmarks differs for each approach.

c. Geometric information based literature studies comparison

A survey on the recent geometric information based methods was presented. Each of these works is based on a specific approach using the geometric information such as: Shape Index (SI), Spin Image(SS), Gaussian (K) and mean Curvatures (H), Curvedness Index , Principal Curvatures (k1,k2), Coefficients of the Fundamental Forms (E, F, G, e, f and g,), Tangent Map, Relief Curves, 2D image Edge Response, Deformable Registration, Local Binary Patterns (LBP), Scale-invariant feature transform (SIFT), Elastic Graph Bunch Matching (EGBM), Principal Component Analysis (PCA)… these works are based on different 3D face databases as well.
Using different 3D face databases, the evaluation of different 3D facial landmarks detection using geometric information based method become one of the complicated tasks. Moreover, even when the same dataset is used, different parts of it could be employed in different experiments.
To evaluate the performance of each work, some authors tend to use the detection rate as performance measure; some others take the error rate. To compare the performance of the surveyed methods on a quite fair basis, we have reported the results from each paper and in Table 1.3 and we summarized them based on the used database.

papers	Authors and date of publication	Database used	Pose and expression variation	Number of landmarks detected
[153]	Gupta et al. 2010	Texas Database	Neutral and frontal scans.	10: Eyes corners, nose tip, nose corners, and mouth corners.
[140]	Perakis et al. 2010	FRGC v2 and UND Ear Databases	Scans with pose variations	8: Eyes corners, nose tip, mouth corners and chin.
[166]	Mehryar et al. 2010	Bosphorus Database	Pose and expression variations	4: Pupils, nose tip and the stomion
[167]	Creusot et al. 2010	FRGC v2 and the Bosphorus database	Pose and expression variations	14: Nose tip and corners, mouth corners, eyes corners, nasion, subnasale, chin, superior and inferior labials.
[168]	Segundo et al. 2010	FRGC and the BU-3DFE databases	Frontal scans with expression variations	5: Nose tip, inner eyes corners and nose corners.
[171]	Berretti et al. 2011	BU-3DFE database	Frontal scans with expression variations	9: Eyes corners, nose tip, nose corners and mouth corners.
[141]	Perakis et al. 2012	FRGC v2 and UND Ear Databases	Pose and expression variations	8: Eyes corners, nose tip, mouth corners and chin tip
[135]	Liang et al. 2013	115 3D facial meshes obtained from a 3dMDR digital stereophoto- grammetry imaging system	Neutral and frontal scans.	20: eyes corners, nose tip, nose corners, mouth corners, nasion, subnasale, superior and inferior labials, stomion, chin, subalars and crista philtries.
[173]	Vezzetti et al. 2013	36 3D face models of nine people.	Frontal scans with expression variations	9: nose tip, nasion, subnasale, nose corners and eyes corners
[155]	Perakis et al. 2013	FRGC v2 and UND Ear databases	Neutral and frontal scans.	8: Eyes corners, nose tip, mouth corners and chin.
[159]	Creusot et al.	FRGC v2 and Bosphorus 3D face	Neutral and	14: Eyes corners, nose tip, nose corners,

	2013	datasets	frontal scans.	nasion, mouth corners and chin.
[160]	Guo et al. 2013	Scans obtained from 3dMDface® system.	Neutral and frontal scans.	17: Eyes corners, nose tip, nose corners, mouth corners, nasion, subnasale, superior and inferior labials, stomion, chin and earlobe tips.
[176]	Sangineto et al. 2013	XM2VTS and BioID for 2D images and FRAV for 3D scans	Pose and expression variations	17: Eyebrows corners, eyes corners, nose points, mouth corners and stomion.
[174]	Vezzetti et al. 2014	79 scanned faces obtained by using Cyberware Head and Face Colour Scanner.	Frontal scans with expression variations	9: Nose tip, nasion, subnasale, nose corners and eyes corners.
[175]	Vezzetti et al. 2014	Bosphorus database + meshes from Minolta Vivid 910 3D laser scanner+ system composed of 4 Canon EOS 1100D cameras	Pose and expression variations	8: Mouth corners, labrum superior and inferior and eyebrows corners.
[177]	Moos et al. 2014	3D reconstructed models of 9 foetus using Simpleware ScanIP software.	-	13: Pronasal, subnasal, nose corners, eyes corners, nasion, inner eyebrow corners, mouth corners, superior and inferior labials.
[161]	Cheng et al. 2014	FRGC database	Neutral and frontal scans.	Points on the contour of the face and some features.
[178]	Gilani et al. 2015	FRGCv2 and BU3DFE Databases.	Frontal scans with expression variations	18: Eyebrows, nose tip and corners, mouth corners, eyes corners, nasion and chin tip.
[164]	Galvanek et al. 2015	Fidentis 3D Face Database	Neutral and frontal scans.	14: Eyes corners, nose tip, mouth corners, stomion, glabela, nasion, superior and inferior labials, chin, and sublabial.
[179]	Sukno et al. 2015	FRGC database, Bosphorus database	Neutral and frontal scans with occlusions	14: Points on the contour of the face and some features.
[181]	Fan et al. 2016	BJUT-3D face database	Pose and expression variations	7: Eyes corners, nose tip and mouth corners.
[165]	Marcolin et al. 2016	Depth map of triangular mesh obtained by Minolta Vivid 910 laser scanner.	Neutral and frontal scans.	6: Nose tip, superior and inferior labials, pupils and subnasale.
[182]	Li et al. 2017	3D facial scans obtained using the Creaform Mega capturor and Gemini 3D camera systems.	Neutral and frontal scans.	25: Points on the contour of the face and some features.
[183]	Vezzetti et al. 2017	Bosphorus database	Expressions variations and occlusions	13: Eyes corners, eyebrows corners, nose tip, nose corners, nasion and the subnasale.

Table 1.3: summary of the geometric information based methods for 3d facial landmarks detection

Databases	Papers	Mean error	Success rate
Bosphorus database	[183] [179] [175] [159] [167] [166]	4.75 mm <3.5 mm 1.3 -3.9 mm - - -	- - - 98.7% 80% 99.2%
FRGCv2 database	[167] [168] [155] [161] [178]	- 5.5 mm 4.26 mm - 3.69 mm	80% - - 98.7% -

	[179]	<3.5 mm	-
BU-3DFE database	[178] [168] [171]	3.69 mm 5.5 mm 3.28 mm	- - -

Table 1.4: performance comparison of 3D Facial landmarks dtection methods

- **Performance evaluation on Bosphorus database**

The performance of the geometric information based methods for 3D facial landmarks detection on the Bosphorus database are presented in Table 1.4. Note that the presented mean errors and success rates are reported based on the original papers.

The Bosphorus dataset has been used in the case of 3D neutral frontal 3D faces as well as 3D faces with pose and expression variations. Among the tested methods on this dataset, the methods presented in [166] and [159] have shown to be the most robust and accurate, these methods are based respectively on Gaussian and mean curvature descriptors that were calculated for each point of the input 3D face, then some constraints were concluded using the manually landmarked 3D faces. The success rate achieved 98.7% and 99.2%, which highlights the power of combining these descriptors with the manually located points.

And the less accurate method on this dataset was the one presented in [183] where the mean error was 4.75 mm. This method is based on the combination of 12 shape descriptors as well as a thresholding technique based on the behaviour of each descriptor.

- **Performance evaluation on FRGCv2 database**

Using the FRGCv2 3D face database, some papers have shown good results of detection for both neutral and frontal 3D faces and for 3D face with pose and expression variations as well. In [161] and[179] a satisfying results were reported using the Histogram of Oriented Normal Vectors (HONV) and Local Normal Binary Patterns (LNBP) and the APSC as the geometric descriptors in addition to fusion the obtained results with those obtained from intensity images data. The success rate achieved 98.7% for [161] and the mean error reported from [179] was inferius to 3.5 mm, which shows the efficiency of such fusions.

The relatively less accurate method using the FRGCv2 dataset was presented in [168] with a mean error of 5.5 mm. this method is based on computing the x and y projections of the depth information relief to localize the 3D landmarks. Therefore, the less accuracy can be related to the projection phase.

- **Performance evaluation on BU-3DFE database**

The BU-3DFE database was used as well in a large number of papers to localize the 3D facial landmarks on frontal faces with facial expressions and occlusions. The reported results show that the methods that were tested on this database have relatively good detection results such as in [171] where authors used Gaussian surface curvature and the mean surface curvature in addition to the Scale Invariant Feature Transform (SIFT), and in [178] where a dense correspondence of 3D facial landmarks has been established. The reported mean errors are 3.28 mm and 3.69 mm respectively, which shows the efficiency of the Gaussian and mean curvature again as well as the robustness of the SIFT.

A relatively high mean error of 5.5 mm was reported by authors in [168] again which was the same using FRGCv2 database. Thereafter, we can conclude that the methods based computing the x and y projections of the depth information relief are less accurate among the presented methods for 3D facial landmarks detection. Which require a reconsidering of this type of approaches.

As can be noticed, a large number of approaches have been proposed to detect the 3D facial landmarks, and a special consideration has been devoted to the methods using the geometric information to localize the 3D landmarks on a 3D face. This kind of methods has received a great attention and become widely used in the field due to the variety of the existed approaches such as the curvature analysis, edge response, SIFT, LBP, EGBM, … and the good results obtained using them.

Despite the metrics used to measure the performance of each approach, for example in the previous subsection, two types of measurements were reported; the detection rate and the error rate, establishing a fair comparison of the presented works still a tedious task as different databases were used in each of them. Although, we tried to compare their performances based on the used database and the results were presented in Table 1.4.
Based on the recent progress in the methods used to localize the 3D facial landmarks based on geometric information, we have noticed a great improvement especially with handling the problems of 3D face pose and expressions variations. Furthermore, some works have explored new tools such as combining the existing geometric descriptors to enhance the accuracy of the landmarks detection, or applying new ones. Even though the reported advancement in 3D facial landmarks detection using geometric information, there is still some points to improve and more accurate algorithms are to be developed. One of the important points is to test further the performance of the existing methods on a large set of 3D face databases in order to evaluate their efficiency as well as their stability.

5.2.2 Approaches based trained statistical feature models

About the recent approaches for 3D facial landmarks detection based on the trained statistical feature models, first of all, these approaches in general aim to use a trained model which learns both the variations between landmarks positions and the local variations of texture and geometry around each landmark and afterwards, to localize the 3D facial landmarks on an input 3D face, the learned model is then used to define the transformation that should be applied between the landmarks on the reference model and the input 3D face.

In the period of (2010-2018), several papers have proposed to detect the 3D facial landmarks using the trained statistical feature models. To the best of our knowledge, the number of the proposed methods using the trained statistical feature models is fewer than those using geometric information techniques. Besides, a large number of the found papers are based on the geometric techniques to train the 3D face model. The rest of this subsection presents some of the proposed work to detect the 3D facial landmarks using trained statistical feature models from 2010 through 2018.

Authors in [184] presented a framework for 3D facial landmarks detection using local coordinates coding. The proposed method can localize the landmarks under expression, pose and resolution variations and also when the 3D face is not fully covered by the data.
Indeed, the framework is composed by two main steps; the first step consists of detecting the nose tip of the input 3D face, and then applying an alignment between the 3D face and the 3D model using an affine transform. Finally, to refine the alignment, the ICP algorithm is applied. The second step aims to build a training dataset for the LCC landmarks localization; this training dataset will allow constructing a coupled dictionary learnt from both the dataset and the corresponding landmarks. Consequently, for a given 3D face, the 3D landmarks are localized using the coupled dictionary by identifying the closest vertices to the calculated landmarks based on the LCC. Figure 1.24 shows an overview of the proposed method.

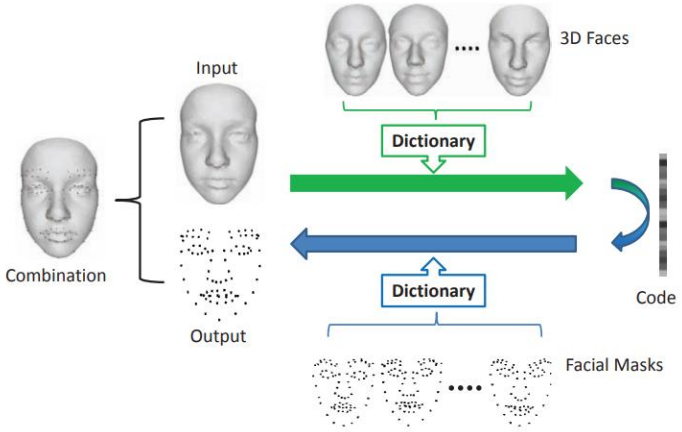

Figure 1.24: 3D facial landmarks localization from [184]**.**

In another work [185], authors have proposed a new method to detect 3D/4D facial landmarks detection using the shape index based statistical shape model (SI-SSM). This method aims first to construct the SI-SSM from both the global shape of 3D facial landmarks and local curvature from patches around each landmark. The global and local shapes are modeled using the annotated 3D facial landmarks in the training set (figure 1.25).

For an input 3D range image, to detect the 3D landmarks, first the shape index values have to be calculated and then apply the SISSM algorithm to the resulted face by finding the correlation between the local shape index patches on the input face and the trained SI-SSM model. This method has been tested using five 3D/4D face databases and showed good results against rotation, occlusion and quality data (figure 1.26).

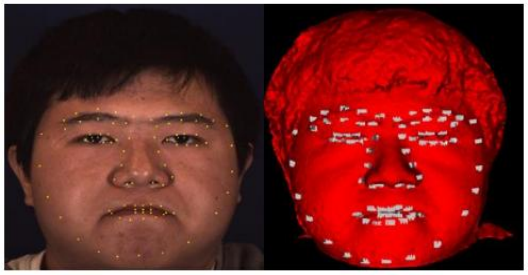

Figure 1.25: Left: 83 landmarks defined on a face; Right: corresponding 3D patches with grey-scale shape index values from [185].

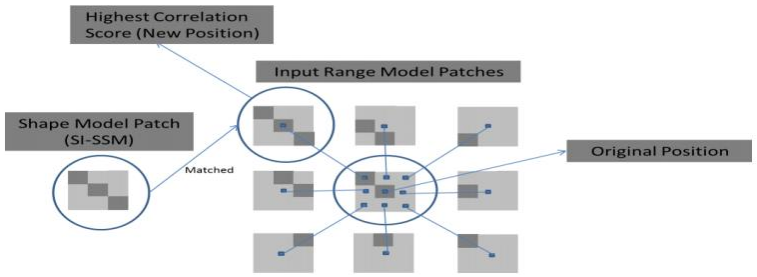

Figure 1.26: Example of correlation search between a SI-SSM patch and input range model patch at size of n×n, (where n=3 for instance) from [185]

In [186], authors proposed a framework to detect 3D facial landmarks learnt from the relationships between the landmarks and their local proprieties by optimizing a global objective function. The proposed framework is based on a statistical model, called 3-D Statistical Facial feAture Model (SFAM), trained using the manually labeled 3D landmarks for each aligned frontal 3D face, then the model is constructed by applying principle component analysis (PCA) to the obtained configuration of the 3D landmarks.

This framework has been tested on three 3D face databases, and the obtained results show that the proposed model can locate the 3D facial landmarks accurately in the presence of occlusions and expression variations.

5.3 3D facial aesthetic quality analysis

In the previous sections, we have reported that the use of the 2D face in image analysis only is limited by the variations of the pose and the illumination, which makes the 3D representation of the face more required to handle these limitations.

Nowadays, with the remarked grow of the 3D acquisition techniques; the analysis using the 3D faces has claimed to be more efficient and accurate comparing to the 2D representation of the face which cannot represent the real structure of the face. For the aesthetic quality analysis of a face, many research studies have claimed the importance of using the 3D representation of the face to analyze its attractiveness as the 3D faces can represent the real structure (geometry and shape) of the original face, which makes it an ultimate way to achieve an accurate attractiveness analysis.

The analysis of facial aesthetic quality using 3D face representation has been discussed in just a few research studies as it is still a newborn topic. The presented research studies have described the analysis of 3D facial attractiveness based on the facial proportions and facial symmetry analysis [187][188], others have introduced the analysis of the 3D facial attractiveness based on the face averageness and its role to enhance the aesthetic quality of the face [189], other paper [190][191] assessed the facial attractiveness based on the facial symmetry only, and other work has used the 3D facial representation to perform a computer aided system for planning plastic and cosmetic surgeries [189][192].

The majority of the proposed works that use the 3D facial representation share similar steps to achieve the analysis of the 3D facial aesthetic quality. These steps in general start by first visualizing the 3D face (shape and texture), localizing its feature and then performing the analysis of the attractiveness. Extracting the facial landmarks is a necessary step in order to get the geometry of the face. These landmarks are located on both the frontal and the profile side of the 3D face and will help the user to calculate and verify if the face needs modifications or not. To localize the 3D facial landmarks, some authors have detected them manually [187], others have localized them automatically using different approaches as presented in previous sections [189], and others have used the already detected landmarks on some 3D face databases [193].

After the detection of the 3D facial landmarks, the goal of facial aesthetic quality analysis can be processed by calculating the different beauty canons on a given face, these canons include the facial symmetry, the facial golden ratio, the facial proportions or neoclassical proportions, and the angular profile, then compare them to the referenced value in the literature studies to conclude the necessary modification to apply to the face to enhance its attractiveness. These are in general the followed steps by the proposed studies to analyze the attractiveness of a 3D face, for example authors in [187] have proposed a geometry based method to analyze the attractiveness of 3D face by first manually labeling the 3D landmarks and then analyzing the 3D facial symmetry and facial frontal proportions based on the golden ration and the neoclassical beauty canons, then a facial angular profile has been processed. Authors in [194] have proposed an automatic system to analyze and to enhance the symmetry of 3D faces by comparing each region of face in both the left and the right side of the bilateral facial axis, then perform a symmetry plan alignment to get global symmetrization. Authors in [189] have studied the relationship between the facial attractiveness and the averageness using a combination of a normalized 3D shape and 2D facial texture. In [195], authors have proposed a Fuzzy Neural Network to assess the 3D facial attractiveness.

6 3D facial attractiveness enhancement

3D facial visualization has become of great importance in the computer graphics field to visualize the 3D objects in general and to manipulate them, therefore to be able to see any modification or deformation applied to them on the screen. These operations are essentially deducted to games interfaces and videos that aim to represent the 3D actors in a realistic way and edit their facial expressions, positions or features according to each specified scene.

The conducted research studies for that purpose have shown very good results which are similar to real life scenes [196] but still suffer from some weakness regarding the visualization after the 3D object editing; this weakness is generally due to the discontinuity and the pose relationship of the object's parts that can be occurred during the 3D deformation [197].

As mentioned before the visualization and the manipulation of the 3D face is a particular case of the 3D object use that is very important in the field of cosmetics and medical analysis of the face. As we mentioned before, the attractiveness of the face plays an important role in individual life and nowadays it is getting more attention in several fields such as the advertizing domain, getting a job as people with an attractive faces are more likely to get better job, earn a higher

salary, and have a better life than people with unattractive face. All of this attractiveness effects apply kind of pressure on people and push them to look more attractive. For this purpose, the suggested solutions are plastic surgeries or cosmetic surgeries.

In fact, the enhancement of the aesthetic quality of a face aims to modify both the geometry and its shape of a face in order to get a more attractive face but with the constraint of keeping the new face looks like the original one. A research study [189] has divided the ways to enhance the facial attractiveness into two types; geometry based enhancement and appearance based enhancement. The first category aims to modify the geometry and the shape of a given face, these kinds of approaches is composed of five main steps; Beauty prototype acquisition, Geometric feature extraction, Nearest prototype(s) search, Geometric feature modification, Image warping and finally Results evaluation. About the appearance-based approaches, they focus on changing the facial skin appearance, in order to become more homogeneous and smooth by removing the face imperfections such as flecks, wrinkles, and unevenness.

The 3D facial aesthetic quality analysis is one of the most active domain that uses the 3D representations of the face in order to have near realistic visualization of the patient's face and moreover to be able to apply the different operations to enhance its aesthetic quality and see the results on the virtual face before the surgeries. This will help the surgeon and the patient at the same time, in one hand to permit to the patient to see the results on his virtual in case of having any other opinions about the surgery, in the other hand for the surgeon to respond the most to the patient requirement and minimize the surgeries errors.

The process of the enhancement of the 3D facial attractiveness starts first by comparing the results obtained from the step of the 3D facial aesthetic quality analysis to the state of the art beauty canons cited in all the previous sections on this chapter. The canons that we are working on in this thesis are; the 3D facial symmetry, the golden ratio and the 3D neoclassical proportions.

Starting from these comparison results, the modification of the 3D face can be processed by manipulating different 3D facial regions that need to be modified in order to get a 3D face that meets the state of the art beauty canons. Finally, to evaluate the performance of the presented methods in the all the previous works, the obtained results were presented to human raters to verify the relevance of the proposed systems.
In this section, we are going to present the most relevant state of the art research studies that aim to edit the 3D facial mesh and provide the final visualization of the obtained results. In the literature, a large number of works discussing the 3D facial mesh deformation and editing were presented, these works can be classified into two categories: facial mesh editing using differential surface representation and 3D facial mesh editing based sketching. Each one of the listed categories has its strengths and limitations as will be described in the following subsections.

6.1 3D facial mesh editing using differential surface representations

3D mesh deformation using differential representations have received a great attention decades ago, and a large number of research studies have addressed the problem of 3D mesh deformation using it. Surface deformation using differential representation is known to be robust, fast and easy to implement, translation invariant and to use surface representation that keep the mesh local information and proprieties invariant during the deformation which leads to a smooth deformation results.

Before using the differential coordinates to represent and manipulate the mesh vertices, they were represented by the absolute coordinates in the majority of works which caused the problems using local operations due to the global misalignment. Authors in [198] have introduced the use of the differential coordinates to represent the mesh geometry and the surface representation in general, and they have claimed that these differential coordinates describe well the local properties of the geometry rather than the absolute position in space. In addition, other papers claimed the same idea and notice that contrary to the traditional Cartesian coordinates which were largely used and that only describe the spatial location of each point, the differential surface representation can tell information about the local shape of the surface, the size and orientation of local details thus, defining operations on surfaces that preserve differential representation. All of this leads to detail-preserving operations. The linearity of the processing framework makes it very efficient, and it has become a promising research direction.

To deform a surface using the differential representations, the surface needs to be represented by the differential coordinates first in order to be able to apply the requested deformations, and then afterwards the surface will be reconstructed using the new differential coordinates to get the final deformation results.

Differential surface representations are inspired by the gradient domain image technique, which was claimed to contain very important visual information to which the human is sensitive. Several image techniques have used this propriety by applying some manipulations to an input image gradient and then reconstructing the resulting by global optimization algorithms that try to find the image with gradients very close to the modified gradients. In general, this is done using the famous Poisson equation, which is known by controlling the gradient and addition the boundaries constraints.

In the following subsections, we present brief review of the different differential representations.

6.1.1 Gradient mesh editing

Using the gradient for surface editing, the results of the deformation are obtained by minimizing functions defined by the 3D coordinates of the surface as following in equation 7, equation 8, and equation 9:

$$\int \|\nabla_{x'} - g_x\|^2 \, dudv \qquad (7)$$

$$\int \left\|\nabla_{y'} - g_y\right\|^2 \, dudv \qquad (8)$$

$$\int \|\nabla_{z'} - g_z\|^2 \, dudv \qquad (9)$$

These functions represent the three coordinates of a surface. g_x represents the gradient of the original surface coordinates. By deriving the Euler-Lagrange equation of the previous functions, the Poisson equation is obtained by equation 10:

$$\Delta_{x'} = div\, g_x \qquad (10)$$

In each triangle, the gradient of the x function is the projection of the unit x-axis vector $(1, 0, 0)^T$ onto the triangle's plane and similarly for the other two coordinate functions. Formally, let a piecewise linear scalar function f on the domain mesh S defined by the barycentre interpolation of per-vertex values $f_i = f(v_i)$ such that (equation 11):

$$f(u, v) = \sum_{i=1}^{n} f_i \, \varphi_i \, (u, v) \qquad (11)$$

Where (u,v) are the parameters over the domain mesh and $\varphi_i(,)$ are the piecewise linear "hat" basis functions associated with the domain mesh vertices, that is $\varphi_i(v_k) = \delta_{ik}$. The gradient of f is then (equation 12):

$$\nabla f(u, v) = \sum_{i=1}^{n} f_i \, \nabla\varphi_i \, (u, v) \qquad (12)$$

If (x, y, z) are the coordinates of a mesh triangle, the gradients of the corresponding hat functions are (see equation 13):

$$\left(\nabla\varphi_x, \nabla\varphi_y, \nabla\varphi_z\right) = \begin{pmatrix} (x-z)^T \\ (y-z)^T \\ n^T \end{pmatrix}^{-1} \begin{pmatrix} 1 & 0 & -1 \\ 0 & 1 & -1 \\ 0 & 0 & 0 \end{pmatrix} \qquad (13)$$

Where n is the unit normal of the triangle.

Several research work have used the gradient based representation to edit and deform 3D meshes, as an example, authors in [199] have presented a new method based sparse data and the gradient for 3D mesh deformation, this method aims to avoid the limitations caused by the combination of the examples based method for mesh deformation. To achieve this purpose, authors in this paper proposed to select small number of deformation mode (pose) and then establish a linear combination to satisfy the user requirements.

In another work [200], authors have developed a new method for facial mesh editing based on gradient field manipulation. This technique consists of using the Poisson equation. This editing function can be achieved by modifying the gradient field and its boundary condition in the 3D mesh (figure 1.27).

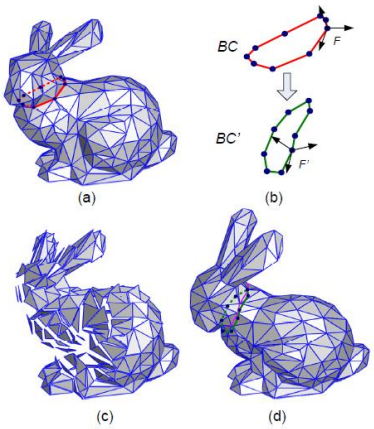

Figure 1.27: the use of Poisson equation to edit 3D meshes. (a) A BUNNY mesh with a curve around its neck. (b)This curve is a generalized boundary condition, BC, for the Poisson equation. Its edited version is BC'. Local frame changes on the curve are propagated to other triangles. (c) Each triangle is locally transformed by the transformation it receives from the propagation. The triangles become disconnected. (d) The Poisson equation stitches together the triangles again in the new pose defined by BC'. from [200]

In [201], authors presented a new approach for bas-relief generation and mesh editing using Gradient based mesh deformation. This approach operates directly on triangulate mesh and ensures the invariance of the mesh topology after the deformation. In this paper, the input 3D object is pre-processed by removing the entire artifact that exists and minimizing the number of vertices using a specified algorithm. After the simplification, the boundaries of the object are matched to the base plan by solving the discrete Poisson equation, which let the deformation produced by the boundaries to propagate in the whole object. The object will then be dragged to the base plan, and the remaining vertices will be transformed to the new location.

6.1.2 Laplacian mesh editing

Mesh editing using the Laplacian is a widely used technique for 3D mesh deformation. Laplacian based technique represents the surface using the Laplacian coordinates. These coordinates are obtained by applying the Laplacian operator to the mesh vertices [198]. In brief, mesh editing based on the Laplacian approach encodes each vertex relative to the centroid of its neighbours [202] and the resulted encoded vertices are a linear function of the global mesh geometry.

The Laplacian coordinates are translation invariant and preserve the intrinsic geometry of the surfaces. To fit the transformed Laplacian coordinates, let's consider the facial mesh M describe by a pair (C,V), where C is the vertices connectivity of the facial mesh and V = $\{v_1, ..., v_n\}$ describes the geometric positions of the facial vertices in R3, and n is the number of model vertices.

The Laplacian coordinate δ_i of the vertex v_i is represented by the difference between v_i and the average of its neighbours is given in equation 14:.

$$\delta_i = v_i - \frac{1}{d_i} \sum_{j \in N_i} v_j \qquad (14)$$

Where $N_i = \{j \mid (i, j) \in C\}$ and $d_i = |N_i|$ is the number of the neighbours of i.

The transformation of the vector from the absolute Cartesian coordinates to the vector of differential coordinates can be represented in matrix form A that describes the connectivity of the mesh. This matrix is called the adjacency matrix of the mesh (equation 15):

$$A_{ij} = \begin{cases} 1 & (i,j) \in C \\ 0 & otherwise \end{cases} \qquad (15)$$

Let the D = diag (d1, . . . ,dn) be the degree matrix, the Laplacian coordinates Δ can be described by the mesh adjacency matrix and the degree matrix as follow in equation 16:

$$\Delta = LV \qquad (16)$$

Where $L = I - D^{-1}A$ and I is the identity matrix.

The rank of L is n − 1, which means V can be recovered from D by fixing part of these vertices and solving a linear system. Thereafter, the matrix *L* is commonly considered as the Laplacian operator of the mesh with connectivity *A*. Thus the Laplacian coordinates of vertex i are given by equation 17:

$$\delta_i = \Delta = (\delta_i^{(x)}, \delta_i^{(y)}, \delta_i^{(z)}) = LV \qquad (17)$$

To perform the facial deformation using Laplacian coordinates Δ, we fix the positions of m points [198] such as in equation 18 :

$$V_i' = U_i \text{ , } i \in \{m, \ldots, n\}, m < n \qquad (18)$$

And then we solve for the remaining vertices $\{V_i', i = m + 1, ..., n\}$ by fitting Laplacian coordinates of geometry V' to the given Laplacian coordinates Δ. We observe that the solution is better if the constraints $\{U_i\}$ are satisfied in a least square sense rather than solved exactly [203][204]. This results in the following error function given by equation 19:

$$E(V') = \sum_{i=1}^{n} || \delta_i(V_i) - \delta_i(V_i') ||^2 + \sum_{i=1}^{m} || V_i' - U_i||^2 \qquad (19)$$

This function has to be minimized to find a suitable set of coordinates *V'*. Solving this quadratic minimization problem, results in a sparse linear system of equations.

The Laplacian coordinates preserve the shape details after the deformation, but still sensitive to linear transformations, which means that the shape detail can be translated but not rotated or scaled.

To edit 3D mesh geometry, author in [205] has defined a process formed by three steps in order to get a global editing of a mesh. These steps are as follows: first, the user defines the region of interest which will be modified, second, he defines a handle inside of the region of interest, finally, he manipulates the handle and the whole surface is reconstructed following the handle.

Other research papers have used the Laplacian approach in order to edit the 3D meshes, authors in [206] have introduced a method to synthesize facial animations using the Laplacian

deformation method. This work is based on cloning the facial expressions on a neutral 3D face using the Laplacian coordinates which transfer the facial expressions from a 3D face example to the same model with neutral expressions. Figure 1.28 presents the global architecture of the proposed approach.

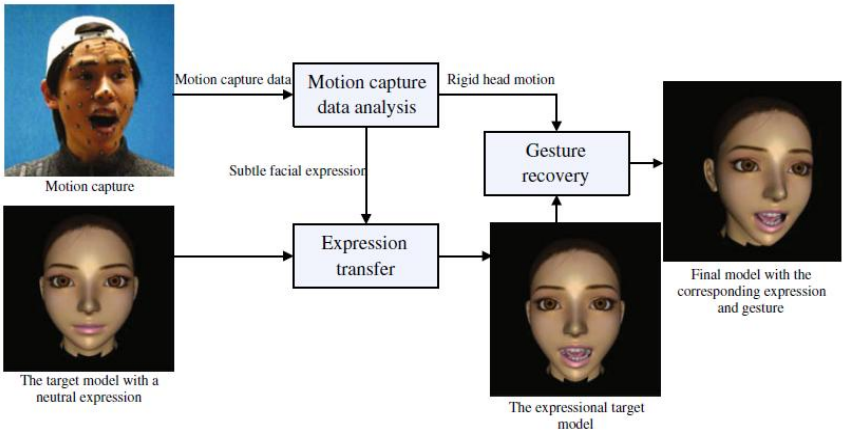

Figure 1.28: the global architecture of the proposed approach for 3D mesh facial expression deformation. From [206]**.**

In a more recent work [207], authors claimed that the Laplacian surface editing can edit locally the surfaces and keep the same 3D details features, but still depending on the 3D object vertices numbers, which makes it time consuming in case of manipulating a large number of vertices are manipulated. In addition, the Laplacian cannot handle the rotation problem as well, for this reason; the authors aim to recover these problems by simplifying the 3D mesh then applying the Laplacian deformation.

Laplacian coordinates have been also used to enhance the attractiveness of a 3D face as described by [187] where authors presented a new geometric enhancement framework for 3D face models. This framework is able to remove facial disharmonies and enhancing frontal and profile appearance using the Laplacian approach, see figure 1.29.

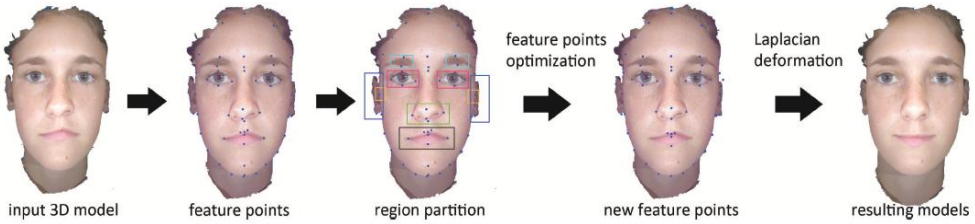

Figure 1.29: 3D facial attractiveness enhancement engine. From [187]

6.2 Sketch based 3D facial mesh editing

Sketch based methods are very popular for creating and deforming 3D surface meshes. These methods consist on drawing different type of sketches that guide the deformation. This kind of mesh deformation techniques give the user the possibility for direct interaction with the 3D model to deform by specifying the desired deformation on an image plan first. The user sketches a 2D curve, a point or a free form strokes to define the region to be deformed as a reference sketch on the input mesh and then he determines the desired deformation by drawing

new sketches on the same 3D mesh, finally, the aims of a sketch based system is making the 3D model following the desired deformation. For more details and classification of sketch based methods for 3D mesh modeling and editing, authors in [208] presented a complete review, (see figure 1.30).

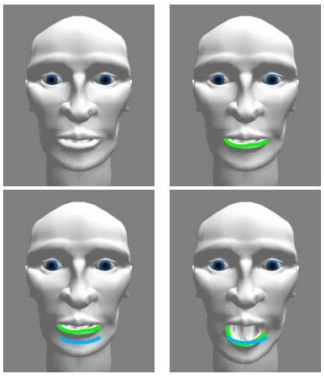

Figure 1.30: Example of 3D mesh editing using a reference curve (green) and a target curve (blue) on an input mesh From [209]

Sketch based method for 3D mesh deformation was first implemented by authors in [210], it allows the user to control the geometric modeling and deformation in a simple way, and it is generally considered as bridge between the hand sketches using pen and paper and the computer based modeling programs. Sketch was developed in order to help and guide the users to perform the geometric creation and modeling of 3D objects. As a simple and primitive example of this method is when a user sketches three segments parallel to the projections of the x-, y-, and z-axes of the scene and these segments meet in one point, then the system creates a cube using the drawn segments. Familiarizing with these kinds of primitive creations, users can create more complex models afterwards. Figure 1.31 illustrates sketch-based method for 3D mesh modeling.

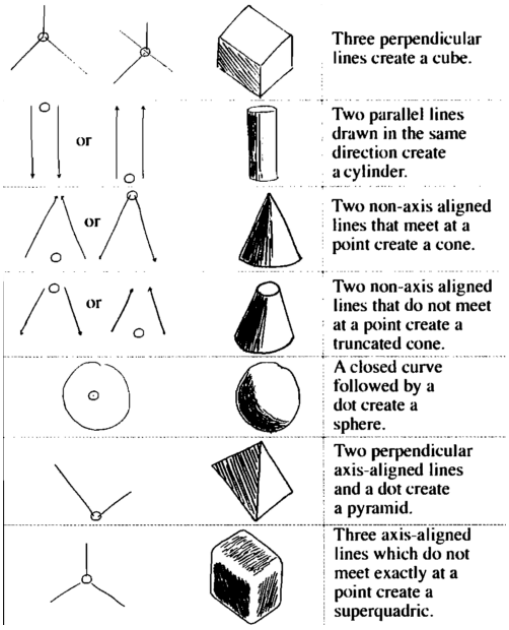

Figure 1.31: Sketch based creating shapes. From [210]

One of the techniques used for sketching is the free form deformation (FFD) [211]. This method provides the possibility to perform a wide variety of 3D mesh deformation; it has been also paid

attention in the industry and the research communities. This method allows the user to manipulate a 3D surface in a large variety of deformation without having to use multiple shapes. Several research studies have used the free form deformation on 2D image plan, and then they transformed the sketch to the 3D representation, the challenge of sketch based mesh deformation is to understand the user input requirements. In addition to interpreting the intent of the user, finding a coherent transformation from 2D to 3D space is a challenging part as well.

In Teddy [212], authors have developed a friendly user interface to create and modeling 3D objects by sketching strokes on the screen and then adding the desired details by editing the mesh with operations like extrusion, cutting, bending, and drawing on the 3D mesh, this system also offers the possibility of deforming the 3D objects using a warp. Teddy's principal limitation can be expressed by the fact that it is not possible to introduce sharp features or creases directly on the models except through cuts. Moreover, the system allows editing only a single mesh at a time. Figure 1.32 shows Teddy's system.

Figure 1.32: Teddy's system on a tablet from [212]

In similar work [213] authors have described a system for creating free-form models from gestural user input. The system use variational implicit surfaces [214] in a modeling tree hierarchy representation which allows the user to edit more than a single object at a time. This system of modeling operations allows the users to construct shapes in a closer way to the way that they draw them.

Authors in [209] presented a novel work that aims to articulate and pose a 3D mesh based on sketching 2D strokes on the input mesh, these strokes define the reference curve that specify the region of the mesh that will be deformed and the target curve that defines the desired deformation. The mesh pose is then optimized by minimizing the distance between the two curves using the downhill complex method.

Another technique for editing 3D meshes is using curves to specify the region to deform and how the results should look like after the deformation. It is similar to the free form based deformation techniques but with more precise user inputs. Previous research studies have investigated in this kind of mesh deformation techniques and have claimed the efficiency of using it. Authors in [215] presented a new method to deform the 3D mesh based on the sketching curves on an image plan. In their method, the user defines the ROI and the handle by drawing the source curve on the original mesh and the new curve that represents the target mesh, and then the system deforms the mesh accordingly. The main contribution of this work is a user interface, which allows even people with no background in 3D complex forms to edit meshes easily.

By combining sketching and 3D mesh editing using Laplacian operator, authors in [216] have performed a 3D mesh deformation while presenting a novel method for feature preserving surface mesh editing. This method consists of first drawing the stroke that defines the desired position of a mesh region, this region must be part of the silhouette forming the mesh. Afterwards, the system segment all the image space silhouette and find the segment from the silhouette that matches the stroke drawn by the user. The next step is to detect the vertices in the mesh that correspond to the silhouette part in order to localize ROI to be deformed. Once the ROI, the handle vertices and their target position have been defined, the Laplacian surface editing is applied to the mesh. Figure 1.33 describe the different steps followed by the authors.

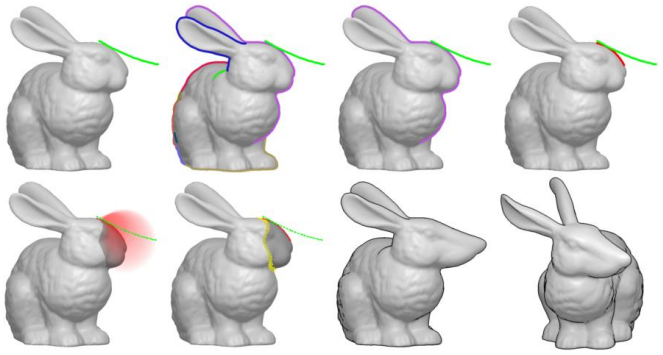

Figure 1.33: Architecture of the 3D mesh editing method presenting in [216]

Mesh deformation can be achieved by using the skeleton of the 3D object as well. This approach is good at extracting the topology and the geometry of the input mesh. to do so, authors in [217] have introduced a method for free form skeleton driving mesh deformations. The aim of these methods is first to extract the skeleton of the 3D object to deform then applying the desired modification. In [217] authors have first extracted the Voronoi-based skeletal mesh from a given original mesh, then the extracted skeletal is deformed using free form deformations finally the shape is reconstructed based on the deformed skeletal mesh. Figure 1.34 presents a description of the proposed method for skeleton-based mesh deformation.

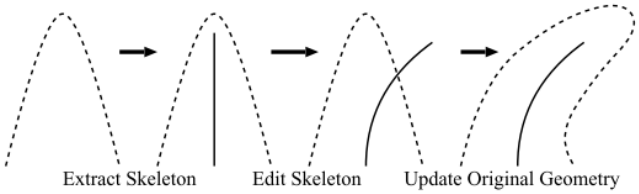

Figure 1.34: Skeleton based mesh deformation. From [217]

7 Conclusion

This chapter initially provides a brief overview about the analysis of the aesthetic quality of faces. As we have four main axes of research, the first one was dedicated to presenting the history of facial attractiveness and the canons used to assess the aesthetic quality of faces. The second axis presented the first part of the analysis using 2D faces that were widely used before starting to work with 3D models. In this axis, we have started by conducting a literature review about the existing methods for 2D face detection on an image, then presenting the existing approaches for 2D facial landmarks detection in order to be able to analyze the aesthetic quality

of 2D faces using the beauty canons defined by the literature studies. From the information described in this subsection, we have concluded that the step of detecting the facial landmarks is a critical one especially when a large number of facial landmarks is needed, and that the results of further analysis depends on the accuracy of the detection, therefore, there is a need for a new method that can detect a large number of landmarks with more accuracy.

The third axis was dedicated to the analysis of facial beauty for 3D face models. Different to the previous axis, we have started by conducting a literature review on the existing methods for 3D face preprocessing to normalize its pose and orientation, this step is necessary as the existing 3D face databases and even in one database, faces don't have the same norms pose and orientation. Later, another literature review was conducted on the existing method for localizing the 3D facial landmarks, and finally the 3D facial attractiveness was analyzed using the same beauty canons used in the 2D part in addition to the analysis of the profile side of the 3D face. From this subsection, we have concluded that there is a need for new method to extract the 3D landmarks on both the frontal and the profile side of 3D the face, moreover this method have to localize a large number of landmarks in order to get efficient results of attractiveness analysis.

In the last axis, we have presented a brief review about the existing approaches for improving the aesthetic quality of 3D faces. The purpose of this part was to visualize the results of applying the beauty canons to 3D faces. Thus robust, fast and geometric details preserving method is needed, this was satisfied using the free form technique for 3D mesh editing.

Chapter 2: 2D facial aesthetic quality analysis

- Manal EL Rhazi, Arsalane Zarghili, Aicha Majda, Ayat Allah Oufkir, Anissa Bouzalmat **" Facial beauty analysis by age and gender."** Int. J. Intelligent Systems Technologies and Applications, Vol. 18, Nos. 1/2, 2019.

- Manal EL Rhazi, Arsalane Zarghili, Aicha Majda **"Comparative Study of Harris and Active Contour Using Viola-Jones Algorithm for Facial Landmarks Detection."** ACMLIS'17 International Conference, Tétouan 19 Mai 2017.

- Manal EL Rhazi, Arsalane Zarghili, Aicha Majda **"Comparative Study of Harris and Active Contour Using Viola-Jones Algorithm for Facial Landmarks Detection."** Transactions on Machine Learning and Artificial Intelligence Vol5, No4, 2017.

1 Introduction

Image analysis is a very rich and active research subject in the field of shape analysis and computer vision. Numerous facial analysis uses have been developed in a number of applications such as authentication, human-machine interfaces, medical diagnosis and treatments...etc. In fact, particular attention has been given to facial images, since they are the part of the body that provides the greatest amount of information about the person [218] such as his: identity, intentions, health and emotional states, attractiveness, age, gender and ethnicity.

Lately, the well-established applications on the face have been facial recognition and facial expression analysis [218]. Although, the analysis of the aesthetic quality of the face has always been a long-standing and debated issue [219][28] due to the various perceptions of attractiveness by individuals.

In this chapter, we suggest a new methodology to analyze the aesthetic quality of 2D faces. The first step to achieve this purpose is to detect the face zone on an image, in our thesis this step is realized using an approach based on the localization of the facial skin. This method has shown interesting results. Indeed, it consists of detecting the pixels that belong to the facial skin zone and those that are not, as a result, the face zone will be extracted from the background. The second step is the localization of the facial landmarks, first of all the facial axes (Eyes axis, nose axis, mouth axis and median axis) are detected using the gradient information variations of the image, this allows us to create rectangles around the facial features to limit the research zone for the landmarks. Then we apply the active contour (Snake) to the whole face and in the drawn rectangles and we detect the intersection of its points with the detected axes belonging to skin zone.

The final step is to study and analyze the attractiveness of the face. Using the detected landmarks, a number of distances and ratios are calculated in order to perform a comparison to the beauty canons cited in the literature and give a result of the analysis with the necessary modification that can enhance the aesthetic quality of the analyzed face.

In brief, the suggested methodology for facial beauty analysis is mainly based on the facial landmarks and proportions detection from a frontal, neutral face, in our specific case 19 landmarks were localized which will be used to evoke and apply the facial beauty canons cited in the previous chapter, by calculating the appropriate distances and ratios then compare it to those of references mentioned in the state-of-the-art canons (see Chapter 1, Section 3.1, 3.2, 3.4). Figure 2.1 describes the proposed approach for the detection and localization of facial landmarks, landmarks and the result of the facial aesthetic quality analysis.

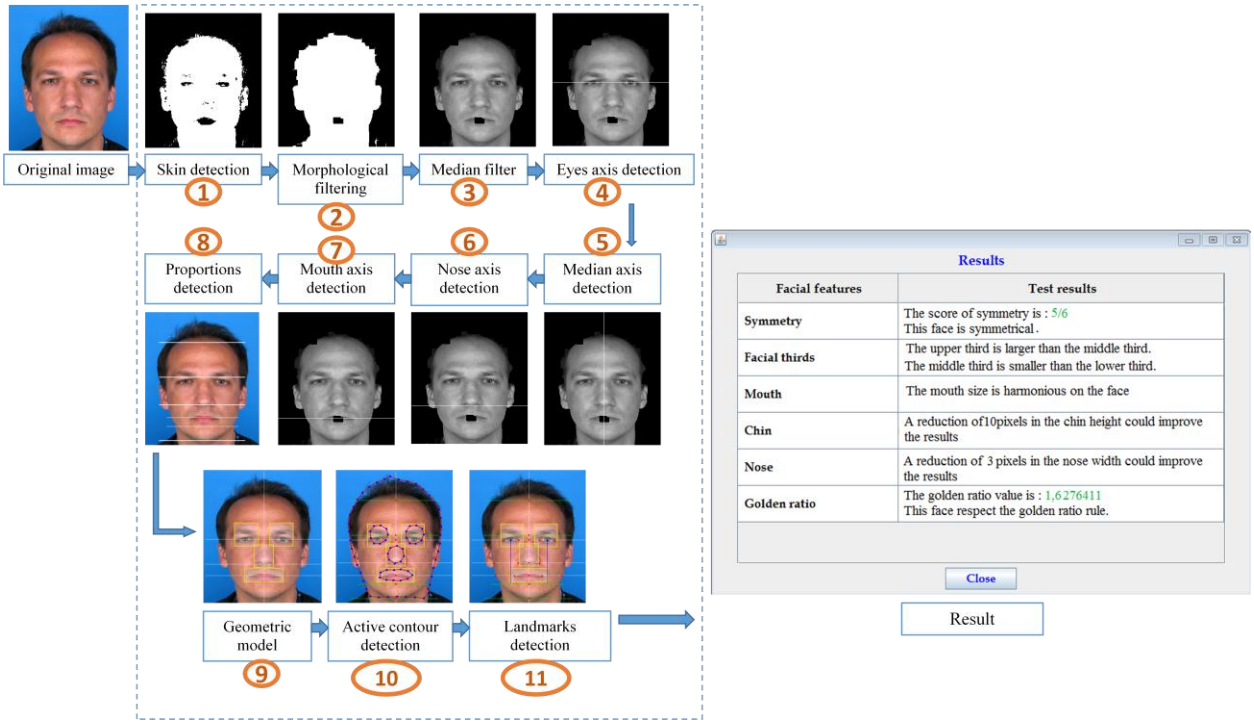

Figure 2.1: Global architecture of the proposed method to analyze the aesthetic quality of faces.

2 2D face detection

Detecting the face on 2D image has received a great attention and many approaches have been proposed to overcome the different problems that can be occurred during the detection process as well as to achieve an accurate localization results. In our thesis, the first step to analyze the aesthetic quality of a face is to detect the face zone in the given image, for this purpose, we propose to localize this zone using the information provided by its color. In fact, it is well known that the image color does not rely on the face pose, skin tones or even the condition of illumination, and each pixel on the image can be represented by a 3 dimensional vector describing its color.

Authors in [220] and [221] have claimed that the color of the skin can be localized in a small interval in the color space of the image, which makes it easy to define a threshold determining the skin zone and non-skin zone on a given image.

2.1 Skin color models

As mentioned before, the skin color can be localized in a short interval in each color space, and then to extract the pixel that belongs to the skin part on the image, a threshold has to be defined to classify the skin pixels and the non-skin pixels. Different spaces of color can be used for that purpose and to represent the pixel's color, each one has its limitation and strength [222]. To classify the pixels of an image into skin and non-skin zones, the most used technique is the histogram; the classification using the histogram allows modeling the skin class based on learning from examples; for a given set of 2D images, the skin pixels are labeled. Indeed, for each labeling step during the learning phase, the probability that the current pixel color is part of

the skin is incremented. This process builds a histogram of the skin color, which can be seen in another way as a probability distribution of the skin color. After the learning stage, a pixel is considered as part of the "skin" class if the value of the model histogram of the color is higher than a specified threshold. Authors in [223] have claimed that modeling the skin pixels using the histogram is more efficient and fast compared to other methods like Modeling by mixtures of Gaussian laws; in their tests, authors have constructed two models using a set of 6822 2D images selected arbitrarily from the web.

In this section, we will describe four types of color spaces that are well used in the computer vision field. These four types can be regrouped as following:

• The primary spaces that provide the possibility to match any color by mixing appropriate amounts of three primary colors, such as the (R, G, B) and (X, Y, Z) color models.

• The luminance–chrominance spaces where one component represents the luminance and the two others the chrominance, the example of the color space that can be found are: Luv, Lab, YIQ and YUV.

• The perceptual spaces which describe the subjective human color perception using the intensity, the hue and the saturation, such as the HSV color space.

• The independent axis spaces resulting from different statistical methods which provide as less correlated components as possible.

In the following subsections, we will discuss in detail some of the color spaces that are widely used, these spaces include the models: the RGB model, the XYZ model, the CMYK model, and the HSV model.

2.1.1 RGB model

The RGB model assembles the primary lights of the Red, Green and the blue together hence the name came from. By mixing these primary colors, we can get a large variety of colors. The RGB color model is also called an additive color model as the combination of the three primary lights with the same quality produces the white light, otherwise different colors as shown in figure 2.2.

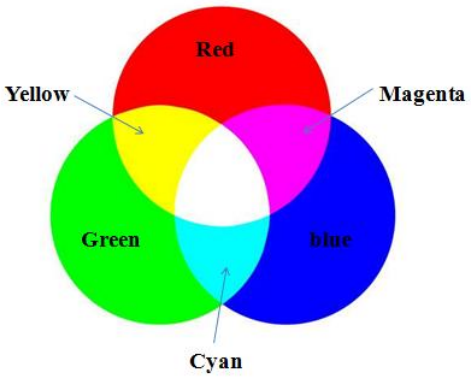

Figure 2.2: representation of the primary colors combination

The RGB color model is often geometrically represented by a cube, where the three main axes correspond to the primary colors; Red, Green and Blue (Figure 2.3). The RGB color model

is considered the most used in the studies based on the analysis and the recognition of the colored images.

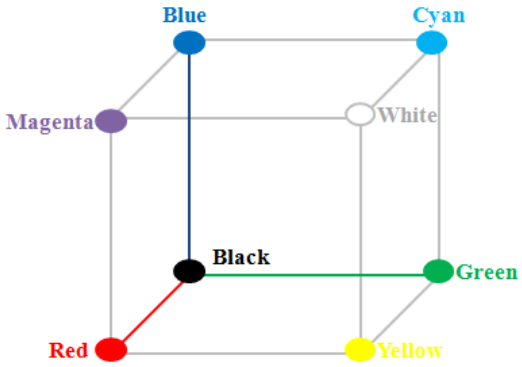

Figure 2.3: The RGB color Cube

2.1.2 XYZ model

The XYZ color model was created by the CIE (International Commission on Illumination) in 1931 that has also created the RGB color model. The XYZ color model was actually derived from the RGB model. The CIE XYZ color model has introduced the notion of luminance a subjective luminous intensity independent of the color, which is represented by the component Y. In addition to Y, the XYZ color model uses two other components X and Z, chosen to have always positive values to describe visible colors. The CIE xyY color space can perfectly separates the notions of luminance Y and chrominance xy and considered to be as a color-independent sensation of intensity.

2.1.3 CMYK model

The CMYK color model is also referred to as the subtractive color model because inks "subtract" the colors red, green and blue from white light. The CMYK color model represents four basic inks: Cyan, Magenta, Yellow and the Key color Black that is produced by the following: White light minus red leaves cyan, white light minus green leaves magenta, and white light minus blue leaves yellow. See Figure 2.4.

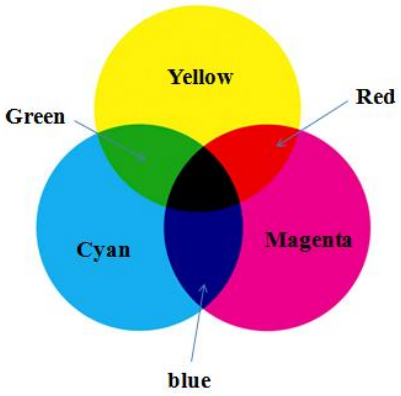

Figure 2.4: CMYK color model

Contrary to the additive color model RGB where the white color is the result of the combination of all primary colors on a black background, the result of combination for the CMYK color model is the black color on a white background.

2.1.4 HSV model

The HSV color model (Hue, Saturation, and Value) is considered the closet color model to the way humans perceive the colors, and an alternative to the RGB color model.
The HSV color model describes color (Hue) using the shade (Saturation) and the brightness (Value). It is very used in computer vision and images analysis and editing.

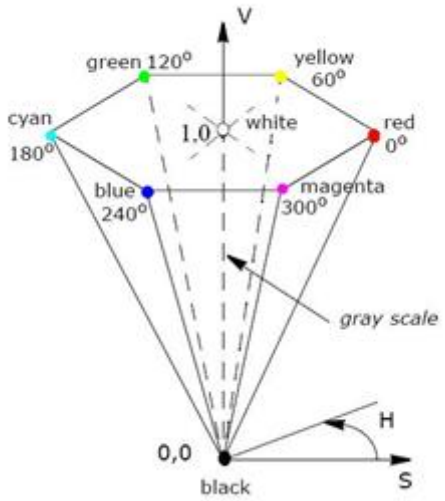

Figure 2.5: HSV color model representation

HSV color model can be represented using a cone as shown in Figure 2.5, the Hue varies from 0 to 360 degree with red at 0 degree, green at 120 degree, blue at 240 degree and magenta at 300 degree. The Saturation component varies from 0 to 100% and the Value component varies from 0 to 100%.

2.2 The proposed method for face zone detection

2D face detection is a key step in many image analysis processes as the more the detection is accurate, the more the analysis is reliable. In our case of the analysis of facial aesthetic quality, the detection of the skin zone has to be efficient as much as possible as a long process of detection is following this first step where each step depends on the previous one.

To detect the face zone on a 2D image based on the skin color, we used a method composed of two main steps; the first step is the detection of face area using the HSV color model proprieties, then the second step is the refinement of the obtained results using morphological filters such as: dilatation, erosion and median filter. The following figure 2.6 presents an overview of the proposed method to detect the face zone on a 2D image.

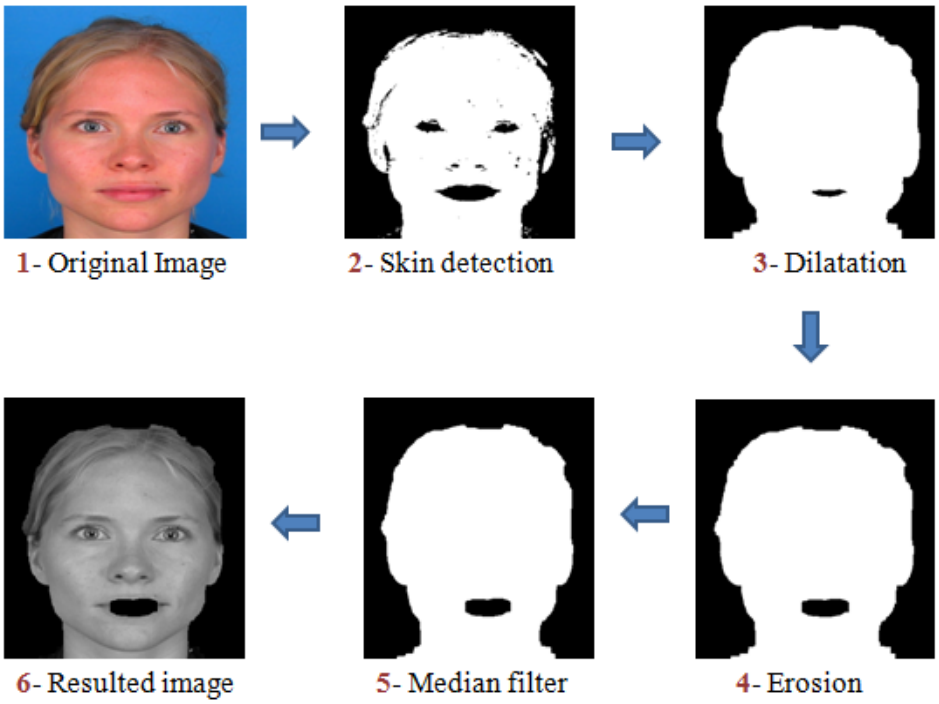

Figure 2.6: Face zone detection steps

2.2.1 Face detection using the skin color proprieties

Detecting the facial zone using the color segmentation based on the skin color proprieties, has been widely used in many studies in the literature [224][225], and has proved to be an efficient and fast method of detection.

To localize the face zone using the skin color proprieties, we have tested the proposed method on two face databases; the FEI database and Utrecht ECVP dataset. The proposed method consists of using the HSV color model to classify the different pixels of the image into the skin or non-skin pixels, consequently, extracting the face zone from the image background. We have chosen the HSV color model for that purpose as it is known by its good results of discrimination between the skin and the non-skin pixels, it is also known by its efficiency compared to other color models such as the RGB model [226]. Moreover, in the HSV color model the threshold used to classify the image's pixels into skin and non-skin pixels is well defined in the literature [225][227][228].

2.2.2 FEI database

The FEI is a Brazilian face database that contains a set of face images taken at the Artificial Intelligence Laboratory of FEI in São Bernardo do Campo, São Paulo, Brazil. There are 14 images for each of the 200 individuals. All images are taken against a white homogenous background in an upright frontal position with profile rotation of up to about 180 degrees, the original size of each image is 640x480 pixels [229]. Figure 2.7 shows an example of the images from the FEI database.

Figure 2.7: Example of images from FEI database

2.2.3 Utrecht ECVP database

The second database used is the Utrecht ECVP face database; it contains 131 images of 49 men and 20 women, [230] Usually in a neutral and smile of each. It was collected at the European Conference on Visual Perception in Utrecht in 2008, with a resolution of: 900x1200. Figure 2.8 shows an example of the images from this database.

Figure 2.8: Example of images from ECVP database

2.2.4 Skin zone detection based on HSV color model

In this subsection, we aim to detect the facial skin pixels using the proprieties of the HSV color model [13]. In RGB, we cannot separate color information from luminance, while in HSV or Hue Saturation Value, we can separate image luminance from color information. Indeed, using the HSV color model, we can extract the pixels Hue independently of their brightness

Value, thus as we have the images represented in the RGB color model, conversion from RGB to HSV model is needed. To perform such conversion the following formulas describe the corresponding values of each HSV component in the RGB model.
To get the Hue "H" value, we find the largest color channel of the R, G, B, values. The smallest two are subtracted off and divided by the difference between the largest and the smallest. We then normalize the hue by adding 0, 2, or 4. The resulting H is any real number. However, any arbitrary number below 0 and above 6 is considered redundant, and it may as well derive a value H mod 6, then (H mod 6) + 6, but it's not necessary, since a relatively decent HSV to RGB conversion algorithm should be able to work with any values of H. (See equation 20).

$$Hue = \begin{cases} undefined & \text{if } \big(\max(\mathrm{R},\mathrm{G},\mathrm{B}) - \min(\mathrm{R},\mathrm{G},\mathrm{B})\big) = 0. \\ \frac{G-B}{\big(\max(\mathrm{R},\mathrm{G},\mathrm{B}) - \min(\mathrm{R},\mathrm{G},\mathrm{B})\big)} & \text{if } \max(\mathrm{R},\mathrm{G},\mathrm{B}) = \mathrm{R}. \\ \frac{B-R}{\big(\max(\mathrm{R},\mathrm{G},\mathrm{B}) - \min(\mathrm{R},\mathrm{G},\mathrm{B})\big)} + 2 & \text{if } \max(\mathrm{R},\mathrm{G},\mathrm{B}) = \mathrm{G}. \\ \frac{R-G}{\big(\max(\mathrm{R},\mathrm{G},\mathrm{B}) - \min(\mathrm{R},\mathrm{G},\mathrm{B})\big)} + 4 & \text{if } \max(\mathrm{R},\mathrm{G},\mathrm{B}) = \mathrm{B}. \end{cases} \quad (20)$$

To obtain the Saturation "S" value, we calculate the difference between the largest and smallest color channel values, divided by the largest color channel value. If the largest color channel value is equal to 0, then the saturation value is 0. (See equation 21).

$$Saturation = \begin{cases} 0 & \text{if } \max(\mathrm{R},\mathrm{G},\mathrm{B}) = 0. \\ \frac{\big(\max(\mathrm{R},\mathrm{G},\mathrm{B}) - \min(\mathrm{R},\mathrm{G},\mathrm{B})\big)}{\max(\mathrm{R},\mathrm{G},\mathrm{B})} & \text{otherwise.} \end{cases} \quad (21)$$

The Value "V" (brightness value) is equal to the brightest color channel as presented in equation 22:

$$Value = \max(\mathrm{R},\mathrm{G},\mathrm{B}) \quad (22)$$

After the conversion of the RGB image to the HSV color model, we need to find the appropriate threshold to classify the image pixels into skin and non-skin pixels. Many authors have investigate this problem in their studies such as authors in [227] and [225] who have proposed a threshold for the values of the Hue "H" and the Saturation "S". As we mentioned previously, the Value "V" component does not affect the process of the skin extraction.
The proposed thresholds for both the saturation and the hue are presented in figure 2.9 and table 2.1.

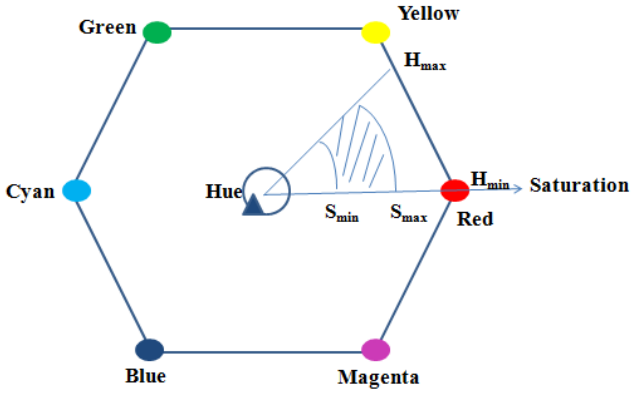

Figure 2.9: Facial skin thresholds in the HS plane

Color channel	Min	Max
Hue "H"	0°	40°
Saturation "S"	0.23	0.69

Table 2.1: Facial skin thresholds proposed by [227]

To achieve our purpose that aims to detect the facial zone on a 2D image, after converting the RGB color image to the HSV color space, we have used very close thresholds to those proposed by [227] as shown in table 2.2. Our proposed threshold for the Hue channel is the same while the Saturation channel is a bit different but still included in the range proposed by [227], using these thresholds we obtained an improved results of skin detection for the both face databases [13].

Color channel	Min	Max
Hue "H"	0°	40°
Saturation "S"	0.25	0.58

Table 2.2: Facial skin thresholds used in our experiments

After choosing the thresholds for the skin color extraction, for each given image in the HSV color model, we segment the image by browsing it pixel by pixel and at each stage verifying if the pixel is included in the range of the skin color as shown in table 2. Therefore, we assign the value 1 to the pixel indicating that this pixel belongs to a skin pixel; otherwise we assign the value 0 indicating that the pixel is a non-skin pixel. The result of this segmentation is a binary image as shown in figure 2.10 for the Utrecht "ECVP" database and figure 2.11 for the FEI face database [13].

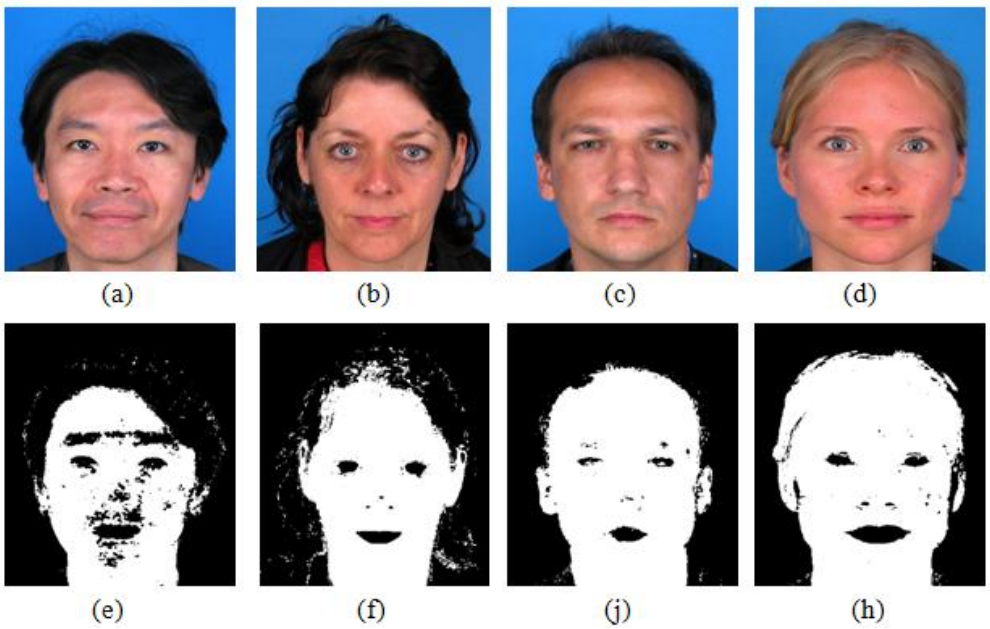

Figure 2.10: Face detection for "ECVP" database: (a), (b), (c) and (d) Original image. (e), (f), (j) and (h) Skin detection

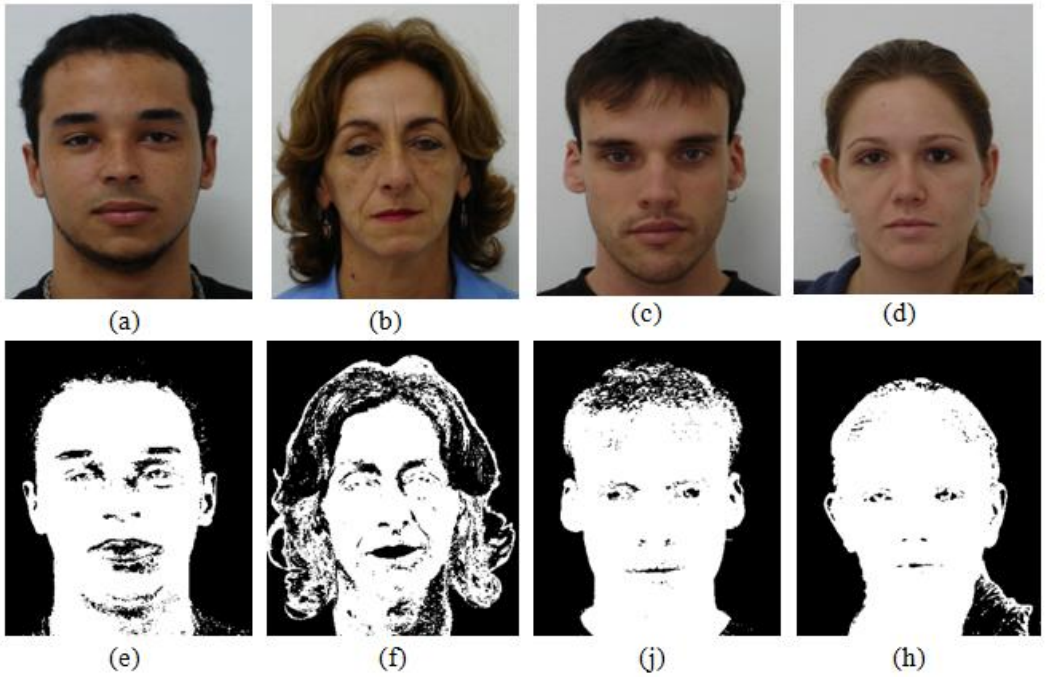

Figure 2.11: Face detection for "FEI" database: (a), (b), (c) and (d) Original images. (e), (f), (j) and (h) Skin detection

As can be seen from the figures above, the pixels in white colour represent the skin zone while the pixels in black represent the non-skin zones. Some facial features like the eyes, the mouth and the nostrils are represented by pixels in black colour because they are not detected as a skin zone. In the other hand, some parts on the face like the hair was detected as a skin zone (figure 2.10 (b)) and (figure 2.11 (j), (h)) and that can be due to the hair colour which is very close to some skin colour.

2.2.5 Skin zone filtering

To improve the results of the skin detection obtained from the previous step, a set of morphological filters followed by a median filter are performed. These filters aim to reduce the false detection zones such as the holes produced by the undetected regions. Thus to achieve that goal, we applied a dilatation then an erosion to the resulted image from the previous step, then finally a median filter is applied to eliminate the noise and make the transitions more homogeneous [13].

a. The morphological filtering

The morphological filtering is applied to the binary image resulted from the skin zone detection step, actually as known, binary images may contain some imperfections especially when it is produced by simple thresholding as in our case, thereafter, some distortion can be produced by noise and texture of the image. Indeed, the morphological filters applied in image processing aim to remove these imperfections by accounting for the form and structure of the image.

In our case, the used morphological filters are based on three operations: the dilatation, the erosion and the concatenation of them known by the closing. These morphological operations use a reference form with which the image signal is compared locally; this form of reference is called the structuring element.

The closing operation smooth the contour of the image fills narrow channels, merges objects close to each other, and fills small holes and gaps. In general, it has the property of filling all the elements in an image smaller than the structuring element. In our tests, we apply a closing with a structuring element acting on the 7 nearest neighbors [231]. The formula of this filter is given as follows in equation 23:

$$Closing(s)(P) = Erosion(s)\,[Dilatation(s)(P)] \qquad (23)$$

Where: P is a pixel in the image.

S is the structuring element.

Erosion (S) represents the erosion of this pixel by the structuring element S.

Dilatation (S) represents dilation with S.

Closing (S) represents the pixel closing by S.

Figure 2.12 and figure 2.13 show the obtained results of the morphological filter for both FEI and Utrecht “ECVP” databases.

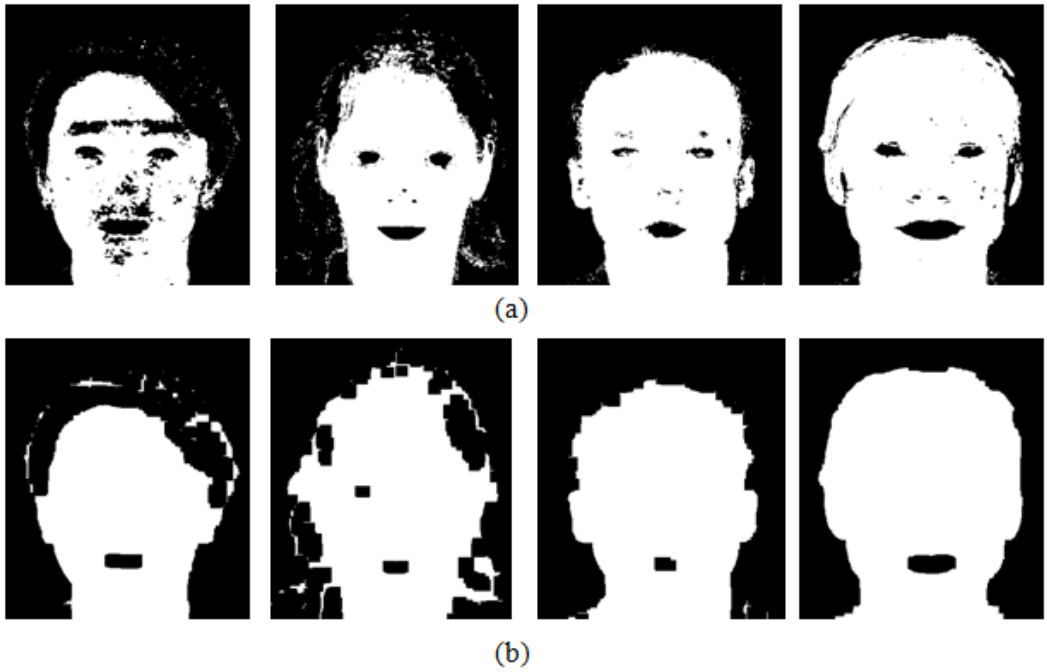

Figure 2.12: Morphological filters for "ECVP" database: (a) before the filtering. (b) After the filtering

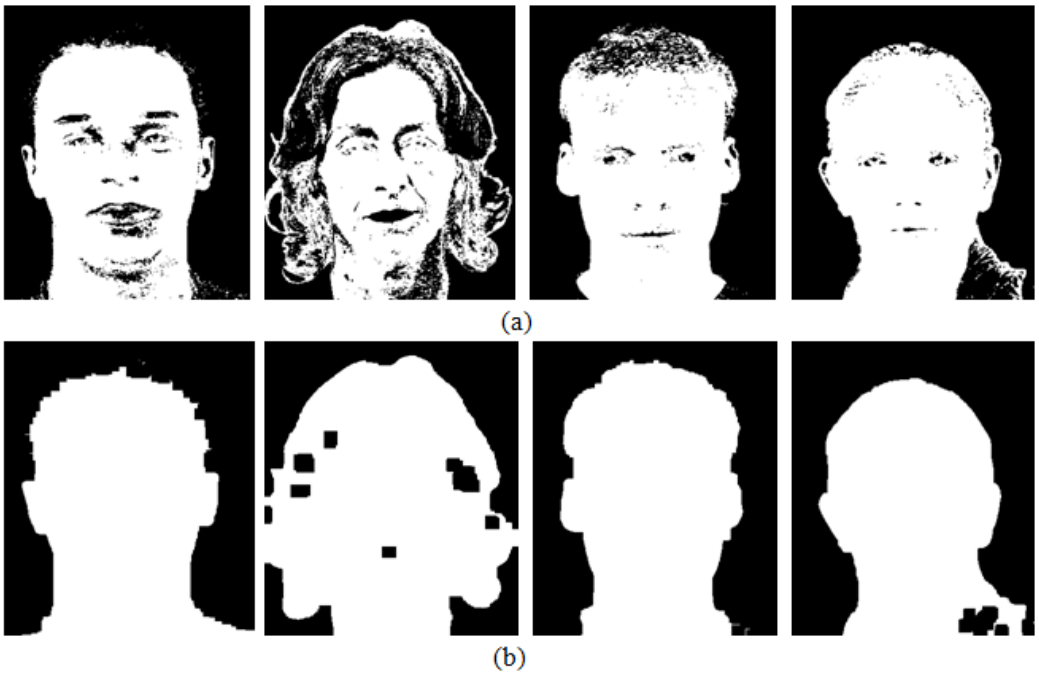

Figure 2.13: Morphological filters for "FEI" database: (a) before the filtering. (b) After the filtering.

After applying the closing to the binary images, we can see that the holes are filled and the small parts detected as non-skin area were merged. However, this morphological filter still insufficient which makes the use of an additional filter (median filter) necessary to improve the results of the face detection.

b. Median filter

The median filter is a method used to reduce noise in an image; it is effective in preserving useful images details. The median filter replaces each pixel by the median of all pixels in a neighborhood, this median is calculated by first sorting all the pixel values from the surrounding neighborhood of the concerning pixel into numerical order and then replacing the pixel being considered with the value of the pixel in the middle.
In our tests, we have used a window of 3*3 to perform the median filter. An example of how the median filter works is presented in figure 2.14.

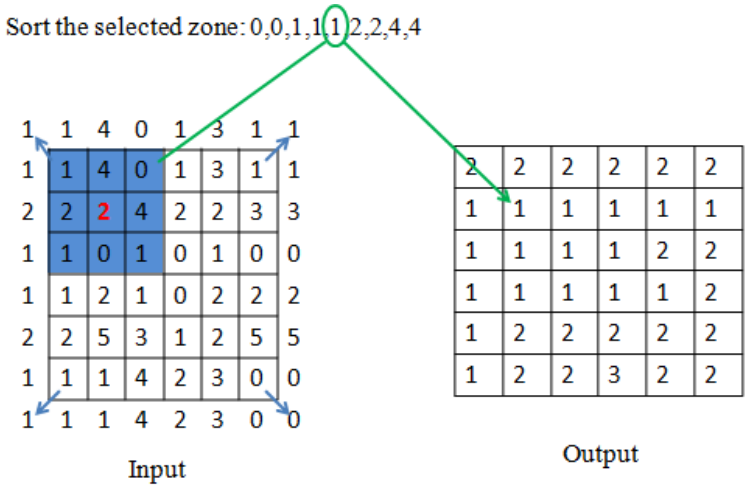

Figure 2.14: Median filter.

The following figures 2.15 and 2.16 present the obtained results after applying the median filter to both the FEI and the Utrecht "ECVP" face databases.

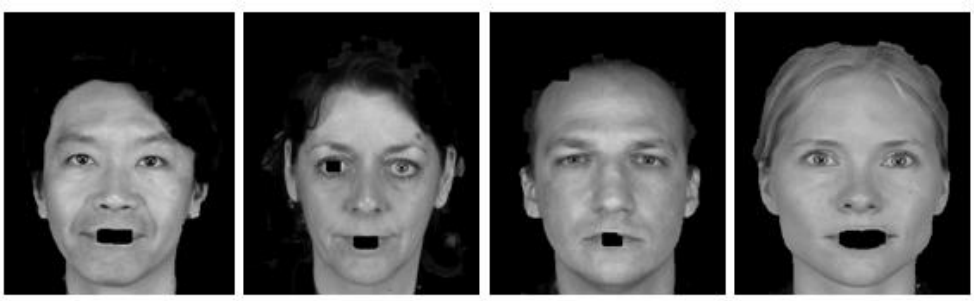

Figure 2.15: Median filter on the "ECVP" database

Figure 2.16: Median filter on the "FEI" database

The obtained results show that the median filter can smooth the region of transitions and fill the holes produced from the segmentation and the morphological steps, which enhance the face zone detection.

3 2D facial landmarks detection

In our thesis, to detect the 2D facial landmarks, many steps have been followed in order to get more accurate detection results and fewer errors. The first step is to detect the facial axes which are the eyes axis, the nose axis, the mouth axis and the median axis; those axes are represented by a number of lines that cross the facial features, the detection of facial axes aims to delimit the facial features zones. After the facial axes detection, the different facial proportions are determined by drawing the lines that specify these proportions. The next step consists of the facial geometric model which is used to draw rectangles around the facial features in order to localize the final research zone of facial landmarks. Once the rectangles are drawn, the active contour (Snake) is applied to the whole face and then to each facial rectangle, furthermore, we detect the intersection of the points given by the active contour and the facial axes, these intersections must be in the skin zone, the resulted intersections are 2D facial landmarks [13].

The following figure 2.17 presents an overview of the proposed method to detect the facial landmarks on a 2D image.

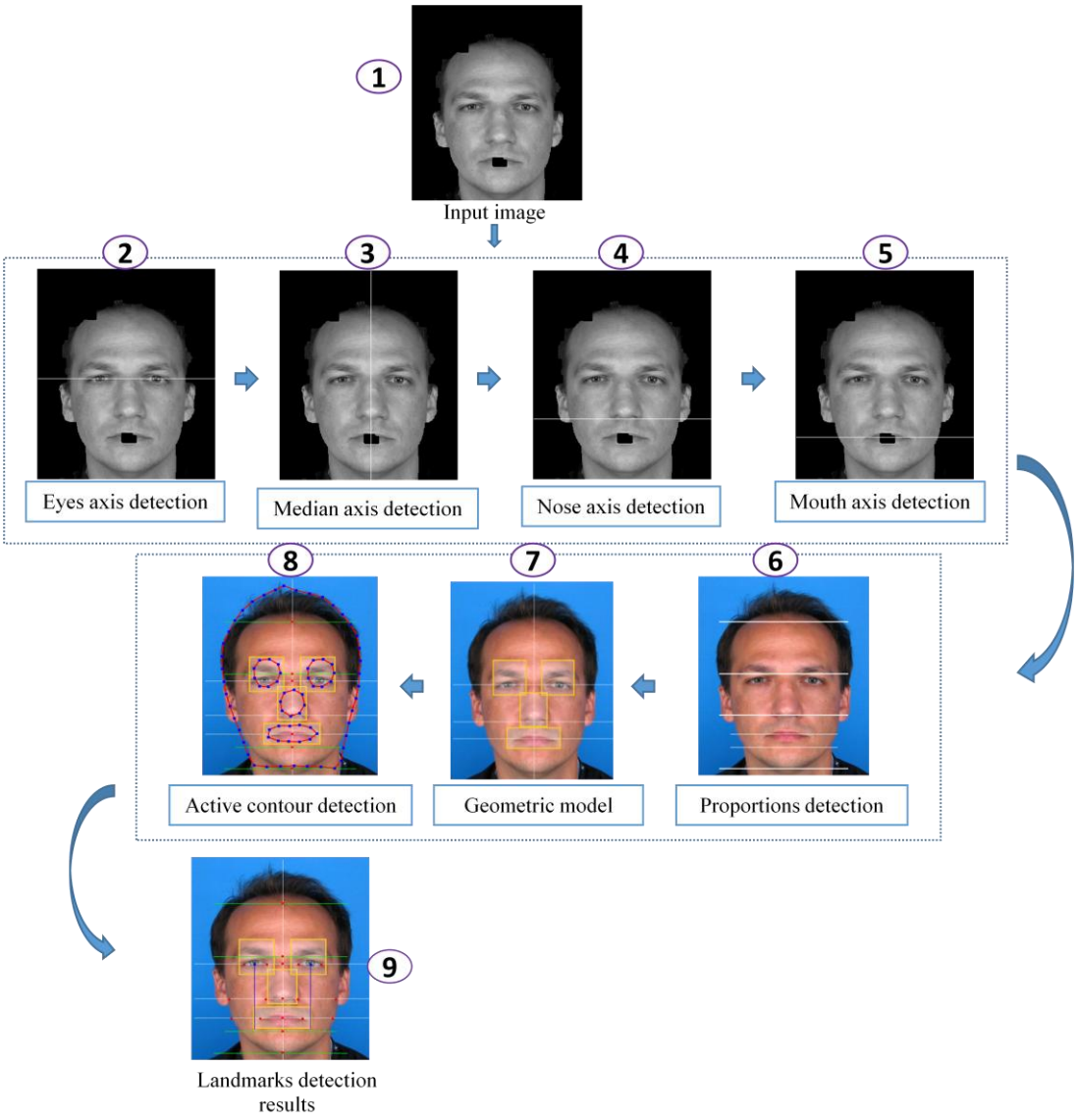

Figure 2.17: 2D facial landmarks detection pipeline.

3.1 Facial axes detection

The detection of facial axis is the first step in the process of the facial landmarks detection. It aims to localize the axes that cross the facial features; the eyes, the nose, the mouth and the median line of the face. Four axes are to be detected; in the following subsections the different steps to detect the facial axes are presented.

3.1.1 Eyes axis detection

The eyes axis (Figure 2.18) corresponds to the line that crosses the two eyes. In our study, to localize the eyes axis in an image, we perform the horizontal projection of the convoluted grayscale image. The reason for choosing the horizontal projection is that it allows us to visualize the different changes in the gradient image [232]. The eyes axis corresponds to the maximum of the resulted projection, it represents several transitions: skin to the eye, white of the

eye to the iris, the iris to the pupil and the same from the other side. In summary, the steps followed to detect the eyes axis are:

1) Convolute the grayscale image I by {-1 0 1} twice and transform the result in absolute value as presented in equation 24:
   $G=| ((I*[-1\ 0\ 1]) * [-1\ 0\ 1]) |$ (24)

2) Horizontal projection of G in given by equation 25:
   $H(y) = \sum_{x=0}^{n-1} G(x, y)$ (25)

3) Find the maximum of the horizontal projection of G.

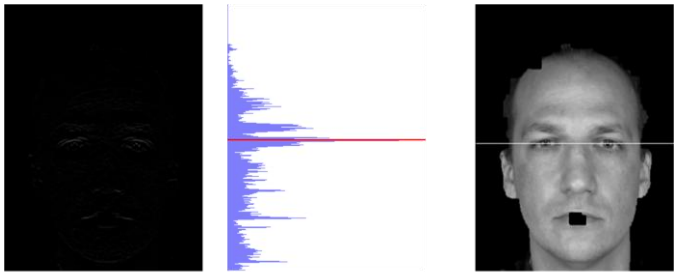

Figure 2.18: Eyes axis detection on an example from the "ECVP" database (a) convoluted image. (b) Image horizontal projection. (c) Eyes axis detection.

As can be seen from Figure 2.18, after performing the image gradient and the horizontal projection Figure 2.18 (b), the curve maximum corresponds to the eyes axis.

3.1.2 Median axis detection

The median axis corresponds to the line that divides the face into two equal parts, to localize the median axis, we use the results obtained from the detection of the eyes axis, indeed, the median axis (Figure 2.19) corresponds to the middle of the area having the maximum change of gradient on the eyes axis [232]. As it is known, the two parts on the left and the right of both the left eye and the right eye respectively have fewer changes in the gradient representation, unlike the eyes part that are characterized by a great gradient change. Finally, the area between the two eyes has an important gradient change because it contains the maximum of the facial skin; this area corresponds to the median axis.

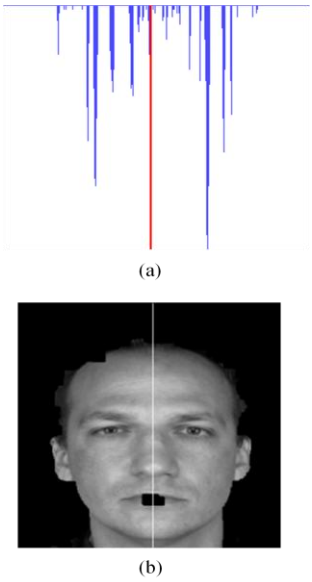

Figure 2.19: Median axis detection on an example from the "ECVP" database (a) Eyes axis gradient. (b) Median axis detection

3.1.3 Nose axis detection

To localize the nostrils axis, we found the line that has the minimum of the skin pixels pixel below the eye axis, and around the median axis [232] using about 18 pixels in width, as shown in Figure 2.20, the nostrils axis can be drawn using the vertical projection of the determined area, and then we detect the minimum of the image gradient curve. The result corresponds to the nostrils axis.

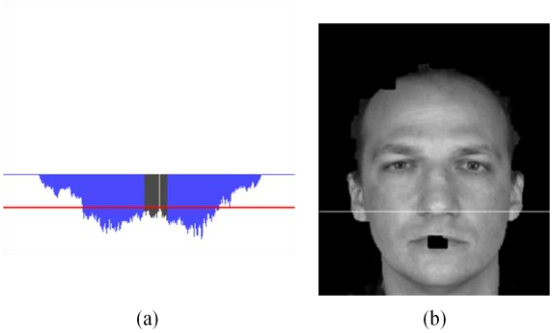

Figure 2.20: Nose axis detection on an example from the "ECVP" database (a) Image vertical projection. (b) Nose axis detection.

3.1.4 Mouth axis detection

To detect the mouth axis, we use the same methodology used to localize the eyes axis, and then we found the line which has the highest gradient below the eyes axis [232], as shown in Figure 2.21. This line corresponds to the mouth axis.

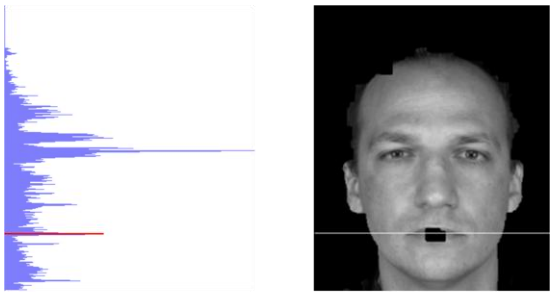

Figure 2.21: Mouth axis detection on an example from the "ECVP" database (a) Image horizontal projection. (b) Mouth axis detection.

The last axes to detect are those that define the facial proportions. Indeed, the detection of facial proportions is based on dividing the face into thirds that must be equal in the perfect case; the upper third extends from the hairline to the glabella, the middle third starts from the glabella to the subnasale, and lower third extends from the subnasale to the chin tip.

The lower third is further divided into thirds: the upper third from the subnasale to stomion, middle third from stomion to the sublabiale crease, and the lower third from the sublabiale crease to the chin tip [71]. Figure 2.22 shows the location of the main point associated to the facial proportions.

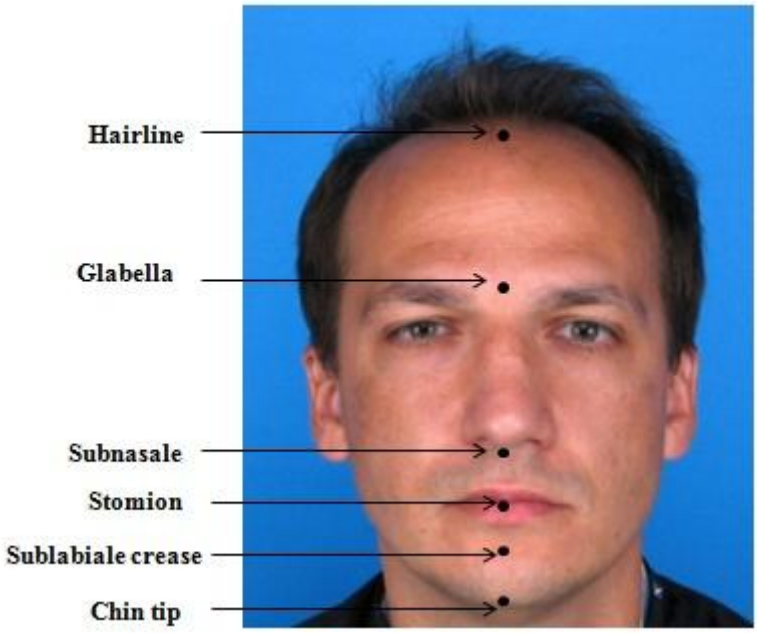

Figure 2.22: Facial proportions landmarks.

3.2 Facial geometric model

Once the axes of facial features are located, we applied the facial geometric model proposed by [233], which allowed us to draw rectangles that surround the facial features (figure 2.23), the model is defined as:

- The vertical distance between the eyes and the centre of the mouth is D.
- The vertical distance between the eyes and the centre of nostrils is 0.6D.
- The mouth width is D.
- The nose width is 0.8D
- The vertical distance between the eyes and eyebrows is 0.4D.

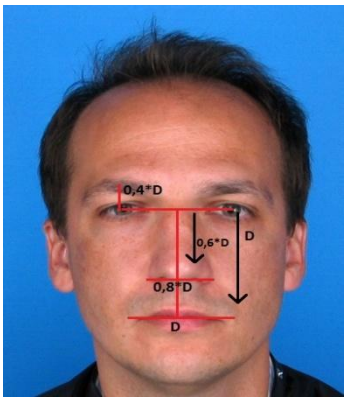

Figure 2.23: Facial geometric model

To draw rectangles that encompass the facial features (eyes, nose and mouth), the coordinates are given by the following formulas, equation 26-33:

1. Rectangle of the mouth:

- Coordinates of the lower left corner:

$$\left(x.median\ axis + \frac{D-1}{2}\ ,\ y.mouth\ axis + \frac{(0.4*D)-1}{2}\right) \quad (26)$$

- Coordinates of the top right corner:

$$\left(x.median\ axis - \frac{D-1}{2}\ ,\ y.mouth\ axis - \frac{(0.4*D)-1}{2}\right) \quad (27)$$

2. Rectangle of the nose:

- Coordinates of the lower left corner:

$$\left(x.median\ axis + \frac{(0.4*D)-\frac{1}{2}-1}{2}\ ,\ y.nose\ axis + (0.1 * D)\right) \quad (28)$$

- Coordinates of the top right corner:

$$\left(x.median\ axis - \frac{(0.4*D)-\frac{1}{2}-1}{2}\ ,\ y.nose\ axis - (0.5 * D)\right) \quad (29)$$

3. Rectangle of the left eye:

- Coordinates of the lower left corner:

$$(x.median\ axis - (0.75 * D)\ ,\ y.eyes\ axis + (0.2 * D)\ ) \quad (30)$$

- Coordinates of the top right corner:

$$(x.median\ axis - (0.2 * D)\ ,\ y.eyes\ axis - (0.45 * D)\ ) \quad (31)$$

4. Rectangle of the right eye:

- Coordinates of the lower left corner:

$$\left(x.median\ axis + (0.75 * D)\ ,\ y.eyes\ axis + (0.2 * D)\right) \quad (32)$$

- Coordinates of the top right corner:

$$(x.median\ axis + (0.2 * D)\ ,\ y.eyes\ axis - (0.45 * D)\ ) \quad (33)$$

Figure 2.24 shows the obtained results after performing both the facial geometric model and drawing of the features rectangles:

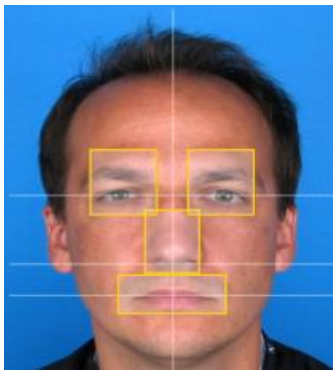

Figure 2.24: Facial rectangles on an example from the "ECVP" database

3.3 Facial landmarks detections

After the localization of facial features and surrounding them by rectangles to limit the areas of research, the next step is to detect the facial landmarks. To achieve that purpose, many approaches have been proposed in the literature (see Chapter 1), in our thesis we first used the anthropometric model of the face [234] to detect 3 landmarks: the sublabiale, the forehead and the nasion which intersect with the median axis, this model assumes that the distances between the facial landmarks are proportional to the vertical distance between the mouth and eyes which is given by the geometric model of the face.

The mouth, nose and the two eyes centre are detected by the intersection of their axis and median axis.

The detection of facial landmarks in the field of facial aesthetic quality analysis is a very sensitive step as the results of the analysis depends of the accuracy the landmarks detection, and since the anthropometric model used before cannot produce the accurate needed facial landmarks, we used the edge detector active contour (Snake) [235]. First, the snake is applied to the entire face to detect its edge, and then it is applied to the determined rectangles to detect the edges of the facial features, thus localize the remaining landmarks.

3.3.1 Combining the active contour with the facial geometric model

The active contour (Snake) is a spline that minimizes the energy; it is directed by external constraint forces, and influenced by image forces that pull it toward features in the form of lines or edges. The basic idea is to bring the points closer to high gradient zones while maintaining certain characteristics such as the contour curvature and the point's distribution.

The used algorithm for this purpose is Greedy [236] known for its speed of execution. The function used in the algorithm is given by equation 34:

$$E_{snake}(i) = (\alpha(i)E_{continuity} + \beta(i)E_{curvature} + \gamma(i)E_{image}) \quad (34)$$

While

α, β, γ = weights according to the term importance. In our study: α = 1, β = 1, γ = 1.

i = index of a point on the snake.

Finally, to localize the facial landmarks (Figure 2.25), we find the intersection of the snake points and the facial axes already detected. These points of intersection must be in the skin area.

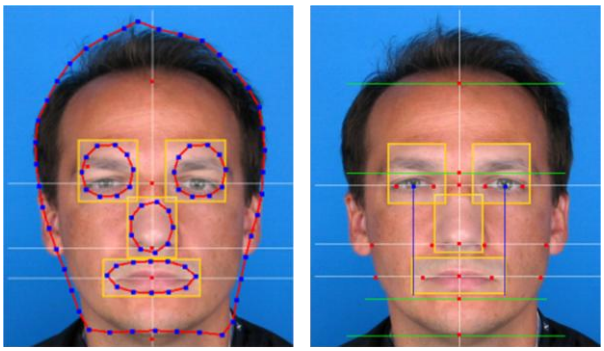

(a) (b)

Figure 2.25: Landmarks detection on an example from the "ECVP" database (a) Snake detector on face. (b) Corners detection

To evaluate the accuracy of our proposed approach for facial landmarks detection, we compared the obtained results to those obtained by a competing method in the literature, in our case we choose the Harris operator approach, which is known by its good results of detection. So after applying the cascade classifier proposed by CascadeObjetDetector of the package vision in Matlab to detect the facial features areas: eyes, nose and mouth. The Harris operator is performed to localize the facial landmarks.

We made statistics on the success rate of the detection for both our proposed approach and the Harris operator method. The two methods were applied to both the "ECVP" Utrecht database and FEI face database, and the results are shown in table 2.3 and table 2.4:

Facial features corners	Success rate of the proposed method	Success rate of Harris approach
Eyes corners	97%	96%
Nose corners	95%	77%
Mouth corners	89%	86%
Chin point	90%	Not allowed
Forehead point	85%	Not allowed
Cheeks extremities	71%	Not allowed

Table 2.3: Success rate of facial corners detection by our system and the competing method using ECVP database

Facial features corners	Success rate of proposed method	Success rate of Harris approach

Eyes corners	94%	92%
Nose corners	89%	81%
Mouth corners	91%	88%
Chin point	83%	Not allowed
Forehead point	80%	Not allowed
Cheeks extremities	65%	Not allowed

Table 2.4: Success rate of facial corners detection by our system and the competing method using FEI database

As remarked from the two tables, the competing method Harris detect only some corners on a specific zones on the face (eyes, nose and mouth) and it does not offer some the other corners like those of the forehead, the chin and the cheeks extremities which are necessary for the analysis of facial attractiveness.

4 2D facial aesthetic quality analyses

The analysis of a 2D facial aesthetic quality is the final step in the proposed work in this chapter; it consists of determining if the given face complies with the beauty canons defined in the literature. For that purpose, after the detection of facial landmarks, we first verify if the face meets the beauty canons which are: the facial symmetry, the golden proportions and the neoclassical proportions by calculating a set of ratios and distances and then compare the obtained results to the state of the art of each canon.

In a special case we analyzed the aesthetic quality of 2D faces and then we tried to categorize the results by age and gender. This means we analyzed different faces belonging to males and females then to young and old people and we tried to figure out the major difference that can exist between these categories. In general, how can gender (men/women) and age (young/old) influence the facial aesthetic quality? [13]

4.1 Facial beauty canons verification

The facial aesthetic quality analysis performed by our system [13] is based on what has been explained previously; for a given face, we localize the regions of interest and their landmarks then we verify whether the face meets the beauty canons or not. An attractive face should respect these canons [40] [42] [39], in our thesis, the following canons were applied:

- The symmetry:

The rule of facial symmetry is easy to verify. The face is divided into regions and for each region, the located landmarks are organized as points pairs and then put into our symmetrization system to calculate the score of the symmetry using the horizontal distances from the median axis. In our case, we took 12 measures (the eyes corners, the nose corners, the mouth corners and the cheeks points); hence the score of symmetry will be noted on 6.

- The golden ratio:

The golden ratio is calculated from the axes that pass through the facial features (eyes axis, nostrils axis and the mouth axis). We calculate the ratio between two distances consecutively, in total we have 4 ratios to calculate. The first ratio is calculated from the forehead point to the chin tip and from the eyes axis to the chin tip, the second ratio is from the eyes axis to the chin tip and from the eyes axis to the mouth axis, the third ratio is calculated from the eyes axis to the mouth axis and from the eyes axis to the nose axis, and the last ratio is calculated from the width of the mouth and the nose width. The calculated ratios are shown in table 2.5.

Number of the golden ratio	Description
1	(forehead point to chin tip) / (eyes axis to chin tip)
2	(eyes axis to chin tip) / (eyes axis to mouth axis)
3	(eyes axis to mouth axis) / (eyes axis to nose axis)
4	Mouth width / nose width

Table 2.5: description of the used Golden ratios

The average of these ratios is then calculated and compared with the golden ratio value: 1.618, when the average is equal to this value or even very close to that number in a specific range, we say that the face meets the golden ratio canon. And if the average is outside that range, then the face does not respect it, thus some modifications are needed to enhance the attractiveness of the face.

For other beauty canons (vertical fifths, horizontal thirds, width of the mouth and the height of the chin), we calculate the different distances and we verify their values by comparing them to the mentioned references in the state of the art of facial attractiveness. The set of the neoclassical proportions verified in our study is shown in table 2.6.

Number of neoclassical proportions	Description
1	Forehead height = nose length = lower face height

2	Face width = 5× nose width
3	Interocular distance = nose width
4	Interocular distance = eye fissure width
5	Mouth width = interpupils distance
6	Chin height = 1/3 of the lower face height

Table 2.6: description of the used neoclassical proportions

4.2 2D facial aesthetic quality analysis

To test our proposed method by gender (men / women), we used the "Utrecht ECVP" and the "FEI" databases that contains images of the two genders. We chose an image as input to the system and as output we obtain the analysis results of its aesthetic quality.

- Women:

First, we tested our proposed method in this thesis to analyze the aesthetic quality of faces of both male and female faces from the "ECVP" database; the results are shown in the following figures. Figure 2.26 represents the obtained results of beauty analysis for women, and figure 2.27 represents the obtained results for men's facial beauty analysis.

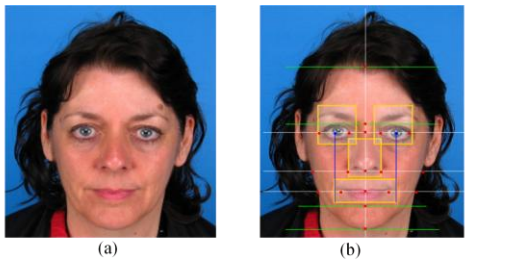

(a) (b)

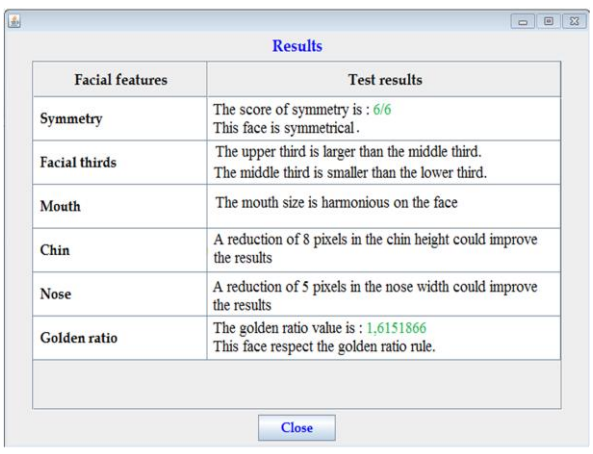

Results

Facial features	Test results
Symmetry	The score of symmetry is : 6/6 This face is symmetrical.
Facial thirds	The upper third is larger than the middle third. The middle third is smaller than the lower third.
Mouth	The mouth size is harmonious on the face
Chin	A reduction of 8 pixels in the chin height could improve the results
Nose	A reduction of 5 pixels in the nose width could improve the results
Golden ratio	The golden ratio value is : 1,6151866 This face respect the golden ratio rule.

Close

(c)

(a) (b)

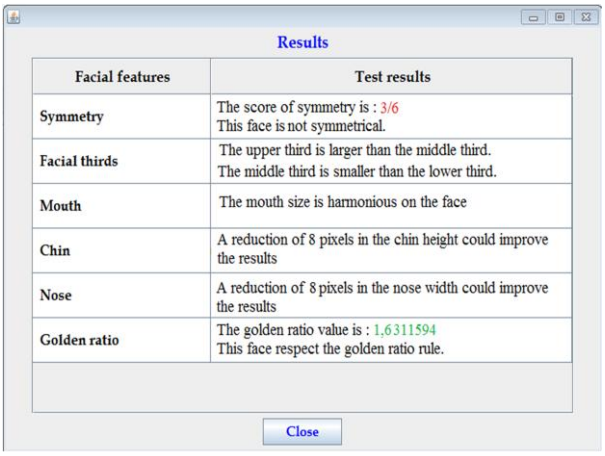

Results

Facial features	Test results
Symmetry	The score of symmetry is : 3/6 This face is not symmetrical.
Facial thirds	The upper third is larger than the middle third. The middle third is smaller than the lower third.
Mouth	The mouth size is harmonious on the face
Chin	A reduction of 8 pixels in the chin height could improve the results
Nose	A reduction of 8 pixels in the nose width could improve the results
Golden ratio	The golden ratio value is : 1,6311594 This face respect the golden ratio rule.

Close

(c)

Figure 2.26: facial attractiveness analyses for women on an example from "ECVP" database (left) and from "FEI" database (right) (a) Original image. (b) Corners detection. (c) Analysis result.

- Men:

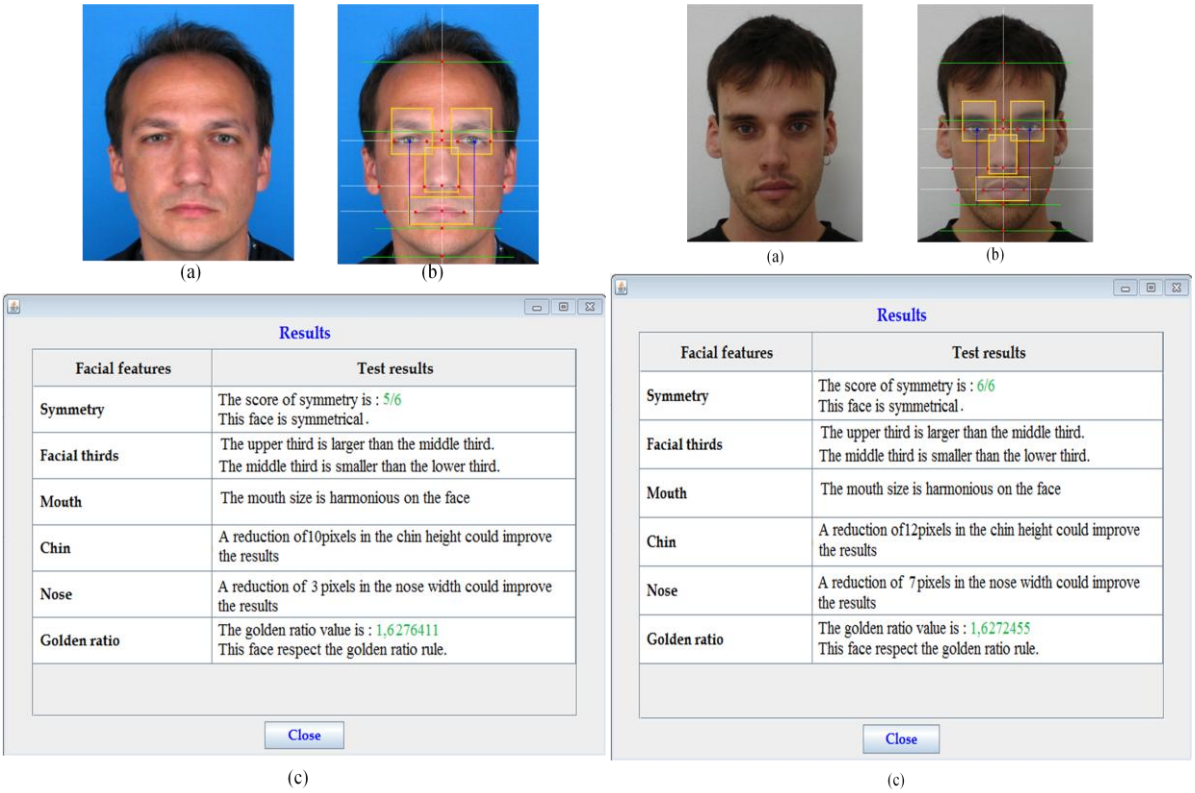

Figure 2.27: facial attractiveness analyses for men on an example from "ECVP" database (left) and from "FEI" database (right) (a) Original image. (b) Corners detection. (c) Analysis result.

In the other hand, we tested our proposed method to analyze the aesthetic quality of faces of both old and young people from the same database, the results are shown in the following figure 2.28 and figure 2.29.

- Old individuals:

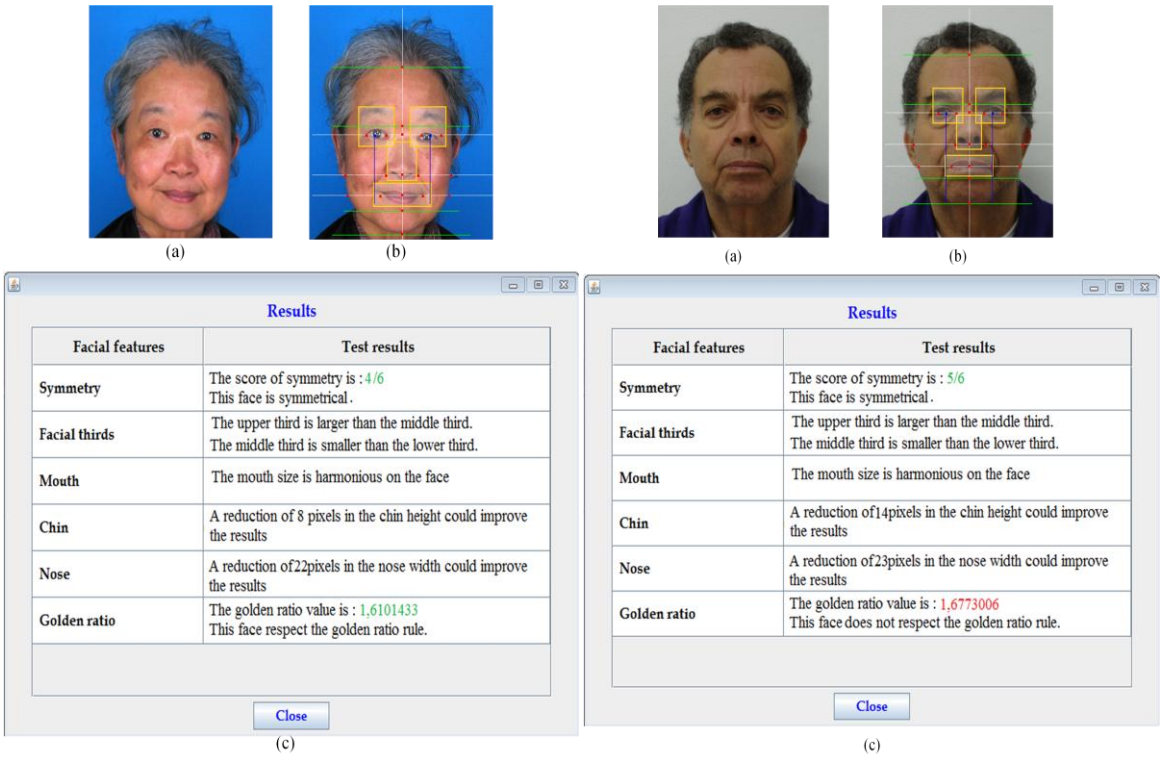

Figure 2.28: facial attractiveness analyses for old people on an example from "ECVP" database (left) and from "FEI" database (right) (a) Original image. (b) Corners detection. (c) Analysis result

- Young individuals :

Figure 2.29: facial attractiveness analyses for young people on an example from "ECVP" database (left) and from "FEI" database (right) (a) Original image. (b) Corners detection. (c) Analysis result.

Based on the previous figures that show the obtained results by performing our proposed method to detect 2D facial landmarks as well as the facial aesthetic quality analysis, we conclude that our

method of landmarks detection is as great as the existing method in the literature and even can outperform some of them, in the other hand, concerning the facial attractiveness analysis by age and gender, we can say that there exist some differences and characteristics corresponding to each category; between man/woman, and young/ old person in specific facial areas.

The main difference by gender is noticed in the forehead and chin parts, as we observed that man's chin and forehead are likely to be more strong and large comparing to those of woman. On the other hand, the main differences by age are observed in areas like the eyebrows, nose and the chin. The eyebrows descend from a high position to a lower one which makes the eyes look smaller. Likewise, the nasal tip gradually descends leading to the enlargement of the nose, and the chin descends in the same manner as the nose and eyebrows. These changes may be due to skull bones which become increasingly thin and weak causing an excess of facial tissue covering the face.
Table 2.7 and table 2.8 present a summary of the main differences in facial attractiveness analysis by gender and age.

Women facial attractiveness characteristics	**Men facial attractiveness characteristics**
less strong and large forehead	More strong and large forehead
less strong chin	More strong chin

Table 2.7: Main facial attractiveness characteristics by gender.

Young individuals facial attractiveness characteristics	**Old individuals facial attractiveness characteristics**
Higher position of the eyebrows	lower position of the eyebrows
Higher nose tip	Enlargement of the nose caused by the descend of the nose tip
Likely higher chin position	Descend of the chin and cheeks area

Table 2.8: Main facial attractiveness characteristics by age.

As in our experiments, in [75], has been explained the difference in facial anatomy according to gender and age, clarifying that there is a difference between man and woman in the specific zones on the face based on the different standards of beauty. These differences include hair distribution and density, the shape of the hairline for women, and beards for men. Also, women eyebrows tend to be curved compared to those of men which are generally horizontal.
On the other hand, to evaluate the obtained results, a domain expert has verified them and proved that the proposed method to analyze the attractiveness of 2D faces (by gender and age) is good enough to perform the analysis. The following table 2.8 presents the evaluation results:

	Satisfying attractiveness analysis results	**Unsatisfying attractiveness analysis results**
ECVP dataset	97.7%	2.3%

FEI dataset	94%	6%

Table 2.9: Domain expert evaluation results

5 Conclusion

In this chapter, we have presented our proposed approach for 2D face aesthetic quality analysis. To achieve that purpose, we first detected the face zone on the image using an approach based on two main steps; the first step consists of the detection of the skin zone based on a segmentation method using the HSV colour model, then a set of morphological analysis was applied in order to enhance the accuracy of the detection. The second step after the detection of the face zone on a 2D image is to localize the facial feature axes using the different characteristics of the greyscale image and the vertical and horizontal projections of the gradient image. Once the axes are detected, the third step consists of the application of the facial geometric model to face to draw the rectangles that surround the facial features; these rectangles will help us to limit the zone of research for the facial landmarks. Afterwards, the fourth step is to apply the active contour (Snake) to the whole face and then to the drawn rectangles to detect the 2D facial landmarks, in this step we found the intersection of the facial axes and the points given by the active contour which have to be located in the skin zone. Finally after detecting the facial landmarks, we were able to analyze the aesthetic quality of the face by verifying first if the face meets the beauty canons defined by the studies in the literature (symmetry, golden ratio, and neoclassical proportions) or not, then suggesting some modification to apply in order to improve its attractiveness.

Chapter 3: 3D facial aesthetic quality analysis

- Manal EL Rhazi, Arsalane Zarghili, Aicha Majda **"Survey on the approaches based geometric information for 3D face landmarks detection."** IET Image Processing, Vol13, Issue8, 2019.

- Manal EL Rhazi, Arsalane Zarghili, Aicha Majda **"Automated detection of craniofacial landmarks on a 3D facial mesh."** 11th edition of the International Conference on Integrated Design and Production CPI, Fez 2019.

1 Introduction

Recently, with the growing accessibility to 3D scans, the use of 3D faces has become a major asset in tackling traditional limitations, including those associated with 2D images, such as lighting conditions and point of view. This is also beneficial for diverse areas such as craniofacial research where manual face manipulation has been the standard technique for the analysis of craniofacial dysmorphology, surgical planning and results evaluation.[135].

As a result, the application of 3D faces has spread widely in different domains, which initially attempt to detect the facial landmarks as an essential step in any subsequent 3D face analysis. 3D facial landmarks have a widespread application in many areas, such as face recognition, face registration, face attractiveness analysis, facial expression analysis, motion capture, facial mesh reconstruction, facial lighting and face animation, making the automatic detection them with accuracy a major challenge, especially when a large number of 3D landmarks are required. In such a case, avoiding time consuming and labor extensive of the manually landmarking process as well as the errors committed during the labeling stage are of high importance.

In this chapter, we present a new approach to analyze the aesthetic quality of a 3D face for both the frontal and the profile sides of the face. To achieve that purpose, the 3D face needs first to be preprocessed in order to normalize its pose and orientation. This step aims to correct the angular rotations of yaw and roll by minimizing the difference between the right and the left sides of the 3D face, and then the pitch is processed by minimizing the difference between the height of the forehead and the height of the chin. The second step is the detection of the 3D facial landmarks; these landmarks will help us to calculate the facial ratios and distances as already done for the 2D faces in the previous chapter. In the current chapter a large number of 3D facial landmarks (30) is detected, this large number is especially needed in the domain of the plastic and aesthetic surgeries, which is our case, to get more details about the facial geometry and moreover to facilitate the application of the suggested modification to the 3D face. The proposed approach to detect the 3D facial landmarks is based on the use of the geometric information provided by the 3D mesh, in fact, our approach is inspired by a previous study that aimed to detect 17 3D facial landmarks. Indeed we extended this method to detect a large number. Among the 30 detected landmarks, 26 landmarks are detected on the frontal side of the 3D face and four landmarks were located on the profile side.

The last step of the 3D facial aesthetic quality analysis is to verify if the face meets the beauty canons defined in the literature studies for the frontal and the profile side of a face; otherwise suggest the necessary modification to enhance its attractiveness. This verification is based on comparing the results obtained from the calculation of the ratios and the distances and those predefined in the literature.

2 3D facial landmarks detection

As explained in chapter 1, the existing 3D facial landmarks detection methods can be divided into two types: those based on the geometric information and those based on the trained statistical features[140]. About the methods that are dependent on the trained statistical feature models, in [237][186][148] authors presented examples of this use. And of those based geometric information and the shape descriptors such as: Shape Index [157], Gaussian curvature [154], Spin Image [156] are the main used to detect the 3D facial landmarks, even though the

suggested method shows a good results, they cannot detect a large number of landmarks, which make the use of other shape descriptors necessary to localize more points on the face. The new descriptors can be different combinations of the first, second and mixed derivatives, the coefficients of the fundamental forms E, F, G, e, f and g, the mean curvatures H, the principal curvature k1 and k2 [177], it can also be different combinations of them or by applying standard functions such as sine, cosine, and logarithm [165].

2.1 Mapping study

In our thesis we used a geometric information based method to detect 3D facial landmarks. First, we classified geometric methods for the detection of landmarks by conducting a systematic mapping study [238]. In the literature, a large number of articles have been proposed for the detection of landmarks from a 3D mesh using geometric methods. The systematic mapping is a technique used to create categories of approaches that share the same techniques using existing works from the same research context. In searching for articles that use geometric methods for the detection of 3D facial landmarks during 2010-2018, 30 papers were selected after eliminating papers that are not in the area. We then classified the obtained papers according to the used approaches for the detection of landmarks. Table 3.1 describes the mapping study.

	Papers	**Authors**	**Method**	**Category**
1	[168]	Silva et al. 2010	Combined relief curves obtained from the depth data and the resulting image of the surface curvature analysis are used to detect 5 3D landmarks.	**Category-1**
2	[155]	Perakis et al. 2014	A fusion method for 8 2D/3D landmarks detection, by using spin image and shape index for 3D scans and edge response for 2D images.	**Category-2**
3	[173]	Vezzetti et al. 2013	A set of differential analysis are used to localize 9 3D landmarks: the first, the second, and the mixed derivates, the coefficients of the Fundamental Forms, the curvatures, Shape and Curvedness Indexes, and Tangent Map.	**Category-1**
4	[141]	Perakis et al. 2013	Candidate landmarks are detected using the Shape Index and Spin Images. Then transformations that align the candidate points to a model trained manually are computed in order to get the best combination of the landmarks.	**Category-3**
5	[175]	Vezzetti et al. 2014	Extension of the previous work: based on the obtained results, new regions are to be detected then minimizing the coefficients of the second fundamental along a specific direction, and maximizing the curvedness index and the shape index.	**Category-1**
6	[165]	Marcolin et al. 2017	105 new 3D shape descriptors by Deriving and composing primary ones are used to localize 6 3D facial landmarks.	**Category-1**

7	[177]	Moos et al. 2017	Different combinations of the first, second and mixed derivatives, the coefficients of the fundamental forms E, F, G, e, f and g, the curvatures K, H, k1 and k2, and shape and curvedness indexes S and C as descriptors have been employed to detect 13 landmarks.	**Category-1**
8	[161]	Cheng et al. 2014	3D Constrained Local Model framework based on the histogram-based 3D facial geometry features: HONV (Histogram of Oriented Normal Vectors) and LNBP(Local Normal Binary Patterns) using 3D Point Distribution Model.	**Category-4**
9	[178]	Gilani et al. 2015	A dense correspondence of 3D faces is established by minimizing the bending energy between seed points of given faces to those of a reference face extracted by adaptive level set curves with adaptive geometric speed functions.	**Category-3**
10	[167]	Creusot et al. 2010	A set of points containing hand placed landmarks is used as input data. For each landmark, a set of geometric descriptors is calculated and then a generic graph model of a face is used in the graph matching process.	**Category-3**
11	[164]	Galvànek et al. 2015	Combining surface curvature analysis (minimal and maximal principal curvature independently for every face feature) and then use the symmetric profile extraction to detect the points on the profile based on peaks or valleys of a curve.	**Category-1**
12	[239]	Jourabloo et al. 2015	By integrating with a 3D point distribution model, a cascaded coupled-regressor approach is developed to estimate the 3D landmark learnt from a labeled 3D scans.	**Category-3**
13	[182]	Li et al. 2017	A set of facial meshes was manually landmarked then used to create a facial atlas of landmarks and a curvature map in order to determine values for curvature thresholds for further meshes to be landmarked.	**Category-3**
14	[166]	Mehryar et al. 2010	Detect the ridges and valleys on the 3D surface using the Gaussian and Mean curvatures, and then group the points that are tightly clustered as the candidate landmarks and discard the remaining. Finally, geometric model imposing a set of distances and angles constraints to the arrangement of the landmarks is utilized to select the final four landmarks.	**Category-1**
15	[160]	Guo et al. 2013	The nose tip is localized using a sphere fitting approach, then to localize 6 salient landmarks, 3D data and texture were transformed into 2D data, and a PCA is used to detect them. To localize an additional 10 points geometric relations and texture constraints are used.	**Category-2**

16	[153]	Gupta et al. 2010	3 facial landmarks are detect using shape informations; Gaussian surface curvature (K), the mean surface curvature (H), and two principal curvatures (κ1, κ2), and the 7 other points are detected using 2D+3D EBGM.	**Category-2**
17	[176]	Sangineto et al. 2013	The proposed method is based on an efficient dense feature extraction (SURF-like descriptors) and a comparison of the 2D local landmark classification outcome with (projected) 3D shape vectors using the multiclass Hausdorff distance.	**Category-2**
18	[179]	Sukno et al. 2015	A shape regression with incomplete local features is presented to detect the landmarks by selecting the candidates through local feature detection (APSC descriptors and calculating the distance to the each manually landmark), finally, a partial set matching is used to infer missing landmarks by regression.	**Category-4**
19	[240]	De Giorgis et al. 2015	To localize 13 3D facial landmarks, Gaussian curvature of the geometrical descriptors is used.	**Category-1**
20	[241]	Fan et al. 2015	Strong shape priors are presented: the characteristic number which includes intrinsic geometries that are common to human faces. It tries to optimize the energy that combines the strong shape prior and relatively simple intensity, and edge/corner models as appearance constraints and finally the solution to facial landmarks extraction can be found by the standard gradient descent.	**Category-2**
21	[242]	Perakis et al. 2010	3D geometry-based information is used to localize the facial landmarks. The results are then filtered out and labeled by matching them with the FLM created by calculating a mean landmark shape using Procrustes Analysis.	**Category-3**
22	[159]	Creusot et al. 2013	Train the system to detect the manually labeled landmarks on a training dataset by calculating a set of shape descriptors for each point on the set and then associating each landmark with a descriptor value.	**Category-3**
23	[243]	Bagchi et al. 2012	New method based on the mean (H) and Gaussian (K) curvatures to extract eye and nose points from faces.	**Category-1**
24	[181]	Fan et al. 2016	The 3D facial models is mapped to 2D geometry image using a conformal mapping, then four 2D landmark detection methods are used to identify the best one. Finally, the landmarks detected in the 2D geometry images are mapped back to the 3D models, using point to point mapping.	**Category-2**
25	[171]	Berretti et al. 2011	3 facial landmarks are detected using the curvature analysis: The Gaussian surface curvature (K) and the mean surface curvature (H). And the remaining points were detected using a solution based on the SIFT detector applied to local search windows.	**Category-4**
26	[135]	Liang et al. 2013	A set of 17 of 3D facial landmarks is localized using	**Category-3**

			the proprieties of the 3D meshes then an additional number of landmarks is detected using a dense a deformable transformation is used between target and destination meshes to determine a set of 20 established landmarks.	
27	[174]	Vezzetti et al. 2014	Different combination of the first, second and mixed derivatives, the Coefficients of the Fundamental Forms E, F, G, e, f and g, the curvatures K, H, 1 k and 2 k , and Shape and Curvedness Indexes S and C as descriptors have been employed to detect 9 landmarks.	**Category-1**
28	[183]	Vezzetti et al. 2017	12 differential Geometry descriptors: coefficients of the fundamental forms, Gaussian, mean, principal curvatures, shape index and curvedness are used to localize 13 3D facial landmarks.	**Category-1**
29	[244]	Vezzetti et al. 2016	To detect 11 3D facial landmarks, a combination of the 3D differential geometry (curvature) descriptors and the RGB image component are used.	**Category-2**
30	[245]	Boukamcha et al. 2015	The mean and Gaussian curvatures information is used to localize 8 3D facial landmarks.	**Category-1**

Table 3.1: Mapping study table

Geometric information based methods used to detect 3D facial landmarks can be classified into four categories:

- **Category-1: Approaches based on curvature analysis:**

Several articles using this approach have been reported, for example in [173], the authors have localized 9 landmarks using differential analysis: the first, the second, and the mixed derivates, the coefficients of the Fundamental Forms, the curvatures, Shape and Curvedness Indexes, and Tangent Map. In another paper [175] they extended this work to detect more points, so they got 17 landmarks. In [165] the same authors introduced 105 new descriptors to detect 6 landmarks by deriving and composing primary ones. Newly developed descriptors are holistic or global and they have shown to have some advantages over local tools. Similarly in [164], to detect 14 landmarks, authors combined different surface curvature analysis descriptors and then used the symmetric profile extraction to detect the points on the profile side of the face based on peaks and valleys of a curve which represent the points with maximal or minimal values of a curvature. In [177] authors have also presented different combinations of the first, second and mixed derivatives, the coefficients of the fundamental forms, the curvatures, shape and curvedness indexes as descriptors to localize 13 landmarks on foetal images suffering from cleft lip pathology. On the other hand, authors in [168] combined relief curves obtained from the depth data and the resulting image of the surface curvature analysis to detect 5 landmarks on 3D scans.

- **Category-2: Approaches based on combining 2D texture with the 3D shape information:**

In [153] authors have firstly localized 3 facial landmarks using curvature analysis, and then to detect 7 additional landmarks, a 2D+3D EBGM algorithm were used. Authors in [176] suggested a method based on the efficient dense feature extraction (SURF-like descriptors) and a comparison of the 2D local landmark classification outcome to the (projected) 3D shape vectors using the multiclass Hausdorff distance in order to detect 17 landmarks. In [181], The authors attempted to map a 3D facial model into a 2D geometry image using conformal mapping, then four 2D landmark detection methods are used to identify the most appropriate one. Finally, the 7 landmarks detected in 2D geometry images are mapped to the 3D models using point-to-point mapping.

- **Category-3: Approaches based on matching the 3D query face with a manually landmarked one and then establishing correspondences:**

An example of such approach is presented in [167] in which authors have detected 14 landmarks using a graph matcher trained using manually labeled landmarks. This approach is based on the use of a query graph and a model graph as input then returns, for each node of the query, a list of most probable candidate labels in the model with corresponding scores, then the best labels are identified using a scale-adapted rigid registration. Moreover in [182], After aligning the face to a frontal position, a set of 25 facial meshes was manually landmarked and used to generate a facial atlas of landmarks and a curvature map reference in order to determine values for curvature thresholds for further face meshes to be landmarked. Authors in [239] have localized 21 landmarks on the edge of the face by integrating with a 3D point distribution model a cascaded coupled-regressor approach in order to estimate the 3D landmarks learnt from labeled 3D scans.

- **Category-4: Approaches based on a generic image descriptors:**

In [171] authors have detected 6 facial landmarks using the Scale Invariant Feature Transform (SIFT) [172] by using windows around each feature, and then identify the points with the largest scale as landmarks. Also in [161], 3D Constrained Local Model framework based on the histogram-based 3D facial geometry features is proposed to detect 3D facial landmarks, the used geometric features are: Histogram of Oriented Normal Vectors (HONV) [163] and Local Normal Binary Patterns (LNBP) [162] using 3D Point Distribution Model.

The first step before detecting the 3D facial landmarks is to normalize the pose and the orientation of the 3D face in order to get plausible results. This step is performed using an approach proposed by [129] as will be demonstrated in the next subsection.

2.2 3D face normalization

Before detecting the 3D facial landmarks, the 3D face must be preprocessed by normalizing its pose and orientation in order to correct the angular rotations of yaw and roll. The preprocessing is achieved by minimizing the difference between the right and the left sides of the 3D face, then the pitch is processed by minimizing the difference between the height of the forehead and the height of the chin [129]. If the face is not symmetric, the 3D face can be aligned

by finding the angular rotations of yaw and roll that minimize the difference between the right and the left side of the face. Indeed, some 3D faces needed a manual correction of the pose and orientation.

The following equation is used to normalize a symmetric face:

$$Diff = \sum_{y=0}^{height} \sum_{x=0}^{width/2} \left| Image_{x,y} - Image_{width-x-1,y} \right| \qquad (35)$$

2.3 3D facial landmarks detection using geometric technique

To detect the 3D landmarks, we followed the technique used in [135] to detect the 10 needed established landmarks that are: the pronasale(5), the subnasale(6), the left and the right alares(20)(21), the left and the right chelion (24)(25), the exocanthion and the endocanthion on the left and the right eye (13)(15)(16)(18) as shown in figure 3.1.

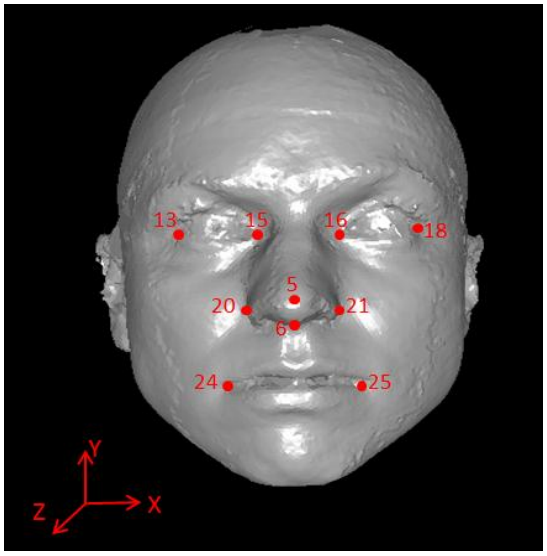

Figure 3.1: the 10 facial landmarks by Liang [135].

Afterwards, we extended this approach to localize 20 additional landmarks on the 3D face, as described in figure 3.2

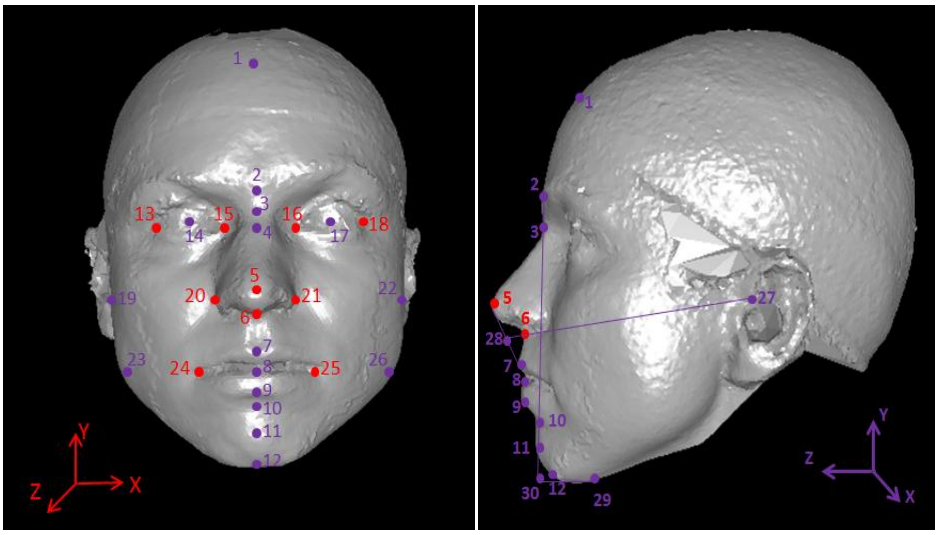

Figure 3.2: 3D facial landmarks on a frontal face (left) and a profile side (right).

The 30 detected facial landmarks shown in figure 3.2 are some of those needed in the craniofacial anthropometry, which is largely used in many fields to analyze and quantify the facial anthropometry such as in the domain of facial aesthetic quality analysis. In [75][246], authors have confirmed that in order to analyze the facial attractiveness, a large set of facial landmarks are needed, which will allow to verify whether a face complies with the aesthetic criteria or not. Based on these aesthetic criteria (see chapter 1), we have concluded that 30 landmarks are sufficient and reliable to analyze the facial attractiveness.

In the proposed method before detecting a new facial landmark, the research zone is restricted using the previously detected landmarks, which makes the step of 3D face pose normalization a crucial and necessary step in the detection process.

2.3.1 A sample data set from CranioGUI dataset

The CranioGUI dataset was created by the Shape-Based Retrieval of 3D Craniofacial Data project investigated by Linda Shapiro and available on the FaceBase Consortium website [247].

The priority of the project is to generate software tools that considerably enhance the accessibility of 3D craniofacial data. CranioGUI can be used by the craniofacial research community to facilitate the analysis of facial anomalies. The software operates on 3D head meshes and is generic in that it can be used for the analysis of several conditions. The dataset has been used by project members to quantify the following conditions: craniosynostosis, plagiocephaly, 22q11.2 deletion syndrome (which includes some medial hypoplasia) and cleft lip and palate.

2.3.2 BaselFaceModel dataset

The Basel Face Model (BFM) is a rich 3DMM for human faces, built from a large group 100 males and 100 females most of them European. The age of the persons was between 8 and

62 years. It has a high mesh density of 53,490 vertices and includes the face, frontal neck and ears. The Base Face Model is a well known 3D morphable model constructed from the 200 3D scans and it is widely used for 3D face recognition and alignment.

The Basel Face model is accompanied by 10 out of sample 3D faces. Each face is rendered in 9 poses and 3 lighting conditions per pose giving 270 renderings in total.

Figure 3.4: Ten example scans of the BaselFaceModel dataset.

2.3.3 The proposed technique to detect 3D facial landmarks

- On the frontal side, to detect the pupils of the two eyes; (14) and (17) in figure 3.2, the research region is restricted to

  - $x(13) \leq x \leq x(15)$ and $y(15) \leq y \leq y(3)$ for the right eye
  - $x(16) \leq x \leq x(18)$ and $y(16) \leq y \leq y(3)$ for the left eye

Then we find for each region the local maxima.

- To detect the point on the middle of the two eyes (4) in figure 3.2, we find the intersection of the line with the same x-value as the pronasale (5) in figure 3.2 and the line with the same y-value as the pupils. We add that the look of the eyes must be forward so that the pupils can be localized at the same line.
- To locate the stomion (8) in figure 3.2, we use the results obtained for the two chelion, and we find the intersection of the line that has the same x-value as the pronasale (5) and the one that goes along the chelion (24) and (25) in figure 3.2.
- To find the ganthion (12) in figure 4.2, the region is restricted to:
  - Below the stomion $y < y(8)$,

Then we find the point with smallest y-value on the pronasale (5) line.

- The sublabiale (10) in figure 3.2 is located by restriction the region to:
  - $y(12) < y < y(8)$,

Then we detect the point with the local minima on the line that has the same x-value as the pronasale (5).

- To detect the pogonion (11) in figure 3.2, we restricted the region to:
  - $y(12) < y < y(10)$

Then we find the local maxima in this area.

- To locate the labiale superius (7) in figure 3.2, we restrict the region to:
  - $y(8) < y < y(6)$,

Then on the line that has the same x-value as the pronasale, we find the local maxima. The same thing for the labiale inferius (9) in figure 3.2, the local maxima is found on the restricted research region $y(10) < y < y(8)$.

- The two upper cheek extremities (19) and (22) in figure 3.2 are detected by restricting the regions to:
    - $x < x(20)$ for the left point and
    - $x > x(21)$ for the right one,

Then on the line that has the same y-value as the pronasale (5), we find the local minima.

- The same thing for the two lower cheek extremities (23) and (26) in figure 3.2, they are detected by restricting the regions to:
    - $x < x(24)$ for the left point and
    - $x > x(25)$ for the right one,

Then on the line that has the same y-value as the stomion (8), we find the smallest x-value on this line.

- To detect the forehead point (1) in figure 3.2, we restrict the research region to:
    - $y > y(3)$,

Then on the line whit the same x-value as the pronasale (5), we find the local minima.

- The last detected point on the frontal side is the nasale (2) in figure 3.2, this point is detected by restricting the research region to:
    - $y(3) < y < y(1)$,

and starting from the sellion (3), we find the first local maxima on the line that has the same x-value as the pronasale (5).

On the profile side we change the position of the head by rotation of 90° then four landmarks are detected.

- First, the tragion (27) is localized by restricting the research zone to:
    - $z < z(18)$ and
    - $y(6) < y < y(18)$,

Then we find the local minima.

- To find the subnasale angle (28), we detect the intersection of the line that connects the tragion (27) and the subnasale (6), and the one that connects the pronasale (5) and the labiale superius (7).

- To locate the point (29), the research region is restricted to:
    - $y < y(11)$ and
    - z$< z(12)$,

Then we find the first point having the tangent to the chin tip.

- To detect the point (30) that forms the mentocervical angle, we find the intersection of the tangent that goes along the chin tip (29) and the line that connects the nasale (2) and the pogonion (11).

The accuracy of the facial landmarks detection is measured by calculating the average distance using the Euclidian distance and the standard deviation of the detected landmarks to those detected manually.

The datasets used in this experiment are the sample data set from the CranioGUI dataset [247], and the BaselFaceModel dataset [248].

For both datasets, we manually locate the same automatically detected landmarks (30 landmarks) on the 3D faces, then to evaluate our extended approach, for a given face we calculate the

average error (mm) of the 3D landmarks detection as well as the standard deviation using the Euclidean distance as shown in table 3.1.

Table 3.2 describes the average distance of the 30 detected landmarks using the presented extended approach to their manually annotated landmarks. The average distance of the automatically detected 30 landmarks to the manually labeled points for the samples from the CranioGUI dataset is 3.59 mm, and the average standard deviation is 2.32 mm. For the BaselFaceModel dataset, the average distance of the 30 detected landmarks to their manually annotated points is 4.01 mm, and the average standard deviation is 2.54 mm. Both of these results indicate the good accuracy of the presented method.

	Facial features	**Average distance and standard deviation for samples from CranioGUI dataset**	**Average distance and standard deviation for BaselFaceModel**
1	Forehead	3.56 ± 3.16 mm	4.27 ±2.41 mm
2	Glabella	2.57 ± 1.19 mm	2.58 ± 2.2 mm
3	Nasion	4.83 ± 5.17 mm	3.41 ± 2.15 mm
4	Eyes centre	1.46 ± 2.68 mm	2.43 ± 1.93 mm
5	Pronasale	2.49 ± 1.65 mm	2.56 ± 2.03 mm
6	Subnasale	2.06 ± 1.48 mm	2.16 ± 1.66 mm
7	Labliale superior	5.47 ± 3.89 mm	3.96 ± 2.86 mm
8	Stomion	2.38 ± 1.54 mm	3.09 ± 3.93 mm
9	Labiale inferior	5.88 ± 4.92 mm	3.34 ± 3.78 mm
10	Sublabiale	3.35 ± 2.91 mm	4.03 ± 2.11 mm
11	Pogonion	1.34 ± 1.89 mm	2.87 ± 2.24 mm
12	Ganthion	3.21 ± 2.75 mm	3.4 ± 3.05 mm
13	Endocanthion Left	4.88 ± 2.85 mm	4.36 ± 1.29 mm
14	Lefts eye pupil	2.96 ± 2.43 mm	2.47 ± 2.06 mm
15	Exocanthion Left	4.05 ± 1.97 mm	3.33 ± 2.51 mm
16	Exocanthion Right	2.98 ± 2.75 mm	3.05 ± 2.28 mm
17	Right eye pupil	2.69 ± 1.68 mm	2.78 ± 1.94 mm
18	Endocanthion Right	2.7 ± 1.47 mm	3.37 ± 2.61 mm
19	Cheek superior Left	4.59 ± 2.5 mm	5.32 ± 1.18 mm
20	Alare Left	2.62 ± 1.52 mm	2.77 ± 1.88 mm
21	Alare Right	1.87 ± 1.52 mm	3.97 ± 1.94 mm

22	Cheek superior Right	6.3 ± 3.67 mm	3.79 ± 2.11 mm
23	Cheek inferior Left	7.6 ± 2.01 mm	8.73 ± 3.5 mm
24	Chelion Left	3.43 ± 2.18 mm	4.29 ± 2.31 mm
25	Chelion Right	3.93 ± 3.88 mm	4.35 ± 2.25 mm
26	Cheek inferior Right	6.61 ± 3.41 mm	6.24 ± 4.09 mm
27	Ear point (Tragion)	8.73 ± 6.04 mm	8.69 ± 5.32 mm
28	Subnasale Angle	1.54 ± 0.95 mm	3.06 ± 2.4 mm
29	Menton	6.72 ± 3.43 mm	6.45 ± 2.72 mm
30	Ganthion 2	6.98 ± 4.19 mm	5.15 ± 3.4 mm

Table 3.2: Average distances and the standard deviations of automatically detected landmarks to the manually located ones for the two 3D face datasets.

By comparing our results to those obtained by [135] and other most recent works in the literature that aim to detect 3D landmarks on a neutral and frontal faces using similar database, we conclude that the results obtained by the extended approach are as good as those obtained by [135] and the other competing methods. Moreover, the presented approach can detect a large number of 30 3D facial landmarks unlike the other approaches presented in the literature that aims to localize the 3D facial landmarks on a neutral frontal faces for different purposes such as the craniofacial anthropometry studies that include a large set of face analysis studies, these studies require a large number of facial landmarks that need to be detected with accuracy in order to get a great and relevant results of analysis, especially in the field the facial aesthetic quality analysis where the more landmarks are detected the more the analysis is reliable.

	Our approach	[135]	[155]	[160]	[174]	[175]	[178]	[179]	[181]	[183]
Average distance	**3.59**	3.12	4.26	1.39	2.67	2.6	3.38	3.34	2.6	4.21
Standard deviation	**2.32**	1.98	-	0.98	10.12	2.7	0.94	1.93	1.95	-
Number of the detected landmarks	**30**	10	8	17	9	8	8	10	7	13

Table 3.3: Comparison of the average distances and the standard deviations of our method against methods in the literature.

Average distance: calculates the distance between the automatically localized landmarks coordinates and the manually annotated ones. It is given by the formula:

$$D = \frac{\sum_1^n (x_i - x)}{n} \qquad (36)$$

Standard deviation: describes how much the localized landmarks coordinates differ from the mean value of the detected landmarks coordinates, and it is given by the formula:

$$\sigma = \sqrt{\frac{\sum_1^n (x_i - \bar{x})^2}{n}} \qquad (37)$$

Where:

n: The total number of the detected landmarks.

x_i: The current automatically localized landmark coordinates.

x: The manually labeled landmark coordinates.

$\bar{x}$: The mean value of the labeled landmarks coordinates.

Experimental results in table 3.3 show that the proposed approach is better than the original work and other works in the literature that detects 3D facial landmarks using geometric information of the mesh. As reported in table 3.3, for our case, the average distance of the automatically detected 30 landmarks to the manually labeled points for the sample data set from the CranioGUI dataset is 3.59 mm and the average standard deviation is 2.32 mm, a competing work has detected 17 landmarks [160], authors have claimed that the average distance to the manually labeling 3D landmarks is 1.39 mm and the average standard deviation is 0.98. then authors in [183] have detected 13 landmarks with an average distance of 4.21 mm to the manually detected 3D face landmarks and the results of the original work of [135] are 3.12 mm as the average distance and 1.98 mm as the average standard deviation to the manually detected 3D landmarks. These results indicate the accuracy of our approach in detecting a large number of landmarks.
Concerning the computational efficiency of the presented approach, a PC with: Intel Core 2 Duo, 2.20 GHz with 3GB RAM is used. Using this machine to detect the 30 3D facial landmarks using a geometric information based method, the required time for the detection and the labeling for each scan is 4.42 (s) as an average which makes it applicable in many face analysis application in the real world. While the required time for the original work in [135] to detect 10 landmarks is 4 (s) as the average. Table 3.4 illustrates the computational cost of the proposed approach for both the sample data set from the CranioGUI dataset and the Basel Face Model dataset.

3D dataset	Average computational cost for each scan
Sample data set from CranioGUI dataset	4.42 (s)
Basel Face Model dataset	6.86 (s)

Table 3.4: Computational cost of the proposed approach

3 3D facial aesthetic quality analysis

The last step to perform after the localization of the 3D facial landmarks is to analyze its aesthetic quality. This step is achieved by verifying if the input 3D face meets the beauty canons predefined in the literature or not, this is similar to what was done in the previous chapter which was dedicated to analyze the aesthetic quality of 2D faces, the only difference between those two studies is that we additionally analyzed the profile side of the 3D face using the criterions cited before that include the different angles that must be respected on the face, and for the frontal side, the symmetry, the golden ratio and the neoclassical proportions are verified by comparing the obtained attractiveness results by our system to those defined in the literature.

3.1 Facial beauty canons verification

As mentioned before, the facial aesthetic quality analysis by our system is based on first normalizing the pose and the orientation of a 3D face and the results of the 3D landmarks detection. These landmarks are keys to analyze the attractiveness of a 3D face. Using them allows us to calculate the different distances, ratios and angles in order to verify if a 3D face verifies the beauty canons or not [40] [42] [39] [249]. In our thesis the following canons were tested:

The symmetry:

Similarly to the aesthetic quality analysis of a 2D face, we analyze the symmetry of a 3D faces. From the detected landmarks on the frontal side of the face, we compare the distances between the different parts of the two half-face from the axe that goes along the nose tip point for the same landmark on both the two sides, in our analysis, we took 12 measures (the eyes corners, the nose corners, the mouth corners and the cheeks points); hence the score of symmetry will be noted on 6.

The golden ratio:

As for the golden ratio, we have calculated it from the axes that pass through the facial features that were detected using the localized 3D landmarks that go along the centre of each feature; the eyes axis is detected using the localized pupils points, the nose axis is detected using the localized subnasale point and the mouth axis is detected using the localized stomion. We calculate the ratio between two distances consecutively, in total we have 4 ratios to calculate. The first ratio is calculated from the forehead point to the chin tip and from the eyes axis to the chin tip, the second ratio is from the eyes axis to the chin tip and from the eyes axis to the mouth axis, the third ratio is calculated from the eyes axis to the mouth axis and from the eyes axis to the nose axis, and the last ratio is calculated from the width of the mouth and the nose width. Details are shown in table 3.5.

Number of the golden ratio	Description
1	(forehead point to chin tip) / (eyes axis to chin tip)
2	(eyes axis to chin tip) / (eyes axis to mouth axis)
3	(eyes axis to mouth axis) / (eyes axis to nose axis)
4	Mouth width / nose width

Table 3.5: Description of the used Golden ratios.

Then the average of these ratios is calculated and compared with the golden ratio value: 1.618 [56][57], if the average of the obtained values of the golden ratio is equal to this value or even very close to that number in a specific range, we can say that the 3D face verifies the golden ratio canon. Otherwise, the face does not respect this canon, thus some modifications are needed to enhance the attractiveness of the 3D face.

The neoclassical proportions:

The neoclassical proportions are verified using the vertical fifths, horizontal thirds, width of the mouth and the height of the chin. To do so, we calculate the different distances and we verify their values and what was mentioned in the references state of the art of facial attractiveness. Table 3.6 shows the different neoclassical proportions tested in our study.

Number of neoclassical proportion	Description
1	Forehead height = nose length = lower face height
2	Face width = 5× nose width
3	Interocular distance = nose width
4	Interocular distance = eye fissure width
5	Mouth width = interpupils distance
6	Chin height = 1/3 of the lower face height

Table 3.6: Description of the used neoclassical proportions

Analyzing the profile side:

To obtain more attractive profile view, a set of angles have been measured to verify whether the person's profile is agreeable or not. Actually, 10 angular measurements have to be determined are explained in chapter 2. Each angle's value is compared to the defined value by the research studies. After calculating all the angles, our system shows the results and then if an angle is not conforming to what was defined as a reference, it indicates the necessary modification to apply as well.

3.2 Facial aesthetic quality analysis

To apply our proposed approach to analyze the aesthetic quality of a 3D face, two 3D face datasets were used; a sample data set from the CranioGUI dataset, and the BaselFaceModel dataset.

For each dataset, we chose a 3D face as an input to our system, and then we get the results of its aesthetic quality analysis for both the frontal and the profile sides as shown in the following figures.

a. Aesthetic quality analysis for the **sample data set from the CranioGUI dataset**:

The following figures (Figure 3.5, 3.6 and 3.7) present the aesthetic quality analysis for three examples of 3D faces from the sample data set from the CranioGUI dataset. For a given 3D face, our system uses it as an input then it analyzes its attractiveness for the frontal and the profile side of the 3D face. The frontal analysis consists of calculating the symmetry, the golden ration and the neoclassical proportions of the 3D face. For the profile side analysis, it is performed by calculating a large number of angles on the face. Afterwards, a comparison of the obtained

results from the both sides to the predefined values defined in the previous research studies is established to verify the conformity. Moreover, our system suggests the necessary modification to apply in order to enhance the aesthetic quality of the input 3D face.

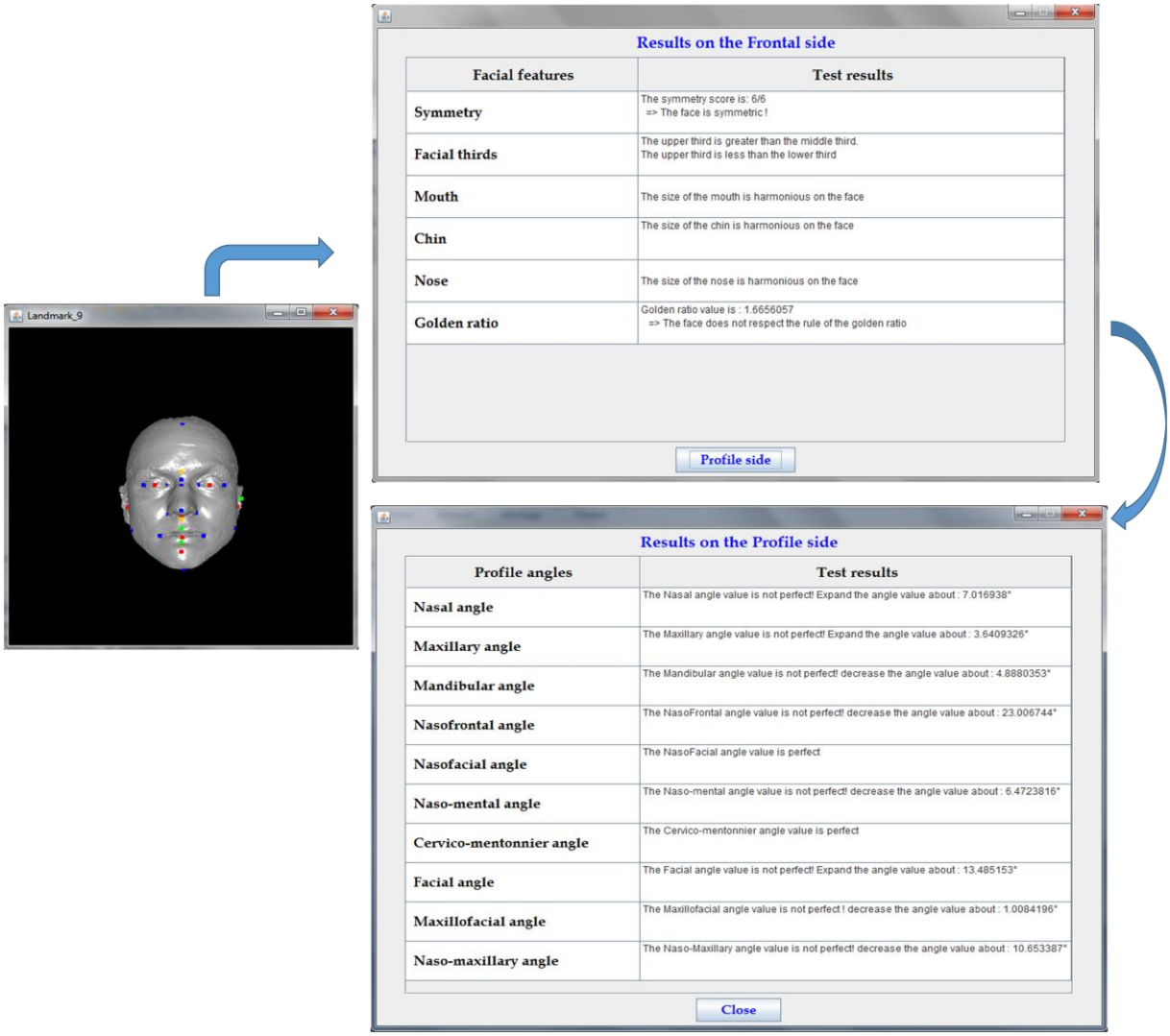

Figure 3.5: Aesthetic quality analysis of 3D face from the sample data set from the CranioGUI dataset (Example 1).

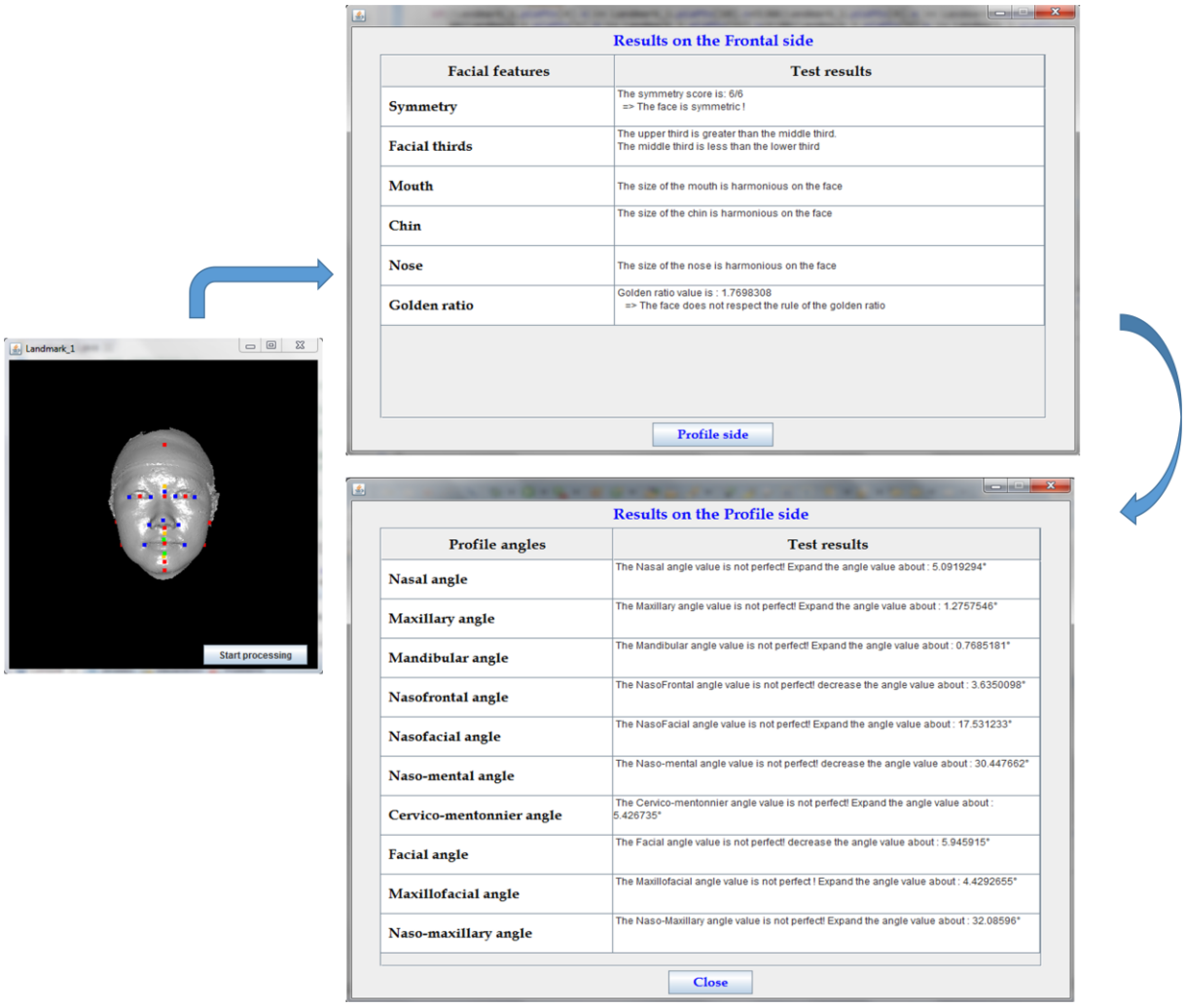

Figure 3.6: Aesthetic quality analysis of 3D face from the sample data set from the CranioGUI dataset (Example 2).

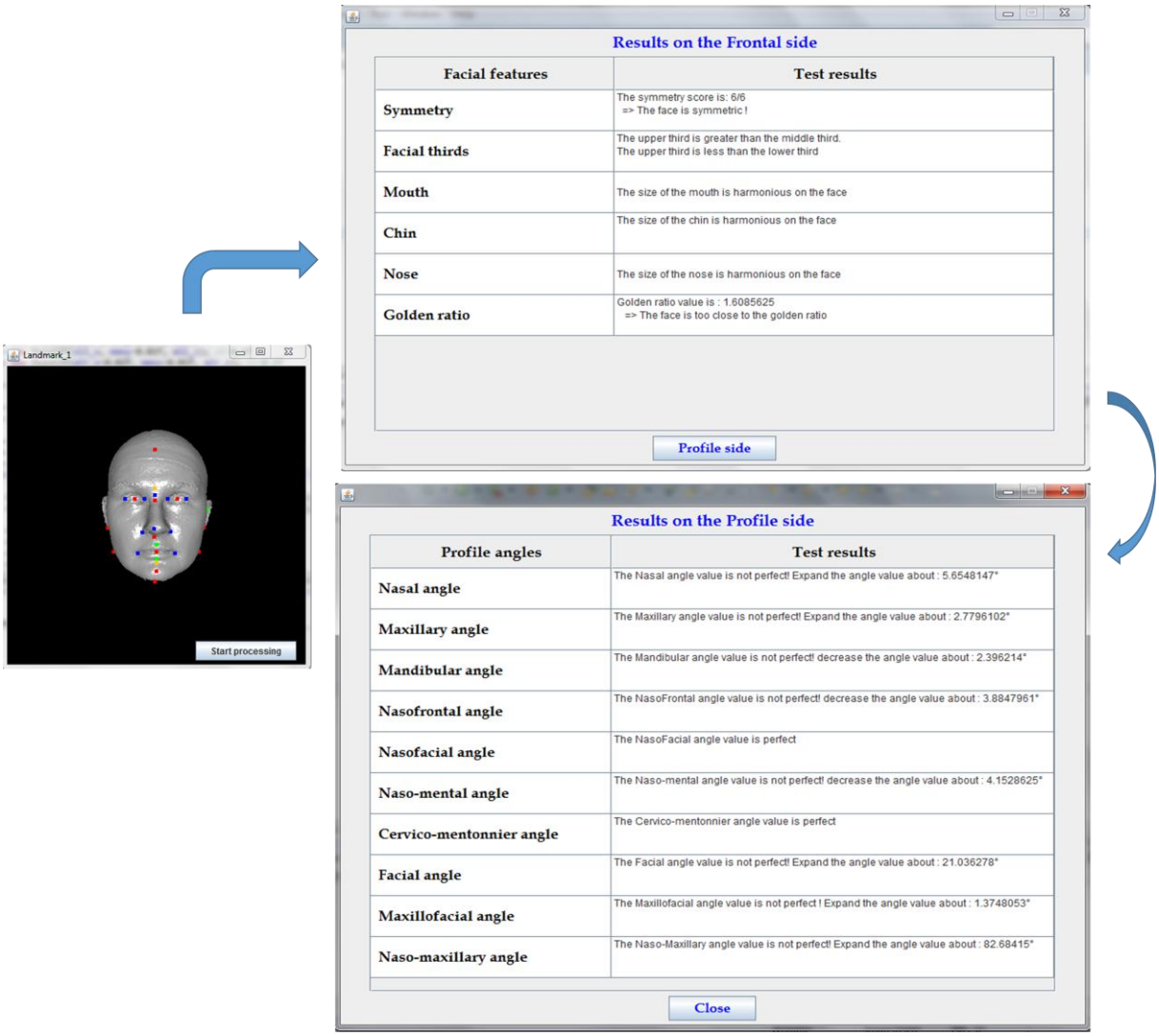

Figure 3.7: Aesthetic quality analysis of 3D face from the sample data set from the CranioGUI dataset (Example 3).

b. Aesthetic quality analysis for BaselFaceModel dataset:

The following figures (Figure 3.8, 3.9 and 3.10) present the results of our system while analyzing the aesthetic quality of some samples of the 3D faces presented in the BaselFaceModel dataset.

The same steps used for the sample data set from the CranioGUI dataset are used for the BaselFaceModel to analyze the attractiveness of the 3D faces and then suggest the necessary modification to apply in order to improve their aesthetic quality.

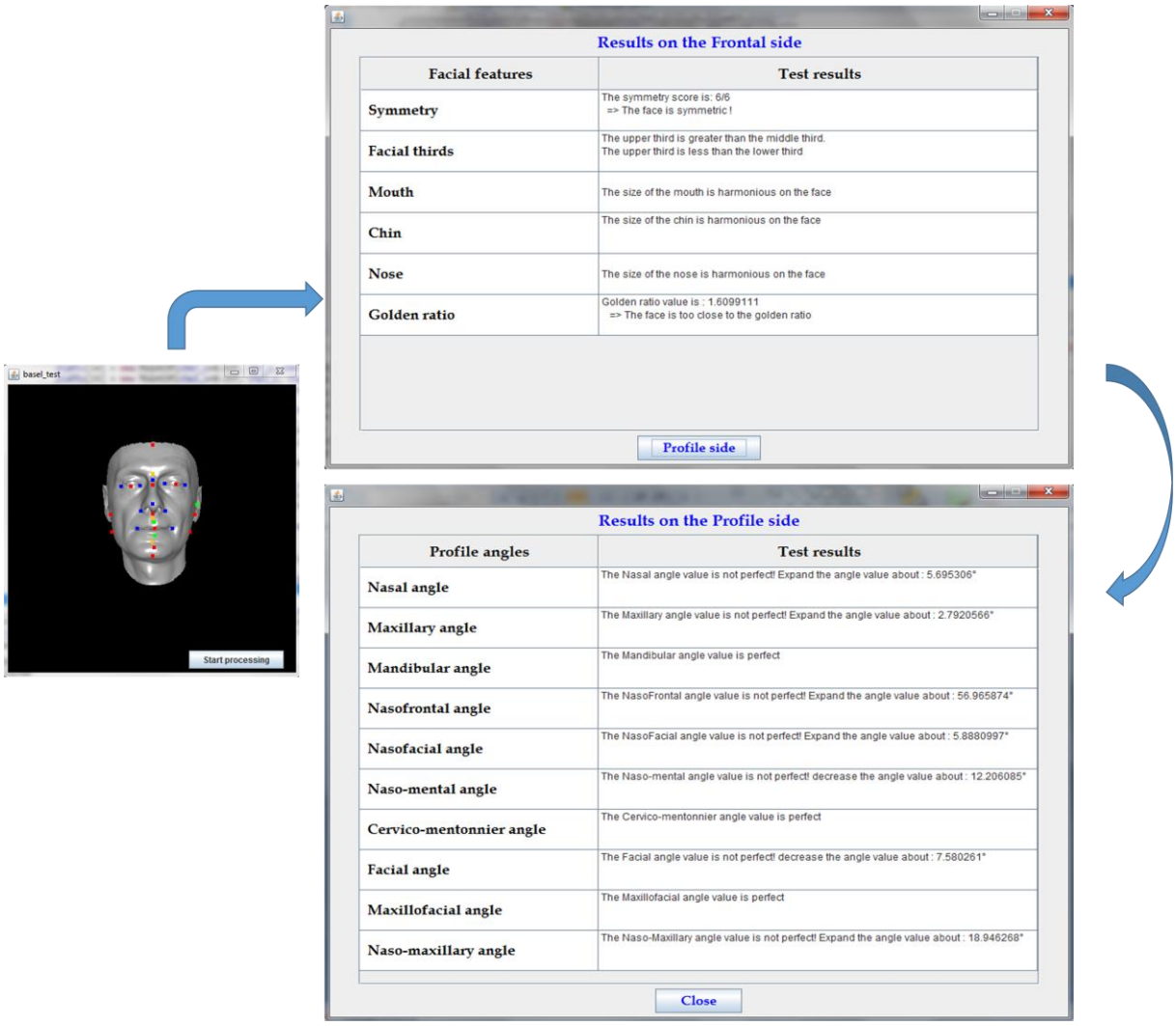

Figure 3.8: Aesthetic quality analysis of 3D face from the BaselFaceModel dataset (Example 1).

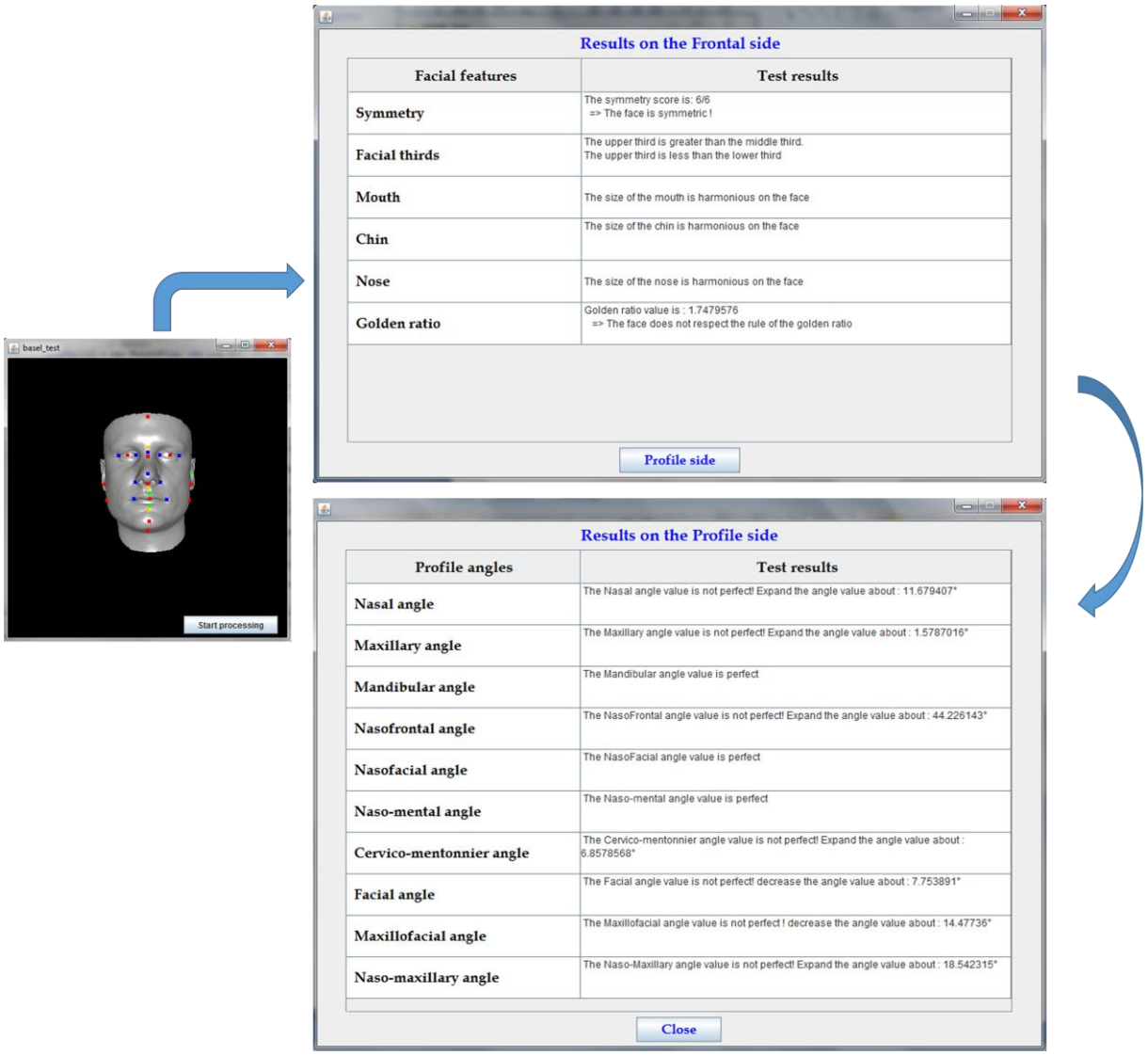

Figure 3.9: Aesthetic quality analysis of 3D face from the BaselFaceModel dataset (Example 2).

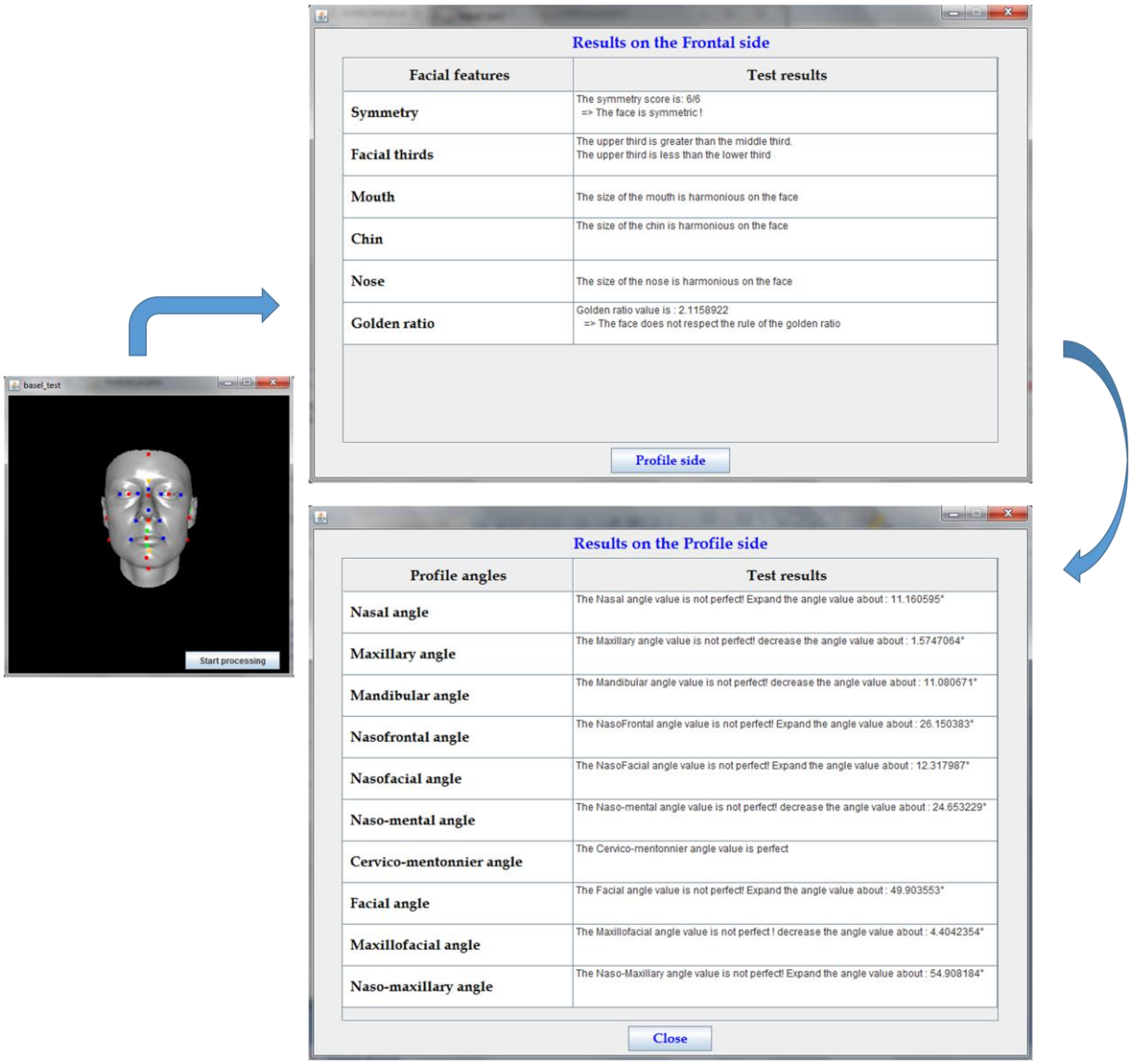

Figure 3.10: Aesthetic quality analysis of 3D face from the BaselFaceModel dataset (Example 3).

To evaluate the performances of the proposed method to analyze the aesthetic quality of 3D faces, the obtained analysis results from both the used datasets (sample data set from the CranioGUI dataset and BaselFaceModel datasets) have been presented to a domain expert for verification.

A plastic surgeon, has assessed the outcomes of our system, and therefore confirmed some of the obtained results and corrected some others. Mostly, the majority of the obtained results were satisfying for both the used datasets in terms of the valuable comments about the aesthetic quality analysis, as well as the reliable suggestions in order to enhance the attractiveness of the input 3D face.

The proposed system to analyze the aesthetic quality of 3D faces owes its remarkable good performance primarily to the use of the suggested approach to localize the 3D facial landmarks which is the key step to successful further analyses.

The following table 3.7 presents the domain expert evaluation of the 3D facial attractiveness analysis obtained results for both the used datasets.

	Satisfying attractiveness analysis results	Unsatisfying attractiveness analysis results
Sample data set from the CranioGUI dataset	88%	12%
BaselFaceModel dataset	92%	8%

Table 3.7: Domain expert evaluation results

4 Conclusion

In this chapter, we have presented our proposed method for 3D aesthetic quality analysis. To do so, we have normalized the pose and the orientation of the 3D face in order to be able to extract the needed landmarks for analyzing the attractiveness of the 3D face. 3D landmarks were detected using an approach inspired by the method presented in [135] that we have extended to detect a large number of 30 landmarks. This number is needed in order to analyze the attractiveness of the 3D face with accuracy. The experimental results of 3D facial landmarks detection show that our approach is better than the original work and many other introduced works in the literature for detecting the 3D facial landmarks using only geometric information provided by the 3D mesh.

After localizing the facial landmarks, we have verified if the 3D face meets the beauty canons defined in the literature or not, this process is performed by comparing the analysis results obtained by our system to those predefined in the research studies. The canons used include the facial symmetry, the golden ration, the neoclassical proportions and the profile angles of the 3D face.

To perform the proposed method for 3D facial aesthetic quality analysis, we have used two 3D face datasets; sample data set from the CranioGUI dataset and the BaselFaceModel, and the obtained results show a good analysis performances as well as an efficient suggestion to enhance the attractiveness of the given face.

Chapter 4: 3D facial attractiveness enhancement

- Manal El Rhazi, Arsalane Zarghili, Aicha Majda, Ayat Allah Oufkir **"3D Facial attractiveness enhancement using Free Form Deformation."** Journal of King Saud University - Computer and Information Sciences, accepted for minor revision.

1 Introduction

Accurate control of geometric models has a significant role to play in several areas such as computer-aided geometric design and digital simulation, and the step of selecting the control parameters and the method of deforming the shape are crucial.

3D mesh deformation has been an active research field recently due to the large and variety range of use. Therefore, while performing the 3D mesh deformation, some criterions have to be respected by the proposed approaches in order to get a satisfying results; the deformation approach has to be sufficiently fast, robust, intuitive, and easy to control. In addition, the result of the deformation must provide physically plausible and aesthetically pleasing deformed mesh and the most important thing is to preserve the original mesh geometric details. This is considering as a challenge for researchers when working with a complex representation like 3D meshes.

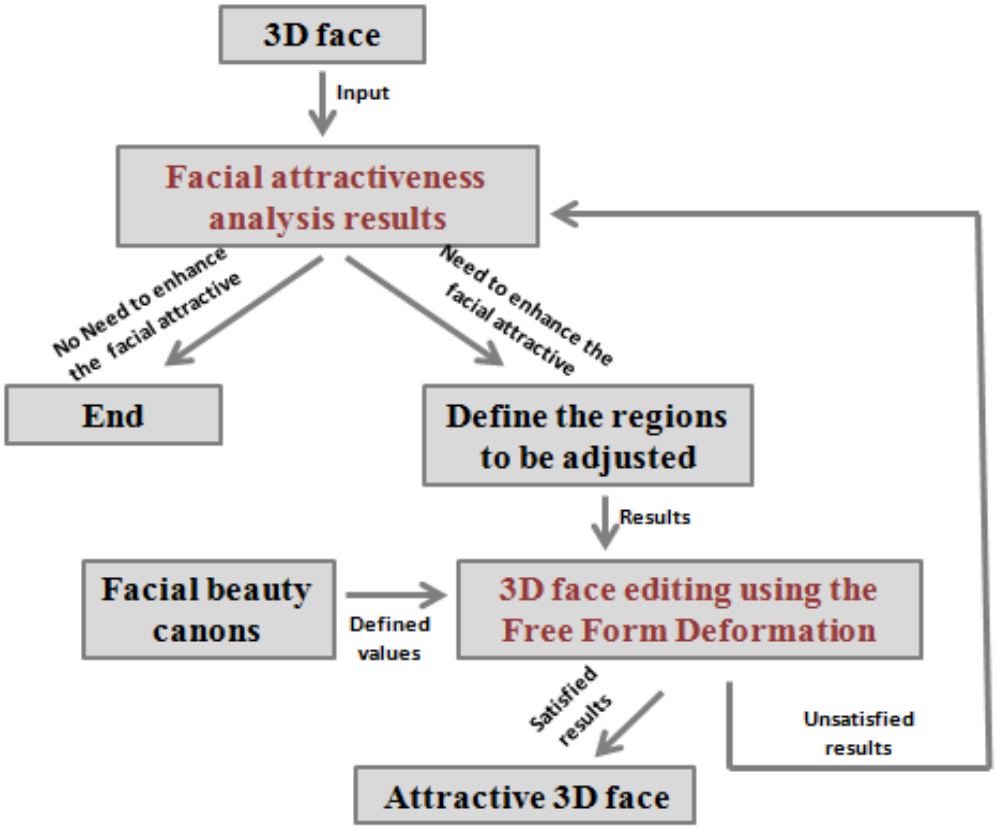

Figure 4.1: Overview of the 3D facial aesthetic quality enhancement process

Different approaches have been proposed in the literature for the purpose of 3D facial editing as described previously in chapter 1. These works aim to generate natural looking deformations of shapes by developing fast, intuitive and accurate approaches for both global and local shape deformation. In particular, the Free Form shape deformation based methods for 3D models editing has been a subject of intensive research studies in the literature, due to their various advantages especially for the domain of digital industries.

To apply the Free form deformation algorithm for 3D mesh editing some steps has to be performed as shown in figure 4.1. Mainly, from the obtained results of the aesthetic quality analysis which are used to determine how much the face must be adjusted, the regions to be edited are identified; these regions represent the set of the vertices to which the deformation will be applied. Thereafter, the editing consists of displacing the vertices from their original positions to new ones on both the frontal and the profile side of the input 3D face in order to get more attractive face respecting the beauty canons discussed in the previous chapters; symmetry, golden ratio, neoclassical proportions and the angular profile.

In the rest of this chapter, we introduce a brief description of the free form deformation technique in the first section (section2), as well as its different functions (Bézier, B-spline, and NURBS) in the subsections 2.1, 2.2, and 2.3 respectively. In section 3, we present the chosen model to enhance the aesthetic quality of 3D faces in term of the beauty canons: symmetry, golden ratio, neoclassical proportions, and the angular profile respectively in the subsections 3.1, 3.2, 3.3, 3.4, and 3.5. The obtained results of 3D facial attractiveness enhancement are presented in section 4, and a conclusion is presented in the last section 5.

2 Free-form deformation

Free form deformation is one of the main methods to edit the geometric shapes. The term free-form deformation (FFD) was first introduced by Sederberg and Perry in 1986. Basically, the main concept was to deform the space in which the object is enclosed; the further modification recalculates the position of the solid points in terms of the modified points in the network.
The Sederberg's technique has been extended later in 1990 by Coquillart; the new version extends the applicability of the first algorithm by using of the irregular lattices. Thereafter, various modifications were applied to the FFD such as by de Casteljau algorithm [250], general spline [251], NURBS [252].
The deformation of 3D shape using the free from approach is based on the use of a polynomial representation to parameterize the shape. The shape to deform is controlled by the use of the control points. Indeed, by changing the position of the control points, the polynomial value describing the curve changes as well. The main used curves for shape deformation are the Bezier, B-splines and NURBS (Non-Uniform Rational B-Spline) curves. The relationship between these types of curves is shown in the following figure 4.2, and we can conclude that the NURBS are the most general type of curves followed by the B-spline curve and finally the Bézier curve.

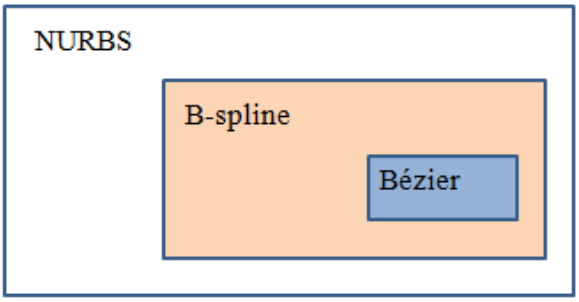

Figure 4.2: Relationship between Bezier, B-splines and NURBS curves

The FFD has proved to be an efficient method to parameterize and manipulate the 3D shape. The free form deformation approaches are known to be independent from the mesh which is used for its discretization, moreover, FFD preserves the shape details after the deformation, and it can be applied locally to deform just a part of the 3D shape or globally to alter the whole shape.

2.1 Free-form deformation based Bézier function

The representation of the Bézier curve is considered to be the most often used representation in computer graphics and geometric modeling. These curve parameters have been defined by two engineers (Pierre Bézier and Paul de Casteljau) in the 1960s to attempt drawing automotive components, thus the curve was called according to Pierre Bézier.
Bézier curve is based on the use of the Bernstein polynomial function, and it is defined by:

$$P_n(t) = \sum_{i=0}^{n} B_i^n(t).P_i$$

Where:

$$B_i^n(t) = \binom{n}{i} t^i(1-t)^{n-i}, i = 0, \dots, n$$

Is the Bernstein polynomial, and P_i are the controls points or the Bézier points.
The Bézier curves have various important proprieties allowed by the de Casteljau algorithm which make them widely used, the main proprieties are:

- **Affine invariance**: The affine map consists of a linear transformation and then a translation between two vectors space. The Bézier curves are unchanged under affine maps which mean that to make things easier, the transformations can be applied to the controls points instead of applying them to the curve. Then the results of the transformation can be constructed from the affine image of its control points.

- **Convex hull property**: The Bézier curve is entirely set in the convex hull of the specified control points, for t ∈ [0, 1], $P_n(t)$ lies in the convex hull of the polygon.

- Modifying the location of a control point results in an overall change in the shape of a Bézier curve.
- **End point interpolation**: The Bézier curve goes through the points P_0 and P_n.

- **Subdivision of the Bézier curve**: In case it is necessary to make a more complex curve, instead of raising the polynomial degree, thereby raising the calculation cost, it is possible to connect several curves of a less complex degree, while respecting continuity and regularity.

The Free Form Deformation based on the Bézier function imposes a parametric hyperpatch on the space to be deformed; the hyperpatch is the surface extension of the Bézier curve and it can be seen as a flexible jelly block that can be twisted, bent and inflated under the effect of a set of control points. Therefore, the deformation process is considered as a trivariate volume of the

polynomial tensor product which extends the one-dimensional curves to the three-dimensional ones.
In order to deform a 3D shape, the user start by first moving the lattice control points, hence deforming the hyperpatch as well. Consequently, any point inside the lattice is deformed accordingly following the hyperpatch.

2.2 Free-form deformation based B-Spline function

In order to have more control on the shape of the curve, B-spline curves (by Greissmair and Purgathofer [1989] and Comninos [1989]) consist of subdividing the domain of the curve into segments instead of the curve directly. This subdivision is performed using the so called knots, control points and a set of coefficients. All the segments created by the subdivision have to respect a continuity conditions.
The form of the B-spline curve of degree p is very similar to the Bézier curve form, and it is defined by:

$$C(u) = \sum_{i=0}^{n} N_{i,p}(u).P_i$$

Where:

$$N_{i,p}(u) = \frac{u - u_i}{u_{i+p} - u_i} N_{i,p-1}(u) + \frac{u_{i+p+1} - u}{u_{i+p+1} - u_{i+1}} N_{i+1,p-1}(u)$$

Is the i-th B-spline basis function of degree p.
Rather than using the control points, the B-spline curve use real coefficients. Same as the spline curves, a B-spline of degree 0 is a constant function, a B-spline of degree 1, a linear per piece and a B-spline of degree 2, a quadratic polynomial per piece.
The first and the quadratic B-spline are presented as follows:

$$B_{0,1}(t) = \begin{cases} t, & 0 \le t < 1 \\ 2 - t, & 1 \le t < 2 \\ 0, & otherwise. \end{cases} \qquad B_{0,2}(t) = \begin{cases} t^2, & 0 \le t < 1 \\ -2t^2 + 6t - 3, & 1 \le t < 2 \\ (3 - t)^2, & 2 \le t < 3 \\ 0, & otherwise. \end{cases}$$

As explained before, the B-spline basis function is similar to the Bézier basis functions, but it is a bit complex due to the subdivision of the curve domain using the knots, as well as the characteristic of being local as the B-spline basis functions are not non-null on the whole interval. The B-spline curve use more shape information comparing to the Bézier curve and thus it is more general. The B-spline has other proprieties such as:

- **Local support**: $N_{i,p}$ (u) is a non-zero polynomial on the intervalle [u_i, u_{i+p+1}).
- **Subdivision propriety**: the B-spline basis function $N_{i,p}$ (u) is a composite curve of degree p polynomials joined at knots in [u_i, u_{i+p+1}).
- **Knots number**: If the number of knots is m+1, the degree of the basis functions is p, and the number of degree p basis functions is n + 1, then m = n + p + 1.

2.3 Free-form deformation based NURBS function

Despite the various proprieties and the important characteristics of the polynomial curves such as the Bézier and the B-spline curves, these curves cannot represent some of the curves which are based on the rational functions such as circles and ellipses for example or require a higher degree of curves to represent simplest. Therefore, the NURBS (by Lamousin and Waggenspack [1994]) curves or the Non-Uniform Rational B-Splines Curves are a generalization of the B-spline curve that cover rational curves using homogenous coordinates.
A NURBS curve of degree p, control points P_0, $P_{1, \ldots,}P_n$, knot vector U = (u_0,u_1,..., u_m), and weights w_0, w_1, … , w_n. Is defined by:

$$C(u) = \sum_{i=0}^{n} R_{i,p}(u).P_i$$

While the basis function is given by:

$$R_{i,p}(u) = \frac{N_{i,p}(u)w_i}{\sum_{j=0}^{n} N_{j,p}(u)w_j}$$

As can be seen from the previous formula, the NURBS curves are rational which will make the representation of rational functions feasible.
Since the NURBS curves are considered as a generalization of the B-spline curves, they have the same proprieties as the B-splines in addition to more others derived from rational characteristics. Thus, the major proprieties of NURBS basis function are:

- **Local support**: $N_{i,p}$ (u) is a non-zero polynomial on the intervalle [u_i, u_{i+p+1}).
- **Subdivision propriety**: the B-spline basis function $N_{i,p}$ (u) is a composite curve of degree p polynomials joined at knots in [u_i, u_{i+p+1}).
- **Knots number**: If the number of knots is m+1, the degree of the basis functions is p, and the number of degree p basis functions is n + 1, then m = n + p + 1.
- **B-spline**: If all the weights are equal w_i = c, the NURBS function turns to a B-spline function, $R_{i,p}$ (u) = $N_{i,p}$ (u).
- **Strong convex hull property**: The NURBS curve is set in the convex hull of its control points.
- **Local modification scheme**: Altering the location of a control point P_i, affect only the curve C(u) on the interval [u_i, u_{i+p+1}).
- **Curve and control points' positions**: By increasing or decreasing the value of weight w_i the curve is pulled or pushed toward or away from control point P_i.

3 3D face attractiveness enhancement based FFD

Since facial attractiveness has a great role in individuals social life, as people with attractive face enjoy many advantages such as: being interesting, nicer, getting good job, having more friends and best partner comparing to others with less attractive faces, most of them tend to enhance the aesthetic quality of their faces to benefit from these advantages.
Several studies have confirmed that the constituent of facial attractiveness are universal, meaning that people from different cultures, ethnicities, ages, gender and socio-economic classes have the same criterion and perception in their judgment on facial beauty [27][29]. The presented studies in the literature about the universal notion of facial attractiveness have suggested some common criterions that a face has to respect in order to be judged as an attractive face. These criterions are known as the beauty canons, indeed they have been defined since ancient time and they include: facial symmetry, golden ratio, neoclassical proportions, and the angular profile.
Improving the appealing of faces has a wild application in photographs retouching and beatification engines which tend to de-blemish and retouch the faces by digitally manipulating them. This manipulation can affect the facial color, texture and its geometry as well, thus, such a tool can be used for various purposes as advertising, social services, facial collages, and faces special effects.
A large number of papers have introduced various tools to enhance the aesthetic quality of 3D faces. In [187] authors proposed a similar work, by enhancing the attractiveness of 3D faces based on the symmetry, the golden ratio, and the neoclassical proportions. Most of the presented works focus on one or two beauty canons in their analysis and improvement of facial attractiveness, moreover, the key step of localizing the 3D facial landmarks is often performed manually in most of the introduced approaches.
From all these issues, we have built a new system to analyze and enhance the attractiveness of 3D faces, the proposed system is more robust and fully automatic at the same time comparing to the existing tools as will be further explained.

In this section we aim to improve the attractiveness of 3D face while keeping a close similarity with the original face. Therefore, a novel system capable of enhancing the aesthetic quality of a given 3D faces (both frontal and profile sides) based on the obtained results of the attractiveness analysis of the same 3D face.
The proposed tool to enhance the attractiveness of 3D faces is based on the use of a free form deformation technique using the Bézier interpolation function. This function has been chosen for the simple reasons that it is easy to use, its computation speed, good results of 3D shape deformation, in addition to other various proprieties as presented in the previous subsection. To the best of our knowledge, this FFD technique has never been used for such a purpose of enhancing the aesthetic quality of 3D faces before.
In the following subsections, the deformation model used to enhance the aesthetic quality of 3D faces is explained, as well as the detailed methodology to improve each of the 3D facial beauty canons (Symmetry, golden ratio, the neoclassical proportions, and the angular profile of the 3D face). At the end, the final results of 3D faces attractiveness enhancement are presented.

3.1 The deformation model

In this subsection, we aim to edit the 3D face, if modifications are needed, in order to enhance its attractiveness following the results of the previous analysis step. These modifications are applied to the main 3D facial region of interest such as: eyes, nostrils, mouth, chin, cheeks, and the profile side.

In the step of 3D face attractiveness enhancement, the localized 3D landmarks are used in order to accurately deform the face.

To deform a 3D face, a local coordinate point is determined on the vertex that has to be deformed and it is called the control point C. Therefore, to shift a vertex from its original position O to P the new one. The following formula is used:

$$P = O + D \qquad (9)$$

Where the displacement vector D is given by:

$$D = \frac{\gamma}{\varepsilon}.B.\vec{N} \quad (10)$$

While the basis function B (Bézier) is calculated using the formula in [253]:

$$B = \exp\left(-\frac{|O-C|^{\alpha}}{2r^2}\right) \quad (11)$$

And:

$$\varepsilon = \exp\left(-\frac{|O_{min}-C|^{\alpha}}{2r^2}\right) \quad (12)$$

$O_{min\ is}$ the closest original vertex to the control point C. and γ, α , and ε are parameters that can be modified depending on the desired deformation. In the displacement formula, $\vec{N}$ is the normal vector of the 3D mesh at the control point, the |.| represents the Euclidian distance between the original point and the deformed one, the parameter γ is used to control the height of the peak after the deformation, and its sign defines the shape form of the deformation whether it is repelling or attracting to the 3D mesh. Thus if $\gamma = -1$ the deformation is shape attracting and if $\gamma = 1$ the deformation is round repelling.

In the case where the control point is not among the mesh vertices, the parameter ε defines height of the deformation as the parameter γ. The parameter α represents the sharpness of the deformation, and r controls the region of the deformation.

By changing the values of the parameters (γ, α , ε, and r) in equation (10), a large variety of shape deformations can be obtained which is considered as one of the advantages of the FFD. On the other hand, in order to deform a set of control points on a 3D mesh, the presented technique can be extended, so the formula of the displacement can be written as:

$$P = O + \sum D \quad (13)$$

Where $\sum D$ is enclosing all the defined control points to be deformed on the 3D mesh.
Indeed, in our work, the set of the parameters guiding the deformation are defined by:

- γ: 1.0
- α: 2.0
- ε: 1.0
- r: 0.1

As been explained previously, the Bernstein polynomial function has several proprieties which can be extended to B-splines or NURBS functions, but in our case, and in order to achieve our goal, the Bernstein or Bézier basis function is enough to get accurate and efficient deformation results.

3.2 Symmetry enhancement

To enhance the aesthetic quality of a 3D face in term of symmetry, we were based on the obtained results from the attractiveness analysis step (Chapter-3, section 3.2) which consists of conducting a symmetrization test for each region in the face and then to the whole face. Indeed this process is based on the use of the localized point pairs 3D craniofacial facial landmarks and the median axis as the central plane. Therefore, for each pair landmarks from the two frontal sides of the 3D face we verify whether the landmark pairs are symmetric or not. In case of non identified symmetry, we perform displacements (translations and rotations) of the associated landmarks according to the obtained results from the symmetrization test.
In our case, we have six point pairs: Exocanthion pair, Endocanthion pair, Alare pair, cheek superior pair, Chelion pair, and cheek inferior pair. As a result of this process, we obtain an adjusted face and facial landmarks and thus a symmetric 3D face so far as shown in figure 4.3.

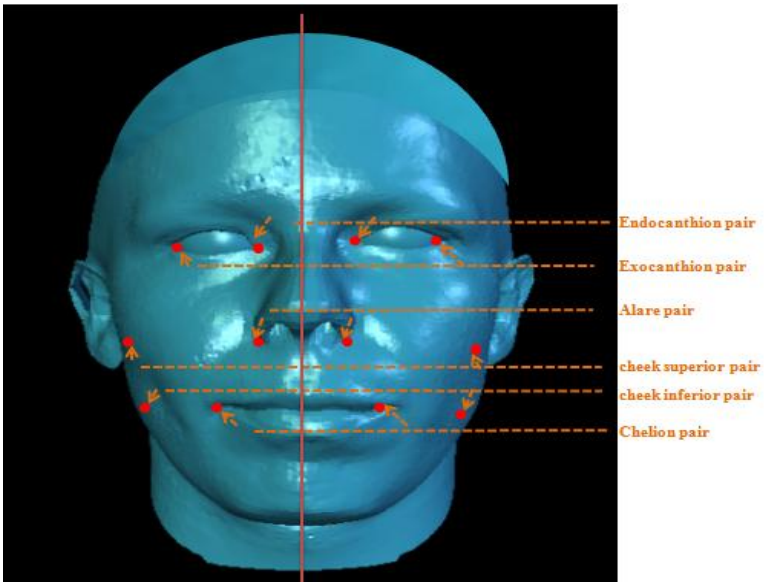

Figure 4.3: Symmetrization of a 3D face

3.3 Neoclassical proportions enhancement

To improve the attractiveness of the frontal side of 3D faces in term of the neoclassical proportions which are the vertical facial fifth, the horizontal facial thirds, the width of the mouth and the height of the chin, we were based on the obtained results from the attractiveness analysis step as well and then for each proportion, after testing whether it complies with the predefined values in the literature or not, we determine the appropriate displacements for each facial features that need to be enhanced in order to get more attractive face. In general the displacement is achieved by moving a set of vertices belonging to the same zone of the original facial proportion to keep the main proprieties of the original face.

In our case, as mentioned previously, a set of four neoclassical facial proportions are verified as demonstrated in the following figure 4.4, figure 4.5, figure 4.6 and figure 4.7.

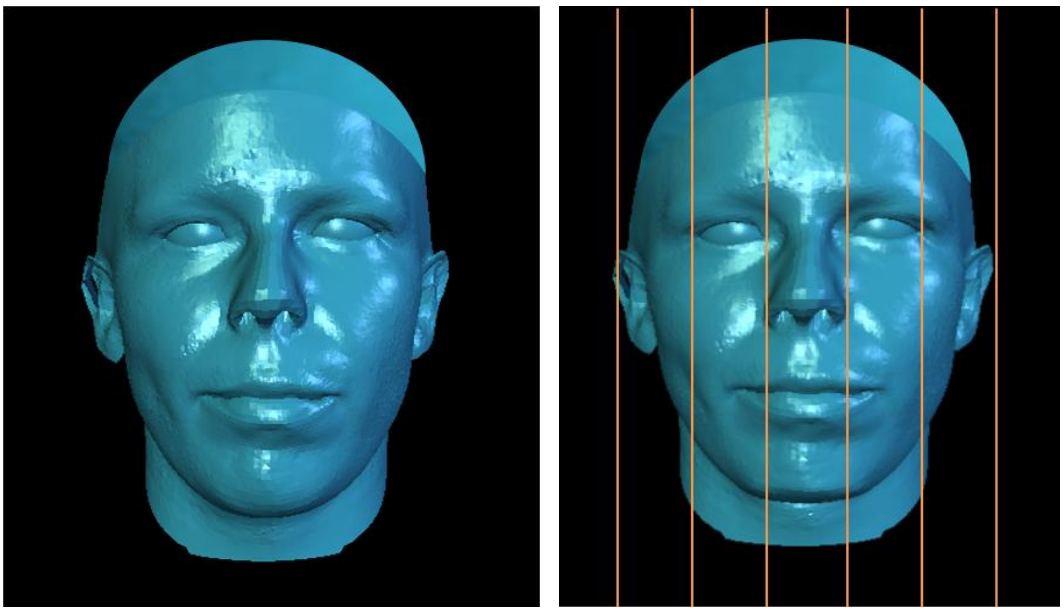

Figure 4.4: Neoclassical proportions enhancement: vertical facial fifth (left face: before the enhancement, right face: after the enhancement).

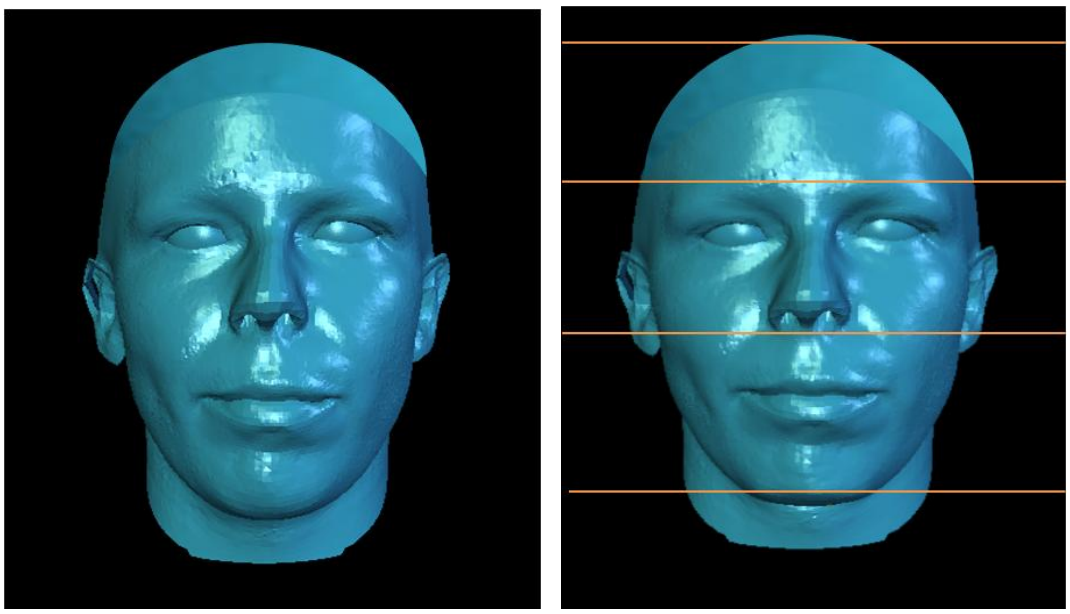

Figure 4.5: Neoclassical proportions enhancement: horizontal facial third (left face: before the enhancement, right face: after the enhancement).

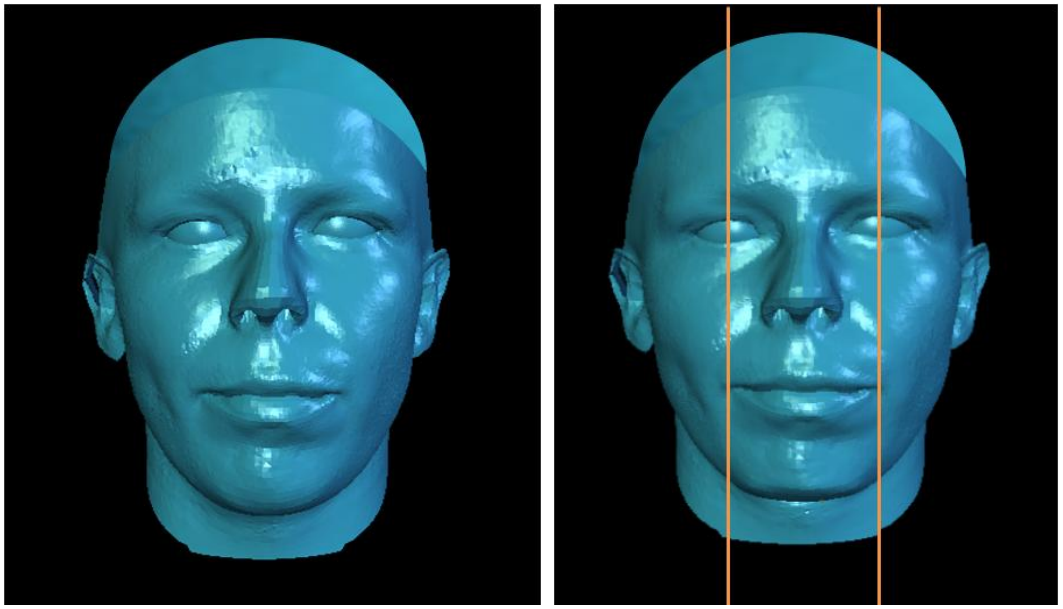

Figure 4.6: Neoclassical proportions enhancement: mouth width (left face: before the enhancement, right face: after the enhancement).

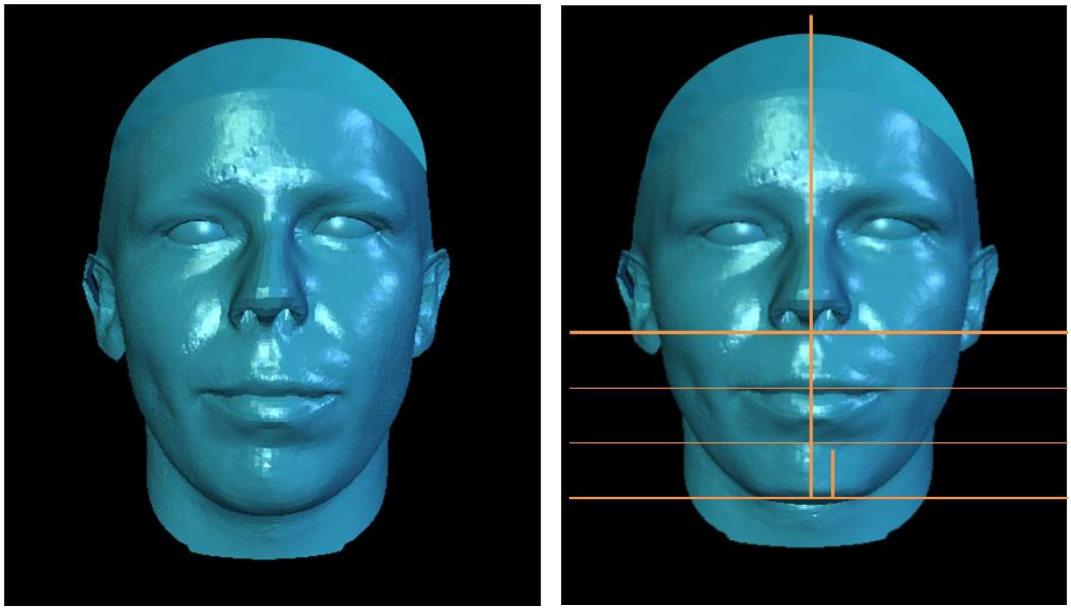

Figure 4.7: Neoclassical proportions enhancement: chin height (left face: before the enhancement, right face: after the enhancement).

3.4 Golden ratio enhancement

A ratio refers to two source landmarks and two destination points; in case of calculating the golden ratio for a given 3D face, the detected facial axes were used. These axes pass through the facial features: eyes axis, nostrils axis, and mouth axis, and the set of the calculated ratios. In our case are; the first ratio is calculated from the forehead point to the chin tip and from the eyes

axis to the chin tip, the second ratio is from the eyes axis to the chin tip and from the eyes axis to the mouth axis, the third ratio is calculated from the eyes axis to the mouth axis and from the eyes axis to the nose axis, and the last ratio is calculated from the width of the mouth and the nose width.

In order to enhance the attractiveness on the frontal side of a 3D face in term of golden ratio, we use of the obtained results from the golden ratio analysis and then for each ratio we define the displacement that should be applied to get more attractive face respecting the golden ratio rule. Thus, firstly the anchoring points are defined and the destination coordinates have to be calculated using the source points and the value of the ratio which is ~1.618. Figure 4.8 shows the set of the calculated golden ratios.

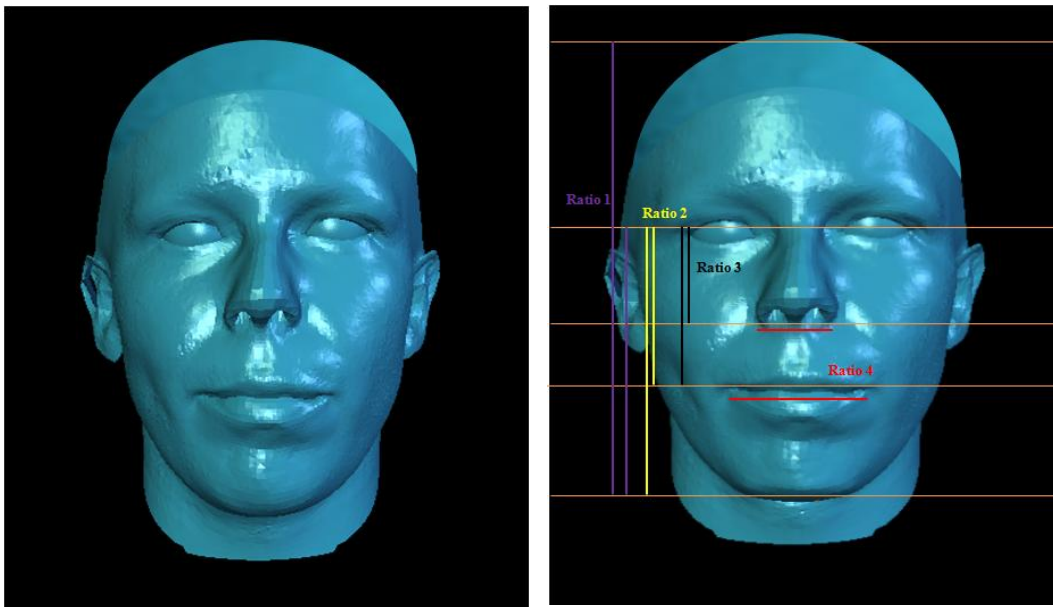

Figure 4.8: 3D facial golden ratios enhancement (left face: before the enhancement, right face: after the enhancement).

3.5 Angular profile enhancement

The aesthetic quality of a face is not only determined from the frontal side of the face but from the profile side as well. The facial profile side editing remains a tedious task as a large modification on this side can affect the proportions of the frontal side. Therefore, in order to enhance the attractiveness of the profile side, the set of 11 angular measurements (table 4.1) have to be conforming to the predefined values in the literature to obtain an agreeable face. To this end, the profile landmarks are adjusted in the YZ plane only without changing their X-coordinates.

The angles	Mean values of the angles
NasoFrontal angle (NFr)	115° - 130°
NasoFacial angle (NFa)	30° - 40°
NasoMental angle (NM)	120° - 130°
Nasal angle (Na)	23.3°

Maxillary angle (Mx)	14.1°
Mandibular angle (Mn)	17.1°
MentoCervical angle (MeC)	80° - 95°
MaxilloFacial angle (MF)	5.9°
Facial angle (F)	102.5°
Nasal Maxillary angle (NM)	106.1°
Holdaway angle (H)	10°

Table 4.1: Profile angles measurements.

The following figure 4.9 and figure 4.10 illustrate the different angular profile on a 3D face.

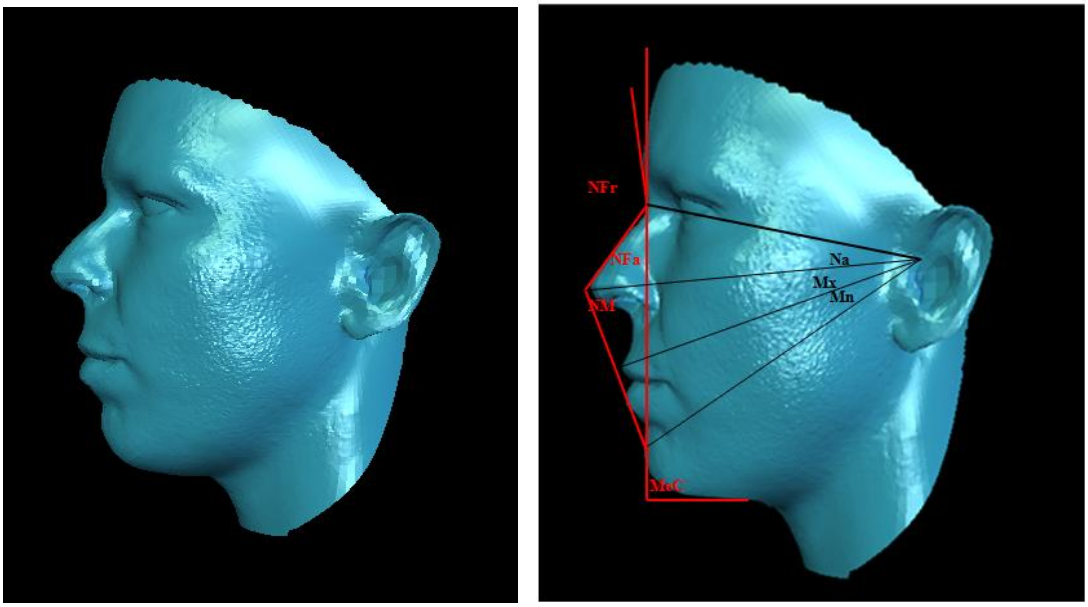

Figure 4.9: Profile angles enhancement (left face: before the enhancement, right face: after the enhancement) (1).

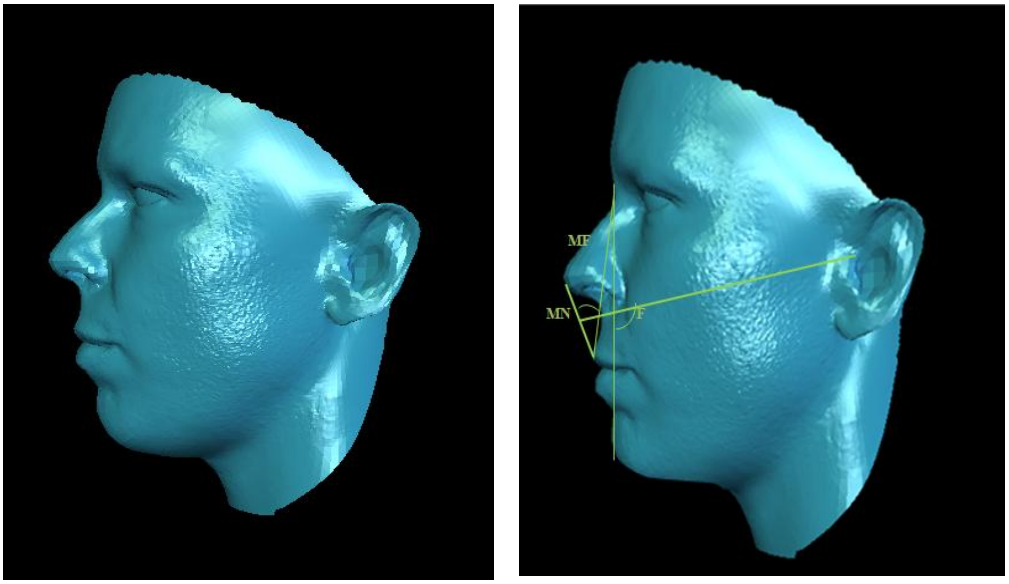

Figure 4.10: Profile angles enhancement (left face: before the enhancement, right face: after the enhancement) (2).

4 Results

Based on the 3D faces aesthetic quality analysis explained in chapter-3, section 3.3.2, which aims to verify whether the input 3D faces comply with the beauty canons (symmetry, golden ratio, neoclassical proportions, and the angular profile) or not, the necessary modifications to apply to get more attractive faces in term of the predefined beauty canons are proposed as well.

As described in the previous subsections, to improve the aesthetic quality of 3D faces, we proceed by enhancing each of the beauty canons using a free form deformation technique based on the Bézier function, while trying to keep the main proprieties of the original face.

To achieve this purpose, we have used the same 3D face datasets as the previous chapter; a sample data set from the CranioGUI dataset [247], and BaselFaceModel dataset [248] and from the obtained results of the attractiveness analysis we have edited the 3D faces to become more attractive.

4.1 3D faces aesthetic quality analysis for a sample data set from the CranioGUI dataset

Input:

3D faces from the sample data set from the CranioGUI dataset + the results of the attractiveness analysis of each face.

Output:

Resulted 3D faces after enhancing their aesthetic quality using the free form deformation technique based on Bézier function.

Results:

The following figures; figure 4.11, and figure 4.12 describe the process of 3D faces enhancement for a set of 3D faces from the sample data set from the CranioGUI dataset, the top rows present the original 3D faces (front and profile), and the bottom rows present the same 3D faces after enhancing their aesthetic quality.

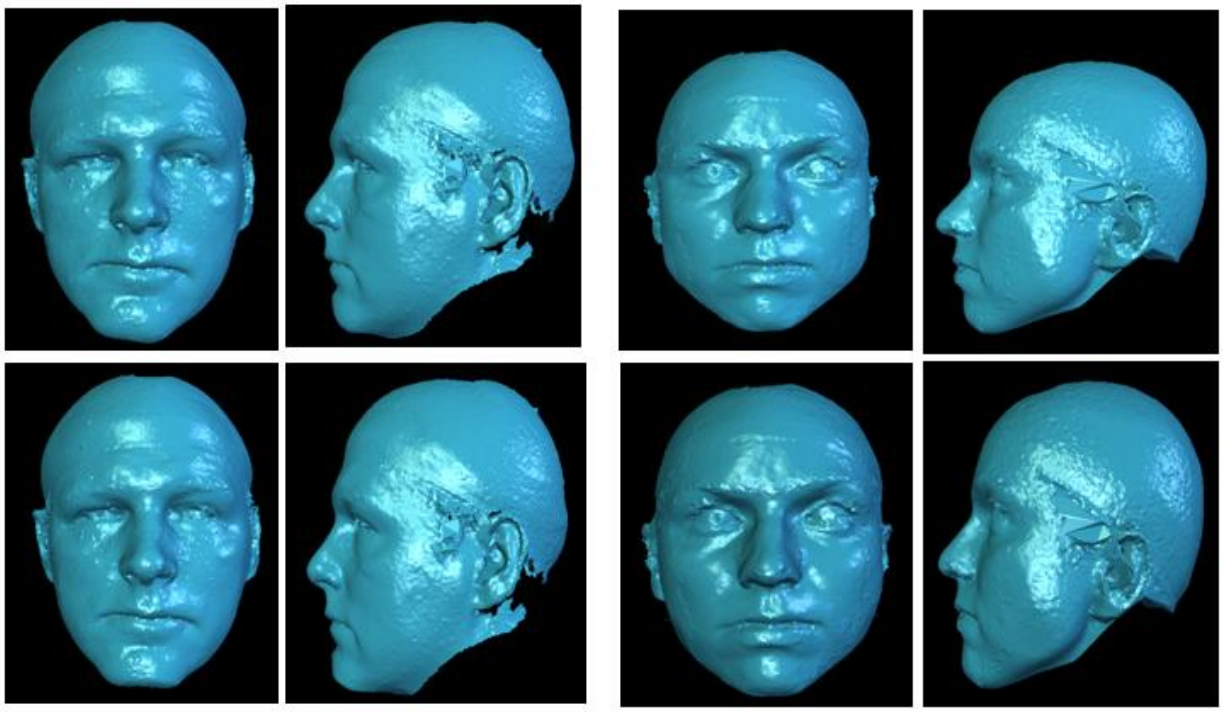

Figure 4.11: 3D face attractiveness enhancement for a sample data set from the CranioGUI dataset (1). Top row: before the enhancement, bottom row: after the enhancement.

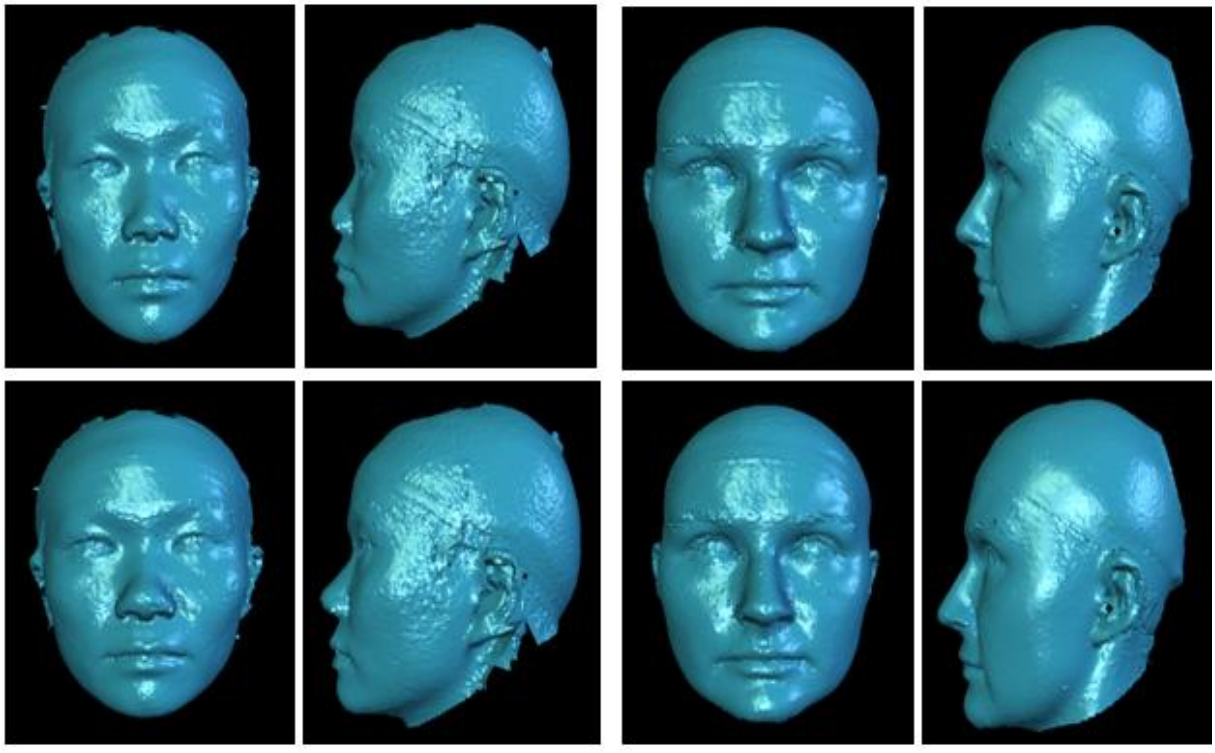

Figure 4.12: 3D face attractiveness enhancement for a sample data set from the CranioGUI dataset (2). Top row: before the enhancement, bottom row: after the enhancement.

4.2 3D faces aesthetic quality analysis for BaselFaceModel dataset:

Input:

3D faces from the BaselFaceModel dataset + the results of the aesthetic quality analysis of each 3D face.

Output:

The obtained 3D face after enhancing its attractiveness using the free form deformation technique based on Bézier function.

Results:

The following figures; figure 4.13, and figure 4.14 present the process of 3D faces enhancement for a set of 3D faces from the BaselFaceModel dataset, the top rows present the original 3D faces (front and profile), and the bottom rows present the same 3D faces after enhancing their aesthetic quality

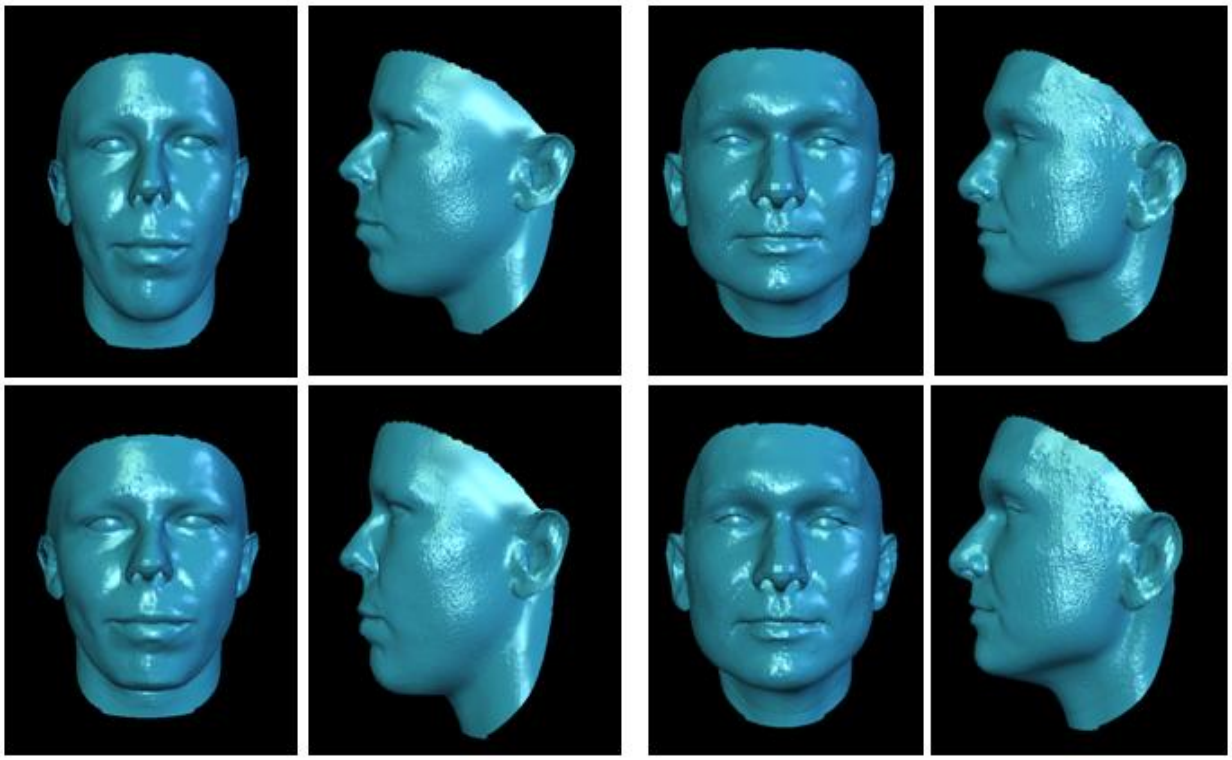

Figure 4.13: 3D face attractiveness enhancement for a sample from BaselFaceModel dataset (1). Top row: before the enhancement, bottom row: after the enhancement.

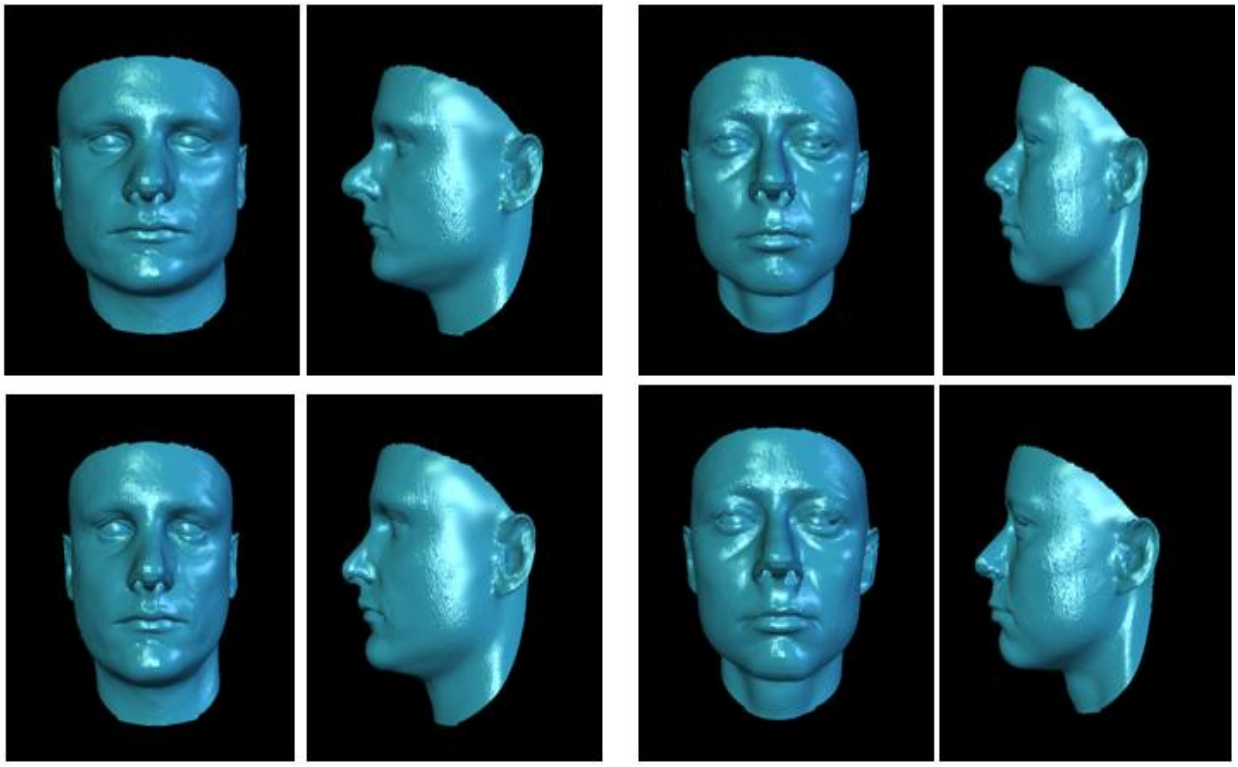

Figure 4.14: 3D face attractiveness enhancement for a sample from BaselFaceModel dataset (2). Top row: before the enhancement, bottom row: after the enhancement.

Concerning the computation cost of the 3D facial aesthetic quality enhancement using the free form deformation technique based on the Bézier function for both the used 3D face datasets, a PC with: Intel Core 2 Duo, 2.20 GHz with 3GB RAM is used. Thus, by using this machine, the required time for enhancing the attractiveness of each 3D face from the sample data set from the CranioGUI dataset is 1.05 (s) as an average, and the required time to enhance the aesthetic quality of each 3D face from the BaselFaceModel is 1.18 (s) as an average. Therefore, we can conclude that the proposed method of using the free form deformation technique based on the Bézier function to enhance the attractiveness of 3D faces is reliable and outstandingly fast making it applicable in many 3D faces editing application in the real world (see table 4.2).

	Sample data set from the CranioGUI dataset	**BaselFaceModel dataset**
Computation cost per scan	1.05 (s)	1.18 (s)

Table 4.2: Computation cost of enhancing the aesthetic quality of the 3D faces for both the used 3D face datasets.

5 Conclusion

In this chapter, we presented the 3D facial aesthetic quality enhancement using a free form deformation technique based on the Bézier function, and the obtained results from the attractiveness analysis as well. This chapter initially introduced the main existing free form deformation techniques; Free-form deformation based Bézier function, Free-form deformation based B-Spline function, Free-form deformation based NURBS function as well as the major

differences between these three types. Afterwards, the used deformation model is described in order to enhance the aesthetic quality of 3D face in term of the defined beauty canons in the literature including the facial symmetry, the golden ratios, the neoclassical proportions, and the angular profile.

The obtained results of 3D facial attractiveness enhancement for both the sample data set from the CranioGUI dataset and the BaselFaceModel dataset show that the proposed system can edit the input 3D face adequately to conform to the predefined beauty canons in the literature; facial symmetry, golden ratio, neoclassical proportions, and the angular profile. These results have clearly indicated the efficiency and the accuracy of the presented system to both analyze and enhance the aesthetic quality of 3D faces.

In the next chapter, we perform an external evaluation step to assess the obtained results from the step of 3D facial attractiveness analysis using the proposed system. During this evaluation, a domain expert is asked to assess the final results of the facial aesthetic quality enhancement, thereafter, we have performed a survey by asking a group of people to vote for the most attractive faces within the original and the enhanced 3D faces using our system.

Chapter 5: Evaluation of the results

1 Introduction

The deformation system presented in the previous chapter aimed at enhancing the aesthetic quality of the 3D faces based on the results of the attractiveness analysis from chapter 4. The aesthetic quality analysis goal is to verify if the given 3D face meets the beauty canons namely the facial symmetry, golden ratio, the neoclassical proportions, and the angular profile. Thus, a 3D face respecting these canons or even being very close to their values is considered as an attractive face and thereafter no need to edit the face, otherwise, the face will have to be modified to improve its attractiveness as proposed in the previous chapter.

The purpose of the current chapter is to evaluate the results of the facial aesthetic quality analysis method as well as the modified 3D face after enhancing its attractiveness using our proposed system. To achieve this end, we have used two methods; the first was to ask a domain expert to assess the obtained results from the 3D facial attractiveness enhancement, and the second method is one of the existing empirical research methodologies, which is the **"survey research"**. The reason for selecting the survey research method to evaluate our final results as well as the other existing empirical research methodologies will be further explained.

This chapter starts with the research questions (in section 2) defined as part of this assessment study. In section 3 the research design used to answer the proposed research questions is described. The main finding from the evaluation regarding the research questions is explained in section 4. Section 5 presents the assessment of the obtained results validity, and finally the last section (section 6) concludes the chapter.

2 Research questions

Overall, the purpose of the evaluation presented in this chapter is to answer the research questions detailed as follows:

- **Research Question-1:** How many landmarks are required to model the attractiveness of a human face?
- **Research Question-2:** Are geometric approaches better than statistical learning techniques for the automatic identification of landmarks in human faces?
- **Research Question-3:** Are the attractiveness analysis and enhancement systems usable?
- **Research Question-4:** Is the edited 3D face attractive?
- **Research Question-5:** Is the used free form deformation technique the best way to enhance the attractiveness of 3D faces?

In Research Question-1, the hypothesis is that there are a specified number of facial landmarks that are required to analyze the aesthetic quality of human faces. Hence in our research we

focused on finding the appropriate number of landmarks in order to accurately modeling the attractiveness of a given face (2D/3D).

In Research Question-2, as we have used a geometric information based technique to identify the landmarks on human 3D faces, we assess the relevance of these methods comparing to the trained statistical feature model techniques in localizing the 3D facial landmarks.

In Research Question-3, we evaluate whether such systems to analyze and enhance the aesthetic quality of face are usable, thereafter we identify the users' perceptions of these tools.

In Research Question-4, and after improving the aesthetic quality of 3D faces, we evaluate the obtained new face whether it is attractive or not.

In Research Question-5, we assess the relevance of the used free form deformation technique in enhancing the aesthetic quality of 3D faces.

3 Research methods

In this section, we explain the followed methodology to address the defined research questions therefore to achieve the final goal of our thesis. In the literature, various empirical research methods were proposed, and they are adopted from other field such as medicine, sociology, and psychology[254]. The most relevant research methods have been identified by [255] and classified into five classes:

- **Controlled experiments:** This method attempts to study a testable hypothesis in which one or more independent variables are varied in order to determine their influence on one or more dependent variables [256]. A clear hypothesis, the basic theory that the hypothesis is derived from, the study variables and the methods to measure them are necessary to perform a controlled experimental design.

- **Survey research:** This is a popular deductive method of collecting conclusive, quantifiable data from a large population in a cost-effective manner, usually through the use of questionnaires [257].A crucial requirement for the researcher in this method is to select a representative sample of the entire population pertinent to the study. Data analysis techniques such as random sampling and stratified sampling are then employed to generalize the results to the whole population. A clear research question is necessary to assess accurately the needed nature of the sample population.

- **Case studies:** This method is divided into two types; the exploratory case studies and confirmatory case studies. The first type is used to make hypotheses and construct theories, while the second type is used to test existing theories. This method can begin with a high-level research question to select cases and then gather the data necessary to study how and why these phenomena occur and the possible causal relationships within these phenomena [258].

- **Ethnographies:** In this method of sociological research, the researcher is ignoring all existing theories and becoming a part of the study group to examine a society or culture and the practices of communication that happen in that group. This method necessitates a research question regarding cultural practices and relevant access to the group for more detailed analysis [255].

- **Action research:** the Action Research method, aims to solve a problem, the researcher is involved to "simultaneously study the experience of solving the problem" [255]. This method can also begin with a high-level research question and requires access to the community concerned.

To evaluate a research study, the choice of a method depends on the researcher's theoretical knowledge, access to the required resources and the proximity between the research method and the posed research objective/question [255]. Given that in our case we aim to test a predefined theory, where the researcher is only an observer of events, the "**survey research**" is used, as the other methods are qualitative in nature, which allow investigating a high-level research question and refining the research context.

4 Research design

To address the defined research questions, we have used two methods; the first method was to analyze again the obtained results from the step of 3D facial aesthetic quality enhancement and verify whether the resulted 3D faces comply with the beauty canons (facial symmetry, golden ratio, neoclassical proportions, and the angular profile) or not, moreover, this method is based on comparing our results to the most relevant works in the literature discussing the same problem. Thereafter, and for further validation of the obtained results, these results were then verified by a domain expert in plastic surgery to whom we have asked to analyze both the aesthetic quality of the original version of the 3D faces and the enhanced version of the same faces by filling in a table which represent each of the used 3D faces IDs from both sample data set from the CranioGUI dataset and the BaselFaceModel datasets, the analysis results of the original 3D faces, the analysis results of the enhanced 3D faces, and if she has any comments to add about the outputs of our system as shown the table 6.1. This method is considered the basic way to evaluating our proposed system to analyze the aesthetic quality of 3D faces and enhance their attractiveness. This method is used as well to answer the set of the five research questions.

And the second method to address the research questions was the use of the survey research method. This method is widely used in similar cases of analysis and evaluation as the researcher can only use existing theories and evaluates them by observation without getting involved in the studied phenomenon or the participant's social life. Therefore, to evaluate the obtained results of 3D facial attractiveness enhancement, we have asked a number of participants' raters to vote for the 3D face that seems more attractive within the original and the new faces (before and after the 3D face aesthetic quality enhancement). This task is related to the last research question, as the participants do not have any idea about the details of the analysis process.

4.1 Domain expert and potential participants raters

Based on the first method to assess the obtained results from the proposed system to analyze and enhance the attractiveness of 3D faces, after analyzing for the second time the attractiveness of the enhanced 3D faces using our system, we have asked a domain expert to validate theses results.

The followed table 6.1, were presented to a domain expert in plastic surgery, in addition to the original versions of the used 3D faces and the enhanced ones. For each 3D face, the results of the aesthetic quality analysis of the original faces were recorded in the second column, the results of the aesthetic quality analysis of the enhanced version of the corresponding 3D face are presented in the third column, and if the surgeon has any additional comments they were filled in the last column.

3D face ID	Attractiveness analysis of the original 3D face	Attractiveness analysis of the enhanced 3D face	Comments
3D face 1	-	-	-
3D face 2	-	-	-
..	..	..	..
3D face n	-	-	-

Table 6.1: Assessment of the proposed system to analyze and enhance the aesthetic quality of 3D faces by the plastic surgeon.

The recorded comments by the plastic surgeon have been considered in order to improve the efficiency and the relevance of our system.

Based on the second method to evaluate the obtained results by our proposed system to analyze and enhance the aesthetic quality of 3D faces, we have asked a number of 50 raters to vote for the most attractive faces within the original and the edited versions of the 3D faces.

The participants to the vote for the most attractive faces were selected from some students from our faculty, and the most valuable informations about them are; educational level and background, age, and sex (see appendix 3).

The educational level of the participants varies in the range: [undergraduate students – postgraduate students], and their age is the range: [19-28] for both male and female raters.

4.2 3D edited face evaluation protocol by the participants raters

In our research, in order to perform the evaluation step of our proposed system to analyze and enhance the aesthetic quality of 3D faces based on the raters' votes, we have followed a set of steps protocol as explained in table 6.2.

Research steps	Description
Step-1	We have presented an overview of our research study to each of the participants. The overview englobes the research problematic, different

	objectives and main results.
Step-2	The selected participants were invited to ask any questions to clarify any ambiguity and avoid any misinterpretations.
Step-3	Each of the selected participants in our study was asked to vote for the face the most attractive within the original and the edited 3D face from both the used 3D face datasets. The 3D faces were presented using our PC so that the details can be seen clearly.
Step-4	The results of the vote were recorder manually. For each 3D face from the used datasets, we have created a table containing the ID of the 3D face, the original version and the editing one. Thereafter, we check for each face within the participants has voted for the original or the edited face.
Step-5	Finally, the obtained results from the created table were then analyzed. And a comparison between the results of our system and the votes of the participant is then established.

Table 6.2: Steps of the evaluation protocol

5 Findings

In the current section, we present the major findings of the previous evaluation study. The findings section explains how we addressed the research questions of the section 6.2 using the research design described previously.

In the following explained each research question and appropriate solutions.

5.1 Research question.1

Research Question-1: How many landmarks are required to model the attractiveness of a human face?

In our proposed system, the first step to proceed the analysis of the aesthetic quality of faces (2D/3D) as well as the enhancement of the attractiveness of 3D faces is to localize the facial landmarks. This is considered to be a key step as the accuracy of any further analysis depends on the efficiency of the localization step.
In our case, and to analyze the aesthetic quality of faces (2D/3D), a number of facial landmarks are needed. This number has not been defined clearly in previous studies in the literature; however, many authors have mentioned in their works that the higher number of facial landmarks is the most the attractiveness analysis as well as the enhancement of the attractiveness gone relevant [259][125]. As mentioned before in Chapters 3 and 4, we have localize a largest number so that the attractiveness of both the 2D and 3D faces can be as accurate as possible. For this purpose, to analyze the aesthetic quality of 2D face, we have detected 19 relevant landmarks automatically, and for the analysis of 3D face we have localized 30 facial landmarks automatically, and this for the best of our knowledge, is considered to be the largest number ever

for that purpose with such determined accuracy. This result will allow us to accurately analyze the aesthetic quality of 3D faces, in addition to an efficient face editing due to the global control of each vertex in the 3D input face.

5.2 Research question.2

Research Question-2: Are geometric approaches better than statistical learning techniques for the automatic identification of landmarks in human faces?

To detect the facial landmarks on 3D faces, we have adopted a geometric information based method. We have explained in Chapter 4 that the existing methods to localize 3D facial landmarks can be classified into two types; those based on the geometric information provided by the 3D mesh, and others based on a trained statistical feature models and we have described each of the approaches and explained their use cases.

In our case, in order to localize the necessary landmarks to analyze the aesthetic quality of faces as well as enhancing their attractiveness, the method based geometric information provided by the 3D mesh were chosen for several reasons. Firstly, regarding the speed of computing and the discriminate capacity as well as the pose invariant, the geometric information based methods are known to be respecting these characteristics comparing to the trained statistical feature models. These characteristics are very important in localizing the landmarks on 3D face meshes. Moreover, the methods based on trained statistical feature models are limited to a fixed number of facial landmarks to create the model, so if there is a need for more landmarks, the whole process has to be performed again in order to create a new model and this can be considered as a drawback for this type of methods, which is not the case for the geometric information based methods.

5.3 Research question.3

Research Question-3: Are the attractiveness analysis and enhancement systems usable?

To answer this research question, neither of the participants nor the reanalysis step of the obtained results are going to be helpful. This question has to be answered by those to whom this system has been created which are the plastic/ aesthetic surgeons. For this purpose, we have asked a plastic surgeon who has been a part of our thesis in the first steps, and the answer was that the surgeons need such system to facilitate their tasks; more specifically concerning the communication with patients as using our system the necessary modifications to enhance the aesthetic quality of a given patient' face are given in short time. Moreover, the patient can visualize the final results on his virtual face before the surgery.

5.4 Research question.4

Research Question-4: Is the edited 3D face attractive?

Answering this researching question was the main objective of evaluation process. Firstly, by reanalyzing the attractiveness (facial symmetry, golden ratio, neoclassical proportions, and

angular profile) of each edited face after enhancing its aesthetic quality using our system, we conclude that some of the edited 3D faces comply with these beauty canons and some others have become closer to the perfect values of the beauty canons. On the other side, by asking a domain expert to assess the obtained results of the attractiveness enhancement, table 6.3 presents the results of aesthetic quality analysis of the enhanced versions of the used 3D faces.
Secondly, by asking a group of about 50 participants (36 females and 14 males) aged between [19-28] years old and from various educational levels to vote for the most attractive face within the two versions of the face (before and after the attractiveness enhancement), we have concluded that the obtained 3D faces after enhancing its aesthetic quality using our system are likely to be more attractive comparing to the original faces as reported by the participants votes. Table 6.4 presents the results of analyzing the different votes for each 3D face of the used 3D face datasets.
All of these conclusions allow us to advocate that the edited 3D face by enhancing its aesthetic quality is more attractive comparing to the original version of the face.

	No attractiveness enhancement	**Attractiveness enhancement**
Analysis results	15%	85%

Table 6.3: Domain expert evaluation results

	Original face	**Edited face**
Participants vote	28%	72%

Table 6.4: Participants votes for 3D face attractiveness

About table 6.3, by analyzing the aesthetic quality of 3D face after improving their attractiveness using our proposed system, we have asked a domain expert to assess the relevance of the obtained results of the attractiveness enhancement. As shown in table 6.3, a domain expert in plastic surgery has confirmed that 85% of the 3D faces from the two used 3D face dataset have become more attractive in term of respecting the beauty canons, while 15% of the 3D faces were found to be less attractive than the original faces or even with no noticed modifications.
From table 6.4 that represents the participants' votes' rate for the most attractive 3D faces within the original and the edited faces, 72% of the edited faces were claimed to be more attractive than the original faces, while 28% of the original 3D faces were considered attractive comparing with the edited faces. From these results we can deduce that our proposed system to analyze and enhance the aesthetic quality of 3D faces is relevant and comparable to the human perception of beauty.
Overall, these results allow us to conclude that the proposed system to analyze and enhance the aesthetic quality of 3D face is reliable enough to be applied to enhance the aesthetic quality of 3D face as well as other similar applications in real world.

5.5 Research question.5

Research Question-5: Is the used free form deformation technique the best way to enhance the attractiveness of 3D faces?

The free form deformation is a technique used in our study to edit the 3D faces in order to enhance their aesthetic quality as previously explained in Chapter 5. The aim of this research question is to assess the relevance of this type of deformation method in enhancing the attractiveness of 3D faces. For this purpose, based on the evaluation of the research question 4, we can conclude that the free form deformation technique used in our thesis is relevant enough to make the analyzed 3D faces more attractive with rate of 85% using the domain expert assessment, and 72% based on votes of the participants to the research survey.

We add that the deformation of 3D faces using the free form technique based on the Bézier interpolation function proposed in our study can edit the 3D faces while keeping the main characteristics of the original face, which is one of the important needed proprieties to enhance the esthetic quality of 3D faces.

6 Results validity

The evaluation process described in this chapter aimed at objectively assessing the proposed five research questions presented in section 6.2 using the analysis process by the domain expert in plastic surgeon, in addition to raters' votes from our university. Afterwards, a richer interpretation of the obtained results is performed.

The presented evaluation helped our research to get more reliability as well as adding the credibility to the obtained results from (2D/3D) facial aesthetic quality analysis and 3D facial attractiveness enhancement. As mentioned before, this is performed through raters' votes from our university which consists of voting for the 3D face perceived the most attractive within the original version and the enhanced version of the used 3D faces. The obtained results from this study have reported the efficiency of the proposed system in enhancing the aesthetic quality of the 3D faces as well as answering the majority of the addressed research questions. The most important evaluation of the obtained results was performed by asking a domain expert to analyze the original 3D faces and the resulted versions of the same faces, and then conclude the efficiency of the proposed system. This is as well have demonstrated the reliability of our proposed system as showed in the previous subsection.

Furthermore, the established and the simplified objective of our research have also helped us to determine the needs and the limitations in the proposed system.

Due to the small number of the raters' participant in the vote for the efficiency of our proposed system in the analysis of facial aesthetic quality (2D/3D) and the enhancement of their attractiveness, yet the reported findings from the evaluation process can be considered as provisional results, and this is due to our restricted time. Mostly, during our evaluation process based on the raters' votes for the most attractive faces, we have adopted to explain and demonstrate the efficiency and the accuracy of both the analysis and the enhancement of faces attractiveness, therefore, as a perspective; we aim to conduct more assessments processes.

7 Conclusion

In this chapter, we have introduced the evaluation process of the proposed system to analyze the aesthetic quality of faces (2D/3D) and thereafter to enhance its attractiveness.

The evaluation process is based on performing a new analysis process of the obtained results from deformation step in order to verify whether the edited 3D face meets the beauty canons or not, and then ask a domain expert to assess the obtained results the edited 3D faces

In addition, to consolidate the obtained results, a short survey have been taken using a number of human raters' votes for the most attractive face within the original version and the edited one.

In general, in the second analysis step of the obtained results from the facial attractiveness analysis, we have stated that the edited 3D faces are more attractive comparing to the original faces in term of respecting the beauty canons, which are facial symmetry, golden ration, neoclassical proportions, and the angular profile which show the relevance of our proposed system. Furthermore, the participants' votes have reported that the new versions of 3D faces after enhancing their aesthetic quality are considered to be more attractive comparing to the original faces.

Conclusion and future work

In the last few years, beauty industries have expanded quickly. Therefore, the analysis and assessment of facial attractiveness has attracted the interest of scientists, doctors and artists for its numerous applications in the entertainment industry, virtual media, plastic surgery and cosmetics. Facial aesthetic quality or attractiveness is one of the most important social characteristics of the individual face. Many studies have demonstrated that facial attractiveness is perceived as a key to both social and intellectual skills.

The attractiveness of faces have been a debated topic since ancient time; as the first idea about beauty is that "beauty is in the eye of the beholder" which mean that each individual has its personal liking that may differs from those of others in a society. However, recent empirical finding have demonstrated that the constituent of attractiveness are not related to person's culture or personal history, and have explored and introduced what makes a face more beautiful. These findings are the beauty canons: facial symmetry, averageness, golden ratios and neoclassical proportions which have been considered as ideal ratios for an attractive face by orthodontists, artists, and physician since ancient times.

Various techniques of machine learning have been developed to analyze the attractiveness of the face by evaluating the characteristics of a given face. Nevertheless, these proposed techniques have not tested and combined the beauty canons in an overall system. Moreover, few of them have enhanced the aesthetic quality of an analyzed face by applying the beauty canons to improve the appeal of faces.

The analysis of facial attractiveness has been proceeded using the 2D representation of the face as the 3D facial scans were not available due to the high price of the used materials. However, nowadays with the expanded availability of the 3D scans analyzing the attractiveness of a 3D face automatically has become more developed option to remedy the limitations of 2D images.

Given all of the above history and importance of facial attractiveness in our social life in addition to the increased demand of cosmetic and aesthetic surgeries, a need for an automatic system to analyze, assess and improve the attractiveness of a face is of a good deal.

To this end, a state of the art on the facial aesthetic quality analysis has been conducted in order to review the predefined canons of beauty in the literature to assess the attractiveness of faces, in addition to the existing methods used to analyze the 2D and the 3D faces as well as the different steps followed to achieve the final results of the analysis and facial attractiveness enhancement. This state of the art allowed us to identify the deficit in the literature, thus to address the existing limitations, this thesis aimed to achieve the following objectives:

- **Research Objective One:** To analyze the 2D facial aesthetic quality and thereafter suggest the necessary modifications in order to improve its attractiveness.

- **Research Objective Two:** To assess the aesthetic quality of 3D faces and as the first research object, recommend the required modifications to enhance its attractiveness.

- **Research Objective Three:** To predict how the face will look like after applying the required modification, thus the post surgery results.

- **Research Objective four:** To assess the resulting face after the surgery by comparing the obtained look to the criterions predefined by the literature and asking a domain expert to assess the final results.

1 Meeting the research objectives

After a good while of studying the state of the art about the facial aesthetic quality analysis, assessment and enhancement, we have addressed four main research objectives, and therefore proposed to divide the thesis into four major parts; the 2D face aesthetic quality analysis, the 3D face aesthetic quality analysis, the 3D face attractiveness enhancement and finally verifying the obtained results from the last part, thus the evaluating the efficiency and performances of the proposed system.

In the first part of our thesis, we have introduced a new technique to analyze the aesthetic quality of 2D faces. For this purpose, our first contribution was a new method to localize the 2D facial landmarks on the input face based on the active contour (Snake) and the set of axes that go across the facial features. Afterwards, the analysis of the face attractiveness can be performed by using the pre-defined beauty canons in the literature; thereafter the necessary modification to apply in order to enhance its appeal can be concluded. Even though the good results of attractiveness analysis, there still some drawbacks especially concerning the details visualization of both the frontal and the profile sides of the face, which makes the use of 3D representation of the face a good deal to remedy all the problems that can occur during the use of the 2D face.

Given the limitations of the first part of our thesis, in the second part, we have introduced a new methodology to analyze the aesthetic quality of 3D faces. To this end, by deriving a literature review of the 3D facial landmarks detection methods followed by a systematic mapping of the methods based geometric information to localize the 3D landmarks, a new method to detect the 3D facial landmarks based on the geometric information of the 3D facial shape has been proposed to detect a high number of 3D landmarks. The analysis of 3D face attractiveness comes then by evaluating if the face complies with the beauty canons or not. These canons are the same as the first part of the thesis for the frontal side of the face, and then we added those related to the profile side. In parallel to the analysis of the 3D face attractiveness, the necessary modifications to apply in order to improve its attractiveness are given by our system. At this stage, to visualize the 3D face after applying the modification is of great requirement.

At the third stage of our thesis, the 3D face editing was performed in order to enhance its aesthetic quality. At first, a literature review of the approach used for that purpose has been conducted, then in our case the editing was achieved using a free form technique based on the Bézier interpolation function. Given the obtained results of the attractiveness analysis, for each region of the 3D face that needs to be edited, the free form approach proposed in our thesis is applied in order to get a 3D face satisfying the beauty canons. After this step, the obtained edited 3D face needs to be evaluated to assess the efficiency of the proposed system in preserving the details of the original face as well as having a pleasing face at the end of editing. For this purpose, we have analyzed the aesthetic quality of the resulted faces from our system by verifying if they comply with the beauty canons and then asking a domain expert to assess the final results, and we have asked to vote for the most attractive face between the two versions of

before and after the editing for each face. The obtained results show that our system can edit the 3D faces and make them more attractive.

2 Contributions

The presented research resulted in the following contributions:

2.1 2D facial landmarks detection

The first contribution of our thesis is new method to localize the 2D facial landmarks using a combination of the active contour (Snake) and the localized facial axes that go across the facial features (eyes axis, nose axis, mouth axis and the median axis). This combination allows us to localize the needed facial landmarks to analyze its aesthetic quality accurately and the followed methodology is as: after localizing the different facial axes (eyes axis, nose axis, mouth axis and the median axis), the geometric model is performed to create the rectangles that encompass the facial features (the eyes, the nose, and the mouth) in order to limit the research zones for the facial landmarks. Afterwards, the active contour is applied to the whole face to detect the landmarks on the border of the face and then to created rectangles to localize the corners of each features. The facial landmarks are finally located as the intersection of the facial axis and the points produced by the active contour as shown in chapter 2, section 3.3.1, and these points of intersection must belong to the skin zone of face.
The suggested methodology has proved to be efficient and accurate compared to one of the well known operator which is the Harris approach, as using the late method some of the needed facial landmarks cannot be localized, thus representing a drawback in analyzing the attractiveness of 2D faces.

2.2 Comparative Study of Harris and Active Contour Using Viola-Jones Algorithm for Facial Landmarks Detection

The second contribution of the presented thesis is a comparative study of Harris and the Active Contour using the Viola-Jones algorithm for 2D facial landmarks detection. Indeed, during this study, we have focused on comparing the success rate of detection for both the competing methods (Harris and the active contour) using the Viola-Jones algorithm in localizing the facial landmarks. These landmarks are detected on the eyes, nose, and mouth zones as they are the common zone that can be located using the two methods.
Experimental results on two different face databases have shown interesting results of 2D facial landmarks (eyes corners, nose corners, and mouth corners) detection for both the Harris and the Active Contour using the Viola-Jones algorithm, still the Active Contour + Viola-Jones has shown an outstanding localization results compared to the Harris+ Viola-Jones algorithm.

2.3 Classification of the geometric information based methods to localize the 3D facial landmarks into four categories

The third contribution of our research is a classification of the geometric information based methods for 3D facial landmarks detection into categories using a mapping study. In the literature, a large number of approaches have been proposed to localize the 3D facial landmarks based on the geometric information provided by the 3D meshes. As previously mentioned, a systematic mapping is a technique used to generate categories of methods that use the same techniques in the same research context, therefore, we have used this study to classify the existing papers that use the geometric information provided by the 3D mesh to localize the facial landmarks in the period between 2010 and 2018 into categories. After a long process, we have excluded the papers that are not in the field and as a result, we found 30 papers. Consequently based on the used approach we classified the obtained papers into four categories; the first type is the methods based curvature analysis, the second type is the methods based on combining 2D texture with 3D shape information, the third type is the methods based on matching the 3D query face with a manually labeled one, and the fourth type is the methods based on generic image descriptors.

2.4 3D facial landmarks detection

The fourth contribution of our thesis is new approach to localize a high number of 3D facial landmarks using the geometric information provided by the shape of the 3D face. The high localized number consists of 30 craniofacial landmarks needed for the analysis of the aesthetic quality of 3D faces, in fact the proposed method was inspired by a previous work as mentioned in chapter 3, section 2.3. The original work has aimed at localizing 17 facial landmarks using the geometric information provided by the 3D face, thus we have used this methodology to localize the 10 needed landmarks, and then we have extended it to obtain a larger number of 30 3D facial landmarks. To achieve that purpose, for each given 3D face, we first perform a normalization process of its pose and orientation to avoid some problems that can be caused later during the landmarks detection process. Thereafter; the 3D facial landmarks are located starting by detecting the nose tip which is considered the key landmark due to its specific location on the face, and then the rest of the 29 3D landmarks are detected successively by limiting for each landmark the zone of research and then using the characteristics of the face geometric information.

Experimental results have shown that the proposed method to localize the 3D facial landmarks is better than the original work and some other suggested works in the literature especially regarding the highest number of the detected landmarks in addition to the minimal errors during the detection process as well.

2.5 3D face editing

The fifth contribution is about the enhancement of the aesthetic quality of 3D faces using the results of the attractiveness analysis step. The enhancement consists of editing the 3D face in

order to become more attractive in term of the beauty canons: facial Symmetry, Golden ratio, neoclassical proportions, and the angular profile. To this end, the proposed method was a Free Form Deformation approach based on the Bézier interpolation function.
Indeed, after the analysis of 3D facial attractiveness (facial symmetry, Golden ratio, Neoclassical proportions, and the angular profile), and if the results of the analysis indicates that the face requires to be edited, the Free Form method constrained by the results of the aesthetic quality analysis form previous stages is applied to each region of the face in order to enhance its appeal in term of the beauty canons. This method has proved to be efficient and robust as it preserves the details of the original face while making it more attractive. To the best of our knowledge this techniques has never been used for such a purpose before.

3 Limitations

Our proposed system to analyze and enhance the aesthetic quality of 3D faces has the following limitations:

- Currently, the suggested method to localize the 2D facial landmarks is used for 2D faces with frontal pose and neutral expression.
- The proposed approach to detect the 3D craniofacial landmarks of 3D facial meshes currently can work only using 3D faces with no expressions and pose variations as well.
- The used 3D faces have to be at the same scale, same distance from the screen, so that the localization of the required facial areas to detect the 3D facial landmarks would be the same as much as possible for all the input 3D faces, thus efficient detection results.

4 Perspectives

The presented research has the following future directions:

- **Real world case study**: the authors aim to apply the presented system to a real world application. Aesthetic or plastic surgeons may used the proposed system in order to analyze the aesthetic quality of patients' face using the 2D or the 3D method, and then to visualize how the face will look like after the surgery following the suggested modifications to enhance its attractiveness.
- **Verifying the proposed system using other 3D face databases**: in the presented study, authors have used two 3D face datasets to analyze the aesthetic quality of the faces which are the BaselFaceModel dataset and a sample data set from the CranioGUI dataset. The system does need to be tested on other 3D face databases, especially those created for the same purpose as our study, in which the facial texture is presented making the visualization of the attractiveness enhancement clearer.

- **Improve the human machine interface of the attractiveness analysis**: our future work will focus on making the proposed human machine interface more developed and pleasing to the eye of the user.

In this conclusion part, we summarized how the proposed four research objectives were achieved in our thesis; first and in order to analyze the aesthetic quality of 2D faces, an automatic and precise method for 2D facial landmarks was proposed which will make the task of the analysis more accurate. Afterwards, to analyze the attractiveness of 3D facial meshes, we have firstly suggested a novel method to automatically localize a larger number of 3D craniofacial landmarks on 3D face meshes, thereafter, the assessment of the aesthetic quality of a 3D face is performed by verifying if the input 3D face meets the beauty canons or not. Thus, in the negative case, the proposed system suggests the necessary modifications to enhance the attractiveness of the 3D face. Consequently, allows the user to visualize the 3D face after applying them.

We described as well the limitations in both the process of analyzing the aesthetic quality of faces and the step of editing them in order to enhance their attractiveness, and thereafter define the future directions in order to explore the limitations that were identified.

References

[1] R. Bull and N. Rumsey, *The social psychology of facial appearance*. Springer Science & Business Media, 2012.

[2] S. Bates, "Survival of the Prettiest: The Science of Beauty," *Wilson Q.*, vol. 23, no. 2, p. 142, 1999.

[3] K. Dion, E. Berscheid, and E. Walster, "What is beautiful is good.," *J. Pers. Soc. Psychol.*, vol. 24, no. 3, p. 285, 1972.

[4] N. Barber, "The evolutionary psychology of physical attractiveness: Sexual selection and human morphology," *Evol. Hum. Behav.*, vol. 16, no. 5, pp. 395–424, 1995.

[5] E. Bradbury, "The psychology of aesthetic plastic surgery," *Aesthetic Plast. Surg.*, vol. 18, no. 3, pp. 301–305, 1994.

[6] L. A. Jackson, "The influence of sex, physical attractiveness, sex role, and occupational sex- linkage on perceptions of occupational suitability," *J. Appl. Soc. Psychol.*, vol. 13, no. 1, pp. 31–44, 1983.

[7] C. M. Marlowe, S. L. Schneider, and C. E. Nelson, "Gender and attractiveness biases in hiring decisions: Are more experienced managers less biased?," *J. Appl. Psychol.*, vol. 81, no. 1, p. 11, 1996.

[8] J. H. Langlois, L. Kalakanis, A. J. Rubenstein, A. Larson, M. Hallam, and M. Smoot, "Maxims or myths of beauty? A meta-analytic and theoretical review.," *Psychol. Bull.*, vol. 126, no. 3, p. 390, 2000.

[9] D. Guo and T. Sim, "Digital face makeup by example," in *2009 IEEE Conference on Computer Vision and Pattern Recognition*, 2009, pp. 73–79.

[10] "VECTRA 3D." [Online]. Available: https://www.canfieldsci.com/imaging-systems/vectra-m3-3d-imaging-system/. [Accessed: 22-Jan-2020].

[11] "MIRRORME 3D." [Online]. Available: https://www.mirrorme3d.com/. [Accessed: 22-Jan-2020].

[12] "CRISALIX." [Online]. Available: https://www.crisalix.com/fr. [Accessed: 22-Feb-2020].

[13] M. El Rhazi, A. Zarghili, A. Majda, A. Bouzalmat, and A. A. Oufkir, "Facial beauty analysis by age and gender," *Int. J. Intell. Syst. Technol. Appl.*, vol. 18, no. 1–2, pp. 179–203, 2019.

[14] M. Castrillón, O. Déniz, D. Hernández, and J. Lorenzo, "A comparison of face and facial feature detectors based on the Viola–Jones general object detection framework," *Mach. Vis. Appl.*, vol. 22, no. 3, pp. 481–494, 2011.

[15] M. El Rhazi, A. Zarghili, and A. Majda, "Comparative Study of Harris and Active Contour using Viola-Jones Algorithm for Facial Landmarks Detection," *Trans. Mach. Learn. Artif. Intell.*, vol. 5, no. 4, 2017.

[16] E. R. ; Manal, Z. Arsalane, and M. ;Aicha, "Survey on the approaches based geometric information for 3D face landmarks detection," *IET Image Process.*, 2019.

[17] E. R. Manal, Z. Arsalane, and M. Aicha, "Automated detection of craniofacial landmarks on a 3D facial mesh," in *International conference on Integrated design and production CPI*, 2019.

[18] S. W. Gangestad and G. J. Scheyd, "The evolution of human physical attractiveness," *Annu. Rev. Anthr.*, vol. 34, pp. 523–548, 2005.

[19] R. Thornhill and S. W. Gangestad, "Human facial beauty," *Hum. Nat.*, vol. 4, no. 3, pp. 237–269, 1993.

[20] A. H. Eagly, R. D. Ashmore, M. G. Makhijani, and L. C. Longo, "What is beautiful is good, but…: A meta-analytic review of research on the physical attractiveness stereotype.," *Psychol. Bull.*, vol. 110, no. 1, p. 109, 1991.

[21] A. G. Miller, *In the eye of the beholder: Contemporary issues in stereotyping*. Praeger Publishers, 1982.

[22] D. S. Berry, L. Zebrowitz-MeArthur, and T. R. Alley, "Social and applied aspects of perceiving faces," 1988.

[23] E. Hatfield and S. Sprecher, *Mirror, mirror: The importance of looks in everyday life*. Suny Press, 1986.

[24] M. Ibáñez-Berganza, A. Amico, and V. Loreto, "Subjectivity and complexity of facial attractiveness," *Sci. Rep.*, vol. 9, no. 1, pp. 1–12, 2019.

[25] Y. Eisenthal, G. Dror, and E. Ruppin, "Facial attractiveness: Beauty and the machine," *Neural Comput.*, vol. 18, no. 1, pp. 119–142, 2006.

[26] C. Darwin, *The descent of man and selection in relation to sex*, vol. 1. Murray, 1888.

[27] D. I. Perrett, K. A. May, and S. Yoshikawa, "Facial shape and judgements of female attractiveness," *Nature*, vol. 368, no. 6468, pp. 239–242, 1994.

[28] B. Fink and N. Neave, "The biology of facial beauty," *Int. J. Cosmet. Sci.*, vol. 27, no. 6, pp. 317–325, 2005.

[29] M. R. Cunningham, A. R. Roberts, A. P. Barbee, P. B. Druen, and C.-H. Wu, "' Their ideas of beauty are, on the whole, the same as ours': Consistency and variability in the cross-cultural perception of female physical attractiveness.," *J. Pers. Soc. Psychol.*, vol. 68, no. 2, p. 261, 1995.

[30] C. A. Samuels and R. Ewy, "Aesthetic perception of faces during infancy," *Br. J. Dev. Psychol.*, vol. 3, no. 3, pp. 221–228, 1985.

[31] A. Slater, P. C. Quinn, R. Hayes, and E. Brown, "The role of facial orientation in newborn infants'

preference for attractive faces," *Dev. Sci.*, vol. 3, no. 2, pp. 181–185, 2000.
[32] K. Kuraguchi, K. Taniguchi, K. Kanari, and S. Itakura, "Face Preference in Infants at Six and Nine Months Old: The Effects of Facial Attractiveness and Observation Experience," *Symmetry (Basel).*, vol. 12, no. 7, p. 1082, 2020.
[33] B. S. Atiyeh and S. N. Hayek, "Numeric expression of aesthetics and beauty," *Aesthetic Plast. Surg.*, vol. 32, no. 2, pp. 209–216, 2008.
[34] M. Bashour, "History and current concepts in the analysis of facial attractiveness," *Plast. Reconstr. Surg.*, vol. 118, no. 3, pp. 741–756, 2006.
[35] F. Vegter and J. J. Hage, "Clinical anthropometry and canons of the face in historical perspective," *Plast. Reconstr. Surg.*, vol. 106, no. 5, pp. 1090–1096, 2000.
[36] M. E. Koury and B. N. Epker, "Maxillofacial esthetics: anthropometrics of the maxillofacial region," *J. oral Maxillofac. Surg.*, vol. 50, no. 8, pp. 806–820, 1992.
[37] L. G. Farkas and J. C. Kolar, "Anthropometrics and art in the aesthetics of women's faces.," *Clin. Plast. Surg.*, vol. 14, no. 4, pp. 599–616, 1987.
[38] L. G. Farkas, *Anthropometry of the Head and Face*. Raven Pr, 1994.
[39] S. R. Marquardt, "Dr. Stephen R. Marquardt on the Golden Decagon and human facial beauty. Interview by Dr. Gottlieb.," *J. Clin. Orthod. JCO*, vol. 36, no. 6, p. 339, 2002.
[40] G. Rhodesô½ *et al.*, "Perceived health contributes to the attractiveness of facial symmetry, averageness, and sexual dimorphism," *Perception*, vol. 36, pp. 1244–1252, 2007.
[41] T. K. Shackelford and R. J. Larsen, "Facial asymmetry as an indicator of psychological, emotional, and physiological distress.," *J. Pers. Soc. Psychol.*, vol. 72, no. 2, p. 456, 1997.
[42] R. Thornhill and S. W. Gangestad, "Human fluctuating asymmetry and sexual behavior," *Psychol. Sci.*, vol. 5, no. 5, pp. 297–302, 1994.
[43] D. C. Waynforth, "Male mating strategies among the Mayas of Belize (men)." Ph. D. thesis, University of New Mexico, 1999.
[44] J. T. Manning, D. Scutt, G. H. Whitehouse, and S. J. Leinster, "Breast asymmetry and phenotypic quality in women," *Evol. Hum. Behav.*, vol. 18, no. 4, pp. 223–236, 1997.
[45] A. P. Møller and J. P. Swaddle, *Asymmetry, developmental stability and evolution*. Oxford University Press, UK, 1997.
[46] A. C. Little, B. C. Jones, and L. M. DeBruine, "Facial attractiveness: evolutionary based research," *Philos. Trans. R. Soc. B Biol. Sci.*, vol. 366, no. 1571, pp. 1638–1659, 2011.
[47] C. Waitt and A. C. Little, "Preferences for symmetry in conspecific facial shape among Macaca mulatta," *Int. J. Primatol.*, vol. 27, no. 1, pp. 133–145, 2006.
[48] C. A. Samuels, G. Butterworth, T. Roberts, L. Graupner, and G. Hole, "Facial aesthetics: Babies prefer attractiveness to symmetry," *Perception*, vol. 23, no. 7, pp. 823–831, 1994.
[49] R. Kowner, "Facial asymmetry and attractiveness judgement in developmental perspective.," *J. Exp. Psychol. Hum. Percept. Perform.*, vol. 22, no. 3, p. 662, 1996.
[50] G. Rhodes, "The evolutionary psychology of facial beauty," *Annu. Rev. Psychol.*, vol. 57, pp. 199–226, 2006.
[51] D. I. Perrett, D. M. Burt, I. S. Penton-Voak, K. J. Lee, D. A. Rowland, and R. Edwards, "Symmetry and human facial attractiveness," *Evol. Hum. Behav.*, vol. 20, no. 5, pp. 295–307, 1999.
[52] G. Rhodes, F. Proffitt, J. M. Grady, and A. Sumich, "Facial symmetry and the perception of beauty," *Psychon. Bull. Rev.*, vol. 5, no. 4, pp. 659–669, 1998.
[53] G. Rhodes, J. Roberts, and L. W. Simmons, "Reflections on symmetry and attractiveness," *Psychol. Evol. Gend.*, vol. 1, pp. 279–296, 1999.
[54] J. H. Langlois, L. A. Roggman, and L. Musselman, "What is average and what is not average about attractive faces?," *Psychol. Sci.*, vol. 5, no. 4, pp. 214–220, 1994.
[55] J. E. Scheib, S. W. Gangestad, and R. Thornhill, "Facial attractiveness, symmetry and cues of good genes," *Proc. R. Soc. London B Biol. Sci.*, vol. 266, no. 1431, pp. 1913–1917, 1999.
[56] H. Pancherz, V. Knapp, C. Erbe, and A. M. Heiss, "Divine proportions in attractive and nonattractive faces.," *World J. Orthod.*, vol. 11, no. 1, pp. 27–36, 2009.
[57] R. Edler, P. Agarwal, D. Wertheim, and D. Greenhill, "The use of anthropometric proportion indices in the measurement of facial attractiveness," *Eur. J. Orthod.*, vol. 28, no. 3, pp. 274–281, 2006.
[58] R. M. Ricketts, "The biologic significance of the divine proportion and Fibonacci series," *Am. J. Orthod.*, vol. 81, no. 5, pp. 351–370, 1982.
[59] R. M. Ricketts, "Devine proportion in facial esthetics," *Clin. Plast. Surg.*, vol. 9, pp. 401–422, 1982.
[60] P. M. Pallett, S. Link, and K. Lee, "New 'golden' ratios for facial beauty," *Vision Res.*, vol. 50, no. 2, pp. 149–154, 2010.
[61] E. Holland, "Marquardt's Phi mask: pitfalls of relying on fashion models and the golden ratio to describe a beautiful face," *Aesthetic Plast. Surg.*, vol. 32, no. 2, pp. 200–208, 2008.

[62] M. Enquist and A. Arak, “Symmetry, beauty and evolution,” *Nature*, vol. 372, no. 6502, p. 169, 1994.
[63] S. C. Roberts *et al.*, “MHC-heterozygosity and human facial attractiveness,” *Evol. Hum. Behav.*, vol. 26, no. 3, pp. 213–226, 2005.
[64] T. R. Alley and M. R. Cunningham, “Article Commentary: Averaged Faces Are Attractive, but Very Attractive Faces Are Not Average,” *Psychol. Sci.*, vol. 2, no. 2, pp. 123–125, 1991.
[65] K. Grammer and R. Thornhill, “Human (Homo sapiens) facial attractiveness and sexual selection: the role of symmetry and averageness.,” *J. Comp. Psychol.*, vol. 108, no. 3, p. 233, 1994.
[66] G. Rhodes and T. Tremewan, “Averageness, exaggeration, and facial attractiveness,” *Psychol. Sci.*, vol. 7, no. 2, pp. 105–110, 1996.
[67] C. L. Apicella, A. C. Little, and F. W. Marlowe, “Facial averageness and attractiveness in an isolated population of hunter-gatherers,” *Perception*, vol. 36, no. 12, pp. 1813–1820, 2007.
[68] J. W. Shepherd and H. D. Ellis, “The effect of attractiveness on recognition memory for faces,” *Am. J. Psychol.*, pp. 627–633, 1973.
[69] L. G. Farkas, T. A. Hreczko, J. C. Kolar, and I. R. Munro, “Vertical and horizontal proportions of the face in young adult North American Caucasians: revision of neoclassical canons.,” *Plast. Reconstr. Surg.*, vol. 75, no. 3, pp. 328–338, 1985.
[70] M. R. Mack, “Vertical dimension: a dynamic concept based on facial form and oropharyngeal function,” *J. Prosthet. Dent.*, vol. 66, no. 4, pp. 478–485, 1991.
[71] J. Milutinovic, K. Zelic, and N. Nedeljkovic, “Evaluation of facial beauty using anthropometric proportions,” *Sci. World J.*, vol. 2014, 2014.
[72] N. Powell and B. Humphreys, *Proportions of the aesthetic face*, vol. 1. Thieme medical pub, 1984.
[73] H. Peck and S. Peck, “A concept of facial esthetics,” *Angle Orthod.*, vol. 40, no. 4, pp. 284–317, 1970.
[74] R. A. Holdaway, “A soft-tissue cephalometric analysis and its use in orthodontic treatment planning. Part I,” *Am. J. Orthod.*, vol. 84, no. 1, pp. 1–28, 1983.
[75] W. F. Larrabee, K. H. Makielski, and J. L. Henderson, *Surgical anatomy of the face*. Lippincott Williams & Wilkins, 2004.
[76] G. Bradski and A. Kaehler, *Learning OpenCV: Computer vision with the OpenCV library*. “ O’Reilly Media, Inc.,” 2008.
[77] Y. Jia *et al.*, “Caffe: Convolutional architecture for fast feature embedding,” in *Proceedings of the 22nd ACM international conference on Multimedia*, 2014, pp. 675–678.
[78] E. Hjelmås and B. K. Low, “Face detection: A survey,” *Comput. Vis. image Underst.*, vol. 83, no. 3, pp. 236–274, 2001.
[79] M.-H. Yang, D. J. Kriegman, and N. Ahuja, “Detecting faces in images: A survey,” *IEEE Trans. Pattern Anal. Mach. Intell.*, vol. 24, no. 1, pp. 34–58, 2002.
[80] S. Zafeiriou, C. Zhang, and Z. Zhang, “A survey on face detection in the wild: past, present and future,” *Comput. Vis. Image Underst.*, vol. 138, pp. 1–24, 2015.
[81] Y. LeCun and Y. Bengio, “Convolutional networks for images, speech, and time series,” *Handb. brain theory neural networks*, vol. 3361, no. 10, p. 1995, 1995.
[82] C. Garcia and M. Delakis, “Convolutional face finder: A neural architecture for fast and robust face detection,” *IEEE Trans. Pattern Anal. Mach. Intell.*, vol. 26, no. 11, pp. 1408–1423, 2004.
[83] H. Qin, J. Yan, X. Li, and X. Hu, “Joint training of cascaded CNN for face detection,” in *Proceedings of the IEEE Conference on Computer Vision and Pattern Recognition*, 2016, pp. 3456–3465.
[84] R. Girshick, J. Donahue, T. Darrell, and J. Malik, “Rich feature hierarchies for accurate object detection and semantic segmentation,” in *Proceedings of the IEEE conference on computer vision and pattern recognition*, 2014, pp. 580–587.
[85] Y. LeCun, K. Kavukcuoglu, and C. Farabet, “Convolutional networks and applications in vision,” in *Proceedings of 2010 IEEE International Symposium on Circuits and Systems*, 2010, pp. 253–256.
[86] Y. Sun, Y. Chen, X. Wang, and X. Tang, “Deep learning face representation by joint identification-verification,” in *Advances in neural information processing systems*, 2014, pp. 1988–1996.
[87] A. Krizhevsky, I. Sutskever, and G. E. Hinton, “Imagenet classification with deep convolutional neural networks,” in *Advances in neural information processing systems*, 2012, pp. 1097–1105.
[88] O. Russakovsky *et al.*, “Imagenet large scale visual recognition challenge,” *Int. J. Comput. Vis.*, vol. 115, no. 3, pp. 211–252, 2015.
[89] C. Zhang and Z. Zhang, “Improving multiview face detection with multi-task deep convolutional neural networks,” in *IEEE Winter Conference on Applications of Computer Vision*, 2014, pp. 1036–1041.
[90] V. Jain and E. Learned-Miller, “Fddb: A benchmark for face detection in unconstrained settings,” UMass Amherst Technical Report, 2010.
[91] S. S. Farfade, M. J. Saberian, and L.-J. Li, “Multi-view face detection using deep convolutional neural networks,” in *Proceedings of the 5th ACM on International Conference on Multimedia Retrieval*, 2015, pp. 643–650.

[92] P. F. Felzenszwalb, R. B. Girshick, D. McAllester, and D. Ramanan, “Object detection with discriminatively trained part-based models,” *IEEE Trans. Pattern Anal. Mach. Intell.*, vol. 32, no. 9, pp. 1627–1645, 2009.
[93] R. Girshick, F. Iandola, T. Darrell, and J. Malik, “Deformable part models are convolutional neural networks,” in *Proceedings of the IEEE conference on Computer Vision and Pattern Recognition*, 2015, pp. 437–446.
[94] C. Dubout and F. Fleuret, “Exact acceleration of linear object detectors,” in *European Conference on Computer Vision*, 2012, pp. 301–311.
[95] P. F. Felzenszwalb, R. B. Girshick, and D. McAllester, “Cascade object detection with deformable part models,” in *2010 IEEE Computer Society Conference on Computer Vision and Pattern Recognition*, 2010, pp. 2241–2248.
[96] A. G. Gray and A. W. Moore, “Nonparametric density estimation: Toward computational tractability,” in *Proceedings of the 2003 SIAM International Conference on Data Mining*, 2003, pp. 203–211.
[97] T. F. Cootes, G. J. Edwards, and C. J. Taylor, “Active appearance models,” *IEEE Trans. Pattern Anal. Mach. Intell.*, no. 6, pp. 681–685, 2001.
[98] R. Toth and A. Madabhushi, “Multifeature landmark-free active appearance models: application to prostate MRI segmentation,” *IEEE Trans. Med. Imaging*, vol. 31, no. 8, pp. 1638–1650, 2012.
[99] S. Rueda and M. Alcaniz, “An approach for the automatic cephalometric landmark detection using mathematical morphology and active appearance models,” in *International Conference on Medical Image Computing and Computer-Assisted Intervention*, 2006, pp. 159–166.
[100] P. Vučinić, Ž. Trpovski, and I. Šćepan, “Automatic landmarking of cephalograms using active appearance models,” *Eur. J. Orthod.*, vol. 32, no. 3, pp. 233–241, 2010.
[101] G. Tzimiropoulos, J. Alabort-i-Medina, S. Zafeiriou, and M. Pantic, “Generic active appearance models revisited,” in *Asian Conference on Computer Vision*, 2012, pp. 650–663.
[102] D. Cristinacce and T. F. Cootes, “Feature detection and tracking with constrained local models.,” in *Bmvc*, 2006, vol. 1, no. 2, p. 3.
[103] T. Baltrusaitis, P. Robinson, and L.-P. Morency, “Constrained local neural fields for robust facial landmark detection in the wild,” in *Proceedings of the IEEE international conference on computer vision workshops*, 2013, pp. 354–361.
[104] A. Asthana, S. Zafeiriou, S. Cheng, and M. Pantic, “Robust discriminative response map fitting with constrained local models,” in *Proceedings of the IEEE conference on computer vision and pattern recognition*, 2013, pp. 3444–3451.
[105] Q. Zhao *et al.*, “Digital facial dysmorphology for genetic screening: Hierarchical constrained local model using ICA,” *Med. Image Anal.*, vol. 18, no. 5, pp. 699–710, 2014.
[106] Y. Wang, S. Lucey, and J. F. Cohn, “Enforcing convexity for improved alignment with constrained local models,” in *2008 IEEE Conference on Computer Vision and Pattern Recognition*, 2008, pp. 1–8.
[107] J. M. Saragih, S. Lucey, and J. F. Cohn, “Deformable model fitting by regularized landmark mean-shift,” *Int. J. Comput. Vis.*, vol. 91, no. 2, pp. 200–215, 2011.
[108] M. Dantone, J. Gall, G. Fanelli, and L. Van Gool, “Real-time facial feature detection using conditional regression forests,” in *2012 IEEE Conference on Computer Vision and Pattern Recognition*, 2012, pp. 2578–2585.
[109] Z. Zhang, P. Luo, C. C. Loy, and X. Tang, “Facial landmark detection by deep multi-task learning,” in *European conference on computer vision*, 2014, pp. 94–108.
[110] S. Ren, X. Cao, Y. Wei, and J. Sun, “Face alignment at 3000 fps via regressing local binary features,” in *Proceedings of the IEEE Conference on Computer Vision and Pattern Recognition*, 2014, pp. 1685–1692.
[111] V. Kazemi and J. Sullivan, “One millisecond face alignment with an ensemble of regression trees,” in *Proceedings of the IEEE conference on computer vision and pattern recognition*, 2014, pp. 1867–1874.
[112] X. Cao, Y. Wei, F. Wen, and J. Sun, “Face alignment by explicit shape regression,” *Int. J. Comput. Vis.*, vol. 107, no. 2, pp. 177–190, 2014.
[113] K. Zhang, Z. Zhang, Z. Li, and Y. Qiao, “Joint face detection and alignment using multitask cascaded convolutional networks,” *IEEE Signal Process. Lett.*, vol. 23, no. 10, pp. 1499–1503, 2016.
[114] Y. Wu and Q. Ji, “Facial landmark detection: A literature survey,” *Int. J. Comput. Vis.*, vol. 127, no. 2, pp. 115–142, 2019.
[115] Z. Zhang, P. Luo, C. C. Loy, and X. Tang, “Learning deep representation for face alignment with auxiliary attributes,” *IEEE Trans. Pattern Anal. Mach. Intell.*, vol. 38, no. 5, pp. 918–930, 2015.
[116] R. Ranjan, V. M. Patel, and R. Chellappa, “Hyperface: A deep multi-task learning framework for face detection, landmark localization, pose estimation, and gender recognition,” *IEEE Trans. Pattern Anal. Mach. Intell.*, vol. 41, no. 1, pp. 121–135, 2017.
[117] J. Zhang, S. Shan, M. Kan, and X. Chen, “Coarse-to-fine auto-encoder networks (cfan) for real-time face alignment,” in *European conference on computer vision*, 2014, pp. 1–16.
[118] G. Trigeorgis, P. Snape, M. A. Nicolaou, E. Antonakos, and S. Zafeiriou, “Mnemonic descent method: A

recurrent process applied for end-to-end face alignment," in *Proceedings of the IEEE Conference on Computer Vision and Pattern Recognition*, 2016, pp. 4177–4187.
[119] E. Tatarunaite, R. Playle, K. Hood, W. Shaw, and S. Richmond, "Facial attractiveness: a longitudinal study," *Am. J. Orthod. Dentofac. Orthop.*, vol. 127, no. 6, pp. 676–682, 2005.
[120] V. S. Johnston, R. Hagel, M. Franklin, B. Fink, and K. Grammer, "Male facial attractiveness: Evidence for hormone-mediated adaptive design," *Evol. Hum. Behav.*, vol. 22, no. 4, pp. 251–267, 2001.
[121] A. Kagian, G. Dror, T. Leyvand, D. Cohen-Or, and E. Ruppin, "A humanlike predictor of facial attractiveness," in *Advances in Neural Information Processing Systems*, 2007, pp. 649–656.
[122] A. J. O'Toole, T. Price, T. Vetter, J. C. Bartlett, and V. Blanz, "3D shape and 2D surface textures of human faces: The role of 'averages' in attractiveness and age," *Image Vis. Comput.*, vol. 18, no. 1, pp. 9–19, 1999.
[123] G. Rhodes, S. Yoshikawa, A. Clark, K. Lee, R. McKay, and S. Akamatsu, "Attractiveness of facial averageness and symmetry in non-Western cultures: In search of biologically based standards of beauty," *Perception*, vol. 30, no. 5, pp. 611–625, 2001.
[124] B. C. Jones, L. M. DeBruine, and A. C. Little, "The role of symmetry in attraction to average faces," *Percept. Psychophys.*, vol. 69, no. 8, pp. 1273–1277, 2007.
[125] K. Schmid, D. Marx, and A. Samal, "Computation of a face attractiveness index based on neoclassical canons, symmetry, and golden ratios," *Pattern Recognit.*, vol. 41, no. 8, pp. 2710–2717, 2008.
[126] H. Gunes and M. Piccardi, "Assessing facial beauty through proportion analysis by image processing and supervised learning," *Int. J. Hum. Comput. Stud.*, vol. 64, no. 12, pp. 1184–1199, 2006.
[127] C. Maes, T. Fabry, J. Keustermans, D. Smeets, P. Suetens, and D. Vandermeulen, "Feature detection on 3D face surfaces for pose normalisation and recognition," in *Biometrics: Theory Applications and Systems (BTAS), 2010 Fourth IEEE International Conference on*, 2010, pp. 1–6.
[128] M. A. Fischler and R. C. Bolles, "Random sample consensus: a paradigm for model fitting with applications to image analysis and automated cartography," *Commun. ACM*, vol. 24, no. 6, pp. 381–395, 1981.
[129] K. Wilamowska, L. Shapiro, and C. Heike, "Classification of 3D face shape in 22q11. 2 deletion syndrome," in *Biomedical Imaging: From Nano to Macro, 2009. ISBI'09. IEEE International Symposium on*, 2009, pp. 534–537.
[130] X. Zhu, Z. Lei, J. Yan, D. Yi, and S. Z. Li, "High-fidelity pose and expression normalization for face recognition in the wild," in *Proceedings of the IEEE Conference on Computer Vision and Pattern Recognition*, 2015, pp. 787–796.
[131] R. Niese, A. Al-Hamadi, and B. Michaelis, "A Novel Method for 3D Face Detection and Normalization.," *J. Multimed.*, vol. 2, no. 5, 2007.
[132] A. Mian, M. Bennamoun, and R. Owens, "Automatic 3d face detection, normalization and recognition," in *3D Data Processing, Visualization, and Transmission, Third International Symposium on*, 2006, pp. 735–742.
[133] C. Ding and D. Tao, "Pose-invariant face recognition with homography-based normalization," *Pattern Recognit.*, vol. 66, pp. 144–152, 2017.
[134] A. Asthana, T. K. Marks, M. J. Jones, K. H. Tieu, and M. V Rohith, "Fully automatic pose-invariant face recognition via 3D pose normalization," in *Computer Vision (ICCV), 2011 IEEE International Conference on*, 2011, pp. 937–944.
[135] S. Liang, J. Wu, S. M. Weinberg, and L. G. Shapiro, "Improved detection of landmarks on 3d human face data," in *Engineering in Medicine and Biology Society (EMBC), 2013 35th Annual International Conference of the IEEE*, 2013, pp. 6482–6485.
[136] D. Colbry, G. Stockman, and A. Jain, "Detection of anchor points for 3d face veri. cation," in *Computer Vision and Pattern Recognition-Workshops, 2005. CVPR Workshops. IEEE Computer Society Conference on*, 2005, p. 118.
[137] X. Lu and A. K. Jain, "Automatic feature extraction for multiview 3D face recognition," in *Automatic Face and Gesture Recognition, 2006. FGR 2006. 7th International Conference on*, 2006, pp. 585–590.
[138] H. Dibeklioglu, A. A. Salah, and L. Akarun, "3D facial landmarking under expression, pose, and occlusion variations," in *2008 IEEE Second International Conference on Biometrics: Theory, Applications and Systems*, 2008, pp. 1–6.
[139] J. D'Hose, J. Colineau, C. Bichon, and B. Dorizzi, "Precise localization of landmarks on 3d faces using gabor wavelets," in *2007 First IEEE International Conference on Biometrics: Theory, Applications, and Systems*, 2007, pp. 1–6.
[140] P. Perakis, G. Passalis, T. Theoharis, and I. A. Kakadiaris, "3d facial landark detection and face registration," *Tech. Rep., Univ. Athens*, 2010.
[141] P. Perakis, G. Passalis, T. Theoharis, and I. A. Kakadiaris, "3D facial landmark detection under large yaw and expression variations," *IEEE Trans. Pattern Anal. Mach. Intell.*, vol. 35, no. 7, pp. 1552–1564, 2013.
[142] A. Colombo, C. Cusano, and R. Schettini, "3D face detection using curvature analysis," *Pattern Recognit.*, vol. 39, no. 3, pp. 444–455, 2006.

[143] M. Romero-Huertas and N. Pears, “3D facial landmark localisation by matching simple descriptors,” in *2008 IEEE Second International Conference on Biometrics: Theory, Applications and Systems*, 2008, pp. 1–6.
[144] M. P. Segundo, C. Queirolo, O. R. P. Bellon, and L. Silva, “Automatic 3D facial segmentation and landmark detection,” in *14th International Conference on Image Analysis and Processing (ICIAP 2007)*, 2007, pp. 431–436.
[145] A. Abu, C. G. Ngo, N. I. A. Abu-Hassan, and S. A. Othman, “Automated craniofacial landmarks detection on 3D image using geometry characteristics information,” *BMC Bioinformatics*, vol. 19, no. 13, p. 548, 2019.
[146] A. Zadeh, Y. Chong Lim, T. Baltrusaitis, and L.-P. Morency, “Convolutional experts constrained local model for 3d facial landmark detection,” in *Proceedings of the IEEE International Conference on Computer Vision*, 2017, pp. 2519–2528.
[147] X. Zhu, Z. Lei, X. Liu, H. Shi, and S. Z. Li, “Face alignment across large poses: A 3d solution,” in *Proceedings of the IEEE conference on computer vision and pattern recognition*, 2016, pp. 146–155.
[148] T.-H. Yu and Y.-S. Moon, “A novel genetic algorithm for 3D facial landmark localization,” in *Biometrics: Theory, Applications and Systems, 2008. BTAS 2008. 2nd IEEE International Conference on*, 2008, pp. 1–6.
[149] P. Nair and A. Cavallaro, “3-D face detection, landmark localization, and registration using a point distribution model,” *IEEE Trans. Multimed.*, vol. 11, no. 4, pp. 611–623, 2009.
[150] I. Matthews and S. Baker, “Active appearance models revisited,” *Int. J. Comput. Vis.*, vol. 60, no. 2, pp. 135–164, 2004.
[151] T. F. Cootes, C. J. Taylor, D. H. Cooper, and J. Graham, “Active shape models-their training and application,” *Comput. Vis. image Underst.*, vol. 61, no. 1, pp. 38–59, 1995.
[152] X. Zhao, E. Dellandréa, and L. Chen, “A 3D statistical facial feature model and its application on locating facial landmarks,” in *International Conference on Advanced Concepts for Intelligent Vision Systems*, 2009, pp. 686–697.
[153] S. Gupta, M. K. Markey, and A. C. Bovik, “Anthropometric 3D face recognition,” *Int. J. Comput. Vis.*, vol. 90, no. 3, pp. 331–349, 2010.
[154] P. J. Besl and R. C. Jain, “Segmentation through variable-order surface fitting,” *IEEE Trans. Pattern Anal. Mach. Intell.*, vol. 10, no. 2, pp. 167–192, 1988.
[155] P. Perakis, T. Theoharis, and I. A. Kakadiaris, “Feature fusion for facial landmark detection,” *Pattern Recognit.*, vol. 47, no. 9, pp. 2783–2793, 2014.
[156] A. E. Johnson, “Spin-images: a representation for 3-D surface matching.” Citeseer, 1997.
[157] C. Dorai and A. K. Jain, “COSMOS-A representation scheme for 3D free-form objects,” *IEEE Trans. Pattern Anal. Mach. Intell.*, vol. 19, no. 10, pp. 1115–1130, 1997.
[158] C. Harris and M. Stephens, “A combined corner and edge detector.,” in *Alvey vision conference*, 1988, vol. 15, p. 50.
[159] C. Creusot, N. Pears, and J. Austin, “A machine-learning approach to keypoint detection and landmarking on 3D meshes,” *Int. J. Comput. Vis.*, vol. 102, no. 1–3, pp. 146–179, 2013.
[160] J. Guo, X. Mei, and K. Tang, “Automatic landmark annotation and dense correspondence registration for 3D human facial images,” *BMC Bioinformatics*, vol. 14, no. 1, p. 232, 2013.
[161] S. Cheng, S. Zafeiriou, A. Asthana, and M. Pantic, “3d facial geometric features for constrained local model,” in *Image Processing (ICIP), 2014 IEEE International Conference on*, 2014, pp. 1425–1429.
[162] G. Sandbach, S. Zafeiriou, and M. Pantic, “Local normal binary patterns for 3D facial action unit detection,” in *Image Processing (ICIP), 2012 19th IEEE International Conference on*, 2012, pp. 1813–1816.
[163] S. Tang *et al.*, “Histogram of oriented normal vectors for object recognition with a depth sensor,” in *Asian conference on computer vision*, 2012, pp. 525–538.
[164] M. Galvánek, K. Furmanová, I. Chalás, and J. Sochor, “Automated facial landmark detection, comparison and visualization,” in *Proceedings of the 31st spring conference on computer graphics*, 2015, pp. 7–14.
[165] F. Marcolin and E. Vezzetti, “Novel descriptors for geometrical 3D face analysis,” *Multimed. Tools Appl.*, vol. 76, no. 12, pp. 13805–13834, 2017.
[166] S. Mehryar, K. Martin, and K. N. Plataniotis, “Automatic landmark detection for 3d face image processing,” in *Evolutionary Computation (CEC), 2010 IEEE Congress on*, 2010, pp. 1–7.
[167] C. Creusot, N. Pears, and J. Austin, “3D face landmark labelling,” in *Proceedings of the ACM workshop on 3D object retrieval*, 2010, pp. 27–32.
[168] M. P. Segundo, L. Silva, O. R. P. Bellon, and C. C. Queirolo, “Automatic face segmentation and facial landmark detection in range images,” *IEEE Trans. Syst. Man, Cybern. Part B*, vol. 40, no. 5, pp. 1319–1330, 2010.
[169] T. C. Faltemier, K. W. Bowyer, and P. J. Flynn, “Rotated profile signatures for robust 3d feature detection,” in *Automatic Face & Gesture Recognition, 2008. FG’08. 8th IEEE International Conference on*, 2008, pp. 1–7.

[170] K. I. Chang, K. W. Bowyer, and P. J. Flynn, “Multiple nose region matching for 3D face recognition under varying facial expression,” *IEEE Trans. Pattern Anal. Mach. Intell.*, vol. 28, no. 10, pp. 1695–1700, 2006.
[171] S. Berretti, B. Ben Amor, M. Daoudi, and A. Del Bimbo, “3D facial expression recognition using SIFT descriptors of automatically detected keypoints,” *Vis. Comput.*, vol. 27, no. 11, p. 1021, 2011.
[172] D. G. Lowe, “Distinctive image features from scale-invariant keypoints,” *Int. J. Comput. Vis.*, vol. 60, no. 2, pp. 91–110, 2004.
[173] E. Vezzetti, F. Marcolin, and V. Stola, “3D human face soft tissues landmarking method: An advanced approach,” *Comput. Ind.*, vol. 64, no. 9, pp. 1326–1354, 2013.
[174] E. Vezzetti and F. Marcolin, “Geometry-based 3D face morphology analysis: soft-tissue landmark formalization,” *Multimed. Tools Appl.*, vol. 68, no. 3, pp. 895–929, 2014.
[175] E. Vezzetti and F. Marcolin, “3D landmarking in multiexpression face analysis: A preliminary study on eyebrows and mouth,” *Aesthetic Plast. Surg.*, vol. 38, no. 4, pp. 796–811, 2014.
[176] E. Sangineto, “Pose and expression independent facial landmark localization using dense-SURF and the Hausdorff distance,” *IEEE Trans. Pattern Anal. Mach. Intell.*, vol. 35, no. 3, pp. 624–638, 2013.
[177] S. Moos *et al.*, “Cleft lip pathology diagnosis and foetal landmark extraction via 3D geometrical analysis,” *Int. J. Interact. Des. Manuf.*, vol. 11, no. 1, pp. 1–18, 2017.
[178] S. Z. Gilani, F. Shafait, and A. Mian, “Shape-based automatic detection of a large number of 3D facial landmarks,” in *Computer Vision and Pattern Recognition (CVPR), 2015 IEEE Conference on*, 2015, pp. 4639–4648.
[179] F. M. Sukno, J. L. Waddington, and P. F. Whelan, “3-D facial landmark localization with asymmetry patterns and shape regression from incomplete local features,” *IEEE Trans. Cybern.*, vol. 45, no. 9, pp. 1717–1730, 2015.
[180] F. M. Sukno and J. L. Waddington, “Rotationally invariant 3D shape contexts using asymmetry patterns,” 2013.
[181] X. Fan, Q. Jia, K. Huyan, X. Gu, and Z. Luo, “3D facial landmark localization using texture regression via conformal mapping,” *Pattern Recognit. Lett.*, vol. 83, pp. 395–402, 2016.
[182] M. Li *et al.*, “Rapid automated landmarking for morphometric analysis of three-dimensional facial scans,” *J. Anat.*, vol. 230, no. 4, pp. 607–618, 2017.
[183] E. Vezzetti, F. Marcolin, S. Tornincasa, L. Ulrich, and N. Dagnes, “3D geometry-based automatic landmark localization in presence of facial occlusions,” *Multimed. Tools Appl.*, pp. 1–29, 2017.
[184] M. Song, D. Tao, S. Sun, C. Chen, and S. J. Maybank, “Robust 3D face landmark localization based on local coordinate coding,” *IEEE Trans. image Process.*, vol. 23, no. 12, pp. 5108–5122, 2014.
[185] S. Canavan, P. Liu, X. Zhang, and L. Yin, “Landmark localization on 3D/4D range data using a shape index-based statistical shape model with global and local constraints,” *Comput. Vis. Image Underst.*, vol. 139, pp. 136–148, 2015.
[186] X. Zhao, E. Dellandrea, L. Chen, and I. A. Kakadiaris, “Accurate landmarking of three-dimensional facial data in the presence of facial expressions and occlusions using a three-dimensional statistical facial feature model,” *IEEE Trans. Syst. Man, Cybern. Part B*, vol. 41, no. 5, pp. 1417–1428, 2011.
[187] Q. Liao, X. Jin, and W. Zeng, “Enhancing the symmetry and proportion of 3D face geometry,” *IEEE Trans. Vis. Comput. Graph.*, vol. 18, no. 10, pp. 1704–1716, 2012.
[188] X. Liang, S. Tong, T. Kumada, and S. Iwaki, “Golden Ratio: The Attributes of Facial Attractiveness Learned By CNN,” in *2019 IEEE International Conference on Image Processing (ICIP)*, 2019, pp. 2124–2128.
[189] S. Liu, Y.-Y. Fan, A. Samal, and Z. Guo, “Advances in computational facial attractiveness methods,” *Multimed. Tools Appl.*, vol. 75, no. 23, pp. 16633–16663, 2016.
[190] V. Lum, M. S. Goonewardene, A. Mian, and P. Eastwood, “Three-dimensional assessment of facial asymmetry using dense correspondence, symmetry, and midline analysis,” *Am. J. Orthod. Dentofac. Orthop.*, 2020.
[191] S. Weiss, C. M. Grewe, S. Olderbak, B. Goecke, L. Kaltwasser, and A. Hildebrandt, “Symmetric or not? A holistic approach to the measurement of fluctuating asymmetry from facial photographs,” *Pers. Individ. Dif.*, vol. 166, p. 110137, 2020.
[192] G. Stern, Z. Fu, and M. Ardabilian, “3D Face Analysis for Healthcare,” in *Biometrics under Biomedical Considerations*, Springer, 2019, pp. 147–160.
[193] A. Bottino, M. De Simone, A. Laurentini, and C. Sforza, “A new 3-D tool for planning plastic surgery,” *IEEE Trans. Biomed. Eng.*, vol. 59, no. 12, pp. 3439–3449, 2012.
[194] J. Kim and S. Choi, “Symmetric deformation of 3D face scans using facial features and curvatures,” *Comput. Animat. Virtual Worlds*, vol. 20, no. 2-3, pp. 289–300, 2009.
[195] W.-C. Chiang, H.-H. Lin, C.-S. Huang, L.-J. Lo, and S.-Y. Wan, “The cluster assessment of facial attractiveness using fuzzy neural network classifier based on 3D Moiré features,” *Pattern Recognit.*, vol. 47, no. 3, pp. 1249–1260, 2014.

[196] W.-C. Ma, M. Barbati, and J. P. Lewis, “A facial composite editor for blendshape characters,” in *Proceedings of the Digital Production Symposium*, 2012, pp. 21–26.
[197] M. Ren, N. Xie, Y. Yang, and H. T. Shen, “Cosmetic-vis: sample-based 3D facial editor for cosmetic medical visualization,” in *ACM SIGGRAPH 2017 Posters*, 2017, p. 21.
[198] M. Alexa, “Differential coordinates for local mesh morphing and deformation,” *Vis. Comput.*, vol. 19, no. 2, pp. 105–114, 2003.
[199] L. Gao, Y.-K. Lai, J. Yang, L.-X. Zhang, L. Kobbelt, and S. Xia, “Sparse Data Driven Mesh Deformation,” *arXiv Prepr. arXiv1709.01250*, 2017.
[200] Y. Yu *et al.*, “Mesh editing with poisson-based gradient field manipulation,” *ACM Trans. Graph.*, vol. 23, no. 3, pp. 644–651, 2004.
[201] Y.-W. Zhang, Y.-Q. Zhou, X.-L. Li, H. Liu, and L.-L. Zhang, “Bas-relief generation and shape editing through gradient-based mesh deformation,” *IEEE Trans. Vis. Comput. Graph.*, vol. 21, no. 3, pp. 328–338, 2015.
[202] O. Sorkine, “Laplacian mesh processing,” in *Eurographics (STARs)*, 2005, pp. 53–70.
[203] O. Sorkine, D. Cohen-Or, and S. Toledo, “High-Pass Quantization for Mesh Encoding.,” in *Symposium on Geometry Processing*, 2003, vol. 42.
[204] Y. Lipman, O. Sorkine, D. Cohen-Or, D. Levin, C. Rossi, and H.-P. Seidel, “Differential coordinates for interactive mesh editing,” in *Shape Modeling Applications, 2004. Proceedings*, 2004, pp. 181–190.
[205] O. Sorkine, D. Cohen-Or, Y. Lipman, M. Alexa, C. Rössl, and H.-P. Seidel, “Laplacian surface editing,” in *Proceedings of the 2004 Eurographics/ACM SIGGRAPH symposium on Geometry processing*, 2004, pp. 175–184.
[206] X. Wan and X. Jin, “Data-driven facial expression synthesis via Laplacian deformation,” *Multimed. Tools Appl.*, vol. 58, no. 1, pp. 109–123, 2012.
[207] J. Sun, Y. Ding, Z. Huang, N. Wang, X. Zhu, and J. Xi, “Laplacian Deformation Algorithm Based on Mesh Model Simplification,” in *2018 IEEE 3rd International Conference on Image, Vision and Computing (ICIVC)*, 2018, pp. 209–213.
[208] F. Naya, J. Jorge, J. Conesa, M. Contero, and J. M. Gomis, “Direct modeling: from sketches to 3D models,” in *Proceedings of the 1st Ibero-American Symposium in Computer Graphics SIACG*, 2002, pp. 109–117.
[209] E. Chang and O. C. Jenkins, “Sketching articulation and pose for facial animation,” in *Proceedings of the 2006 ACM SIGGRAPH/Eurographics symposium on Computer animation*, 2006, pp. 271–280.
[210] R. C. Zeleznik, K. P. Herndon, and J. F. Hughes, “SKETCH: An interface for sketching 3D scenes,” in *ACM SIGGRAPH 2007 courses*, 2007, p. 19.
[211] T. W. Sederberg and S. R. Parry, “Free-form deformation of solid geometric models,” *ACM SIGGRAPH Comput. Graph.*, vol. 20, no. 4, pp. 151–160, 1986.
[212] T. Igarashi, T. Igarashi, S. Matsuoka, and H. Tanaka, “Teddy: a sketching interface for 3D freeform design,” in *Acm siggraph 2007 courses*, 2007, p. 21.
[213] O. Karpenko, J. F. Hughes, and R. Raskar, “Free-form sketching with variational implicit surfaces,” in *Computer Graphics Forum*, 2002, vol. 21, no. 3, pp. 585–594.
[214] G. Turk and J. F. O’brien, “Shape transformation using variational implicit functions,” in *ACM SIGGRAPH 2005 Courses*, 2005, p. 13.
[215] Y. Kho and M. Garland, “Sketching mesh deformations,” in *Proceedings of the 2005 symposium on Interactive 3D graphics and games*, 2005, pp. 147–154.
[216] J. Zimmermann, A. Nealen, and M. Alexa, “SilSketch: automated sketch-based editing of surface meshes,” in *Proceedings of the 4th Eurographics workshop on Sketch-based interfaces and modeling*, 2007, pp. 23–30.
[217] S. Yoshizawa, A. G. Belyaev, and H.-P. Seidel, “Free-form skeleton-driven mesh deformations,” in *Proceedings of the eighth ACM symposium on Solid modeling and applications*, 2003, pp. 247–253.
[218] A. Laurentini and A. Bottino, “Computer analysis of face beauty: A survey,” *Comput. Vis. Image Underst.*, vol. 125, pp. 184–199, 2014.
[219] K. Kościński, “Current status and future directions of research on facial attractiveness,” *Anthropol. Rev.*, vol. 72, no. 1, pp. 45–65, 2009.
[220] M. M. Fleck, D. A. Forsyth, and C. Bregler, “Finding naked people,” in *European Conference on Computer Vision*, 1996, pp. 593–602.
[221] R. Kjeldsen and J. Kender, “Finding skin in color images,” in *Automatic Face and Gesture Recognition, 1996., Proceedings of the Second International Conference on*, 1996, pp. 312–317.
[222] N. Vandenbroucke, L. Macaire, and J.-G. Postaire, “Color image segmentation by pixel classification in an adapted hybrid color space. Application to soccer image analysis,” *Comput. Vis. Image Underst.*, vol. 90, no. 2, pp. 190–216, 2003.
[223] M. J. Jones and J. M. Rehg, “Statistical color models with application to skin detection,” *Int. J. Comput. Vis.*, vol. 46, no. 1, pp. 81–96, 2002.

[224] R.-L. Hsu, M. Abdel-Mottaleb, and A. K. Jain, “Face detection in color images,” *IEEE Trans. Pattern Anal. Mach. Intell.*, vol. 24, no. 5, pp. 696–706, 2002.
[225] K. Sobottka and I. Pitas, “Extraction of facial regions and features using color and shape information,” in *Pattern Recognition, 1996., Proceedings of the 13th International Conference on*, 1996, vol. 3, pp. 421–425.
[226] K. Sandeep and A. N. Rajagopalan, “Human Face Detection in Cluttered Color Images Using Skin Color, Edge Information.,” in *ICVGIP*, 2002.
[227] S. Baskan, M. M. Bulut, and V. Atalay, “Projection based method for segmentation of human face and its evaluation,” *Pattern Recognit. Lett.*, vol. 23, no. 14, pp. 1623–1629, 2002.
[228] K. Sobottka and I. Pitas, “A novel method for automatic face segmentation, facial feature extraction and tracking,” *Signal Process. Image Commun.*, vol. 12, no. 3, pp. 263–281, 1998.
[229] D. C. E. Thomaz, “FEI Face Database.” .
[230] A. 2D face sets-U. E. Peter Hancock. (2014, “No Title.” [Online]. Available: http://pics.psych.stir.ac.uk/2D_face_sets.htm.
[231] M. Gay, “Caractérisation de la neige, du névé et de la glace par traitement d’images.” Université Joseph-Fourier-Grenoble I, 1999.
[232] F. Abdat, C. Maaoui, and A. Pruski, “Suivi du gradient pour la localisation des caractéristiques faciales dans des images statiques,” in *21° Colloque GRETSI, Troyes, FRA, 11-14 septembre 2007*, 2007.
[233] F. Y. Shih and C.-F. Chuang, “Automatic extraction of head and face boundaries and facial features,” *Inf. Sci. (Ny).*, vol. 158, pp. 117–130, 2004.
[234] S. G. Ababsa, “Authentification d’individus par reconnaissance de caractéristiques biométriques liées aux visages 2D/3D.” THÈSE pour obtenir le titre de Docteur de l’Université Evry Val d’Essonne Spécialité: Sciences de l’Ingénieur université d’Evry val d’Essonne, 2008.
[235] M. Kass, A. Witkin, and D. Terzopoulos, “Snakes: Active contour models,” *Int. J. Comput. Vis.*, vol. 1, no. 4, pp. 321–331, 1988.
[236] D. J. Williams and M. Shah, “A fast algorithm for active contours and curvature estimation,” *CVGIP Image Underst.*, vol. 55, no. 1, pp. 14–26, 1992.
[237] C. Xu, Y. Wang, T. Tan, and L. Quan, “Robust nose detection in 3D facial data using local characteristics,” in *Image Processing, 2004. ICIP’04. 2004 International Conference on*, 2004, vol. 3, pp. 1995–1998.
[238] K. Petersen, R. Feldt, S. Mujtaba, and M. Mattsson, “Systematic Mapping Studies in Software Engineering.,” in *EASE*, 2008, vol. 8, pp. 68–77.
[239] A. Jourabloo and X. Liu, “Pose-invariant 3D face alignment,” in *Proceedings of the IEEE International Conference on Computer Vision*, 2015, pp. 3694–3702.
[240] N. De Giorgis, L. Rocca, and E. Puppo, “Scale-space techniques for fiducial points extraction from 3D faces,” in *International Conference on Image Analysis and Processing*, 2015, pp. 421–431.
[241] X. Fan, H. Wang, Z. Luo, Y. Li, W. Hu, and D. Luo, “Fiducial facial point extraction using a novel projective invariant,” *IEEE Trans. Image Process.*, vol. 24, no. 3, pp. 1164–1177, 2015.
[242] P. Perakis, G. Passalis, T. Theoharis, and I. Kakadiaris, “3D facial landmark detection & face registration: A 3D facial landmark model & 3D local shape descriptors approach,” *Tech. Rep. TP-2010-01*, 2010.
[243] P. Bagchi, D. Bhattacharjee, M. Nasipuri, and D. K. Basu, “A novel approach to nose-tip and eye corners detection using HK curvature analysis in case of 3D images,” in *2012 Third International Conference on Emerging Applications of Information Technology*, 2012, pp. 311–315.
[244] E. Vezzetti, F. Marcolin, S. Tornincasa, and P. Maroso, “Application of geometry to rgb images for facial landmark localisation-a preliminary approach,” *Int. J. Biom.*, vol. 8, no. 3–4, pp. 216–236, 2016.
[245] H. Boukamcha, M. Elhallek, M. Atri, and F. Smach, “3D face landmark auto detection,” in *2015 World Symposium on Computer Networks and Information Security (WSCNIS)*, 2015, pp. 1–6.
[246] R. J. Rohrich, J. E. Janis, and J. M. Kenkel, “Male rhinoplasty,” *Plast. Reconstr. Surg.*, vol. 112, no. 4, pp. 1071–1086, 2003.
[247] C. Y. Brinkley JF, Fisher S, Harris MP, Holmes G, Hooper JE, Jabs EW, Jones KL, Kesselman C, Klein OD, Maas RL, Marazita ML, Selleri L, Spritz RA, van Bakel H, Visel A, Williams TJ, Wysocka J; FaceBase Consortium, “The FaceBase Consortium: a comprehensive resource for craniofacial researchers.” .
[248] P. Paysan, R. Knothe, B. Amberg, S. Romdhani, and T. Vetter, “A 3D face model for pose and illumination invariant face recognition,” in *Advanced video and signal based surveillance, 2009. AVSS’09. Sixth IEEE International Conference on*, 2009, pp. 296–301.
[249] L. Ulrich, J.-L. Dugelay, E. Vezzetti, S. Moos, and F. Marcolin, “Perspective Morphometric Criteria for Facial Beauty and Proportion Assessment,” *Appl. Sci.*, vol. 10, no. 1, p. 8, 2020.
[250] Y.-K. Chang and A. P. Rockwood, “A generalized de Casteljau approach to 3D free-form deformation,” in *Proceedings of the 21st annual conference on Computer graphics and interactive techniques*, 1994, pp. 257–260.
[251] S. Lee, G. Wolberg, K.-Y. Chwa, and S. Y. Shin, “Image metamorphosis with scattered feature constraints,”

IEEE Trans. Vis. Comput. Graph., vol. 2, no. 4, pp. 337–354, 1996.
[252] S.-M. Hu, H. Zhang, C.-L. Tai, and J.-G. Sun, "Direct manipulation of FFD: efficient explicit solutions and decomposible multiple point constraints," *Vis. Comput.*, vol. 17, no. 6, pp. 370–379, 2001.
[253] S. Yoshizawa, A. G. Belyaev, and H.-P. Seidel, "A simple approach to interactive free-form shape deformations," in *10th Pacific Conference on Computer Graphics and Applications, 2002. Proceedings.*, 2002, pp. 471–474.
[254] V. Basili and S. Elbaum, "Better Empirical Science for Software Engineering," in *28th International Conference on Software Engineering (ICSE 2006), invited talk*, 2006.
[255] S. Easterbrook, J. Singer, M.-A. Storey, and D. Damian, "Selecting empirical methods for software engineering research," in *Guide to advanced empirical software engineering*, Springer, 2008, pp. 285–311.
[256] C. Hakim, *Research design: Successful designs for social and economic research*. Psychology Press, 2000.
[257] A. Thornhill, M. Saunders, and P. Lewis, *Research methods for business students*. Prentice Hall: London, 2009.
[258] R. K. Yin, "Case study research: Design and methods sage," *Thousand Oaks*, 2003.
[259] H. S. Park, S. C. Rhee, S. R. Kang, and J. H. Lee, "Harmonized profiloplasty using balanced angular profile analysis," *Aesthetic Plast. Surg.*, vol. 28, no. 2, pp. 89–97, 2004.

Appendix-1

Interfaces of our system of analyzing the aesthetic quality of 2D and 3D faces:

The following figures present the interfaces of our system to analyzing the aesthetic quality of frontal side of 2D faces.

Figure A-1: Input 2D face.

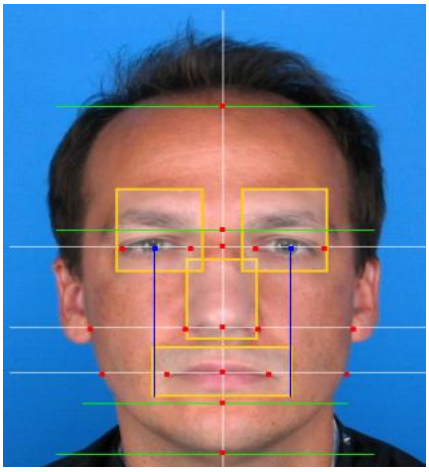

Figure A-2: 2D facial landmarks localization.

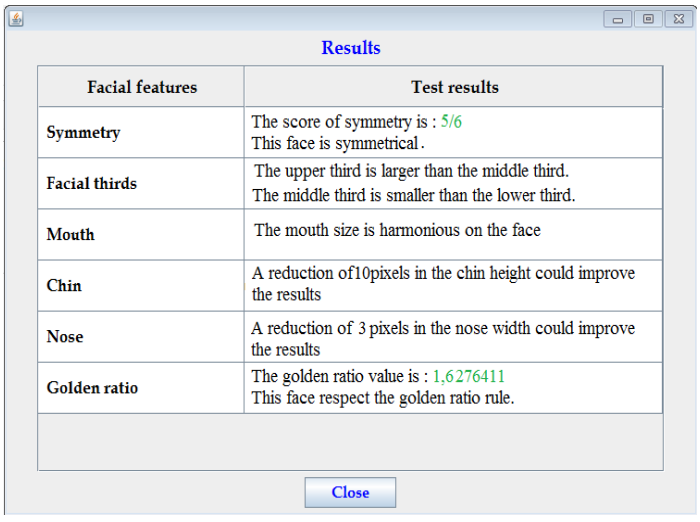

Figure A-3: Results of the aesthetic quality analysis of the frontal side of the 2D face.

The following figures describe the process of our proposed system to analyze and enhance the aesthetic quality of 3D face.

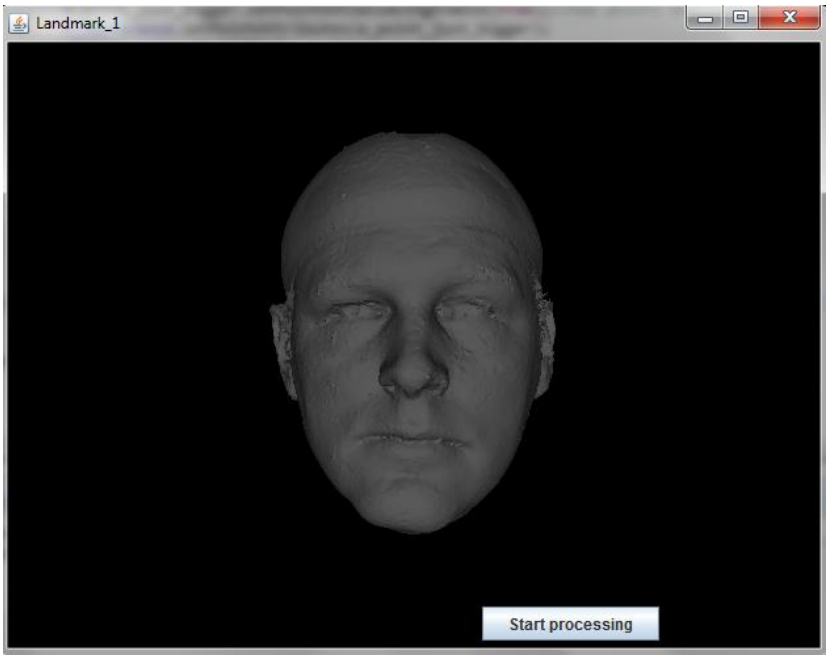

Figure A-4: The input 3D face.

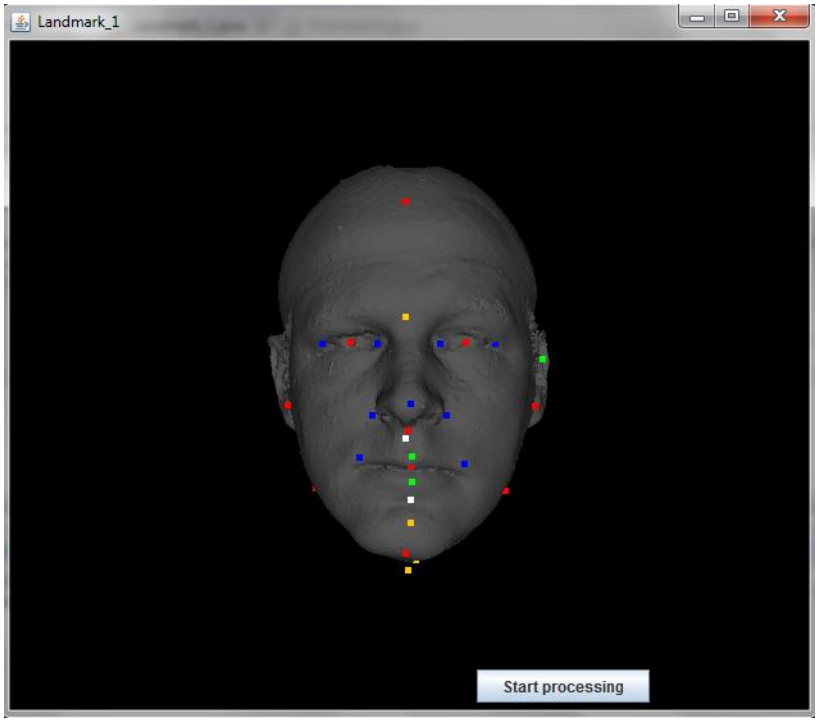

Figure A-5: 3D facial landmarks localization.

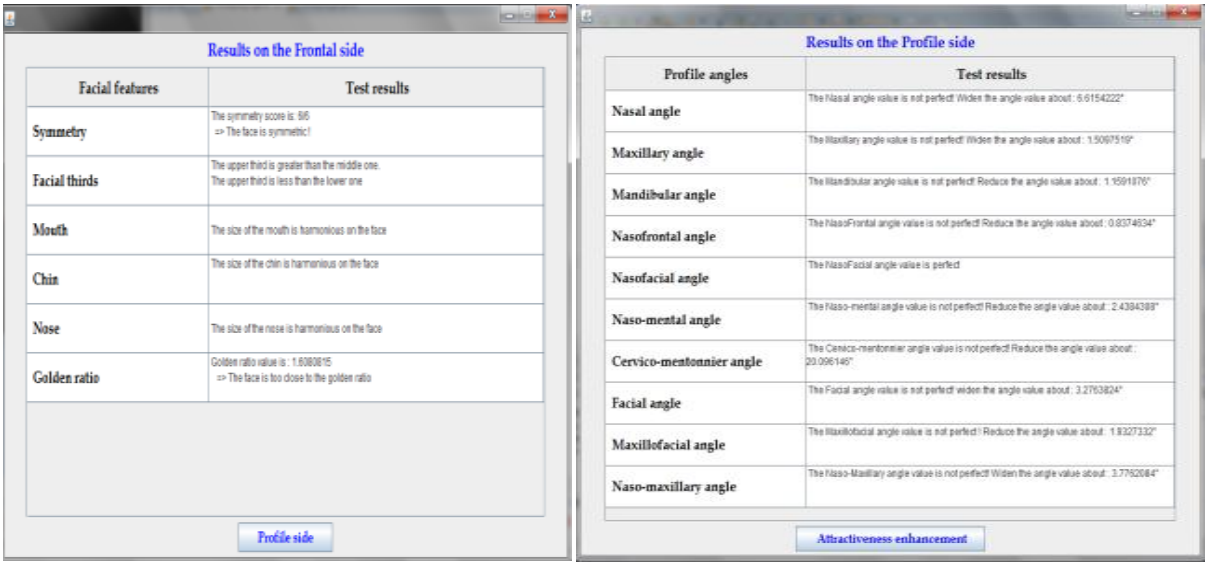

Figure A-6: 3D facial aesthetic quality analysis results on both the frontal and profile sides.

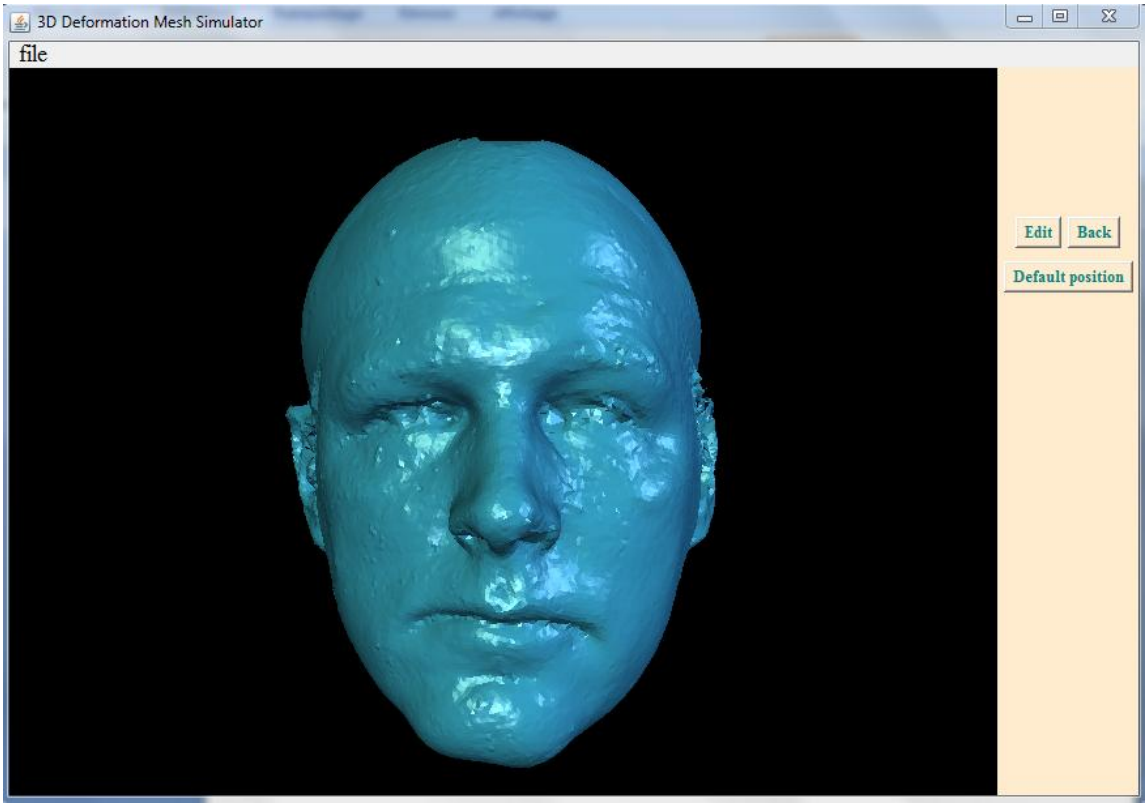

Figure A-7: 3D facial aesthetic quality enhancement interface.

Appendix-2

3D facial aesthetic quality enhancement results assessment: survey protocol

The survey was conducted in order to assess the obtained results from the step of the aesthetic quality enhancement by our system. For this purpose, this survey took place in the Faculty of Science and Technology (FST) at the University of Sidi Mohammed Ben Abdellah (USMBA- Fez) covering about 50 students from different specialties in the FST.

Objective:

The aim of the survey is to evaluate the obtained results of our system in term of enhancing the aesthetic quality of 3D faces; each of the enhanced 3D faces are presented to the students, afterwards, it is to the student to vote for the face the most attractive within the original and the edited face.

Participants:

The participants to the survey were chosen randomly from the Faculty of Science and Technology of the University of Sidi Mohamed Ben Abdellah. Indeed, after a brief explanation of the purpose of our research study to each of the participants, they were invited to ask any questions to clarify any ambiguity and avoid any misinterpretations before the vote.

Data collection:

The presented survey was conducted using a simple self administered questionnaire. For each of the participants, we have collected the information detained in the next appendix, and then ask them to vote for the most attractive 3D face within the original and the edited one by our system. The 3D face before and after the attractiveness enhancement were presented to the participants using our PC so that the details can be seen clearly, thereafter, the results of the vote for each 3D faces from the used datasets were recorder manually to create a table of comparison containing the ID of the 3D face, the original version, the editing one and the vote of each of the participants.

Appendix-3

Evaluation Questionnaire

Profile information
Sex : Age: Educational level: Have you used such a tool before? : If yes, please indicate the name:

Please fill in the following table by voting for the most attractive face (Before or after the enhancement of its attractiveness using our system).

3D face ID	Before the aesthetic quality enhancement	After the aesthetic quality enhancement
Face-1		
Face-2		
Face-3		
...		
Face-N		

جامعة سيدي محمد بن عبد الله بفاس
UNIVERSITÉ SIDI MOHAMED BEN ABDELLAH DE FES

كلية العلوم والتقنيات فاس
FACULTÉ DES SCIENCES ET TECHNIQUES DE FÈS

Centre d'Etudes Doctorales : Sciences et Techniques de l'Ingénieur

Résumé de la thèse intitulée:

3D facial aesthetic quality: Analysis and enhancement system

Doctorante :
M^lle^: Manal EL RHAZI

Directeurs de thèse :
Pr. Arsalane ZARGHILI
Pr. Aicha MAJDA

Laboratoire d'accueil : Systèmes Intelligents et Applications.
Etablissement : Faculté des Sciences et Techniques de Fès

1 Introduction

a. Motivation

L'attractivité faciale joue un rôle important dans la vie humaine et a toujours été l'un des sujets les plus débattus dans de nombreux domaines en raison des différentes perceptions de l'attractivité par les individus. Dans la littérature, de nombreuses études ont défini ce qui rend un visage attirant, unifiant ainsi les critères d'attractivité et les rendant universels et non liés à l'époque historique ou à l'ethnicité d'une personne.

L'attractivité physique a une influence importante et considérable dans la vie sociale humaine, comme l'ont démontré plusieurs recherches au cours des dernières décennies. Elle est également largement liée à la possession d'une variété de qualités positives qui rendent un individu meilleur que les autres, comme le résume la déclaration de Dion, Berscheid et Walster en 1972, qui affirmait que "ce qui est beau est bon". En effet, l'attrait physique offre de nombreux avantages à la vie individuelle, surtout dans une société obsédée par la beauté et l'attrait. Ces avantages sont prouvés par des expériences quotidiennes comme la sélection intersexuelle. L'attirance physique peut également affecter l'estime de soi et provoquer des troubles psychologiques.

En conséquence de l'influence de l'attractivité, les gens ont tendance à être de plus en plus attirants en utilisant du maquillage ou en ayant recours à des opérations de chirurgie plastique. C'est pourquoi, depuis 2000, le nombre total de chirurgies plastiques a considérablement augmenté en raison de la croissance continue du nombre de chirurgies exigeantes ainsi que de l'argent dépensé à cette fin.

Parallèlement à l'augmentation des besoins en matière de chirurgie plastique, il est recommandé de simplifier et de montrer comment le visage sera après l'opération, de planifier les procédures, de vérifier la satisfaction du patient et de réduire les risques pendant l'opération également. Par conséquent, un outil automatique d'analyse de l'attractivité faciale basé sur les canons de beauté définis dans la littérature est nécessaire, ce qui est considéré comme un grand défi pour les chercheurs.

b. Objectifs de recherche

Aujourd'hui, la visualisation 3D est largement utilisée dans le domaine médical ; cependant, peu de systèmes sont dédiés aux domaines de la chirurgie plastique en raison du prix élevé des matériaux. Les logiciels existants pour planifier les procédures faciales en 3D et évaluer la post-chirurgie sont manipulés en fonction du patient et à quoi il veut ressembler comme résultat, sans tenir compte du caractère réellement attrayant du visage.

Les systèmes existants de visualisation du visage en 3D (VECTRA 3D , MIRRORME 3D , CRISALIX) ne proposent aucun standard d'attractivité faciale en 3D, ce qui fait du développement d'un tel outil une tâche nécessaire pour faciliter le travail des chirurgiens et du patient en même temps, et pour remédier au manque de systèmes 3D permettant d'analyser l'attractivité du visage en 3D, et proposer les modifications nécessaires afin d'améliorer son attractivité.

Dans notre thèse, nous visons à répondre aux objectifs de recherche suivants :

- **Premier objectif de recherche :** analyser la qualité esthétique du visage 2D et ensuite suggérer les modifications nécessaires afin d'améliorer son attractivité.

- **Deuxième objectif de recherche :** évaluer la qualité esthétique des visages 3D et, comme premier objet de recherche, recommander les modifications nécessaires pour améliorer son attractivité.
- **Troisième objectif de recherche :** Prévoir l'aspect du visage après l'application de la modification requise, et donc les résultats post-opératoires.
- **Quatrième objectif de recherche :** Évaluer le visage obtenu après l'opération en interrogeant un expert du domaine de la chirurgie plastique et en réalisant une enquête.

c. Méthodologie de recherche

Pour répondre aux objectifs de recherche cités précédemment, la figure ci-dessous présente un résumé de la méthodologie suivie dans notre thèse.

Le projet a été divisé en quatre étapes ; chacune est liée à l'étape suivante, nous avons commencé par une analyse bibliographique globale afin de localiser notre travail et d'établir les besoins existants. Ensuite, comme première tentative, nous avons analysé la qualité esthétique du visage 2D en utilisant une nouvelle méthode pour détecter les points de repère du visage 2D et nous avons ensuite suggéré les modifications nécessaires pour améliorer son attractivité. La deuxième étape est de commencer à travailler en profondeur sur notre projet d'analyse de l'attractivité faciale en 3D. Après une revue systématique de la littérature et une analyse cartographique, nous avons sélectionné la méthode appropriée pour détecter les points de repère faciaux en 3D afin de pouvoir analyser l'attractivité du visage en 3D et enfin de prédire comment ce visage peut être plus attrayant. La troisième étape est la visualisation du visage en 3D après les modifications appliquées pour vérifier la satisfaction du patient et du chirurgien. Enfin, la dernière étape est l'évaluation des résultats obtenus, en demandant à un expert du domaine de la chirurgie plastique et en réalisant un sondage en demandant aux participants de voter pour le visage le plus attrayant.

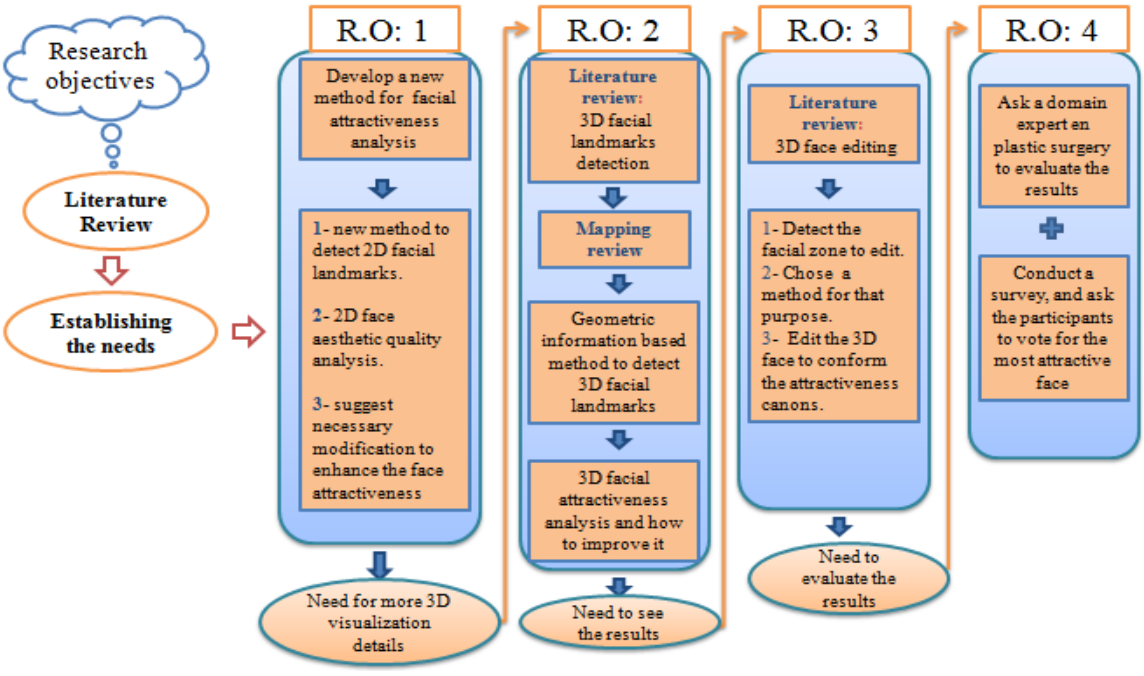

La méthodologie de recherche proposée

2 Analyse de la qualité esthétique des visages 2D

Dans cette partie, nous proposons une nouvelle méthodologie pour analyser la qualité esthétique des visages en 2D. La première étape pour atteindre cet objectif est de détecter la zone du visage sur une image, dans notre thèse cette étape est réalisée en utilisant une approche basée sur la localisation de la peau du visage. Cette méthode a donné des résultats intéressants. En effet, elle consiste à détecter les pixels qui appartiennent à la zone de la peau du visage et ceux qui n'en font pas partie, par conséquent, la zone du visage sera extraite du fond. La deuxième étape est la localisation des points de repère du visage, tout d'abord les axes du visage (axe des yeux, axe du nez, axe de la bouche et axe médian) sont détectés en utilisant les variations des informations de gradient de l'image, cela nous permet de créer des rectangles autour des traits du visage pour limiter la zone de recherche des points de repère. Ensuite, nous appliquons le contour actif sur l'ensemble du visage et dans les rectangles dessinés et nous détectons l'intersection de ses points avec les axes détectés faisant partie de la zone de la peau.

L'étape finale consiste à étudier et à analyser l'attractivité du visage. En utilisant les points de repère détectés, un certain nombre de distances et de rapports sont calculés afin d'effectuer une comparaison avec les canons de beauté cités dans la littérature et de donner un résultat de l'analyse avec les modifications nécessaires qui peuvent améliorer la qualité esthétique du visage analysé.

La figure ci dessous décrit l'approche proposée pour la détection et la localisation des repères faciaux, des points de repère et du résultat de l'analyse de la qualité esthétique du visage.

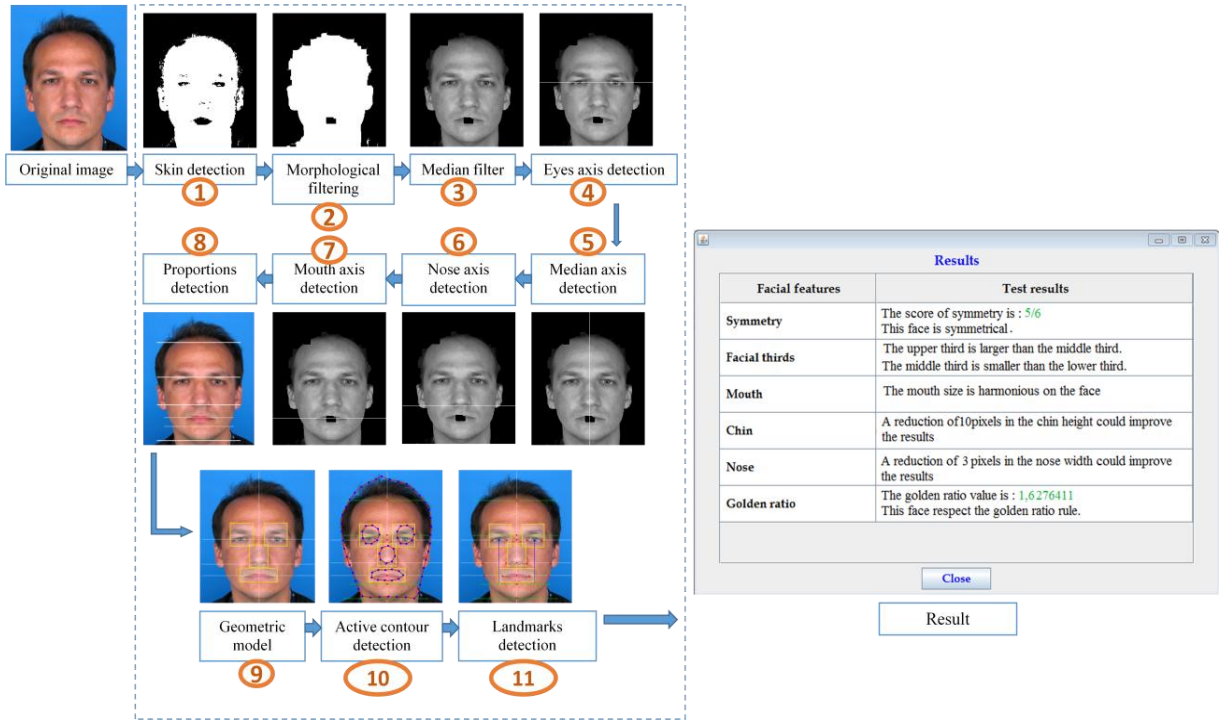

Architecture globale de la méthode proposée pour analyser la qualité esthétique des visages 2D

a. Les canons de beauté

Selon la nature universelle de l'attrait du visage, diverses hypothèses ont été avancées pour décrire les préférences communes en matière de beauté faciale et répondre ainsi à la question : qu'est-ce qui rend un visage attrayant ? Ces hypothèses sont nées de l'idée qu'un visage doit respecter certains critères qui sont connus des canons de la beauté pour être jugés attrayants. Dans notre thèse, nous nous sommes concentrés sur trois canons qui sont les plus utilisés et qui ont été largement discutés dans de nombreuses études de recherche qui ont prouvé l'importance de ces canons dans l'évaluation de la beauté du visage.

- **Symétrie :**

Une caractéristique commune des visages jugés beaux est que leur harmonie provient de l'équilibre, la symétrie faisant référence à la capacité de diviser un visage en deux moitiés égales. La psychologie de l'évolution s'est concentrée sur la perception de la symétrie faciale et a rapporté qu'elle est un facteur d'attractivité, et de nombreuses études prouvent que la symétrie reflète l'état psychologique et les conditions génétiques, car la symétrie bilatérale des traits du visage est un signe d'hétérozygotie génétique et elle reflète également la capacité à résister aux parasites et aux différentes perturbations, elle peut donc être considérée comme un signe de bonne santé. D'autre part, l'asymétrie du visage peut être liée à une anomalie génétique qui se produit chez les personnes qui ont été exposées à des perturbations environnementales ou à des maladies.

- **Le nombre d'or :**

Le nombre d'or est une célèbre proportion mathématique, qui est appliquée en peinture, en sculpture, en architecture, et également observée dans la nature. Il est presque devenu synonyme d'une forme belle et équilibrée. Le nombre d'or Φ est dérivé du nom du sculpteur grec Phidias et est un nombre irrationnel de l'ordre de 1,618033988. Il est obtenu lorsqu'un segment a + b peut être divisé en deux sections telles que a + b/a = a/b.

- **Les proportions néoclassiques :**

De plus, malgré un visage parfaitement proportionné, il existe des variations infinies de couleur et de forme de chaque trait du visage (sourcils, yeux, nez, lèvres, etc.) ce qui conduit à l'aspect distinctif de chaque race et permet des variations infinies de beauté. Les proportions du visage ou les canons néoclassiques ont été formulés dès la renaissance par certains artistes comme Durer et da Vinci, et ils sont cependant encore très célèbres et largement utilisés dans le domaine de la chirurgie plastique, de l'art et de la sculpture. Les canons néoclassiques populaires sont les suivants :

- Sur la face frontale du visage, le visage "idéal" peut être divisé en cinq segments verticaux égaux, chaque cinquième étant égal à la largeur d'un œil.

- Horizontalement, entre la racine des cheveux et le menton, le visage peut être divisé en tiers égaux, le tiers supérieur s'étendant de la racine des cheveux à la glabelle, le tiers

médian de la glabelle à la sous-nasale, et le tiers inférieur de la sous-nasale à la pointe du menton.

- De plus, le tiers inférieur peut également être subdivisé en tiers égaux qui déterminent la lèvre supérieure, la lèvre inférieure et la zone du menton. Le premier tiers s'étend de la sous-nasale à la ligne horizontale entre la lèvre supérieure et la lèvre inférieure, le deuxième tiers s'étend de la ligne entre la lèvre supérieure et la lèvre inférieure à la sous-nasale et le dernier tiers s'étend de la sous-nasale à la pointe du menton.

- Les coins de la bouche doivent être projetés dans la verticale descendant de la pupille lorsque le regard est neutre et vers l'avant.

- Finalement, la hauteur du menton doit représenter 1/9 de la hauteur du visage (1/3 du tiers inférieur).

- **Le profil angulaire :**

Du côté du profil, un certain nombre d'angles doivent être vérifiés afin de refléter les proportions du profil du visage.

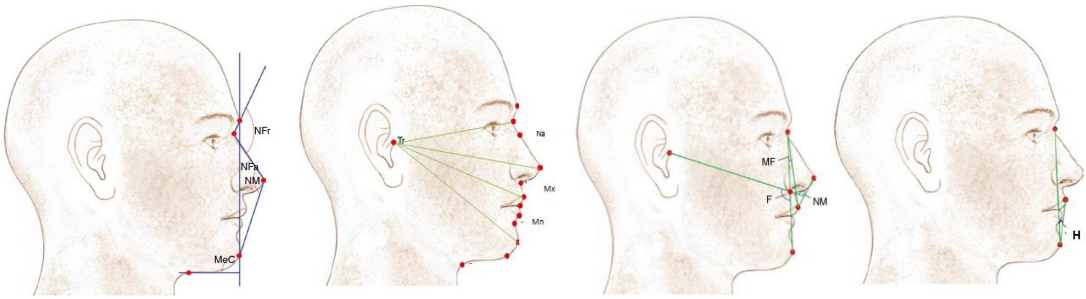

Les angles	La valeur moyenne
NasoFrontal angle (NFr)	115° - 130°
NasoFacial angle (NFa)	30° - 40°
NasoMental angle (NM)	120° - 130°
MentoCervical angle(MeC)	80° - 95°
Nasal angle (Na)	23.3°
Maxillary angle (Mx)	14.1°
Mandibular angle (Mn)	17.1°
MaxilloFacial angle (MF)	5.9°
Facial angle (F)	102.5°
Nasal Maxillary angle (NM)	106.1°
Angle (H)	10°

b. Détection du visage 2D dans une image

La détection des visages en 2D est une étape clé dans de nombreux processus d'analyse d'images car plus la détection est précise, plus l'analyse est fiable. Dans notre cas de l'analyse de la qualité esthétique du visage, la détection de la zone cutanée doit être aussi efficace que possible car un long processus de détection suit cette première étape où chaque étape dépend de la précédente.
Pour détecter la zone du visage sur une image 2D basée sur la couleur de la peau, nous avons utilisé une méthode composée de deux étapes principales ; la première étape est la détection de la zone du visage en utilisant les propriétés du modèle de couleur HSV, puis la seconde étape est le raffinement des résultats obtenus en utilisant des filtres morphologiques tels que : dilatation, érosion et filtre médian.

c. Détection de points de repère faciaux 2D

Dans notre thèse, pour détecter les points de repère faciaux en 2D, de nombreuses étapes ont été suivies afin d'obtenir des résultats de détection plus précis et moins d'erreurs. La première étape consiste à détecter les axes du visage qui sont l'axe des yeux, l'axe du nez, l'axe de la bouche et l'axe médian ; ces axes sont représentés par un certain nombre de lignes qui croisent les traits du visage, la détection des axes du visage vise à délimiter les zones des traits du visage. Après la détection des axes faciaux, les différentes proportions du visage sont déterminées en traçant les lignes qui spécifient ces proportions. L'étape suivante consiste en un modèle géométrique facial qui est utilisé pour dessiner des rectangles autour des traits du visage afin de délimiter la zone de recherche finale des points de repère faciaux. Une fois les rectangles dessinés, le contour actif est appliqué sur l'ensemble du visage puis sur chaque rectangle facial, et nous détectons l'intersection des points donnés par le contour actif et les axes faciaux, ces intersections doivent être dans la zone de la peau, les intersections résultantes sont des points de repère faciaux 2D.

d. Analyse de la qualité esthétique des visages 2D

L'analyse de la qualité esthétique d'un visage en 2D est la dernière étape du travail proposé ; elle consiste à déterminer si le visage donné est conforme aux canons de beauté définis dans la littérature. Pour cela, après la détection des repères faciaux, nous vérifions d'abord si le visage répond aux canons de beauté qui sont : la symétrie faciale, le nombre d'or et les proportions néoclassiques en calculant un ensemble de ratios et de distances, puis nous comparons les résultats obtenus à l'état de l'art de chaque canon.

L'analyse de la symétrie :

La règle de la symétrie faciale est facile à vérifier. Le visage est divisé en régions et pour chaque région, les points de repère localisés sont organisés en paires de points et ensuite mis dans notre système pour calculer le score de la symétrie en utilisant les distances horizontales par rapport à l'axe médian. Dans notre cas, nous avons pris 12 mesures (les coins des yeux, les coins du nez, les coins de la bouche et les points des joues) ; le score de symétrie sera donc noté sur 6.

L'analyse du nombre d'or :

Le nombre d'or est calculé à partir des axes qui passent par les traits du visage (axe des yeux, axe des narines et axe de la bouche). Nous calculons le rapport entre deux distances consécutives, au total nous avons 4 rapports à calculer. Le premier rapport est calculé de la

pointe du front à la pointe du menton et de l'axe des yeux à la pointe du menton, le deuxième rapport est calculé de l'axe des yeux à la pointe du menton et de l'axe des yeux à l'axe de la bouche, le troisième rapport est calculé de l'axe des yeux à l'axe de la bouche et de l'axe des yeux à l'axe du nez, et le dernier rapport est calculé de la largeur de la bouche et de la largeur du nez.

L'analyse des proportions néoclassique :

Pour les autres canons de la beauté (quintes verticales, tierces horizontales, largeur de la bouche et hauteur du menton), on calcule les différentes distances et on vérifie leurs valeurs en les comparants aux références mentionnées dans l'état de l'art de l'esthétique faciale.

3 Analyse de la qualité esthétique des visages 3D

Récemment, avec l'accessibilité croissante aux scanners 3D, l'utilisation de visages 3D est devenue un atout majeur pour faire face aux limitations traditionnelles, y compris celles associées aux images 2D, telles que les conditions d'éclairage et le point de vision. Cela est également bénéfique pour divers domaines tels que la recherche craniofaciale où la manipulation manuelle des visages a été la technique standard pour l'analyse de la dysmorphologie craniofaciale, la planification chirurgicale et l'évaluation des résultats.

Dans cette partie, nous présentons une nouvelle approche pour analyser la qualité esthétique d'un visage en 3D, tant pour la face frontale que pour la face de profil.

a. La normalisation du visage3D :

Pour analyser la qualité esthétique des visages 3D, le visage doit d'abord être prétraité afin de normaliser sa pose et son orientation. Cette étape vise à corriger les rotations angulaires de lacet et de roulis en minimisant la différence entre les côtés droit et gauche du visage 3D, puis le tangage est traité en minimisant la différence entre la hauteur du front et la hauteur du menton.

b. La détection des points repères en 3D :

Après avoir prétraité le visage 3D, la deuxième étape est la détection des points de repère; ces points de repère nous aideront à calculer les rapports et les distances faciales comme cela a déjà été fait pour les visages en 2D dans le chapitre précédent. Dans la présente partie, un grand nombre de repères faciaux 3D (30) est détecté, ce grand nombre est particulièrement nécessaire dans le domaine des chirurgies plastiques et esthétiques, ce qui est notre cas, pour obtenir plus de détails sur la géométrie du visage et en outre pour faciliter l'application de la modification suggérée au visage 3D. L'approche proposée pour détecter les points de repère faciaux en 3D est basée sur l'utilisation des informations géométriques fournies par le maillage 3D. En fait, notre approche s'inspire d'une étude précédente qui visait à détecter 17 points de repère faciaux en 3D. En effet, nous avons étendu cette méthode pour en détecter un grand nombre. Parmi les 30 points de repère détectés, 26 points de repère sont détectés sur la face frontale de la face 3D et quatre points de repère ont été localisés sur la face de profil, comme le montre les figures ci-dessous.

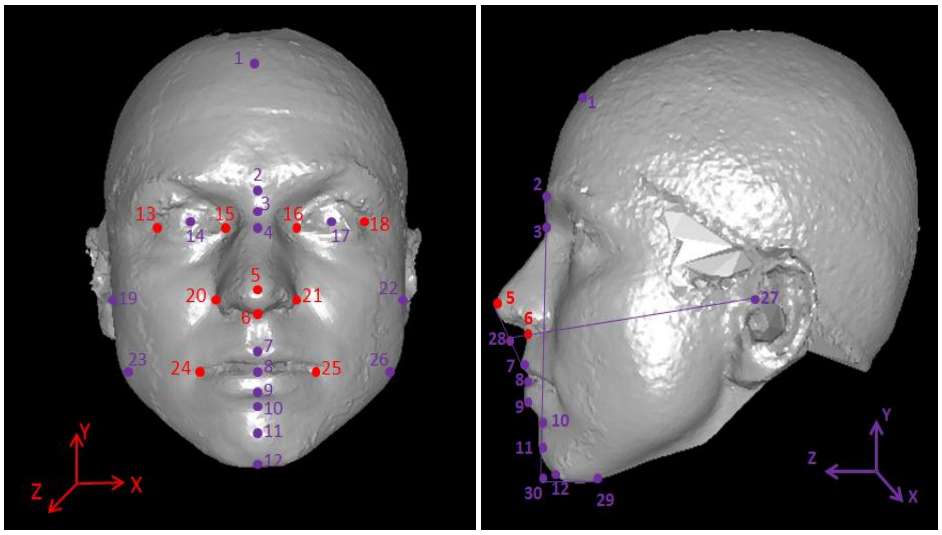

Les points de repère faciaux en 3D

Les 30 points de repère faciaux détectés sont quelques-uns de ceux qui sont nécessaires à l'anthropométrie cranio-faciale, qui est largement utilisée dans de nombreux domaines pour analyser et quantifier l'anthropométrie faciale, comme par exemple dans le domaine de l'analyse de la qualité esthétique du visage. Des auteurs ont confirmé que pour analyser l'attractivité faciale, un large ensemble de points de repère faciaux est nécessaire, ce qui permettra de vérifier si un visage répond ou non aux critères esthétiques. Sur la base de ces critères esthétiques, nous avons conclu que 30 points de repère sont suffisants et fiables pour analyser l'attractivité faciale.
Dans la méthode proposée, avant de détecter un nouveau point de repère facial, la zone de recherche est limitée en utilisant les points de repère précédemment détectés, ce qui fait de l'étape de normalisation de la pose du visage en 3D une étape cruciale et nécessaire dans le processus de détection.

c. Analyse de la qualité esthétique des visages 3D :

La dernière étape de l'analyse de la qualité esthétique du visage en 3D consiste à vérifier si le visage répond aux canons de beauté définis dans les études de la littérature pour le côté frontal et le côté profil d'un visage ; sinon, à suggérer les modifications nécessaires pour améliorer son attractivité. Cette vérification est basée sur la comparaison des résultats obtenus à partir du calcul des ratios et des distances avec ceux prédéfinis dans la littérature.

L'analyse de la symétrie :

Comme pour l'analyse de la qualité esthétique d'un visage en 2D, nous analysons la symétrie d'un visage en 3D. A partir des points de repère détectés sur la face frontale du visage, nous comparons les distances entre les différentes parties des deux demi-faces à partir de l'axe qui longe le point de la pointe du nez pour un même point de repère sur les deux faces, dans notre analyse, nous avons pris 12 mesures (les points des coins des yeux, des coins du nez, des coins de la bouche et des joues) ; ainsi le score de symétrie sera noté sur 6.

L'analyse du nombre d'or :

Les différents ratios utilisés sont les mêmes déjà utilisé dans la partie 2D, et sont comme suit :

Number of the golden ratio	Description
1	(forehead point to chin tip) / (eyes axis to chin tip)
2	(eyes axis to chin tip) / (eyes axis to mouth axis)
3	(eyes axis to mouth axis) / (eyes axis to nose axis)
4	Mouth width / nose width

Ensuite, la moyenne de ces ratios est calculée et comparée à la valeur du nombre d'or : 1,618, si la moyenne des valeurs obtenues du nombre d'or est égale à cette valeur ou même très proche de ce nombre dans une plage spécifique, on peut dire que le visage 3D vérifie le canon du nombre d'or. Dans le cas contraire, le visage ne respecte pas ce canon, il faut donc procéder à quelques modifications pour améliorer l'attractivité du visage 3D.

L'analyse des proportions néoclassique :

Les différentes proportions néoclassiques testées dans notre étude sont :

Number of neoclassical proportion	Description
1	Forehead height = nose length = lower face height
2	Face width = 5× nose width
3	Interocular distance = nose width
4	Interocular distance = eye fissure width
5	Mouth width = interpupils distance
6	Chin height = 1/3 of the lower face height

L'analyse de profil:

Pour obtenir une vue plus attrayante du profil, une série d'angles a été mesurée pour vérifier si le profil de la personne est agréable ou non. En fait, 11 mesures angulaires doivent être déterminées, comme déjà expliqué. La valeur de chaque angle est comparée à la valeur définie par les études de recherche. Après avoir calculé tous les angles, notre système montre les résultats et si un angle n'est pas conforme à ce qui a été défini comme référence, il indique la modification nécessaire à appliquer également.

La figure ci-dessous présente un exemple d'analyse de la qualité esthétique d'un visage 3D.

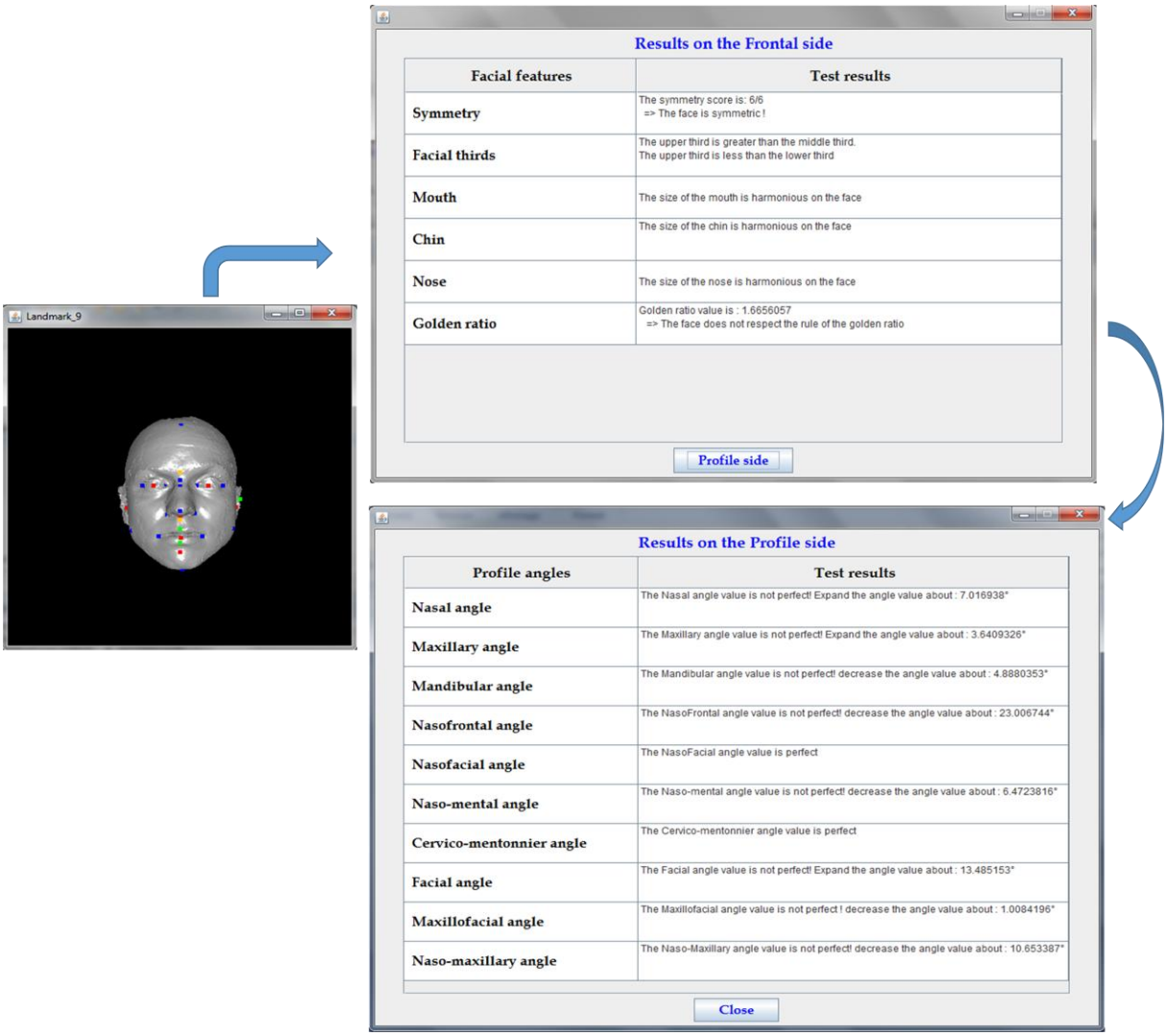

Analyse de la qualité esthétique d'un visage 3D

4 Amélioration de la qualité esthétique des visages 3D

Apres avoir analyser la qualité esthétique des visages 3D, le système proposé dans notre thèse propose les modifications nécessaires pour améliorer l'attractivité du visage donné. D'où l'étape suivante est l'application de ces modifications sur le visage 3D.

La déformation des maillages 3D est un domaine de recherche actif depuis quelque temps en raison de la grande diversité des utilisations. Par conséquent, tout en effectuant la déformation du maillage 3D, certains critères doivent être respectés par les approches proposées afin d'obtenir des résultats satisfaisants ; l'approche de la déformation doit être suffisamment rapide, robuste, intuitive et facile à contrôler. En outre, le résultat de la déformation doit fournir un maillage déformé physiquement plausible et esthétiquement agréable et le plus important est de préserver les détails géométriques du maillage original. Ceci est considéré comme un défi pour les chercheurs lorsqu'ils travaillent avec une représentation complexe comme les maillages 3D.

Différentes approches ont été proposées dans la littérature pour effectuer les modifications faciale en 3D comme décrit dans notre thèse. Ces travaux visent à générer des déformations de formes d'aspect naturel en développant des approches rapides, intuitives et précises pour la déformation globale et locale des formes. En particulier, les méthodes de déformation libre des formes (FFD) pour la déformation de modèles 3D ont fait l'objet de recherches intensives dans la littérature, en raison de leurs divers avantages, notamment dans le domaine des industries numériques.

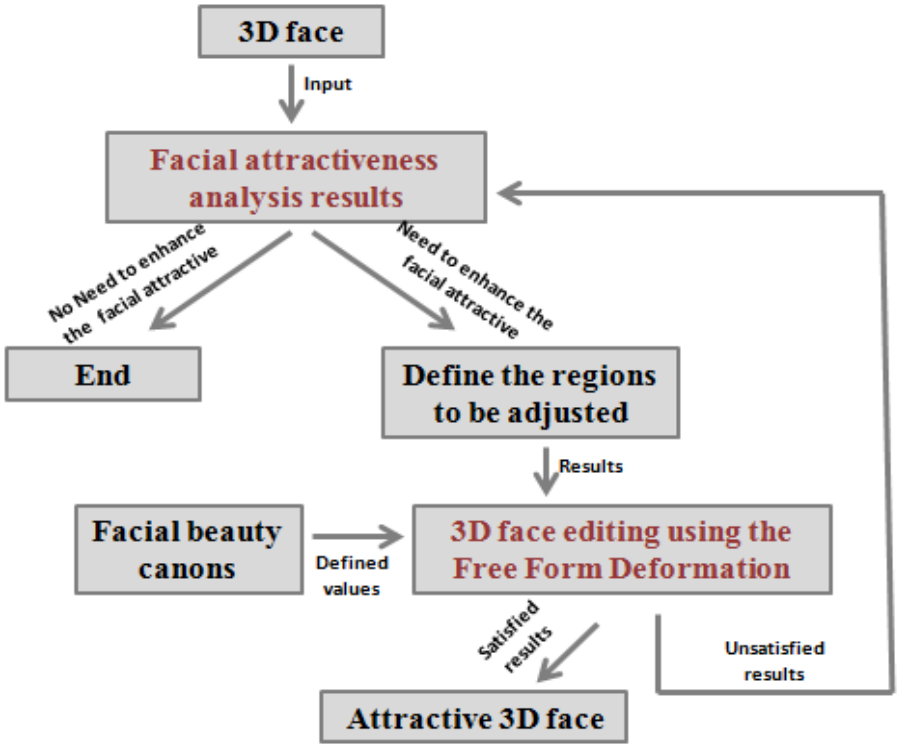

Architecture d'amélioration de la qualité esthétique des visages 3D

Pour appliquer l'algorithme de déformation de forme libre à l'édition de maillages 3D, certaines étapes doivent être effectuées comme indiqué dans la figure ci dessus. Principalement, à partir

des résultats obtenus de l'analyse de la qualité esthétique qui sont utilisés pour déterminer la mesure dans laquelle le visage doit être ajusté, les régions à éditer sont identifiées ; ces régions représentent l'ensemble des points sur lesquels la déformation sera appliquée. Par la suite, la modification consiste à déplacer les points d'origine vers de nouveaux points, tant du côté frontal que du côté du profil du visage 3D d'entrée, afin d'obtenir un visage plus attrayant respectant les canons de beauté abordés précédemment dans les chapitres précédents : symétrie, golden ratio, proportions néoclassiques et profil angulaire.

a. Le modèle de déformation

Dans cette sous-section, nous visons à éditer le visage 3D, si des modifications sont nécessaires, afin d'améliorer son attractivité suite aux résultats de l'étape d'analyse précédente. Ces modifications sont appliquées aux principales régions d'intérêt du visage 3D, à savoir : les yeux, les narines, la bouche, le menton, les joues et le côté profilé.
Dans l'étape d'amélioration de l'attractivité du visage 3D, les points de repère 3D localisés sont utilisés afin de déformer le visage avec précision.
Pour déformer un visage 3D, un point de coordonnées local est déterminé sur le sommet qui doit être déformé et il est appelé le point de contrôle C. Par conséquent, pour déplacer un sommet de sa position initiale O à P le nouveau. La formule suivante est utilisée :

$$P = O + D$$

Où le vecteur de déplacement D est donné par :

$$D = \frac{\gamma}{\varepsilon}.B.\vec{N}$$

Alors que la fonction de base B (Bézier) est calculée selon la formule :

$$B = \exp\left(-\frac{|O - C|^{\alpha}}{2r^2}\right)$$

Et :

$$\varepsilon = \exp\left(-\frac{|O_{min} - C|^{\alpha}}{2r^2}\right)$$

O_{min} est le sommet d'origine le plus proche du point de contrôle C. et γ, α et ε sont des paramètres qui peuvent être modifiés en fonction de la déformation souhaitée. Dans la formule de déplacement, $\vec{N}$ est le vecteur normal du maillage 3D au point de contrôle, le |.| représente la distance euclidienne entre le point d'origine et le point déformé, le paramètre γ est utilisé pour contrôler la hauteur du pic après la déformation.

b. Résultats

Basé sur l'analyse de la qualité esthétique des visages 3D expliquée précédemment, qui vise à vérifier si les visages 3D d'entrée sont conformes aux canons de beauté (symétrie, golden ratio, proportions néoclassiques et profil angulaire) ou non, les modifications nécessaires à appliquer pour obtenir des visages plus attrayants en termes de canons de beauté prédéfinis sont également proposées.
Comme décrit dans la sous-section précédente, pour améliorer la qualité esthétique des visages 3D, nous procédons à l'amélioration de chacun des canons de beauté en utilisant une technique

de déformation libre basée sur la fonction de Bézier, tout en essayant de préserver les principales propriétés du visage original.

Entrée du système :
Visages en 3D + les résultats de l'analyse de l'attractivité de chaque visage.

Sortie du système:
Visages 3D résultants après amélioration de leur qualité esthétique par la technique de déformation de forme libre basée sur la fonction de Bézier.

Résultats :
La figure ci-dessous décrit le processus d'amélioration des faces 3D pour un ensemble de visages 3D. Les lignes supérieures présentent les faces 3D originales (face et profil) et les lignes inférieures présentent les mêmes faces 3D après amélioration de leur qualité esthétique.

Amélioration de la qualité esthétique des visages 3D

5 Evaluation des résultats

Le système de déformation présenté dans la partie précédente visait à améliorer la qualité esthétique des visages 3D en se basant sur les résultats de l'analyse de l'attractivité de la partie 3. L'objectif de l'analyse de la qualité esthétique est de vérifier si le visage 3D donné répond aux canons de la beauté, à savoir la symétrie faciale, le nombre d'or, les proportions néoclassiques et le profil angulaire. Ainsi, un visage 3D respectant ces canons ou même étant très proche de leurs valeurs est considéré comme un visage attractif et par la suite il n'est pas nécessaire de modifier le visage, sinon, le visage devra être modifié pour améliorer son attractivité comme proposé dans la partie précédente.
L'objectif de la présente partie est d'évaluer les résultats de la méthode d'analyse de la qualité esthétique du visage ainsi que le visage 3D modifié après avoir amélioré son attractivité à l'aide du système que nous proposons. Pour ce faire, nous avons utilisé deux méthodes ; la première a consisté à demander à un expert du domaine d'évaluer les résultats obtenus par l'amélioration de l'attractivité faciale en 3D, et la seconde est l'une des méthodes de recherche empirique existantes, qui est la "recherche par sondage".

a. Questions de recherche

En général, l'objectif de l'évaluation présentée dans cette partie est de répondre aux questions de recherche détaillées comme suit :

- **Question de recherche 1** : Combien de points de repère sont nécessaires pour modéliser l'attractivité d'un visage humain ?
- **Question de recherche 2** : Les approches géométriques sont-elles meilleures que les techniques d'apprentissage statistique pour l'identification automatique de points de repère dans les visages humains ?
- **Question de recherche 3** : Les systèmes d'analyse et d'amélioration de l'attractivité sont-ils utilisables ?
- **Question de recherche 4** : Le visage 3D édité est-il attractif ?
- **Question de recherche 5** : La technique de déformation de forme libre utilisée est-elle la meilleure façon d'améliorer l'attractivité des visages 3D ?

Pour répondre aux questions de recherche définies, nous avons utilisé deux méthodes ; la première consistait à analyser à nouveau les résultats obtenus lors de l'étape d'amélioration de la qualité esthétique des visages en 3D et à vérifier si les visages en 3D résultants sont conformes aux canons de la beauté (symétrie faciale, golden ratio, proportions néoclassiques et profil angulaire) ou non ; en outre, cette méthode est basée sur la comparaison de nos résultats avec les ouvrages les plus pertinents de la littérature traitant du même problème. Par la suite, et pour une validation plus précise des résultats obtenus, ces résultats ont ensuite été vérifiés par un expert du domaine de la chirurgie plastique à qui nous avons demandé d'analyser à la fois la qualité esthétique de la version originale des visages 3D et de la version améliorée des mêmes visages en remplissant un tableau qui représente chacun des ID des visages 3D utilisés, les résultats d'analyse des visages 3D originaux, les résultats d'analyse des visages 3D améliorés, et si elle a

des commentaires à ajouter sur les résultats de notre système. Cette méthode est considérée comme le moyen de base pour évaluer le système que nous proposons pour analyser la qualité esthétique des visages en 3D et améliorer leur attractivité. Cette méthode est également utilisée pour répondre à l'ensemble des cinq questions de recherche.
Et la deuxième méthode pour répondre aux questions de recherche a été l'utilisation de la méthode de recherche par sondage. Cette méthode est largement utilisée dans des cas similaires d'analyse et d'évaluation car le chercheur ne peut qu'utiliser des théories existantes et les évaluer par l'observation sans s'impliquer dans le phénomène étudié ou la vie sociale du participant. Par conséquent, pour évaluer les résultats obtenus en matière d'amélioration de l'attractivité du visage en 3D, nous avons demandé à un certain nombre de participants de voter pour le visage en 3D qui semble le plus attrayant parmi le visage original et les nouveaux visages (avant et après l'amélioration de la qualité esthétique du visage en 3D). Cette tâche est liée à la dernière question de recherche, car les participants n'ont aucune idée des détails du processus d'analyse.

b. Validation des résultats

Le processus d'évaluation décrit dans cette partie visait à évaluer objectivement les cinq questions de recherche proposées présentées dans la section précédante en utilisant le processus d'analyse par l'expert en chirurgie plastique, en plus des votes des évaluateurs de notre université. Par la suite, une interprétation plus riche des résultats obtenus est effectuée.
L'évaluation présentée a permis à notre recherche d'être plus fiable et d'ajouter de la crédibilité aux résultats obtenus par l'analyse de la qualité esthétique du visage (2D/3D) et l'amélioration de l'attrait du visage en 3D. Comme nous l'avons déjà mentionné, cette évaluation est réalisée par le biais des votes des évaluateurs de notre université, qui consiste à voter pour le visage 3D perçu comme le plus attrayant dans la version originale et la version améliorée des visages 3D utilisés. Les résultats de cette étude ont montré l'efficacité du système proposé pour améliorer la qualité esthétique des visages en 3D et répondre à la majorité des questions de recherche abordées. L'évaluation la plus importante des résultats obtenus a été réalisée en demandant à un expert du domaine d'analyser les visages 3D originaux et les versions résultantes des mêmes visages, puis de conclure à l'efficacité du système proposé. Cela a également permis de démontrer la fiabilité du système proposé, comme indiqué dans la sous-section précédente.
En outre, l'objectif établi et simplifié de notre recherche nous a également permis de déterminer les besoins et les limites du système proposé.
En raison du petit nombre de participants au vote des évaluateurs pour l'efficacité de notre système proposé dans l'analyse de la qualité esthétique du visage (2D/3D) et l'amélioration de leur attractivité, les résultats rapportés du processus d'évaluation peuvent être considérés comme des résultats provisoires, et ceci est dû à notre temps limité. La plupart du temps, au cours de notre processus d'évaluation basé sur les votes des évaluateurs pour les visages les plus attractifs, nous avons adopté pour expliquer et démontrer l'efficacité et la précision de l'analyse et de l'amélioration de l'attractivité des visages, donc, comme une perspective ; nous visons à mener plus de processus d'évaluation.

6 Conclusion

a. La réalisation des objectifs de recherche

Après avoir étudié l'état de l'art en matière d'analyse, d'évaluation et d'amélioration de la qualité esthétique du visage, nous avons abordé quatre objectifs de recherche principaux, et avons donc proposé de diviser la thèse en quatre grandes parties : l'analyse de la qualité esthétique du visage en 2D, l'analyse de la qualité esthétique du visage en 3D, l'amélioration de l'attractivité du visage en 3D et enfin la vérification des résultats obtenus dans la dernière partie, donc l'évaluation de l'efficacité et des performances du système proposé.

Dans la première partie de notre thèse, nous avons introduit une nouvelle technique pour analyser la qualité esthétique des visages 2D. À cette fin, notre première contribution a été une nouvelle méthode pour localiser les points de repère faciaux 2D sur le visage d'entrée, basée sur le contour actif et l'ensemble des axes qui traversent les traits du visage. Ensuite, l'analyse de l'attractivité du visage peut être effectuée en utilisant les canons de beauté prédéfinis dans la littérature ; ensuite, la modification nécessaire à appliquer afin d'améliorer son attractivité peut être conclue. Même si les résultats de l'analyse de l'attractivité sont bons, il y a cependant quelques inconvénients, notamment en ce qui concerne la visualisation des détails des côtés frontal et profil du visage, ce qui rend l'utilisation de la représentation 3D du visage très utile pour remédier à tous les problèmes qui peuvent survenir lors de l'utilisation du visage 2D.

Étant donné les limites de la première partie de notre thèse, nous avons introduit dans la deuxième partie une nouvelle méthodologie pour analyser la qualité esthétique des visages en 3D. À cette fin, en réalisant une analyse documentaire des méthodes de détection des points de repère du visage en 3D, suivie d'une cartographie systématique des méthodes basées sur les informations géométriques pour localiser les points de repère en 3D, une nouvelle méthode de détection des points de repère du visage en 3D basée sur les informations géométriques de la forme du visage en 3D a été proposée pour détecter un grand nombre de points de repère en 3D. L'analyse de l'attractivité des visages en 3D vient alors en évaluant si le visage est conforme ou non aux canons de la beauté. Ces canons sont les mêmes que ceux de la première partie de la thèse pour la face frontale du visage, puis nous avons ajouté ceux relatifs à la face de profil. Parallèlement à l'analyse de l'attractivité du visage en 3D, les modifications nécessaires à appliquer pour améliorer son attractivité sont données par notre système. À ce stade, il est très important de visualiser le visage en 3D après avoir appliqué la modification.

Au troisième stade de notre thèse, la modification du visage en 3D a été effectuée afin d'améliorer sa qualité esthétique. Dans un premier temps, une analyse documentaire de l'approche utilisée à cet effet a été réalisée, puis dans notre cas, la déformation a été réalisé en utilisant une technique de Free Form sur la fonction d'interpolation de Bézier. Compte tenu des résultats obtenus de l'analyse de l'attractivité, pour chaque région du visage 3D qui doit être éditée, l'approche libre proposée dans notre thèse est appliquée afin d'obtenir un visage 3D satisfaisant les canons de la beauté. Après cette étape, le visage 3D édité obtenu doit être évalué afin d'apprécier l'efficacité du système proposé pour préserver les détails du visage original ainsi que pour obtenir un visage agréable à la fin de l'édition. À cette fin, nous avons analysé la qualité esthétique des visages résultant de notre système en vérifiant s'ils sont conformes aux canons de beauté et en demandant ensuite à un expert du domaine d'évaluer les résultats finaux, et nous

avons demandé de voter pour le visage le plus attrayant entre les deux versions de avant et après la modification de chaque visage. Les résultats obtenus montrent que notre système peut éditer les visages en 3D et les rendre plus attrayants.

b. Synthèse des contributions

Les contributions de notre thèse sont comme suit :

1. **Une nouvelle méthode pour détecter les points de repère du visage sur une image 2D.** Cette méthode est une combinaison de deux approches : le contour actif et l'approche basée sur la détection des axes 2D du visage qui passent par les traits du visage : les yeux, le nez, la bouche et l'axe médian. Cette nouvelle méthode s'avère plus efficace pour détecter un grand nombre de points de repère que les autres approches les plus utilisées dans la littérature comme l'ondelette de Haar.

2. La deuxième contribution est **une étude comparative de Harris et Active Contour utilisant l'algorithme Viola-Jones pour la détection des points de repère faciaux**. Sur la base de la première contribution, nous avons mené une étude comparative de l'opérateur bien connu Harris et de l'Active Contour (Snake) en utilisant l'algorithme Viola-Jones pour la localisation des points de repère faciaux en 2D.
   Les résultats expérimentaux ont montré que l'Active Contour + Viola-Jones a montré des résultats de localisation intéressants comparés à l'algorithme Harris+ Viola-Jones.

3. La troisième contribution est une **classification des méthodes d'information géométrique pour localiser les points de repère faciaux en 3D en catégories**. Une étude cartographique est réalisée pour caractériser les méthodes existantes basées sur l'information géométrique pour localiser les points de repère faciaux en 3D et pour les classer en catégories. Ainsi, les méthodes basées sur l'information géométrique pour localiser les points de repère faciaux en 3D peuvent être classées en quatre catégories.

4. La quatrième contribution est **une nouvelle approche pour détecter 30 points de repère faciaux en 3D**, cette approche est basée sur les informations géométriques du visage en 3D. Cette méthode est capable de localiser le grand nombre de 30 points de repère sur un visage en 3D avec un minimum d'erreur et d'écart-type par rapport aux autres études de la littérature.

5. La cinquième contribution est **une nouvelle méthode pour éditer le modèle de visage en 3D afin d'appliquer les modifications nécessaires pour améliorer son attractivité**. Cette méthode est basée sur l'utilisation d'une technique de déformation Free Form utilisant la fonction d'interpolation de Bézier. En effet, pour chaque zone du visage qui doit être modifiée, la technique Free Form est utilisée pour appliquer les modifications nécessaires afin d'améliorer son attrait en termes de canons de beauté.

c. Perspectives

La recherche présentée a les orientations futures suivantes :

- **Étude de cas du monde réel :** les auteurs visent à appliquer le système présenté à une application du monde réel. Les chirurgiens esthétiques ou plastiques peuvent utiliser le système proposé afin d'analyser la qualité esthétique du visage des patients en utilisant la méthode 2D ou 3D, puis de visualiser l'aspect du visage après l'opération en suivant les modifications suggérées pour améliorer son attrait.

- **Vérification du système proposé en utilisant d'autres bases de données de visages en 3D :** dans l'étude présentée, les auteurs ont utilisé deux bases de données de visages en 3D pour analyser la qualité esthétique des visages. Le système doit être testé sur d'autres bases de données de visages en 3D, en particulier celles créées dans le même but que notre étude, dans lesquelles la texture du visage est présentée de manière à rendre la visualisation de l'amélioration de l'attractivité plus claire.

- **Améliorer l'interface homme-machine de l'analyse de l'attractivité :** nos travaux futurs se concentreront sur la mise au point de l'interface homme-machine proposée, afin qu'elle soit plus développée et plus agréable à l'œil de l'utilisateur.